

ENGINEERING AND TECHNOLOGY MANAGEMENT



EDITORS

Prof. Dr. Ashok JAMMI

Prof. Dr. Abdulkadir GÜLLÜ

Assist. Prof. Zeynep YAMAN

Assist. Prof. Senai YALÇINKAYA

ENGINEERING AND TECHNOLOGY MANAGEMENT

EDITORS

Prof. Dr. Ashok JAMMI

Prof. Dr. Abdulkadir GÜLLÜ

Assist. Prof. Zeynep YAMAN

Assist. Prof. Senai YALÇINKAYA

ENGINEERING AND TECHNOLOGY MANAGEMENT

EDITORS

Prof. Dr. Ashok JAMMI
Prof. Dr. Abdulkadir GÜLLÜ
Assist. Prof. Zeynep YAMAN
Assist. Prof. Senai YALÇINKAYA

Güven Plus Group Inc. Publications: 49/2021
15 DECEMBER 2021

Publisher Certificate No: 52866
E-ISBN: 978-625-7367-05-9
Güven Plus Group Inc. Publications

All kinds of publication rights of this scientific book belong to GÜVEN PLUS GROUP CONSULTANCY INC. CO. PUBLICATIONS. Without the written permission of the publisher, the whole or part of the book cannot be printed, broadcast, reproduced or distributed electronically, mechanically or by photocopying. ***In case of any legal negativity, the institutions that support the preparation of the book, especially GÜVEN PLUS GROUP CONSULTANCY INC. CO. PUBLISHING, the institution (s) responsible for the editing and design of the book, and the book editors and other person (s) do not accept any "material and moral" liability and legal responsibility and cannot be taken under legal obligation. We reserve our rights in this respect as GÜVEN GROUP CONSULTANCY "PUBLISHING" INC. CO. in material and moral aspects. In any legal problem/situation TURKEY/ISTANBUL courts are authorized.*** This work, prepared and published by Güven Plus Group Consultancy Inc. Co., has ISO: 10002: 2014-14001: 2004-9001: 2008-18001: 2007 certificates. This work is a branded work by the TPI "Turkish Patent Institute" with the registration number "Güven Plus Group Consultancy Inc. Co. 2016/73232" and "2015/03940". This scientific/academic book is of national and international quality and has been officially documented with the information of Istanbul Governorship Provincial Culture and Tourism Directorate Istanbul Printed Letters and Pictures Compilation Directorate No: 37666426-207.01[207.02.02]-E.62175 Date: 21.01.2019. ***This scientific/academic book is "within the scope of academic incentive criteria for 2019, and it is evaluated within the scope of the related regulation published in accordance with the Presidential Decision numbered 2043 dated 16/1/2020 and published in the Official Gazette numbered 31011 dated 17/01/2020" and meets the academic incentive criteria.*** This multi-author book has E-ISBN and is scanned by the National Libraries of the Ministry of Culture and the E Access system of the National Library, which has an agreement with 18 different World Countries. This book cannot be bought or sold with a monetary value. Güven Plus Group Consultancy Inc. Co. Publishing has not earned any financial income or made any requests from the authors of the book chapter, supporters, and contributors. Provided that the chapter and content in this scientific book is quoted and cited to the relevant book, it can be used by scientific or relevant researchers for reference. ***Our publishing house and the editorial board of the book act in accordance with the laws on the protection of personal data and privacy. It obliges the authors of scientific book chapters to act in this direction. Individuals who own this academic/scientific book regarding the protection of personal data are obliged to act in accordance with the relevant laws, regulations and practices. It is deemed to have accepted in advance the legal, material and moral problems and obligations that arise about those who act contrary to this.***

Text and Language Editors

Assoc. Prof. Gökşen ARAS (Turkish – English)
Assist. Prof. L. Santhosh KUMAR (English)

Cover and Graphic Design

Prof. Dr. Pelin AVŞAR KARABAŞ
Lec. Ozan KARABAŞ
Ozan DÜZ

Page Layout

Burhan MADEN

Print-Binding

GÜVEN PLUS GROUP CONSULTANCY INC. CO. PUBLICATIONS®
Kayaşehir Neighborhood Evliya Çelebi Street Emlakkonut Başakşehir Houses 1/A D Block Floor 4 Number 29
Başakşehir İstanbul - Turkey Phone: +902128014061- 62 Fax: +902128014063 Mobile: +9053331447861

BOOK LICENSEE

GÜVEN PLUS GROUP CONSULTANCY INC. CO. PUBLICATIONS®
Kayaşehir Neighborhood Evliya Çelebi Street Emlakkonut Başakşehir Houses 1/A D Block Floor 4 Number
29 Başakşehir İstanbul - Turkey Phone: +902128014061- 62 Fax: +902128014063 info@guvenplus.com.tr,
www.guvenplus.com.tr

TABLE OF CONTENTS

PREFACE.....	1
THE ROLE OF OPTICAL AND ULTRASOUND IMAGING IN MEDICINE: SAMPLE APPLICATIONS OF PHANTOM IMAGING	2
<i>Tuğba Özge ONUR, Gülhan USTABAŞ KAYA</i>	
NOISE MEASUREMENT RESULTS IN WOOD PANEL MANUFACTURING WORKPLACE.....	26
<i>Zehra Gülten YALÇIN, Mustafa DAĞ, Ercan AYDOĞMUŞ</i>	
CIRCULAR BUILDING DESIGN THAT CONTRIBUTES TO THE CIRCULAR ECONOMY	62
<i>Ebru DOĞAN, Fatma Berfin YAMAK</i>	
HVAC PRACTICES FOR DATA CENTERS.....	85
<i>Kaan YILMAZKARASU, Ayhan ONAT</i>	
ASSESSMENT ON OPERATING INLET PRESSURE HEAD FOR IRRIGATION SUBMAINS INCORPORATING DIFFERENT TYPES OF PRESSURE PROFILES-II: DESIGN APPLICATIONS	124
<i>Gürol YILDIRIM</i>	
ON THE VISCOELASTIC DYNAMICS AND STABILITY OF AXIALLY FUNCTIONALLY GRADED FLUID CONVEYING PIPES	148
<i>Reza AGHAZADEH</i>	
DESIGN AND ASSESSMENT OF A MATERIAL RECYCLING FACILITY IN THE MIDDLE-SCALE RESIDENTIAL AREA.....	168
<i>Nesli AYDIN</i>	
NUMERICAL METHODS IN HEAT CONDUCTION AND PLOTTING THE TEMPERATURE DISTRIBUTION IN MATLAB PROGRAM.....	187
<i>Abdull Ghafoor SHAIB, Senai YALÇINKAYA, Bahadır ALYAVUZ</i>	

THE HISTORIC CONCRETE: CONSTRUCTION AND ARCHITECTURE	210
<i>Hilal Tuğba ÖRMECİOĞLU</i>	
REACTION DIFFUSION EQUATION IN ENGINEERING.....	229
<i>Esen HANAÇ</i>	
SUSTAINABLE SMART CITY CONCEPT: DEVELOPMENT PROCESS OF KONYA	250
<i>Nazmiye Nur ŞENYİL, Süheyla BÜYÜKŞAHİN</i>	
INFORMATION SECURITY WITH STEGANOGRAPHY	287
<i>İnan GÜLER</i>	
STRUCTURAL PROPERTIES OF THE SUPER ALLOYS AND THEIR MACHINABILITY	305
<i>Abdullah ALTIN</i>	
OPERATING PRINCIPLE OF AUTOMATIC ARTICULATOR	348
<i>Mohammad RAFIGHI, Abdulkadir GÜLLÜ, Metin ORHAN</i>	

PREFACE

Technological advances in the field of engineering are followed by major and important developments. Güven Plus Grup A.Ş., whose publications are mostly academic books, has gained a lot of prestige with its national and international activities. The “Engineering and Technology Management” book has been published by this publisher that consists of fifteen different chapters which cover various issues and researches of valuable academicians.

Activities that benefit humanity such as development, change, progress, and innovation are a product of labor. Sharing scientific studies that benefit all humanity is of great importance. As scientists, it is our pleasure to touch people’s world positively, by publishing works that make their lives easier.

Each chapter in the book consists of original studies which are written by valuable academicians and researchers. We would like to express our gratitude to each of our authors who collected these works in our book and became a part of it.

May everyone who reads and examines this book find it helpful in terms of solving a problem, getting an answer to a question, and getting an opportunity for their further work. Presenting such scientific studies aimed at making a positive contribution to humanity for the benefit of scientists, researchers and industrialists will take our human feelings further and make people look at life more positively.

We believe that this book, which includes chapters on many interesting topics of engineering technologies, will shed light on the academic studies of many researchers and will find a valuable place in the catalogs of the Higher Education Institution, university libraries, and personal archives.

We would like to thank our esteemed authors, referees, technical team, and our dear readers, who have contributed to the realization of this book, which is the result of long efforts and meticulous studies.

Prof. Dr. Ashok JAMMI
Prof. Dr. Abdulkadir GÜLLÜ
Assist. Prof. Zeynep YAMAN
Assist. Prof. Senai YALÇINKAYA
December 2021

THE ROLE OF OPTICAL AND ULTRASOUND IMAGING IN MEDICINE: SAMPLE APPLICATIONS OF PHANTOM IMAGING

Tuğba Özge ONUR¹, Gülhan USTABAŞ KAYA²

Abstract: Today, in the medical field, ultrasound is frequently used for both diagnostic and therapeutic purposes. Ultrasound waves are generated with the help of a transducer that can both emit high-frequency sound waves and detect reflected echoes of them. In this way, by applying a gel that prevents the formation of air gaps between the transducer and the dermis, ultrasound enables the imaging of internal organs, the detection of a specific target, the ablation or disintegration of a tissue or a specific target. Thus, ultrasound imaging is a non-invasively method that is generally considered safe since it does not produce ionizing radiation. However, the requirement to move the transducer over the dermis, ie contact, can be a disadvantage of ultrasound imaging for some situations. In these cases, optical imaging, where light is used for imaging in medical applications, can be used alternatively. In optical imaging, non-ionizing radiation including visible, ultraviolet, and infrared light is used. In this way, the patient's exposure to harmful radiation can be significantly reduced, and it can be used for both the diagnosis and the treatment. However, the major disadvantage of optical imaging can be its high cost. In this study, the lateral shearing digital holographic microscopy (LSDHM) method is used for both providing nondestructive, full-field, and high-resolution imaging and reducing the cost which is the major disadvantage in optical medical imaging. In this context, it has been shown that optical medical imaging can

1 Zonguldak Bülent Ecevit University, Dept. of Electrical-Electronics Engineering, Zonguldak / Turkey, tozge.ozdinc@beun.edu.tr, Orcid No: 0000-0002-8736-2615

2 Zonguldak Bülent Ecevit University, Dept. of Electrical-Electronics Engineering, Zonguldak / Turkey, gulhan.ustabas@beun.edu.tr, Orcid No: 0000-0002-5643-0531

be performed at a low cost and with fewer components with various exemplary imaging applications. For this purpose, some tissue-mimicking phantoms have been produced by using agar gel to mimic the human vascular system and cystic masses in tissues or organs for use in imaging applications. It can be also concluded that phantom structures can be used for all kinds of calibration, testing, reliability testing, etc. of imaging systems without the need for any living tissue and provides great convenience. In other respects, since phantom structures can be generated to model all kinds of tissues and organs, they help to speed up diagnosis and treatment without the need for any biopsy or additional operations and are used frequently in medical fields.

Keywords: Medical Imaging, Ultrasound, Optic, Lateral Shearing Digital Holographic Microscopy, Image Formation

INTRODUCTION

Medical imaging is used to aid diagnosis and treatment by obtaining images of various parts of the human body. There have been various medical imaging techniques such as radiography, magnetic resonance imaging (MRI), tomography, ultrasound, photoacoustic imaging, optical imaging, etc. (Jafari et al., 2018). In the 1940s, ultrasonic technology, which was first used in radars during World War II, began to be used in diagnostic medicine studies after this date, and after the 1970s, it was fully accepted for diagnostic medicine studies. In general, ultrasonic imaging is a diagnostic imaging method that uses high-frequency sound waves to display internal parts of the body and organs. Today, medical ultrasound with a frequency between 2 and 40 MHz is a frequently used clinical imaging method due to its low cost, non-radiation and easy application. The frequency can be increased to 100 MHz levels for ophthalmology, skin imaging and intravenous imaging studies that require special applications (Bonnet et al., 2019). Medical ultrasound can be used for both diagnostic and therapeutic applications. Since the tissues and organs in the human body have different properties such as elasticity, density, etc., the value of the speed of sound varies in each region of the human body. The sound velocity in the brain tissue is 1530 ms^{-1} whereas it is about 1568 ms^{-1} in the muscles and 3600 ms^{-1} in the bones (Bonnet et al., 2019). In addition, sound waves are reflected while propagating in the

human body due to the different regions and borders. For example, they are reflected and partially transmitted at the boundaries between organs and fluids or other tissues. While using ultrasound imaging for diagnosing, an ultrasound transducer is used to convert mechanical energy into electrical energy and vice versa. In ultrasound imaging, ultrasound waves are directed to the body by pressing the transducer against the dermis and to reduce the air gaps between the transducer and the skin and to fill the gap, any type of gel is applied to the dermis. While the waves propagate throughout the body, the sound echoes due to reflection and scattering caused by body fluids and tissues are collected by the transducer. Back reflections from tissue interfaces occur because the tissue layers have different acoustic resistances. The high resistance difference between the tissues causes more energy to be reflected back and thus it is echoed at a higher amplitude. Soft transition interfaces between tissues allow the propagation of the ultrasonic signal. However, since there is a certain difference between the basic soft tissues and bone acoustic resistances in the body, most of the acoustic energy is reflected by the bone, and the rest is absorbed. The acoustic resistances of biological tissues are given in Table 1.

Tablo 1. The Acoustic Resistances of Biological Tissues (Kobayashi et al., 2014)

Biological Medium	Acoustic Resistance x 10 ⁵ (g.cm ⁻² s ⁻¹)
Fatty Tissue	1.38
Ophthalmic	1.52
Encephalon	1.58
Hemal	1.61
Nephritic	1.62
Hepatic	1.65
Muscle	1.7
Bone	7.8
Air	0.0004

In addition, beam deflection and refraction also cause attenuation. Because when smooth interfaces are considered, according to the angle of incidence in ultrasonic imaging, ultrasonic waves are reflected, refracted and transferred to the other medium. If the interface is smooth and the direction of propagation of the ultrasonic wave is perpendicular to the interface, as in the Figure 1, some of the ultrasonic beam is reflected and some passes to the other medium.

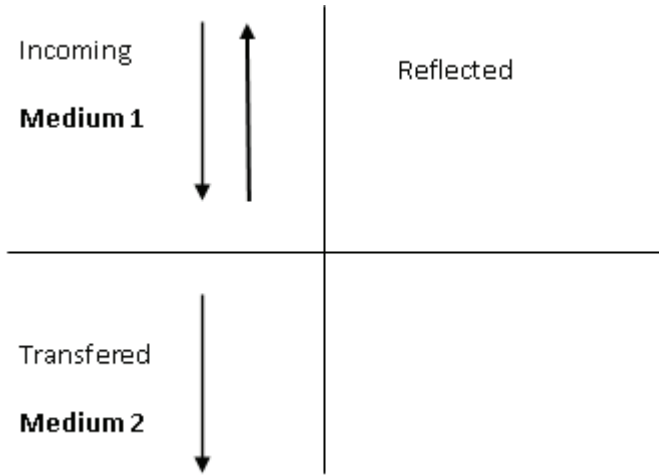


Figure 1. The Case of Perpendicular Arrival Angle and Smooth Interface (Fish, 1991)

Depending on the strength and nature of these sound echoes gathered by the transducer, user viewable 1-dimensional (1-D), 2-dimensional (2-D) or 3-dimensional (3-D) images can be created (Hermawati and Sugiono, 2017). In addition to this, ultrasound imaging is frequently used for diagnosis and treatment in many applications today, since it does not require injection or needle in most cases, is mostly painless, provides fast images, and does not have radiation. However, ultrasound imaging may have two disadvantages. One of them is that ultrasound waves can cause minor damage to the body due to the cavitation which occurs in the low pressures and falls in the high pressures. But despite this, medical ultrasound can be regarded as one of the least harmful imaging techniques that have opportunity to use present day and is used even if

there is a pregnancy. The other one is that ultrasound imaging requires contact, that is, the transducer needs to be moved in the skin to create the image. Therefore, optical imaging can be an alternative to ultrasound imaging.

In optical imaging for medicine, light is used for imaging. Although optical devices to be used according to the type of examination performed by physicians vary greatly, optics have an important role in medical imaging. It can be used in pathology, microscopic surgery, some types of eye testing/treatment systems, laparoscopy, colonoscopy, endoscopy, deep tissue imaging, etc due to providing appropriate spatial resolution (He et al., 2021). The most important reason why optical imaging is used more limitedly than ultrasound imaging is the high cost of optical devices and systems. Most components of each optical system have to be designed specifically for the device, which increases the design cost of optical systems. However, the cost can be reduced while increasing the modularity of the design by using digital holography.

In recent years, by using digital holographic microscopy (DHM) methods, the cost of medical imaging with digital holographic devices has been reduced, while non-destructive, full-field and high resolution are achieved. The quantitative phase and amplitude information of biological specimens are recorded with these methods. Hence, very small transparent objects and biological microorganisms are visualized from various depths and viewed with high resolution (Di et al., 2016). To encode the phase and amplitude image, coherent light is combined with reference and object waves. Then the interference pattern (hologram) is occurred. The information about specimen is extracted by using numerical processing techniques (Singh et al., 2012). There are various optical configurations to form the digital holographic microscopy. They use the superposition of the object beam and background reference beams that travel on two arms as bases. Mach-Zehnder and Michelson interferometers are the examples of two-beam setup. Although two beams pass through the separate arms in these methods, the stability of the system is disrupted due to having mechanical vibrations and minor disturbances (Anand et al., 2017; Vora et al., 2017).

On the other hand, the in-line holography setup that increases the stability and has less expensive components, can be used for medical imaging. The phase can be retrieved with eliminating the defocus aberration in LSDHM, which has self referencing configuration (Devinder et al., 2019). LSDHM is preferred for many researchers due to displaying micro-sized samples (Seo et al. 2014). For instance, *Chilomonas* protozoa microorganisms that have 20–40 μm size is displayed via LSDHM by Singh et al. (Singh et al., 2012). Moreover, polystyrene grains are imaged with DHM based on single reference phase microscopy method (Jang et al. 2010). In the aforementioned studies, the temporary phase stability was obtained by numerically subtracting the phase information from the recorded hologram. In this context, various studies are conducted by using several signal processing algorithms and applying artificial intelligence methods (Rivenson et al., 2019; Jo et al., 2019; Nguyen et al., 2017).

In other respects, phantoms are needed to verify the position (calibration) of both ultrasonic and optical devices used for diagnosis and treatment, to improve the signal and noise ratios of existing systems, to ensure the awareness and interpretation of the images taken during the practical work of the users before using the device and during the application. In these applications, phantoms serve as test materials that can describe the special characteristics of human tissues. For this reason, it is important for both ultrasonic and optical systems in medical imaging to create phantoms that are easy to manufacture, do not contain any harmful chemicals, and cost low. In addition, commercial phantoms are produced for many markets and major applications and cannot be personalized. The prices of these phantoms which represent many tissues and organs, can reach high values. For this reason, producing phantoms closest to the tissues to be applied, easy to use and low cost is another important issue (Onur et al., 2021).

In this study, imaging applications have been performed to visualize the veins or cystic masses in the created phantoms by using LSDHM and it is shown that optical medical imaging is also non-invasive and can be performed with low cost and less components. The study is organized as follows: the procedure of image formation for ultrasound systems is described in the Image Formation In Ultrasound Imaging Systems secti-

on. Image Formation In Optical Systems section is designated for the optical imaging systems by using optical holography. Experimental results are presented in The Applications of Image Formation By Using Optical Holography section and Results and Discussion section accomplishes this paper.

IMAGE FORMATION in ULTRASOUND IMAGING SYSTEMS

In ultrasound imaging systems, the image acquisition is based on the generation and the detection of ultrasonic waves utilizing the piezoelectric effect of the transducer. This effect is provided by a piezoelectric material in the transducer which is generally barium titanate (BaTiO_3) or lead zirconium titanate (PZT) (Qian et al., 2020). The electrical energy is converted to the mechanical energy or vice versa in these materials. By using the contraction and stretching in piezoelectric material due to the electrical fields, ultrasound waves are generated. In ultrasound imaging, axial and lateral resolutions are used. Axial resolution depends on the frequency of sound wave and the better axial resolution provides the transducer to distinguish the shorter ranges between the structures. On the other hand, the structures which are located in the same lateral range to the transducer can be distinguished by using lateral resolution and it also depends on the frequency and accordingly wavelength of the ultrasound. The use of ultrasound enables to acquire 1-D signals or images and also 2-D or 3-D images. It can be obtained by using different imaging modes such as A, B or M modes in ultrasound (Ward et al., 1997).

A-mode which is the amplitude mode displays the magnitude of the reflected ultrasound wave (Szabo, 2014). The disadvantage of this imaging mode is to acquire the information only in the sonic ray direction means that only one single line in the body.

B-mode images are generated with the combination of A-mode scans and intensity. This is the commonly used mode for ultrasound imaging (Sassaroli et al., 2017). In this mode, since the visuals of the inter body are acquired as bidimensionally to obtain samples on 2-D or 3-D planes, mechanical or electronic scanners in linear or phased arrays are used. In the case of mechanical scanners, a cross section of the human body is

displayed as a circle segment and the echo intensity of this segment is converted to a gray scale. The image matrix is formed by combining the obtained gray scales and a B-mode image is obtained. Electronic scanners consist of transducers whose number and diameter can range from 60 to 100 and 0.5 mm to 1 mm, respectively and these are designated in a linear or curved array (Nikolov and Jensen, 2002). For scanning, one group of transducers is activated at the same time and then all group items are shifted. The difference of electronic scanners which have a phase array structure is that each transducer is reached with a separate adjustable delay for both sending and receiving.

M-mode is the motion mode. In this mode, the transducer emits ultrasonic pulses without any moving, and an A or a B mode scan is gathered every time. In this way, time-dependent measurement for organ motion according to the probe can be obtained. It can be useful in applications such as examining the movement of the heart wall that is myocardium (Li and Min, 2020).

Since B-mode scanning which provides visualization of various tissue structures in the body, is the most common used ultrasound mode by clinicians, in this section image formation in B-mode will be detailed. In B mode image, first the amplitude of the quadrature signal is taken that means envelope determination. Then, to reduce the dynamic range from the sampled range (about 12 bit) to output image (8 bit), the signal is compressed logarithmically or histogram equalization is used (Maini and Aggarwal, 2010).

Logarithmic Compression

Logarithmic compression can be used to enhance the image quality or to shrink the dynamic range of the received signals (Brandner et al., 2021). The variation in RF data amplitude is quite much. Therefore, if the same image is linearly mapped to 0-255 gray scale image, the most important tissue structures will only have 0-9 image values. In other words, due to the several very high amplitude points in the image, the others will be overshadowed. To gain a compensation, the amplitude

values are mapped with the logarithmic function that adjusts the dynamic range. Logarithmic compression can be defined as in Equation 1,

$$g(x) = c \log(1 + x)g(x) = c \log(1 + x) \quad (1)$$

where c is a constant. This kind of compression enables more compression for the differences in high gray values than the differences in low gray values.

Histogram Equalization

The histogram is very important to determine the contrast of the image. If the histogram is concentrated to the left, the image will be dark. If the histogram is to the right condensed, the image will be bright. The best contrast images will have a nearly uniform scattered histogram in all their amplitudes. Therefore, histogram equalization is one of the best known image enhancement methods. The main purpose of histogram equalization-based methods is to reappoint the intensity values of pixels to make uniform the density distribution (Moniruzzaman et al., 2013). Let's assume that the original the image is normalized and its intensity range is $[0, 1]$ and the function of intensity distribution for it is $p(x)$. Here, x determines the intensity value of the normalized image. The density distribution of the output image is set to 1 after the desired density function equalization. Histogram equalization can be defined as in Equation 2,

$$y = \int_0^x p(u) du \quad (2)$$

where y and x are the intensities of output and input images, respectively; u is a variable. In addition, both x and y values are in the range of $[0,1]$.

An Example for Image Formation in B-Mode Scanning

In this study, the data used is obtained from a linear array transducer that includes various transducers. The data is acquired by sampling at 40 MHz with 128 beamlines and in the example where the speed of sound is 1540 m/s. The beamlines are 15 mm apart. The phantoms used were generated with random scattered glass beads in an agar. The diameters of glass beads are in the range of 5-43 μm (Onur and Hacıoğlu, 2016). The amplitude of the obtained RF signal and the generated phantom image is shown in Figure 2 and Figure 3, respectively.

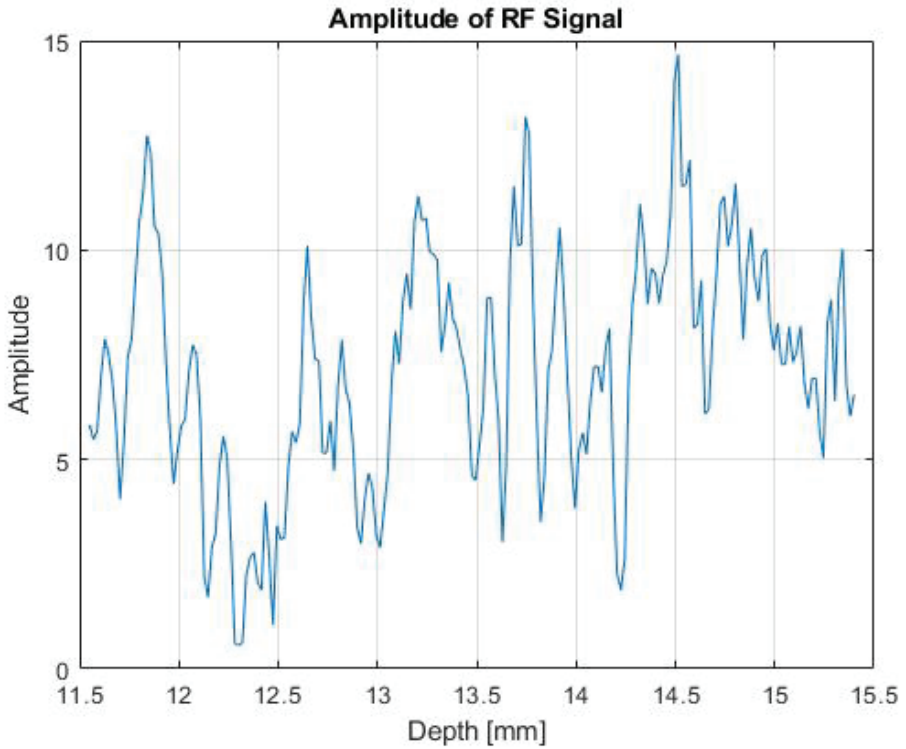


Figure 2. The Amplitude of RF Signal

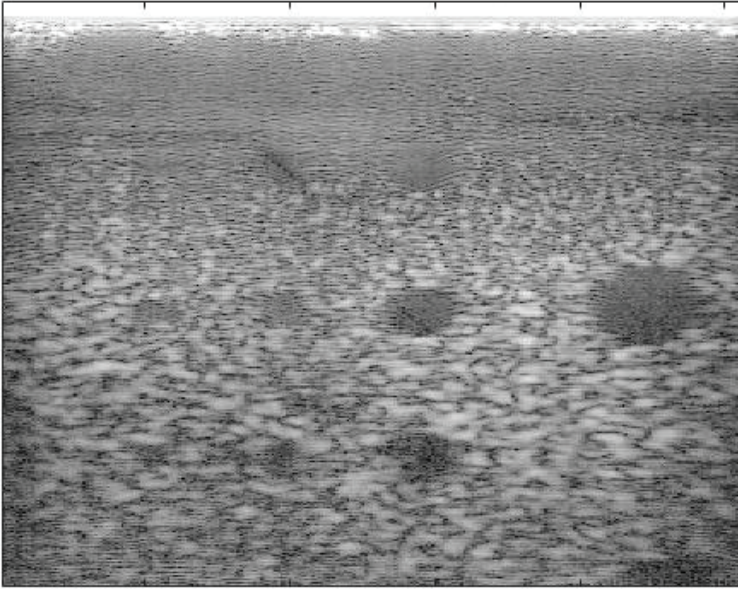


Figure 3. The Image of Generated Phantom

It can be seen from Figure 3 that the image includes resolution cylinders which are indistinct at some points. Logarithmic compression or histogram equalization methods can be used to highlight these resolution cylinders that are not specific in the darker regions of image. The obtained figure after logarithmic compression and histogram equalization is applied is shown in Figure 4.

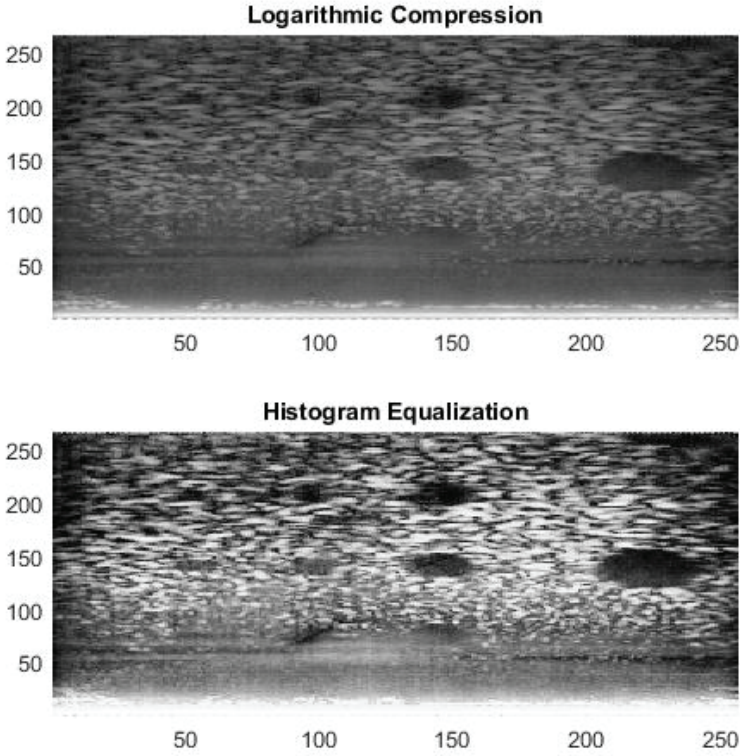


Figure 4. The Image of Generated Phantom After Logarithmic Compression and Histogram Equalization

It can be easily seen from Figure 4 that only the resolution cylinders become more prominent by using logarithmic compression, while histogram equalization makes background details more clear.

IMAGE FORMATION in OPTICAL SYSTEMS

The quantitative phase and amplitude information of biological samples are imaged with nondestructive and full-field technique of digital holographic microscopy (DHM) (Di et al., 2016). Small lesions, biological microorganisms, transparent objects can be captured with high

resolution in various depths. Various optical systems such as Mach-Zehnder and Michelson interferometers are used for this purpose.

In these methods called as two-beam path configurations, a coherent beam divided into two beams. One path represent the object beam, which illuminate the sample, and the second one is reference beam is kept unaltered (Devinder et al., 2019). In Mach-Zehnder interferometer (MZI), these beams move in different paths in space. Thereafter they are combined by using beamsplitter to form an interference fringe on image sensor. The configuration of MZI is depicted in Figure 5 (Ustabaş Kaya and Saraç, 2019).

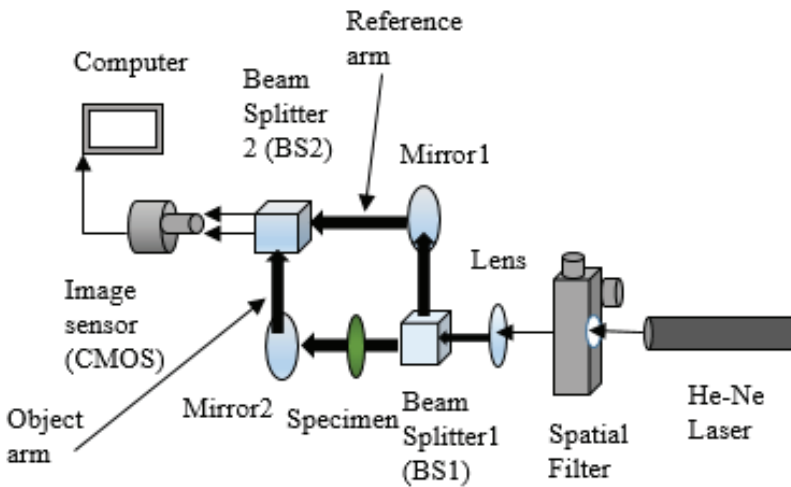


Figure 5. Configuration of Mach-Zehnder Interferometry

In MZI, He-Ne laser that has 632nm wavelength and 10mW output power can be used as a beam source. Three-axis spatial filter, lens and beam splitter are used for filtering the beam spatially, expanding the beam and splitting the beam into two path, respectively. The splitting beam constitutes the reference and objects arms. After the reference and object beams are directed to the mirrors that located at approximately 45°, these beams are sent to second beam splitter and imaging sensor of camera, respectively. On the way of object beam, specimen is located to create the phase difference between two-path. The combined two be-

ams, that are object and reference beams, create an interference pattern (hologram) on the imaging sensor.

On the other hand, to separate the wavefronts of illuminated beam Michelson interferometer can be used. As in the Mach-Zehnder interferometry, in this system, the laser beam is split into two branches with the help of a beam splitter. In Mach-Zehnder interferometry, the beam traveling in two separate arms is combined with the help of a second beam splitter, while a single beam splitter is used in Michelson Interferometry (MI). This beam splitter both splits the beam in two path and then combines the amplitudes of the two split beams using the principle of superposition. Figure 6 shows the Michelson Interferometry configuration (Min et al., 2019).

He-Ne laser ($\lambda = 632\text{m}$, $P_{\text{max}} = 0 \text{ W}$) is used as a coherent illumination source for MI. The beam is filtered by three-axis SF (spatial filter) and expanded by Lens (L). The expanded beam is splitted into two beam path by using beam splitter (BS). The first beam is reflected to Mirror1 (M1) and the second one continues on its way to direct toward the Mirror2 (M2). The first one is reflected to Mirror1 and the second one continues on its way to direct toward the Mirror2. Thereafter, two beams of the same amplitude, reflected by hitting the mirrors, are combined in the same beam splitter to observe interference on the image sensor. In two beam paths configuration, materials under the sample can be incorporate. Moreover, the phase and amplitude informations can be obtained numerically due to different path lengths.

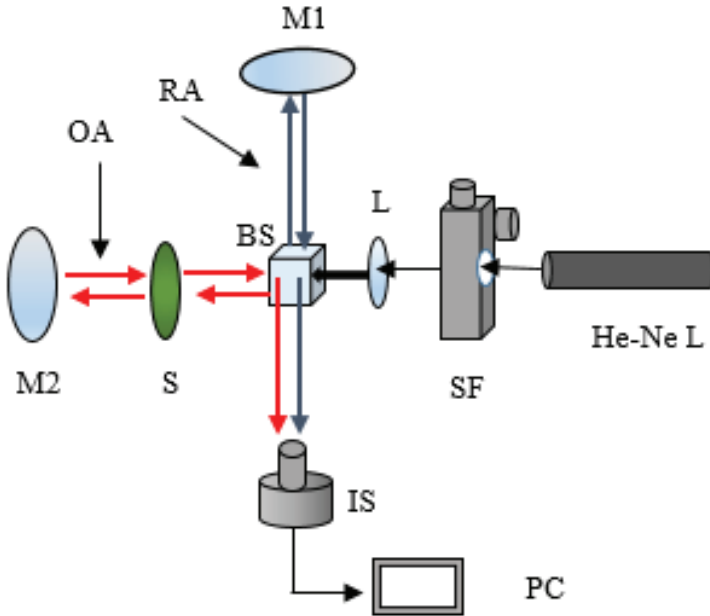


Figure 6. Configuration of Michelson Interferometry (He-Ne L: Lazer, SF: Spatial Filter, L: Lens, BS: Beam Splitter, M1: Mirror 1, S: Sample, M2: Mirror 2, IS: Image Sensor, PC: Personal Computer, OA: Object Arm, RA: Reference Arm)

In two beam path configurations such as MZI and MI, small disturbances and mechanical vibrations occur due to using high cost of optical components. To overcome the stability problem of these systems, the usage of single beam path self-referencing LSDHM system can be proposed. Figure 7 shows a single beam path self-referencing LSDHM system. This system has advantages over MZI systems. One of them is the decrease in the number of components used in the system. In addition, the stability increases since the vibrations and disturbances that may occur in any of the arms in the MZI system are not in the lateral cutting system. Moreover, as the bandwidth of the imaging sensor is fully used, finer spatial details can be captured (Devinder et al., 2019).

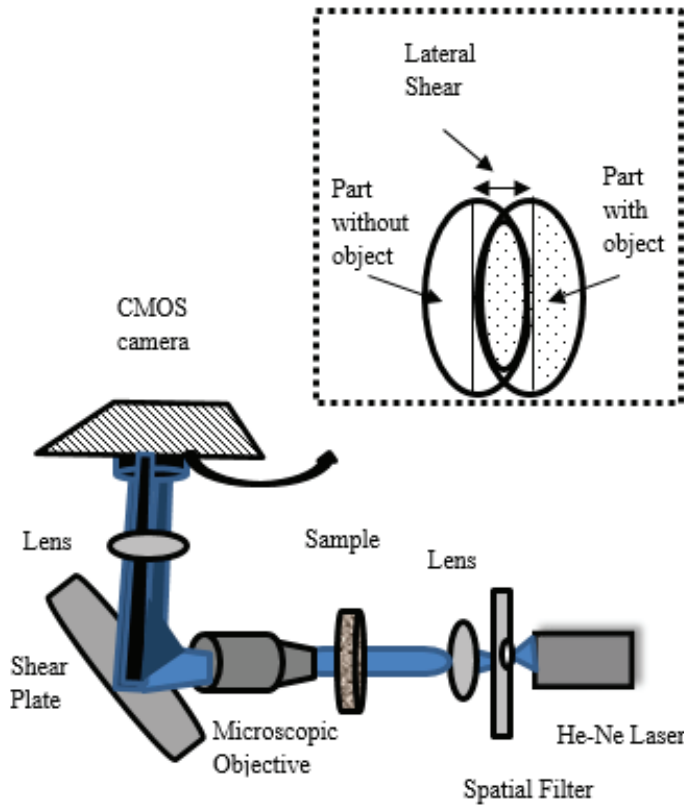


Figure 7. Configuration of Lateral Shearing Digital Holographic Microscopy

In LSDHM, the laser beam is filtered and collimated by SF and L respectively. Thereafter, the collimated beam is reflected from the front and back surfaces of the shearing plate after passing through the sample (transparent objects or biological microorganisms) and microscopic lens with 6X magnification. The plate thickness causes lateral shear and the two beams interfere in the lateral shear zone. To eliminate the twin image problem that occurs in optical configurations, second lens is used. To eliminate the duplicate image problem that occurs due to overlapping the object information, the second lens is placed between the shear plate and imaging sensor (CMOS camera). The angle of placed lens is controlled and oriented to alleviate the overlapping (Seo et al. 2014). In addi-

tion, the size of magnified samples are chosen small, where the lateral shear is big. Hence, the sample and its second copies are not overlapped. In final, the interference pattern (hologram) is consituted on imaging sensor (Onur et al., 2021).

The mathematical expression of captured hologram is given in Equation 3 (Yaroslavsky, 2004),

$$I(x, y) = O^2(x, y) + R^2(x, y) + 2OR(\varphi(x, y)) \quad (3)$$

The sheared object has altered and unaltered regions. These regions and the coordinates of the hologram plane are defined as $O(x, y)$, $R(x, y)$ and (x, y) , respectively. In DHM, the object wavefront ($I(x, y)$) includes an intensity and phase informations. It can be possible that, these informations are reconstructed from the complex amplitude of $I(x, y)$. In this work, the Hilbert-Huang Transform (HHT) is used for reconstruction process. (Yaroslavsky, 2004). The phase information is obtained from recorded hologram by using HHT in reconstrcution process. Equation 4 defines the phase information of HHT .

$$\varphi(x, y) = \tan^{-1} \left(\frac{\text{Im}(HHT(x))}{\text{Re}(HHT(x))} \right) \quad (4)$$

where, Im is the imaginer part and Re is te real parts of HHT. The purpose of using Hilbert transform in this study is to remove the redundancies in symmetry of real-valued signals in traditional Fourier transform used in reconstruction process. In other words, it directly eliminates the negative frequency components with HHT (Medoued et al., 2013).

THE APPLICATIONS of IMAGE FORMATION by USING OPTICAL HOLOGRAPHY

Digital holographic microscopy is preferred for various applications such as cancer cell detection, characterization of small lesions, disease identification and etc. In the field of medicine. There have been many researches related to DHM imaging in the current literature. For instance, the cancer cell morphology is examined with DHM in combination of machine learning algorithm (Lam et al., 2018). The cancer detection is also studied by El Schich et al., with using DHM (El-Schich et al. 2018). On the other hand, biological cells are visualized by Ziemczonok et al., with Mach-Zehnder digital holographic microscope (Ziemczonok et al. 2019). In addition, the phantom mimicking samples are visualized by Onur et al., via LSDHM system (Onur et al., 2021).

Studies with phantom mimicking tissue samples aforementioned in the case studies given above have recently found a wide range of applications as they are used in the diagnosis of diseases without contacting humans. In this study, various applications to image the vein or cystic masses have been performed to show that the LSDHM system can be an alternative to ultrasonic imaging in the cases where contact is not desired. The simulations are performed on Matlab 2018(b) program and we captured different samples with LSDHM system. In Figure 8, the samples of created phantom models are presented.

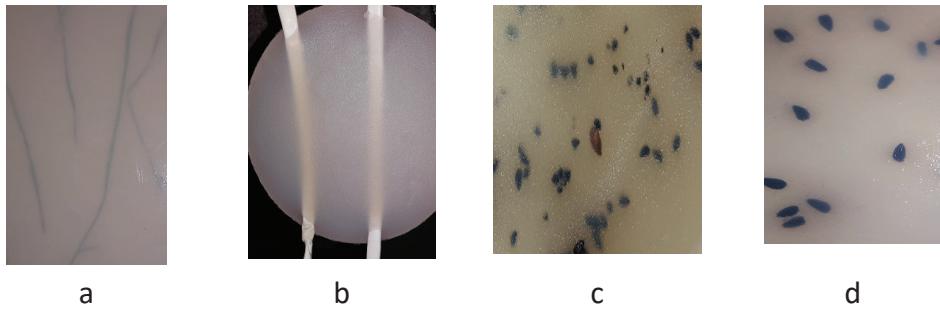


Figure 8. Created Phantom Models With a) Grass b) Balloons, c) Broken Black Cumin d) Black Cumin

The used phantom models are created with a mixture of agar powder and distilled water. While preparing the phantom models, a homogeneous mixture was obtained by continuously mixing distilled water with a certain degree of boiling water and agar. Then, some agar mixture was poured into the mold and the materials used were placed on it. Then the material surfaces were covered with the agar mixture again. To prevent the formation of air bubbles during the formation of the phantoms, the mixture was obtained by continuous mixing. Because the air bubbles that form in the medium will cause deterioration of the image quality to be obtained. At first stage, the grass is used in the generated mixture to create a representative vascular structure. It is shown in Figure 8a. The aim here is to visualize the thin veins that are not obvious and can hardly be located with the proposed system. Secondly, transparent and thin tube type balloons, which are filled with water, are used in the generated mixtures to see the full vascular structure. These balloons are considered to represent the human vein and vein in soft tissue-mimicking phantoms are obtained. The created second phantom is given in Figure 8b. In the third stage of the study, phantom tissue model was created to detect the presence of cystic masses using various black cumin seeds. In Figure 8c and Figure 8d show the used broken black cumin (Onur et al., 2021) and black cumin in normal size in created phantom model, respectively.

These samples are recorded with LSDHM system represented in Figure 7. The interference pattern of each created phantoms given in Figure 8 are depicted in Figure 9, respectively. The resolution of the camera

used in the system is adjusted according to the transparency level of the phantom sample to be displayed.

It can be seen from Figure 9a that when the grass is used for mimicking the thin veins, it can be detected easily. On the other hand, in the case of using white colored transparent balloon as shown in Figure 9b, the image is obtained much clearer and vascular structure is much more pronounced. To prove that the proposed system is suitable for imaging artificial tissues, not only tissues representing vascular structures were examined, but also artificial tissues produced for small cystic masses were imaged. In this context, the holographic patterns are captured for soft tissue-mimicking phantom samples obtained with broken black cumin and black cumin in normal size. These images are given in Figure 9c and Figure 9d respectively.

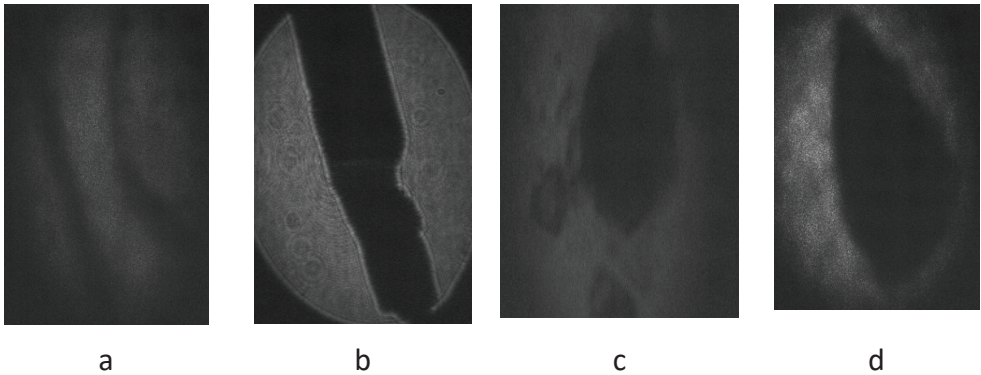


Figure 9. The Interference Pattern of Soft Tissue-Mimicking Phantom Samples a) Obtained with Grass b) Obtained with Balloons, c) Obtained with Broken Black Cumin d) Obtained with Black Cumin

RESULTS and DISCUSSION

In this study, sample applications have been carried out to show that digital holography can be used as an alternative method to ultrasound, which is frequently used in medical imaging. For this purpose, the LS-DHM method, which minimizes the high-cost problem in optical systems and provides high resolution, has been used. It has been observed that cystic masses and vascular structures in phantom models created using black cumin and different types of balloons respectively in the

laboratory environment can be imaged by using the LSDHM method. Thus, the LSDHM method enables the visualization of the veins and detects the vascular structures. On the other hand, small cystic masses can be detected by using LSDHM. This is also an important issue in terms of early diagnosis of small masses and initiating treatment at an early stage. Apart from all these, LSDHM can be used as an alternative for ultrasound imaging in some diagnosing cases since it is also non-invasive. In further researches, the study can be improved by imaging other phantoms that mimic different tissue or organ structures and LSDHM performance can be presented in more detail. In addition, by using the produced phantom structures, it can be ensured to determine which imaging method is more suitable for which depth and medium. In addition, studies will be advanced to produce phantoms with different structures closest to human tissues, easy to use and low cost, to be used in medical imaging applications. In this sense, it will be tried to produce phantoms with long storage times with materials that can be easily used and found by everyone without requiring special attention during construction, and are also chemically harmless and cheap.

REFERENCES

Anand, A., Moon, I., and Javidi, B. (2017). Automated disease identification with 3D optical imaging: a medical diagnostic tool. *Proceedings of IEEE*, 105, 924-946.

Brandner, D.M., Cai, X., Foiret, J., Ferrara, K.W., and Zagar, B.G. (2021). Estimation of tissue attenuation from ultrasonic B-mode images-spectral-log-difference and method-of-moments algorithms compared. *Sensors*, 21, 2548-2567.

Bonnet, N., Bourgoin, L., Biver, E., Douni, E., and Ferrari, S. (2019). RANKL inhibition improves muscle strength and insulin sensitivity and restores bone mass. *Journal of Clinical Investigation.*, 129(8), 3214-3223.

Devinder, S., Lal, A., Dastidar, T.R., and Dubey, S.K. (2019). Quantitative analysis of numerically focused red blood cells using subdivided two-beam interference (STBI) based lateral-shearing digital holographic, arXiv:1909.03454 [eess.IV] (2019).

Di, J., Li, Y., Xie, M., Zhang, J., Ma, C., Xi, T., Li, E., and Zhao, J. (2016). Dual-wavelength common-path digital holographic microscopy for quantitative phase imaging based on lateral shearing interferometry. *Applied Optics*, 55 (26), 7287- 7293.

El-Schich, Z., Mölder, A.L., and Wingren, A.G. (2018). Quantitative phase imaging for label-free analysis of cancer cells-focus on digital holographic microscopy. *Applied Sciences*, 8(7), 1027.

Fish, P. (1991). *Physics and instrumentation of diagnostic medical ultrasound*. Wiley.

He, Z., Wang, P., Liang, Y., Fu, Z., and Ye, X. (2021). Clinically available optical imaging technologies in endoscopic lesion detection: current status and future perspective. *Journal of Healthcare Engineering*, 2021, 7594513.

Hermawati, F.A., and Sugiono, E. (2017). *Ultrasound image formation from Doppler transducer*. In: Parinov I., Chang SH., Jani M. (eds) *Advanced Materials*. Springer Proceedings in Physics, vol 193. Springer, Cham.

Jafari, S.H., Saadatpour, Z., Salmaninejad, A., Momeni, F., Mokhtari, M., Nahand, J.S., Rahmati, M., Mirzaei, H., and Kianmehr, M. (2018). Breast cancer diagnosis: Imaging techniques and biochemical markers. *Journal of Cellular Physiology*, 233(7), 5200-5213.

Jang, J., Yun Bae, C., Park, J.K., and Ye, J.C. (2010). Self-reference quantitative phase microscopy for microfluidic devices. *Optics Letters*, 35(4), 514-516.

Jo, Y., Cho, H., Lee, S.Y., Choi, G., Kim, G., Min, H., and Park, Y. (2019). Quantitative phase imaging and artificial intelligence: a review. *IEEE Journal of Selected Topics in Quantum Electronics*, 25: 1-14.

Kobayashi, K., Yoshida, S., Saijo, Y., and Hozumi, N. (2014). Acoustic impedance microscopy for biological tissue characterization. *Ultrasonics*, 54(7), 1922-1928.

Lam, V.K., Nguyen, T.C., Chung, B.M., Nehmetallah, G., and Raub, C.B. (2018). Quantitative assessment of cancer cell morphology and motility using telecentric digital holographic microscopy and machine learning. *Cytometry A*, 93(3), 334-345.

Li, X., and Min, X. (2020). The role of M-mode echocardiography in patients with heart failure and preserved ejection fraction: A prospective cohort study. *Experimental and Therapeutic Medicine*, 19(3), 1969-1976.

Maini, R., and Aggarwal, H. (2010). A comprehensive review of image enhancement techniques. *Journal of Computing*, 2, 8-13.

Medoued, A., Lebaroud, A. and Sayad, D. (2013). Application of Hilbert transform to fault detection in electric machines. *Advances in Difference Equations*, 2013, 2.

Min, J., Yao, B., Trendafilova, V., Ketelhut, S., Kastl, L., Greve, B., and Kemper, B. (2019). Quantitative phase imaging of cells in a flow cytometry arrangement utilizing Michelson interferometer-based off-axis digital holographic microscopy. *Journal of Biophotonics*, 12, e201900085.

Moniruzzaman M., Shafuzzaman M., and Hossain M.F. (2013, 13-15 February). Brightness preserving Bi-histogram equalization using edge pixels information. International Conference on Electrical Information and Communication Technology (EICT), Khulna, Bangladesh.

Nikolov, S.I., and Jensen, J.A. (2002). Virtual ultrasound sources in high-resolution ultrasound imaging. *Proceedings of SPIE - The International Society for Optical Engineering*, 4687, 395-405.

Nguyen, T., Bui, V., Lam, V., Raub, C.B., Chang, L.C., and Nehmetallah, G. (2017). Automatic phase aberration compensation for digital holographic microscopy based on deep learning background detection. *Optics Express*, 25: 15043–15057.

Onur, T.Ö., and Hacıoğlu, R. (2016, 16-19 May). Image enhancement in ultrasound imaging, 2016 24th Signal Processing and Communication Application Conference (SIU), Zonguldak, Turkey.

Onur, T.Ö., Ustaşaş Kaya, G., and Kaya, C. (2021). Phase shifted.lateral shearing digital holographic microscopy imaging for early diagnosis of cysts in soft tissue.mimicking phantom. *Applied Physics B*, 127, 61-74.

Qian, W., Yang, W., Zhang, Y., Bowen, C.R., and Yang, Y. (2020). Piezoelectric materials for controlling electro-chemical processes. *Nano-Micro Letters*, 12(149), 2-39.

Rivenson, Y., Liu, T., Wei, Z., Yibo Zhang, Y., Haan, K., and Ozcan, A. (2019). PhaseStain: the digital staining of label-free quantitative phase microscopy images using deep learning. *Light: Science & Applications*, 8: 23.

Sassaroli, E., Scorza, A., Crake, C., Sciuto, S.A., and Park, M. (2017). Breast ultrasound technology and performance evaluation of ultrasound equipment: B-mode. *IEEE Transactions on Ultrasonics, Ferroelectrics and Frequency Control*, 64, 192– 205.

Singh, A.S.G., Anand, A., Leitgeb, R.A., and Javidi, B. (2012). Lateral shearing digital holographic imaging of small biological specimens. *Optics Express*, 20(1), 23617-23622.

Seo, K.B., Kim, B.M., and Kim, E.S. (2014). Digital holographic microscopy based on modified lateral shearing interferometer for three-dimensional visual inspection of nanoscale defects on transparent objects. *Nanoscale Research Letters*, 9, 471.

Szabo, T.L. (2014). *Diagnostic ultrasound imaging: inside out*. New York City, NY: Elsevier Inc., 519– 537.

Ustabaş Kaya, G., and Saraç, Z. (2019). Crack detection by optical voice recorder based on digital holography. *Photonic Sensors*, 9(4), 327-336.

Vora, P., Trivedi, V., Mahajan, S., Patel, N., Joglekar, M., Chhaniwal, V., Moradi, A.R., Javidi, B., and Anand, A. (2017). Wide field of view common-path lateral shearing digital holographic interference microscope. *Journal of Biomedical Optics*, 22(126001), 1-11.

Ward, B., Baker, A.C., and Humphrey, V.F. (1997). Nonlinear propagation applied to the improvement of resolution in diagnostic medical ultrasound. *Journal of the Acoustical Society of America*, 101, 143– 154.

Yaroslavsky, L. (2004). *Digital holography and digital signal processing: principles, methods, algorithms*. Kluwer Academic Publishers Group, MA, USA.

Ziemczonok, M., A. Kuś, A., Wasylczyk, P., and Kujawińska, M. (2019). 3D-printed biological cell phantom for testing 3D quantitative phase imaging systems. *Scientific Reports*, 9(1), 1–9.

NOISE MEASUREMENT RESULTS IN WOOD PANEL MANUFACTURING WORKPLACE

Zehra Gülten YALÇIN¹, Mustafa DAĞ², Ercan AYDOĞMUŞ³

Abstract: In this study, noise exposure and ambient noise measurement studies were carried out in accordance with the Occupational Health and Safety Law No. 6331 in a workplace where wood panels are produced. This workplace is included in the dangerous workplace class defined as 16.21.01 Production of veneer plates, plates, etc. Made of wood, bamboo and other woody materials (in leaf form, not pressed) in working class) according to the NACE Rev.2_Six Code. With this study, measurements were taken during the 8-hour daily period and the results of the working environment measurement results, temperature, humidity, pressure measurement results and the noise results of the working environment during the production phase were calculated. In accordance with the relevant legislation, the lowest exposure effective limit value and the highest exposure effective limit value were calculated for the solution of risk factors that cause health problems, and it was seen that personal protective ear should be worn by the employees.

Keywords: Occupational Health and Safety Law No. 6331, Risk Analysis-Factors, Hazard Classes, Noise Measurement Studies

-
- 1 Çankırı Karatekin University, Faculty of Engineering, Department of Chemical Engineering, Uluyazı Campus Çankırı / Turkey, zaltin@karatekin.edu.tr, Orcid No: 0000-0001-5460-289X
 - 2 Çankırı Karatekin University, Faculty of Engineering, Department of Chemical Engineering, Uluyazı Campus Çankırı / Turkey, mudag@karatekin.edu.tr, Orcid No: 0000-0001-9540-3475
 - 3 Elazığ Fırat University, Faculty of Engineering, Department of Chemical Engineering, Elazığ / Turkey, ercanaydogmus@firat.edu.tr, Orcid No: 0000-0002-1643-248

INTRODUCTION

Occupational Health and Safety

The definitions of the International Labor Organization (ILO) and the World Health Organization regarding Occupational Health and Safety are as follows;

“Occupational Health is a branch of science that aims to maximize and maintain the physical, mental and social well-being of employees in every profession, to prevent harm to their health, to place the worker in jobs that are suitable for their physiological and psychological abilities, and thus to adapt the job to the person and the person to the job” (ILO). “Health is a state of complete well-being in physical, spiritual and social aspects” (WHO).

Occupational safety refers to the complete set of technical rules for obligations imposed to reduce the hazards faced by employees at work and in the workplace if it is not possible to eliminate them. Occupational safety mostly aims to eliminate the risks to the life and body integrity of the employee. Based on these definitions, it seems that occupational health and safety are actually complementary concepts. Improvements in the field of health will improve the overall situation of employees and isolate threats, while improving occupational safety will obviously prevent occupational accidents and occupational diseases and thus contribute to occupational health. Historically, it is seen that the history of occupational health and safety concepts emerged in the years following the industrial revolution. While this revolution brought about socio-economic changes, it also led to an increase in occupational accidents and occupational diseases.⁴ Systematic and scientific studies conducted in order to protect against situations that may harm health caused by various reasons in any workplace are explained by the concept of “Occupational Health and safety” and three main goals are defined with it. Protecting Employees; Occupational health and safety is the main purpose of the studies. It aims to protect the existing and employees in the working environment from negative effects and protect them from

4 İş Sağlığı ve Güvenliği, Yönetim Sistemleri ve Risk Değerlendirme Metodolojileri Ö Özkılıç- TİSK Yayınları, Ankara, 2005.

accidents and occupational diseases in a comfortable and safe environment, and to ensure mental and physical integrity. Ensuring production safety; ensuring production safety at work by protecting the employee at work, it will reduce the labor force and working day losses caused by occupational diseases and accidents, so production will be protected, with the confidence that a healthier and safer working environment gives to the employee, there will be an increase in work efficiency.

Ensuring business Safety; Business safety is ensured as measures to be taken at work and machine failures that may arise due to work accidents or unsafe and unhealthy working environment will be eliminated, such as explosion and fire situations that may endanger the business.

Although the history of industrialization in our country goes back to old times, the acceleration after the 80s and its efforts to become involved in the international system made it easier for the problems of the employees to come to the agenda.

As a result of the OHS (occupational health and safety) studies that gained momentum in the 21st century, the Ministry of Health, Labor and Employer Unions and trade association, especially the Ministry of Labor and Social Security in Turkey, have become parties to the law. According to the figures of the International Labor Organization (ILO), approximately every year in the world; 2.050.00 people die due to work accidents and occupational diseases, and about 6.000 people die every day due to work accidents and occupational diseases. It is seen from the data obtained that 350.00 people die from work accidents and 1.700.000 people die from occupational diseases in total annually. Every year, 270.000.000 work accidents

occur and 160.000.000 people suffer from occupational diseases. 438.000 workers die each year due to toxic substances, and 10% of the skin cancer that occurs in the world is caused by contact with toxic substances in the workplace. It is estimated that 100.000 people die each year due to asbestos.⁵ Below are data on occupational accidents and occupational diseases in Tables 1 and 2.

⁵ DR Group/Vital OSGB

Table 1. 2018 and 2019 SSI Work Accidents and Occupational Diseases ⁶

	SGK	
	2018	2019
Number of compulsory insurance holders within the scope of article 4-1/a of Law No. 5510	14.229.170	14.324.000
Work accident	430.985	422.463
Occupational disease	1.044	1.088
Number of deaths as a result of work accidents	1.541	1.149
fatal work accident	9.15	9.97
Number of deaths as a result of occupational disease	0	0

6 <http://www.2dr.com.tr/issagligi> 2020[Erişim Tarihi:20.12.2020]

Table 2. Occupational Accidents and Occupational Diseases in Turkey by Years⁷

Years	Number of Occupational Accidents	Number of Occupational Diseases	Number of Occupational Accident Deaths	Number of Deaths as a result of Occupational Disease	Total Number of Deaths as a result of Work Accident and Occupational Disease
2000	74.847	803	731	6	737
2001	72.367	883	1.002	6	1.008
2002	72.344	601	872	6	878
2003	76.668	440	810	1	811
2004	83.830	384	841	2	843
2005	73.923	519	1.072	24	1.096
2006	79.027	574	1.592	9	1.601
2007	80.602	1.208	1.043	1	1.044
2008	72.963	539	865	1	866
2009	64.316	429	1.171	0	1.171
2010	62.903	533	1.144	1	1.454
2011	69.227	638	1.563	10	1.573
2012	74.871	395	744	1	745
2013	191.389	371	1.360	3	1.363
2014	221.366	4944	1.626	29	1.886
2015	241.547	510	1.252	13	1.265
2016	286.068	597	1.405	0	1.405
2017	359.653	691	1.633	0	1.633
2018	430.985	1.044	1.541	0	1.541
2019	422.463	1.088	1.149	0	1.149

7 http://www.sgk.gov.tr/wps/portal/sgk/tr/kurumsal/istatistik/sgk_istatistik_yilliklari

Historical Development of Occupational Health and Safety in Turkey

The first studies on Occupational Health and safety in Turkey were carried out before the establishment of the Republic in 1921. In order to ensure uninterrupted maintenance of coal production, the necessary regulations have been made in Zonguldak and Ereğli coal enterprises in order to regulate the working conditions of the employees here. New regulations and laws numbered 114 and 151 were made to improve working conditions for those working in coal enterprises. Many problems have been encountered in working conditions with the developing industrialization. For this reason, many laws, statutes and regulations related to worker health and Occupational Safety were composed during the Republic period. The first legal regulation was arranged as the Week Holiday Law No. 394, dated January 2, 1924. With the legal regulation, it is observed that the first positive studies were carried out in the field of worker health and safety in the history of the Republic. However, with Article 332 of the debt Law, which came into force in 1926, it is seen that all employees involved in the employer's working life have the responsibility to organize and implement their work in a healthy and safe environment (Akbulut, 2015).

The Public Health Law and the Municipalities Law were put into effect in 1930. It is seen that the Public Health Law No. 1593 covers the first studies which are of great importance even today in terms of worker health and safety. The first foundations of working in a healthy and safe environment have been raised by this law. Articles 173-178 of this law governed the working conditions of children and women in industrial organizations, night services for workers, conditions of employment of pregnant women before and after birth, and the Prohibition of workers in workplaces (Çiçek and Öcal, 2016).

After that, with the Labor Law No. 3008, which entered into force in 1936 and covers many problems of working life, it is worth noting that for the first time in our country, a detailed and systematic regulation on worker health and occupational safety was made. According to the provisions of this law, the establishment of the Ministry of Labour, which

was planned to be established within 1 year, could only take place in 1945. With the first article of the Ministry of Labor Law No. 4841 dated 28 January 1946, social security was among the duties of the Ministry (Altan, 2004).

In 1971, the Labor Law No. 1475 was put into effect. In terms of occupational health and safety, modern and comprehensive regulations have been introduced with the Labor Law No. 1475 and the regulations and regulations issued in accordance with it (Talas, 1992).

Due to the effects of the European Union integration process, the Labour Law No. 4857 was adopted in 2003. Many regulations have been adopted in the field of Occupational Health and safety based on the Labor Law No. 4857 (Gerek, 2008).

Finally, the Occupational Health and Safety Law No. 6331 dated 20.06.2012 was adopted and some articles of Law No. 4857 were repealed within 6 months of the publication of the law (Arıcı, 1999).

Occupational Health and Safety Law No. 6331

The Occupational Health and Safety Law was regulated in Articles 73 to 82 in the Fifth Section of the Labor Law No. 1475, and the sub-regulations were renewed with a number of regulations, especially the Occupational Health and Safety Regulation. In the Labor Law No. 4857, which entered into force on 10 June 2003, this subject was examined under the heading of Occupational Health and Safety and in the Fifth Chapter, in articles 77 to 89, and the sub-regulations were determined by regulations. Due to the fact that this law has some shortcomings in the work of the employee in a healthy and safe working environment, the Occupational Health and safety law 6331 was adopted. The difference between law 4857 and law 6331 is that law 6331 contains a proactive approach. In other words, it is based on determining the possible risks in advance and taking precautions before the danger occurs at work.

The law was accepted by the Turkish Grand National Assembly on 20 June 2012 and was published in the Official Gazette dated 30 June 2012, but entered into force on 30 December 2012. As of the same date,

the articles and provisions of the Labor Law No. 4857 regarding occupational health and safety were repealed.

With the Law No. 6331; It has regulated the duties, authorities, responsibilities, rights and obligations of employers and employees in order to ensure occupational health and safety at workplaces and to improve existing health and safety conditions. Law; Apart from the exceptions specified in article 2, regardless of their field of activity; It covers all jobs and workplaces belonging to the public and private sectors, employers and employer representatives of these workplaces, all employees including apprentices and interns.

One of the most important innovations brought by this law is the obligation to make/have risk analysis and assessment, and the other is the obligation to employ/assign occupational physicians and occupational safety specialists in all workplaces. The law introduced a six-fold NACE coding for workplaces, and within this framework, workplaces were classified as less dangerous, dangerous and very dangerous. In public workplaces and private sector workplaces with less than 50 employees and in the hazardous class, the obligation to employ/assign an occupational physician and occupational safety specialist started on 1 June 2016. With this law, the amount of administrative fines has also been increased and a high amount of administrative fines has been foreseen (Çiçek ve Öçal, 2016).

Workplace Hazard Classes

Based on the 9th article of the Occupational Health and Safety Law No. 6331, the “Workplace Hazard Classes Communiqué on Occupational Health and Safety” issued by the Ministry of Labor and Social Security by being published in the Official Gazette dated 26.12.2012 and numbered 28509; According to the first article; In accordance with Article 9 of the Occupational Health and Safety Law dated 20.6.2012 and numbered 6331, the hazard classes in which the workplaces take place in terms of occupational health and safety are specified in the Workplace Hazard Classes List attached to the Workplace Hazard Classes Communiqué on Occupational Health and Safety.

According to the second article;

1. The hazard class of the main work carried out in a workplace is taken into account in the determination of the hazard class.

2. The employer shall notify the Ministry of Labour and Social Security of the actual change of business activity within one month at the latest.

3. In case of hesitation in determining the main work, the purpose of the establishment of the workplace is taken into consideration.

If more than one activity is carried out in the workplace in accordance with the main work description, the job with a higher hazard class is taken as the basis. In case the field of activity is expanded in addition to or as a continuation of the main work performed in the workplaces included in the workplace definition of the Law No. 6331, this workplace is determined in accordance with the rule based on this paragraph.

In order to determine the hazard class of the workplace from the list in the annex of the "Communiqué on Workplace Hazard Classes on Occupational Health and Safety", it is necessary to first know the "NACE" code of the workplace.

Workplace Hazard class is determined by the "NACE" code. The Statistical Classification of Economic Activities in the European Community (NACE); It is a reference source for the producing and disseminating of statistics on economic activity in Europe. In Nace coding, workplace/enterprises are given a six-digit code according to their field of activity topics. As part of the European Union alignment studies carried out in many areas in our country, the application of the NACE code has also begun to be used.

NACE Code consists of 3, 4, 5, 6 and 7 digits starting from the 2nd digit (after) of the workplace SSI registration number. So it will be a 6 digit code (Gerek, 2008) (Table 3).

Table 3. NACE Code Determination Criteria (Çiçek ve Öçal, 2016)

SSI REGISTRY NUMBER			A-BCDE-FGHI-JKLMNOÖ-041-PR-SŞ/TUV					
SSI expansion	A	BCDE	FGHI	JKLMNOÖ	041	PR	SŞ	TUV
Digit	1 Digit	4 Digit	4 Digit	7 Digit	3 Digit	2 Digit	2 Digit	3 Digit
codes	Content Code	Line Of Business Code (Nace Code)	Unit Code	Workplace No	City Code	County Code	Control Code	Agent code components

For Example;

Let the SSI registration number of the workplace studied be 242110202001260000602-58. This workplace includes the numbers starting from the 2nd digit from the left to the 7th digit of the SGK registration number. The NACE code, which determines the hazard class of the workplace, is the 6-digit number 421102. The following result will be obtained when searched by typing 42.11.02 from the list in ANNEX-1 in the “Communiqué on Workplace Hazard Classes on Occupational Health and Safety”.

According to NACE code 42.11.02 “Asphalt and repair of road surfaces, pavement, bumps, bicycle paths, etc. construction of roads, roads, etc. road, tunnel, etc., such as marking surfaces with paint, road barrier, installation of traffic signs and plates, etc. If working with “surface works in places”, the workplace is in the “very dangerous” workplace class (Kırtaş ve Altundağ, 2019)

Risk Analysis and Evaluation

According to article 4 of the Occupational Health and Safety Law No. 6331, the risk assessment is expressed as follows: determining the dangers that exist in the workplace or that may come from outside, analyzing and rating the factors that cause these hazards to become risks and the risks arising from the hazards, and to be done in order to decide on control measures. In addition, according to Article 10 of the Occupational Health and Safety Law No. 6331, employers are obliged to make or have a risk assessment done in terms of occupational health and safety.

In this direction, the methods and principles of risk assessment studies are specified in the Occupational Health and Safety Risk Assessment Regulation, which was published in the Official Gazette dated 29.12.2012 and numbered 28512.

In accordance with the Occupational Health and Safety Risk Assessment Regulation by the relevant organizations, the following stages are followed in the risk assessment work to be carried out in the companies. Risk assessment studies are carried out together with the risk assessment team formed in accordance with the provisions of the regulation. Risk assessment steps consist of 4 steps. These; (Çiçek, 2016).

Hazard identification

- a) Determination and analysis of risks
- b) Risk control steps
- c) Documentation

Hazard Identification

When identifying hazards, the following information is collected as a minimum according to the work environment, employees and their interest in the workplace.

- a. Workplace building and add-ons.
- b. Business and operations with activities carried out in the workplace.
- c. Production process and techniques.
- d. Business equipment.
- e. Substances used.
- f. Processes related to residual and waste.
- g. Organization and hierarchical structure, duties, powers and responsibilities.
- h. Experience and thoughts of employees.
- i. Work permit documents to be obtained in accordance with the relevant legislation before starting work.
- j. Health surveillance records with employee training, age, gender and similar characteristics.

- k. Status of women employees with groups requiring special policies, such as young, old, disabled, pregnant or lactating employees.
- l. Workplace inspection results.
- m. Occupational disease records.
- n. Occupational accident records.
- o. Records of events that occurred in the workplace, but did not cause injury or death, but led to damage to the workplace or work equipment.
- p. Near miss event records.
- q. Material safety data sheets.
- r. Environmental and personal exposure level measurement results.
- s. Previously conducted risk assessment studies, if any.
- t. Emergency action plan.
- u. Documents that must be prepared in certain workplaces, such as a health and safety plan and an explosion Protection document.

When collecting information about hazards, occupational accidents and occupational diseases that occur in similar workplaces that produce with the same production, methods and techniques are also evaluated.

In the light of the information collected; also take into consideration the provisions of the legislation on occupational health and safety in the working environment physical, chemical, biological, psychosocial, ergonomic, and so sources of danger or the hazards that may arise as a result of their interaction is determined and recorded.⁸

Risk Identification and Analysis

By taking into account each of the identified hazards separately, it is determined how often the risks that may arise from these hazards may occur, and who, what, in what way and in what severity may be harmed

⁸ <https://www.isvesosyalguvenlik.com/is-sagligi-ve-guvenligi-kanunu/>

by these risks. The impact of existing control measures is also taken into account when making this determination.

The risks identified in the light of the information and data collected; it is analyzed by using factors such as the characteristics of the enterprise's activity, the nature of hazards or risks in the workplace and the constraints of the workplace or by using a combination of one or more methods selected on the basis of national or international standards. If the analysis is performed for separate sections, taking into account the interactions of the sections are considered and concluded as a whole. The risks analyzed are sorted and written, starting with the one with the highest risk level according to the size and importance of their effects, so that control measures are decided (Küçükoğlu, 2020).

Risk Control Steps

The following steps are applied to control risks.

- **Planning:** A planning is carried out in order to control the risks that are analyzed and sorted according to the size and importance of their effects.
- **Decision on risk control measures:** The following steps are applied in order to completely eliminate the risk, and if this is not possible, to reduce the risk to an acceptable level.
- **Replacing the dangerous with the non-dangerous or less dangerous.**
- **Elimination of hazard or hazard sources.**
- **struggle with risks at source.**
- **Implementation of risk control measures:** plans are prepared that include the work and transaction steps of the agreed measures, the person or workplace section that will perform the transaction, the person or workplace section responsible, the start and end date, and similar information. These plans are put into practice by the employer.
- **Monitoring of applications:** the implementation steps of the prepared plans are regularly monitored and inspected, and neces-

sary corrective and preventive actions are completed by identifying the conflicting directions.

In the implementation of Risk control steps, it is ensured that collective protection measures are given priority according to personal protection measures and that the measures to be applied do not cause new risks (Arpat ve Özkan, 2018).

Documentation

- Risk assessment is documented to cover the following minimum considerations. Business title, address and employer's name. The names and titles of the people who perform them, as well as the document information provided by the Ministry of those who have an occupational safety specialist and a workplace doctor. Date performed and effective date. The name of each, if the risk assessment was conducted separately for different departments in the workplace. Identified sources of danger and hazards. Identified risks. The method or methods used in risk analysis. Analysis results, including the order of importance and priority of the identified risks. Corrective and preventive control measures, the dates of their execution and the level of risk determined thereafter.

The risk assessment is carried out by a team formed by the employer. The risk assessment team consists of the following.

- Employer or employer's representative.
- Occupational safety specialists and occupational physicians who carry out health and safety services in the workplace.
- Employee representatives in the workplace.
- Support staff in the workplace.
- Employees who are identified to represent all units in the workplace and have knowledge of the work carried out in the workplace, current or possible sources of danger and risks.

The employer may receive services from persons and organizations outside the workplace to support this team when necessary.

Coordination of risk assessment work can also be provided by the employer or a person appointed by the employer from within the team. The employer meets all the necessary needs such as tools, equipment,

space and time for the person or persons assigned in risk assessment work to fulfill their duties, and cannot restrict their rights and authorities due to their duties. The person or persons assigned to risk assessment studies protect and keep confidential the information and documents provided by the employer.

According to the hazard class, the risk assessment is renewed every two, four and six years at the latest, respectively, in very dangerous, dangerous and less dangerous workplaces.

The risk assessment is fully or partially renewed, taking into account that new risks that may arise in the following cases affect all or part of the workplace.

- Moving the workplace or making changes to buildings.
- Changes in the technology, materials and equipment used in the workplace.
- Changes in production method.
- Accident at work, occupational disease or near miss.
- A change in legislation regarding the boundary values of the working environment.
- Requirement according to work environment measurement and health surveillance results.
- The emergence of a new danger arising from outside the workplace that may affect the workplace.

In order to fulfill the control measures determined as a result of the Risk assessment, an implementation plan must be made in which the necessary resources are specified by the responsible person. It is also of great importance to determine deficiencies and inadequacies by following the implementation plan. Each page of the report prepared by the Risk assessment team must be initialed and the last page must be signed by the team members.⁹

⁹ <https://www.resmigazete.gov.tr/eskiler/2012/06/20120630-1.htm>

Occupational Hygiene

Occupational hygiene can be defined as identifying physical, chemical and biological factors that may negatively affect employee health, evaluating and controlling their effects. Even AIHA (American Industrial Hygiene Association) defined the concept of occupational hygiene as “occupational hygiene is the science and art that detects, evaluates and controls environmental factors, stresses that occur in workplaces and cause illness, deterioration of Health and anxiety in industrial society.”

For this reason, protecting the health and well-being of the working population is of great importance in terms of increasing work efficiency and contributing to the social security system by reducing treatment costs. The field of occupational hygiene includes the determination of the physical, chemical and biological factors mentioned above by measurement tests and analyses and the evaluation of their health effects and the design and application of the necessary measures (Çavuş, 2015).

The regulation on “Laboratories Performing Occupational Hygiene Measurement, Test and Analysis” was published by the Ministry of Labor and Social Security on 20.08.2013. This regulation regulates the subject of measurement testing and analysis and sets out the procedures and principles for authorizing laboratories that will conduct occupational hygiene measurement testing and analysis. Again, in accordance with this regulation occupational hygiene measurement, testing and analysis, “in the working environment, the health of the employees, which may adversely affect any noise, vibration, lighting, non-ionizing radiation, such as physical and dust, gas, chemical and Steam, such as viruses, bacteria, fungi biological factors such as qualitative and quantitative determination to be made” defines.¹⁰

Occupational Hygiene measurement parameters and selection of parameters

Risk factors that can be evaluated by measurement are grouped in the form of physical, chemical and biological factors. Parameters such as

¹⁰<http://pastelosg.com/assets/files/isg-risk-degerlendirme.pdf>

noise, vibration, lighting, thermal comfort, dust are evaluated physically while, parameters such as volatile organic compounds, acid vapors are evaluated chemically. Biological factors, on the other hand, are microorganisms that cause diseases, such as infection or an outbreak of disease. The parameters that must be measured according to the line of work studied differ. Even between departments in the same workplace, measurement parameters may be different from each other. This is due to the fact that the processes in the relevant departments are different, and therefore the emergence of different factors that will threaten human health during the relevant processes.

Table 4. Some Occupational Hygiene Parameters and Standards¹¹

EXPERIMENTAL AREA	EXPERIMENT NAME	EXPERIMENT METHOD
OCCUPATIONAL HYGIENE-NOISE	Measuring the level of noise that people are exposed to and detecting hearing loss	TS 2607 ISO 1999
	Description, measurement and evaluation of acoustic-environmental noise	TS EN ISO 1996-2
	Acoustics-noise emitted from machinery and equipment - Determination of emission sound pressure levels at a workstation and other specified locations with similar environmental Corrections applied	TS EN ISO 11202

¹¹<https://www.resmigazete.gov.tr/eskiler/2013/08/20130820-3.htm>

OCCUPATIONAL HYGIENE-VIBRATION	Determination of vibration emission value by experimenting with moving machines	TS EN 1032+A1
	Measurement and evaluation of hand-transmitted vibration that people are exposed to	TS EN ISO 5349-1 TS EN ISO 5349-2
OCCUPATIONAL HYGIENE-LIGHTING	Measurement of lighting/light intensity level in workplaces	COHSR-928-1-IPG-039
OCCUPATIONAL HYGIENE-THERMAL COMFORT	Heat oppression of employee according to WBGT (age-Hopper sphere Temperature) Index for hot environments and determination of thermal comfort conditions according to PMV-PPD indices	TS EN ISO 7730 TS EN 7243
	Determination of PMV and PPD Indices for Moderate Thermal Environments, Determination of Conditions for Thermal Comfort	TS EN ISO 7730
OCCUPATIONAL HYGIENE - DUST MEASUREMENT	Determination of Total and Respirable Dust Sampling: Sampling the filter with the pump Analysis: Gravimetric	HSE MDHS 14/3
	Determination of Total, Respirable and Thoracic Aerosols Sampling: Taking samples to the filter by pump Measurement: Gravimetric	HSE / MDHS 14/4

NOISE MEASUREMENT RESULTS IN WOOD PANEL MANUFACTURING WORKPLACE

OCCUPATIONAL HYGIENE-INSTANT GAS MEASUREMENT

Determination of Carbon Monoxide (CO)
Sampling and Measurement: Electrochemical Cell Method

NIOSH-NMAM 6604

Determination of Oxygen (O₂)
Sampling and Measurement: Electrochemical Cell Method

NIOSH-NMAM 6601

OCCUPATIONAL HYGIENE-INSTANT GAS MEASUREMENT WITH DETECTOR TUBE

Determination of Toxic Gas or Vapor Concentrations (Acetic Acid, Ammonia, Benzene, Carbon Dioxide, Carbon Monoxide, Ethyl alcohol(ethanol), Ethylene Oxide, Formaldehyde, Hydrogen, Hydrogen Chloride, Hydrogen Cyanide, Hydrogen Fluoride, Hydrogen Sulphide, Nitric Acid Vapour, Nitrogen Oxides, Ozone, Phenol, Sulfur Dioxide, Sulfuric Acid, Oil Mist)
Sampling and measurement: instantaneous measurement with detector tube

ASTM D 4490-96

DETERMINATION OF TIRE STEAM AND TIRE DUST

Determination of Tire Vapor and Tire Dust

MDHS 47/2

ACOUSTIC-NOI- SE	Detection of Sound Power Level (ΔL_s , ΔL_F , ΔL_M , ΔL_α , L_{pA} , L_w) from Sound Pressure Level Measurements in Industrial Facilities with Multiple Noise Sources	TS ISO 8297
	Determination of Sound Power Level (L_{peq} , T , ΔL_s , K_1 , K_2 , L_{pf} , LW) from Sound Pressure Level Measurements from Noise Sources Using the Observation Method	TS EN ISO 3746
	Detection of Noise Reduction Factors (f , L_f , L_fT) when Spreading Sound in Open Areas in Residential Areas	TS ISO 9613-1
	Reduction of sound when spreading outside Part 2: General calculation method	TS ISO 9613-2
	Detection of Environmental Noise Level (L_{aeq} , L_{aeqt} , L_{regt} , L_{day} , L_e , $L_{evening}$, L_{AFNT} , L_E , L_{afmax} , L_{cenmax} , L_{rden} , L_{rden})	TS 9315 ISO 1996-1 ve TS 9315 ISO 1996-1/T1 TS ISO 1996-2 ve TS ISO 1996-2/T1

Measurement parameters should be selected by trained and experienced specialists. Because if the parameters are selected incomplete or incorrectly, they will be evaluated differently than the corresponding environment, and the results will be misleading. When the working environment is a sand quarry, dust harmful to health will be effective, and measurement and evaluation will be necessary for health during the working period. Here, only personal dust measurement and comparison with the limit value will not indicate that the environment is suitable for health. Dust can be consist of many different elements or compounds. Knowing what the dust content is of great importance that is both as a

measurement method and measurement method and for evaluation. Because the measurement methods and limit values vary depending on the content of the dust. At this point, the parameter that should be understood well is inert dust. Personal respirable or total dust measurements only evaluate inert dusts. Inert dusts are generally dusts containing a very low amount (less than 1%) of silica and having small and curable effects when it reaches the lungs. But some health problems arise when it comes to exposure to high concentrations of these dusts. For this reason, although the silica content is low, separate limit values have been determined for dusts that threaten health due to other elements or compounds contained in them. These dusts and their limit values are specified in the annex of the Dust Control Regulation.

If a more practical and understandable definition for inert dust is required, all dusts that do not have a limit value in the corresponding annex are inert dust. For this reason, it is not correct to measure and evaluate the dust in every environment as inert dust. It is necessary to act according to the content of the dust. Therefore, it will only be possible to make personal dust measurement for employees at the sand quarry by evaluating inert dust there. But since the content of the dust there will contain a high percentage of silica, the main parameter we need to measure should be silica dust. The measurement method and limit value of silica dust are different from that of inert dust. Therefore, it would be wrong to measure personal dust in the sand quarry.¹²

Repetition Period of Occupational Hygiene Measurements

The following statement is included in the second paragraph of Article 5 of the Regulation on Laboratories Performing Occupational Hygiene Measurement, Testing and Analysis regarding the repetition period of Occupational Hygiene measurements; The employer performs occupational hygiene measurements, tests and analyzes depending on the risk assessment. When personal exposures as a result of the workplace environment or work also differ, occupational hygiene measurements,

¹²<http://haberisg.com/gundem/is-hijyeni-olcumleri-neden-yapilir/>

tests and analyzes are repeated if the workplace physician or occupational safety specialist deems it necessary.

From this statement it becomes clear that the measurements should be repeated if the risks in the working environment change qualitatively or quantitatively. In other words, new measurements should be made if the amount of use of the pollutant source in the workplace environment increases or a new that previously undefined pollutant enters the relevant environment. This approach is correct if the environmental conditions change, but it remains incomplete if they do not change. In cases where the environmental conditions have not changed, the TS EN 689 standard, which the regulation requires to be taken into account, takes a measurement-based approach to the issue. In the appendix "F" of the relevant standard, a method is proposed to determine the measurement period as follows. According to the corresponding method, the measurement results made are: If the measurement result does not exceed 1/4 of the relevant limit value, 64 weeks, If the measurement result exceeds 1/4 of the relevant limit value and is below 1/2, 32 weeks, If the measurement result exceeds 1/2 of the relevant limit value and falls below the limit value, the measurements should be repeated every 16 weeks.

As a result, according to International Labour Organization (ILO) data, 160,000,000 people suffer from occupational diseases per year and 6,000 people die from occupational diseases per day. All institutions, from the smallest to the largest, should not ignore the occupational hygiene measures, which are the most important pillars of the concept of occupational hygiene, in order not to cause more material and moral losses due to all preventable occupational diseases. It should always be known that the time, labor and capital that will be spent on occupational hygiene measurements will be much less than the negative situations and consequences that occur when the requirements are not met.¹³¹⁴

13<https://www.resmigazete.gov.tr/eskiler/2013/08/20130820-3.htm>

14<https://www.resmigazete.gov.tr/eskiler/2017/01/20170124-6.htm>

Occupational Hygiene Noise Measurement

Noise is defined as “unwanted sound” that causes discomfort and makes you restless. Sound, on the other hand, is the waves emitted by a substance vibrating in the environment by moving air molecules around it.

The human ear is a highly sensitive organ that begins to detect sound vibrations in the range of 20-20000 Hertz (symbol Hz) or 0-140 decibels (dB) from a pressure level of 20 μ Pa (micropascal). When measuring sound pressure, a logarithmic proportional scale is used that the unit of which is decibels (dB) [12]

In accordance with the Labor Law No. 4857 and the “Regulation on the Protection of Employees from Risks Related to Noise”; The employer is obliged to have noise measurements made in the workplaces in order to diagnose any hearing loss due to noise and to protect the hearing ability of the employees.

- Personal Noise Exposure Measurement is the measurement of personal noise exposure value and reporting of measurement results using a noise measuring device and a microphone (dosimeter) attached to the ear of the worker connected to the device (Figure 1).

- Ambient Noise Measurement is the reporting of measurement results by keeping a certain period of time in the environment with a noise measuring device (Figure 1).



Figure 1. Ambient Noise Dosimeter (a-b), Personal Noise Dosimeter Used in Noise Measurement (Svantek-c)

Noise levels of workplaces or working areas of factories are measured in accordance with the legislation. A noise map is prepared by showing the points where ambient noise is measured in the workplace layout plan and coloring the measured values.¹⁵

Noise Measurement

Before starting the noise measurement, information is collected about the noise source to be measured and the environment exposed to noise. A planning is made on how long the noise will be evaluated. Pre-checks are completed by checking noise measuring instruments, equipment and hardware, calibrating the device. In order to get the correct result with high accuracy and compare it with previous measurements, it is necessary to calibrate the measuring device (microphone).

After all the preparations are completed by the specialist who will carry out the noise measurement, the noise measurement process is started. When choosing a measurement point, the point at which the highest noise level in the environment is measured is selected. When measuring, situations such as rain, wind or loud music coming from the outside environment that will affect the measurement are taken into account. In noise measurements, some parameters that are equivalent in noise regulation are used. These parameters are as follows:

Equivalent Noise Level [Leq, Leq (T), Leq, LAeqT]

- Sound Impact Level (FLOOD, LE)
- The highest volume (Lmax)
- Lowest volume (Min)
- The highest peak value (MaxP, Peak), Instant volume (SPL)

The measurement values recorded after the noise measurements made for occupational health and safety are prepared by the Occupational Safety Specialist as a noise measurement report.¹⁶

¹⁵<https://www.resmigazete.gov.tr/eskiler/2013/08/20130820-3.htm>

¹⁶https://webdosya.csb.gov.tr/db/cygm/editordosya/Agac_Agac_urunleri_ve_Mobilya_imalati_Kilavuzu.pdf

Duration of Noise Measurement

The purpose of noise measurement is to protect human health and to provide a safe working environment in workplaces. In the following cases, the noise measurement is repeated.

- In cases where the relevant risk factor is found as a result of the risk assessment,
- In cases where occupational disease occurs,
- In cases where the employee uses the workplace environment or the working environment machine equipment changes,
- Increase in the noise source.

Measurements that are not performed in accordance with the correct technical and noise regulations will make the noise measurement report worthless.

Noise Exposure Limit Value

In the “Regulation on the Protection of Employees from Noise-Related Risks”, exposure action values and exposure limit values are given below:

- Lowest exposure action values: (LEX, 8h) = 80 dB(A) or peak (P_{peak}) = 112 Pa [135 dB(C)]
- Peak exposure action values: (LEX, 8 hours) = 85 dB(A) or peak (P_{peak}) = 140 Pa [137 dB(C)]
- Exposure limit values: (LEX, hour) = 87 dB(A) or peak (P_{peak}) = 200 Pa [140 dB(C)]

When applying exposure limit values, the protective effect of personal ear protective equipment used by the employee is also taken into account when determining the exposure of employees. The effect of ear protectors is not taken into account in the exposure action values.

Daily noise exposure can be detected vary significantly from day to day with the certainty that if the exposure limit values exposure action value in the implementation of daily noise exposure level, instead of weekly noise exposure level can be used.

In these works;

a) The weekly noise exposure level determined by adequate measurement cannot exceed the exposure limit value of 87 dB(A).

b) Appropriate measures are taken to minimize the risks associated with these works.¹⁷

WOOD PRODUCTS

In the forest products industry; bending, splitting, cutting, peeling, mowing, chipping, fibering, gluing, pressing, steaming, drying, impregnating, etc. of wood raw materials production is carried out by processing methods. Wood and wood products are mainly used in two different ways today. The first of these are products made from raw wood, which is the traditional method. The second is wood panel products such as MDF, particle board, particle board (wood products that are divided into fiber and chips and reassembled) made of wood.

Wood Panel Products

Particleboard and Fiberboard Industry

Particle boards are defined as sheets obtained by mixing wood or other woody plant chips with synthetic resin glues and gluing and forming them under certain temperatures and pressures. It is a material that has recently been increasing in use in the furniture industry both in the world and in our country.¹⁸

Fiberboard production is carried out by two methods: dry and wet. While hard board is produced by wet method, both hard (HDF) and medium hard fiber board (MDF) are produced by dry method. The most fundamental difference between these methods is due to the environment in which the fiber draft is formed. In the wet method, this formation is achieved using water, while in dry and semi-dry methods, pneumatic and mechanical methods are used. Due to the fact that the binders

17<https://docplayer.biz.tr/188668625-Ts-2607-iso-1999-standardi-gurultu-maruziyeti-olcumlalimati.html>

18<https://docplayer.biz.tr/9060737-Turk-standardi-turkish-standard.html>

in the wood are sufficient in the wet system, no binder is used. But in dry and semi-dry systems, glue is used as a binding agent.

Melamine Coated Board and Glossy Board Industry

Impregnated paper, melamine coating and glossy board are used as the main raw materials of the industry. Unlike raw wood products here, the impregnation process is applied to wood-looking melamine papers that are glued onto the boards instead of the chips and fiber boards produced. The produced particle board and fiber board do not need impregnation, because they are both heat treated and produced with chemical additives. In the impregnation line, special glue mixtures (prescription) are impregnated into tree-looking papers and dried and stored ready to be glued to chip/fiber board.

Laminate Flooring Industry

Laminate flooring consists of decorative paper with a transparent film layer and a tree pattern at the top, plates such as particle board in the middle and a lining containing melamine at the bottom [29]. In the production of laminate flooring, melamine paper is coated on chip board or fiber board according to the desired parquet pattern, melamine boards are sized to the desired parquet size. Then the channel is drilled into the parquet and packed.

Noise Measurement Studies in the Facility where Wood Panel Production is Made

Indoor Noise Measurements

These measurements with EN ISO 11202 (Acoustics - description of environmental noise, measurement and evaluation) and TS EN ISO 1996-2 (Acoustic - radiated noise from machinery and equipment - a workstation and at other locations with similar environmental corrections applied to the determination of emission sound pressure level specified) were determined on the basis of the standards (Table 5).

Table 5. Indoor Noise Measurement Results

	Measurement Section	1st measurement	2nd measurement	3.measurement	Measurement Time (min.)
1	MDF Press Sizing Front	75.4	76.9	76.8	5
2	MDF Press Line Laying Front	76.1	75.7	75.6	5
3	Impregnation Section Head of Line	70.5	75.7	70.3	5
4	shipment area	70.4	70.6	70.1	5
5	Melamine Section Sheet Feeding	77.6	78.5	78.8	5
6	Melamine Press Packaging Department	74.8	74.7	71.8	5
7	Sanding Line Sheet Feeding	82.0	87.7	87.6	5
	Background	43.7	46.3	41.2	5
8	MSF Press Line Sheet Section	81.4	82.2	82.0	5
9	Impregnation Section End of Line	73.7	73.8	74.5	5
10	Warehouse Department	74.9	74.0	74.3	5
11	Melamine Section Press Control Panel Front	77.6	76.5	78.2	5
12	Melamine Department Quality Control	79.6	82.2	82.2	5
13	Sanding Line Operation Room	80.3	80.7	81.5	5
14	Maintenance Shop Lathe Machine Front	78.4	78.5	81.1	5
15	Compressor Room	88.1	88.6	86.5	5
16	Boiler Control Room	70.6	70.5	70.8	5
17	Fibering Front	80.2	80.6	80.3	5
18	Fiber Operation Room	61.0	60.3	62.3	5
	Background	41.5	47.8	45.7	5

The measurement of the temperature, humidity and pressure values of the experimental points are shown in Table 6. These measurements were made on 20.07.2020 with the Svantek 971 Noise Dosimeter (Device Brand/Model/Serial No. Svantek/SC001/T200001) in accordance with the requirements of TS EN ISO 11200. Svantek Noise Dosimeter verification calibrator was used for verification before and after measurement (Calibrator Brand/Model/Serial No-Svantek/ND9/N000001).

Table 6. The Results of Measuring the Working Environment in the Workplace Where Wood Panel Production is Carried Out

Measurement No.	Temperature (°C)	Humidity (%)	Pressure (hpa)
1	24.9	64	986.4
2	27.1	65	986.5
3	28.6	64	986.4
4	27.6	66	986.5
5	36.0	40	986.7
6	36.1	40	986.7
7	28.1	63	986.1
8	29.6	64	986.4
9	27.2	65	986.5
10	26.4	66	986.9
11	35.7	40	986.7
12	36.1	40	986.6
13	36.1	41	986.7
14	28.7	41	986.5
15	28.6	60	986.9
16	29.4	61	987.8
17	27.9	60	986.9
18	28.7	61	986.5

After the measurement is made, the data recorded on the device is transferred to the computer environment. Then, the measurement re-

sults are analyzed in detail with the appropriate software and the values to be calculated are determined. The necessary calculations are made within the framework of the "Instruction for Using a Computer Program for Acoustic Calculations". In the report, a comparison is made with the limit values within the scope of the relevant legislation.

Table 7. Calculated Ambient Noise Results in Various Sections of Wood Panel Production

Measurement No.	Measurement Section	L_{eq} (dBA)	Evaluation
1	MDF Press Sizing Front	76.37	exceeds
2	MDF Press Line Laying Front	75.8	exceeds
3	Impregnation Section Head of Line	70.37	exceeds
4	shipment area	70.37	exceeds
5	Melamine Section Sheet Feeding	78.3	exceeds
6	Melamine Press Packaging Department	73.77	exceeds
7	Sanding Line Sheet Feeding	85.77	exceeds
8	MSF Press Line Sheet Section	81.87	exceeds
9	Impregnation Section End of Line	74	exceeds
10	Warehouse Department	74	exceeds
11	Melamine Section Press Control Panel Front	77.43	exceeds
12	Melamine Department Quality Control	81.33	exceeds
13	Sanding Line Operation Room	80.83	exceeds
14	Maintenance Shop Lathe Machine Front	79.33	exceeds
15	Compressor Room	87.73	exceeds
16	Boiler Control Room	70.63	exceeds
17	Fibering Front	80.37	exceeds
18	Fiber Operation Room	61.2	well

As can be seen in Table 7, Leq values were measured in the sections where wood panel was produced. As a result of the measurement, those who exceed the limit values and those who are within the scope of the limit value were determined.

Environmental Noise Criteria for Industrial Facilities

Article 25-The following are the criteria for the environmental noise level and noise prevention arising from industrial facilities.

a) Depending on the area where the industrial facilities are located and the defined time period; Environmental noise levels for industrial facilities cannot exceed the limit values in Table 8 in terms of L_{day} and L_{night}. These values apply to all facilities other than entertainment venues listed in Annex-VII Lists A and B.

Table 8. Environmental Noise Limit Values for Industrial Facilities¹⁹

Areas	L _{day} (dBA)	L _{night} (dBA)
Industrial areas (industrial zones)	70	60
Industrial and residential areas (mainly industrial)	68	58
Industrial and residential areas (mainly residential)	65	55
Rural areas and residential areas	60	50

b) List given in Annex VII of this regulation for industrial facilities A and B given in Table 8 environmental noise limit values are exceeded; workers exposed to noise on the basis of each machine and equipment prepared by the institution or institutions responsible under the relevant legislation brought in conjunction with the principles of environmental control measures to ensure effective and enforceable measures are taken ^[30].

¹⁹<https://www.resmigazete.gov.tr/eskiler/2010/06/20100604-5.htm>

Noise Exposure Measurements

Noise exposure measurements were carried out in accordance with the "TS 2607 ISO 1999 Acoustic - Determination of Noise Exposed at Work and the Estimated Standard of Hearing Loss Caused by This Noise".

Personal noise exposure measurements were evaluated according to the articles of the "Regulation on Protection of Employees from Noise-Related Risks" dated 28.07.2013 and numbered 28721.

Exposure Action Values and Exposure Limit Values

ARTICLE 5 - (1) In terms of the application of this regulation, the exposure action values and exposure limit values are given below.

a) Lowest exposure action values: (LEX, 8h) = 80 dB(A) or (P_{peak}) = 112 Pa [135 dB(C) re. 20 µPa] (calculated value of 135 dB (C) with reference to 20 µPa).

b) Peak exposure action values: (LEX, 8h) = 85 dB(A) or (P_{peak}) = 140 Pa [137 dB(C) re. 20 µPa].

c) Exposure limit values: (LEX, 8h) = 87 dB(A) or (P_{peak}) = 200 Pa [140 dB(C) re. 20 µPa].

(2) When applying exposure limit values, the protective effect of personal ear protective equipment used by the employee is also taken into account when determining the exposure of employees.

(3) The effect of ear protectors is not taken into account in the exposure action values.

(4) Daily noise exposure vary significantly from day to day with the certainty that can be detected if the exposure limit values exposure action value in the implementation of daily noise exposure level, instead of weekly noise exposure level can be used. In these works;

The weekly noise exposure level determined by adequate measurement cannot exceed the exposure limit value of 87 dB(A).

Noise Exposure Measurement Results

Noise exposure measurement results (Table 9), thermal comfort conditions (Table10) in the plant where wood panel production is made, and the noise measurement value in Table 11 are given below.

Table 9. Noise Exposure Measurement Results in the Facility where Wood Panel Production is Made

Measurement No.	Working Time(Hours)	Exposure Time (Hours)	Measurement Time (min.)	Measuring Device Brand/Model/ Serial Number	Calibrator Brand/Model/ Serial Number
1.	8	7.5	121	Svantek/SC001/ T200001	Svantek /ND9/N000001

Table 10. Thermal Comfort Ambient Conditions in the Facility where Wood Panel Production is Made

Measurement No.	Temperature (°C)	Humidity (%)	Pressure (hpa)
1.	27.1	65	987.6

Table 11. Measurement Result of Chipping Section in the Facility where Wood Panel Production is Made

Measurement No.	Measurement Section	Person/Task Being Measured	Measurement Result $L_{EX,8H}$ (dBA)	L_{peak}
1.	Chipping Section	Technical staff /75866354895/ Opr.	92.52	151.8

As a result, since the exposure limit values exceed $L_{(EX,8hours)}=85$ dBA or $L_{peak} =137$ dBC according to the articles of “Regulation on Protection of Employees from Risks Related to Noise”, it is obligatory for the employer to take measures to reduce noise.

CONCLUSION

In the facility where wood panel production is carried out, ambient noise measurement result values have been determined. The data on these measurement values are recorded on the computer. Within the scope of this program, the software measurement results were analyzed and the necessary calculations were evaluated within the framework of the “Instruction for Using a Computer for Acoustic Calculations”. As a

result, according to the calculated ambient noise results, it was determined that it exceeded the standard measurement values during production. Accordingly, noise reduction measures have become mandatory. The results of the lowest and highest exposure values calculated and the precautions to be taken are given below.

When the lowest exposure effective limit value ($L_{(EX,8hr)}=80$ dBA or $L_{peak}=135$ dBC) is exceeded, earphones should be kept ready for use by workers.

When the highest exposure effective value ($L_{(EX,8hr)}=85$ dBA or $L_{peak}=137$ dBC) is exceeded, workers must use earplugs.

When the exposure limit value ($L_{(EX,8hr)}=87$ dBA or $L_{peak}=140$ dBC) is exceeded, technical measures should be taken by the employer according to the Regulation on the Protection of Employees from Risks Related to Noise.

REFERENCES

Akbulut, M.C. İSG Tarihsel Gelişim ve İlgili Kuruluşlar. İSG Ders Notu, A.Ü. Beypazarı MYO.

Altan, Ö. Z. (2004). *Sosyal Politika Dersleri*. Eskişehir: Anadolu Üniversitesi Yayınları

Arıcı, K. (1999). *İşçi Sağlığı ve İş Güvenliği Dersleri*. Ankara: TES-İŞ Eğitim Yayınları

Arpat, B., Özkan, Y. (2018). İşletmelerde Ölçek, Ekonomik Faaliyet Grubu ve Tehlike Sınıfı Değişkenlerinin İş Güvenliği Kültürü Üzerine Etkisi Metal Sektörü Denizli İli Örneği. *İŞ, GÜÇ Endüstri İlişkileri ve İnsan Kaynakları Dergisi*. 20, 359-382.

ÇSGB 20.08.2013. İş Hijyeni Ölçüm Test ve Analizi Yapan Laboratuvarlar Hakkında Yönetmelik <https://www.resmigazete.gov.tr/eskiler/2013/08/20130820-3.htm> (E.T. 22.09.2021).

Çavuş, Ö.H. (2015). 6331 Sayılı İş Sağlığı ve Güvenliği Kanunu Kapsamında Ofis İşyerlerinde Risk Değerlendirmesi, *Çalışma İlişkileri Dergisi*, 6(2), 1-14.

Çevresel Gürültünün Değerlendirilmesi ve Yönetimi Yönetmeliği(2002/49/EC) <https://www.resmigazete.gov.tr/eskiler/2010/06/20100604-5.htm> (E.T. 03.10.2021).

Çiçek, Ö., Öçal, M. (2016). Dünyada ve Türkiye’de İş Sağlığı ve İş Güvenliğinin Tarihsel Gelişimi. *Hak-İş Uluslararası Emek ve Toplum Dergisi*. 5(5) , 106-129.

DR Group/Vital OSGB. <http://www.2dr.com.tr/issagligi> 2020 (E.T.20.12.2020).

Gerek, H. N. (2008). *İş Sağlığı ve İş Güvenliği*. Eskişehir. Anadolu Üniversitesi AÖF Yayınları.

Haber İSG. (2019). Gündem İş Hijyeni Ölçümleri Neden Yapılır? <http://haberisg.com/gundem/is-hijyeni-olcumleri-neden-yapilir/> (E.T. 20.06.2019)

İsg Laboratuvarlar Derneği, İş Hijyeni Ölçüm Parametreleri ve Parametrelerin Seçimi İş Hijyeni Ölçüm Test ve Analizi Yapan Laboratuvarlar Hakkında Yönetmeliği

<https://www.resmigazete.gov.tr/eskiler/2017/01/20170124-6.htm> (E.T. 22.09.2021).

Özkılıç, Ö. (2005). İş Sağlığı ve Güvenliği, Yönetim Sistemleri ve Risk Değerlendirme Metodolojileri - TİSK Yayınları, Ankara.

İş Sağlığı ve Güvenliği Risk Değerlendirmesi Yönetmeliği Resmi Gazete, 29.Aralık.2012, sayı:28512. <http://pastelosgb.com/assets/files/isg-risk-degerlendirme.pdf> (E.T. 22.09.2021).

Kırtaş, H.A., Altundağ, H. (2019). İş Yeri Acil Durum Ekiplerinin Eğitimi, *İSG Akademik – OHS Academic*. 1(1), 49-57.

Küçüköğlü, M.T. (2020). Risk yönetiminin neresindeyiz? Otomotiv sektörü örneği. *Trakya Üniversitesi Sosyal Bilimler Dergisi*, 2 (2), 1001-1020.

T.C. Yasalar (20.06.2012) 6331 Sayılı İş Sağlığı ve Güvenliği Kanunu. Ankara. Resmî Gazete (28339 sayılı). <https://www.resmigazete.gov.tr/eskiler/2012/06/20120630-1.htm> (E.T. 22.09.2021).

Yetiş, Ü. (2016). Sektörel Atık Klavuzları https://webdosya.csb.gov.tr/db/cygm/editedosya/Agac_Agac_urunleri_ve_Mobilya_imalati_Kilavuzu.pdf (E.T. 30 .08.2021).

TS 2607 ISO 1999 İş Yerinde Maruz Kalınan Gürültünün Tayini ve Bu Gürültünün Sebep Olduğu İşitme Kaybının Tahmini Standardı. Nisan 2015 ICS 13.140; 17.140.20 <https://docplayer.biz.tr/188668625-Ts-2607-i-so-1999-standardi-gurultu-maruziyeti-olcum-talimati.html> (E.T. 03.10.2021).

TS 2607 ISO 1999, Akustik- iş yerinde maruz kalınan gürültünün tayini ve bu gürültünün sebep olduğu işitme kaybının tahmini, Nisan 2005. <https://docplayer.biz.tr/9060737-Turk-standardi-turkish-standard.html>(E.T.03.10.2021).

TÜİK,2018/2019 SGK Meslek hastalıkları ve İş kazaları Verileri http://www.sgk.gov.tr/wps/portal/sgk/tr/kurumsal/istatistik/sgk_istatistik_yilliklari

Talas, C. (1992). Türkiye'nin Açıklamalı Sosyal Politika Tarihi, Ankara: Bilgi Yayınevi 6331 Sayılı İş Sağlığı ve Güvenliği Kanunu/ 14.04.2013 [Erişim Tarihi:20.12.2020]) <https://www.isvesosyalguvenlik.com/is-sagligi-ve-guvenligi-kanunu/>

CIRCULAR BUILDING DESIGN THAT CONTRIBUTES TO THE CIRCULAR ECONOMY

Ebru DOĞAN¹, Fatma Berfin YAMAK²

Abstract: The rapidly developing technology since the industrial revolution, the increase in the population, the change in the understanding of global consumption, uncontrollable urbanization practices and industrial wastes cause the depletion of natural resources, climate change, loss of biodiversity and global environmental problems. In other words, in the Anthropocene period, all kinds of activities carried out by human beings cause permanent damage on the earth. Epidemics such as COVID-19, natural disasters and ecological crises experienced around the world recently are irreversible damages caused by humans. In the face of the negativities that have arisen, societies have again questioned the economic and ecological system. Accordingly, many countries, institutions, councils and academic circles have started to work on sustainable solutions and strategies that are more environmentally friendly, contribute positively to the global economy and create new employment areas. Along with the new social order that has emerged around the world, circular economy and circular building concepts have been developed as an approach that directs the society to renewable energy sources and recovery opportunities, encourages sustainable business and life models, and reduces the general understanding of consumption in the process from the source of raw materials to waste generation. Conventional construction activities that take place in the building design, application, use and post-use processes constitute a major obstacle to the formation of sustainable built envi-

1 Malatya Turgut Özal University, Faculty of Art, Design and Architecture, Malatya / Turkey, ebru.dogan@ozal.edu.tr, Orcid No: 0000-0002-3143-347X

2 Malatya Turgut Özal University, Faculty of Art, Design and Architecture, Malatya / Turkey, fatmaberfin.yamak@ozal.edu.tr, Orcid No: 0000-0003-0303-4057

ronments, which the circular economy aims to create. In recent years, research has focused on the concept of circular building, which provides easy and undamaged disassembly, adaptation, recovery and durability of a building, in order to reduce the environmental, economic and social negativities caused by building construction activities and contribute to the circular economy. By introducing and applying the purpose, scope and basic principles of the concept at the international level, the impact of environmental problems reaching global dimensions is reduced or completely eliminated. In this context, within the scope of the study, first of all, general definitions of circular economy, circular building and circular building design concepts, which contribute to reducing the negative burdens on natural and built environments, are explained. Then, the design principles included in the circular building design approach, which contributes to the circular economy, are determined and expressed within the scope of the literature study. The opportunities offered by the circularity approach, the effect of which has yet to be noticed in building design, and the obstacles to its implementation are explained. At the end of the study, in the light of the obtained data, suggestions are presented for the extensive application of the circular building design approach. In the study, a guideline was created that all actors (architects, engineers, academics... etc.) working in the field of building design and implementation can benefit from while applying the circular building design approach.

Keywords: Circular Economy, Circular Building Design

INTRODUCTION

The circular economy model, the formation of which dates back to the 1970s, is an approach that includes many models such as the Club of Rome theory of 'Limits to Growth', Braungart and McDonough's 'Cradle to Cradle' concept, Stahel's 'Performance Economics', Lyle's 'Regenerative Design' and Benyus' 'Biomimicry'.

Various definitions have been made for the circular economy model in scientific studies. In most of these definitions, it is mentioned that the concept emerged in order to reduce the negative effects of the Linear Economy model (Figure 1), which works with the "take-make-waste" system. In the linear economy model, the raw material is extracted from its main source and turned into a product, and after it is used, the products are sent to waste areas.

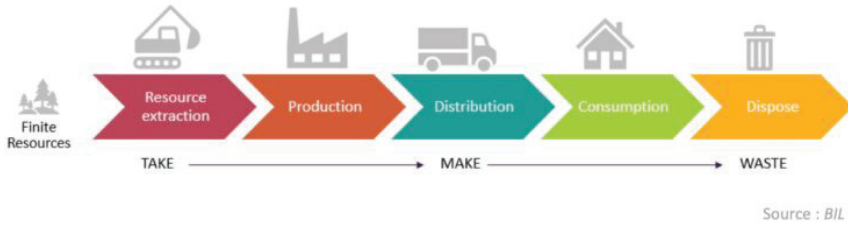


Figure 1. Linear Economy Model (My LIFE Team, 2021)

The circular economy aims to reduce or eliminate the negative effects of the Linear Economy model by providing sustainable development and economic benefit (creating value and saving through reducing resource input), environmental benefit (reducing negative environmental impacts) and social benefit (creating employment) (Saidani ve diğerleri, 2017). In this context, the main goal of the circular economy is to achieve sustainable development through the improvement of resource efficiency, while ensuring environmental improvement, economic welfare and social justice.

The Ellen MacArthur Foundation, which has done extensive research on the circular economy in recent years, developed the “butterfly” diagram (Figure 2), arguing that material flows can be divided into two interactive cycles, technical and biological cycles. The biological cycle uses renewable and plant-derived resources to safely return them to the biosphere. It also contributes to the bio-economy by reducing raw material consumption and waste generation, benefiting from the possibility of reuse, and transforming products at a higher value. The technical cycle requires that man-made products be designed to be reused or recycled when they reach the end of their service life or become unusable. Thus, products are prevented from being sent to waste areas (ARUP, 2016).

In a circular economy, waste generation is reduced and resource use is kept under control to protect human and environmental health. While this provides a systematic benefit to the economy, it also contributes to a sustainable ecosystem.

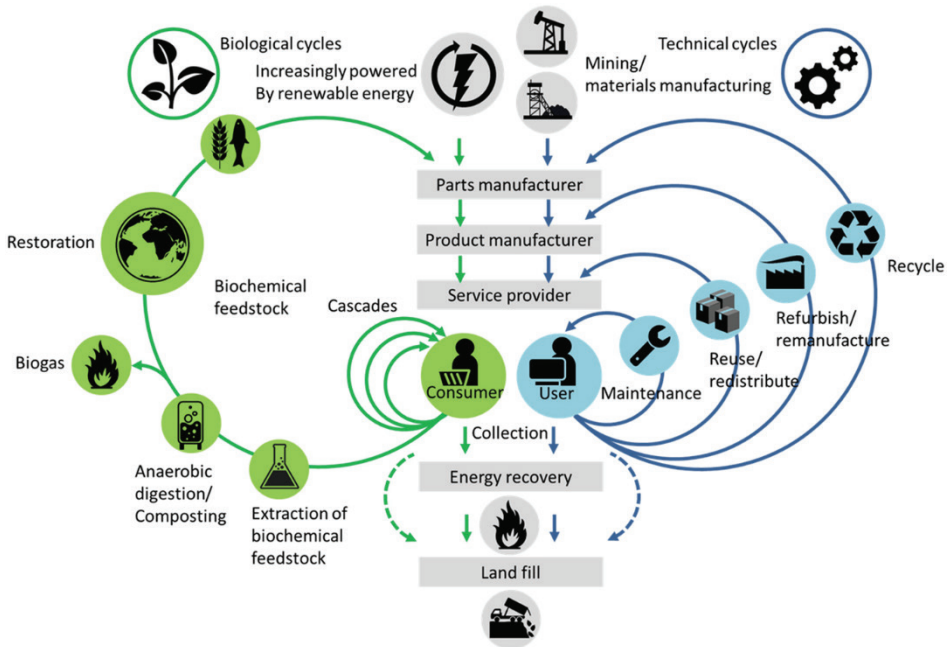


Figure 2. The “Butterfly Diagram” Developed by the Ellen MacArthur Foundation (MacArthur, 2015)

The circular economy can be explained as an industrial system design that is either restorative or regenerative. It uses the restoration approach instead of the end-of-life concept, turns to the use of renewable energy, eliminates the use of toxic chemicals that restrict reuse, and ensures the elimination of waste with superior materials, products and system design (Ellen MacArthur Foundation, 2012).

This framework considers the optimal use of material, energy and water resources, while simultaneously promoting positive effects on biodiversity, human culture, society, health, well-being and the creation of multiple forms of value (Metabolic, 2019).

Cyclality is the amount of renewal of resource flows (EMF et al., 2015). It can be evaluated at different systematic levels. In general, there are four levels of circularity: macro level (built environment including large areas such as cities, provinces, regions), medium level (eco-industrial areas), micro level (single company or consumer) and nano level

(buildings, products, components and materials) (Saidani ve diğerleri, 2017). Tüm düzeyler birbirini etkiler ve etkileşime girer (Linder et al., 2017). In particular, there are few scientific studies on the concept of circularity at the nano level. For this reason, the concept of circularity is discussed at the nano level, that is, at the building level. At the nano level, circularity happens in two ways:

Circular Material Use: The use of cyclic materials includes renewable biological cycles or technical cycles that can be reused after use.

Circular Building Design: Products and components are designed and manufactured so that they can be easily disassembled at the end of their use and reapplied in a new condition (Geldermans, 2016; Loppies, 2015).

There are several circular design strategies that focus on products, components, and materials at the nano level. Circular building design is a Design for Circularity (DfC) strategy that is specific to or compatible with buildings. In the field of architecture, circular building design can be defined as “a building designed, planned, constructed, operated, maintained and disassembled in accordance with the principles of the circular economy”. (Pomponi and Moncaster, 2017).

In this context, solutions have been proposed for the inclusion of built environments in the circular economy:

- Incorporate materials into the economy in a constantly high value and circular manner.
- To ensure maximum energy efficiency by using renewable energy sources.
- To ensure the successful recovery of natural resources.
- To protect biodiversity by preventing it from being damaged by human activities.
- To protect societies by avoiding costly activities that adversely affect the well-being and existence of their cultures, using appropriate processes and management models.

- To protect the health or well-being of humans and other living things in activities that take place in a circular economy, by finally eliminating toxic and dangerous substances.
- Maximize the use of resources, not only in financial returns, but also by raising the value of many elements.

The application of circular economy principles in built environments prevents environmental problems and at the same time increases the added value of buildings. Within the scope of the study, the concept of circularity, which contributes to the circular economy, is discussed at the building level.

MATERIAL and METHOD

The circular economy includes purposes such as the protection of the built environment and natural resources, the health of people and all other living things, and the provision of new employment areas. Conventional building design and application methods cause many negative environmental problems. It is possible to solve this problem with a circular building design approach that contributes to the circular economy. In this context, within the scope of the study, circular building design strategies, the benefits and obstacles in front of them were investigated.

In the light of the information obtained, it is aimed to provide guidance about the circular building design approach to many disciplines such as architects, engineers, contractors, academics, etc. involved in building construction.

The main method followed in the study is the current literature analysis, evaluation and interpretation. The necessary information about the theoretical infrastructure of the concepts that are the subject of the study has been obtained from various scientific publications, guide books and internet resources. In this context, first of all, the concepts of circular economy and circular building are defined. Then, the circular building design approach discussed in the study was explained and the strategies revealed by the approach were determined. Based on the data obtained, the benefits of the circular building design approach and the obstacles to its implementation have been identified. At the end of the

study, suggestions are presented for the effective implementation of the concept.

FINDINGS and DISCUSSION

1. Circular Building

The circular building represents a temporary and dynamic material warehouse that is designed and managed in accordance with DE principles throughout its life cycle. At the same time, it aims at high-value recovery and prolonging the life of materials, products and components as much as possible in the construction chain in a way that does not harm the environment by reducing the consumption of raw materials. In this context, in order to apply the concept of circularity in buildings, the system organization of the building should be done, physical parts with different service life intervals should be separated from each other and independence between the parts should be ensured. Brand’s “Shearing Layers of Change” diagram (Figure 3) explains how building parts with different life spans should be separated into a building system and how they should be put together.

According to Brand (1994), the various physical parts that make up the building system should be brought together in accordance with their associated service life. In addition, Brand claimed that the building system is formed by the coming together of the layers he defined as “Site, Structure, Skin, Services, Space Plan, Stuff”, which undertake different functions and each have different life spans. In his study, he assigned the longest life span for the site on which the building is located.

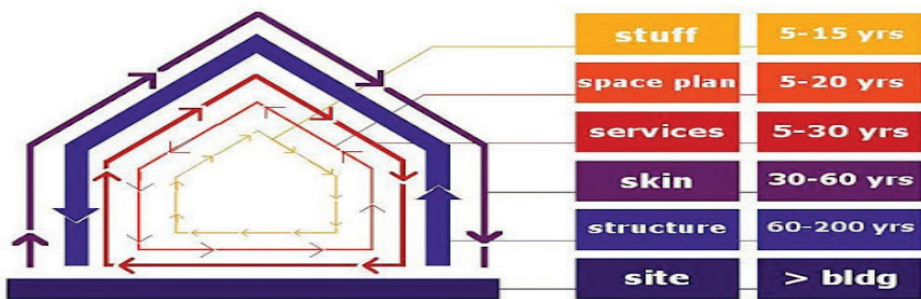


Figure 3. Shearing Layers of Change (Brand, 1994)

The use of the concept of circularity in a building is related to the functional, technical and aesthetic values of the building parts as well as their economic value. All layers of the structure are expected to meet certain performance and features at a certain service value level during their lifetime. Consideration should be given to how and in what way the building layers will be included in the circular process without sending them to landfills when their performance and features fall below a certain service value or expire. Because natural living conditions do not accept waste generation. In nature, it is a food source for another living thing left over from a living thing. While nature includes a circular process from one life to another, in today's society, the conventional design product is sent to waste areas at the end of its service life (McDonough ve Braungart, 2002).

For this reason, when the building parts come to the end of their service life, they should be reused for the same or another purpose without going to waste areas and buildings with a circular life process should be created. The service values of the components of a circular building must be determined. The service values of a building are as follows:

Technical Value: The technical features of the circular building include the use of circular materials and circular design approaches. It aims to use recovery (reuse or recycle) materials that do not contain toxic materials. In addition, it is ensured that the structural parts are designed and produced in such a way that they can be easily disassembled and adapted.

İşlevsel Değer: Functional values in a circular building; It includes sustainable values related to environmental impact, energy and water use. In recent years, both building and material/product evaluation and management systems have been developed to analyze environmental impacts with the effective use of natural resources and energy. It uses internationally valid systems such as "Environmental Impact Assessment (EIA), Environmental Product Declaration (EPD), Life Cycle Assessment (LCA), Building Research Establishment Environmental Assessment Method (BREEAM), Municipal Practice Guideline (MPG), C2C", while determining the functional values of circular buildings.

Aesthetic Value: In the circular building, aesthetic value includes elements based on people's perception such as comfort, acoustics and light. It is very difficult to determine the aesthetic value of a building, as aesthetic perception varies from person to person.

Economic Value: In a circular building, economic value; material price differentials, material supply chain risks, and material shortage measures.

The lifetime and service values of each layer of the building differ from each other (SenterNovem, 2007). When the concept of circularity is applied in a structure, all layers of that building should be considered separately. Within the scope of the study, the use of circular materials and circular building design approaches, which constitute the technical values of the building, were examined in detail.

2. Circular Material Use

In circular buildings, raw material input is refused or reduced by using highly recovery materials. Economic benefit is provided by recovery. During the process of collecting raw materials from waste areas and second-hand products, attention should be paid to human health. In addition, durable and prolong use materials should be used by avoiding the use of deteriorated and worn / rotten materials.

In order to ensure a high level of recycling in a building, it is necessary to have detailed information about the material composition of the buildings. Due to the increasing complexity in construction and the use of a large number of materials and products, digitization, process automation and data standards must be used.

3. Circular Building Design

A circular design has been defined as material selection and advances in product design (standardization of components, modularity, pure material input, design for easier disassembly) at the heart of the circular economy (MacArthur, 2013). Design for Circular Economy (DfCE) is closely related to Design for Sustainability (DfS). Design for sustainability aims to better implement and develop the concept defined as X in the emerging DfX paradigm to take an environmental approach.

In order to realize the circular building design, the structural system, spaces and materials of the building must be separated from each other and reused in different ways (Durmisevic ve Brouwer, 2006). For this, it uses two different design approaches, namely Design for Disassembly and Design for Adaptability.

Design for Disassembly (DfD): DfD is a design approach that aims to extend service life by recovering the end-of-service built environment and its parts. With the DfD approach, it is possible to systematically disassemble the structural parts that make up the building at the end of their service life, without causing damage/ damage, and prolonging the life of these parts by reusing or recycling them in the future. Instead of consuming the natural environment, this approach reintroduces the material extracted from the existing building stock as a raw material into the cycle.

There are several strategies that can be implemented for recovery purposes, from complete reuse to recycling of parts when the building and its parts reach the end of their service life. It is possible to consider recycling strategies under two headings as reuse and recycling.

- Reuse: Bu geri kazanım stratejisi, bir bina parçasının, hizmet ömrü sonunda bütün olarak orijinal yerinden alınarak, orijinal işlevine uygun şekilde veya farklı bir işlev için başka bir yerde tekrar kullanılmasını amaçlar.
- Recycling: It includes the processes of converting building parts that have reached the end of their service life into their own raw materials and remanufacturing them by processing into other parts.

Recovery strategies (recovery scenarios or life cycle scenarios) for building systems and components can be adapted to the hierarchical organization of the building system as follows (Morgan and Stevenson, 2005) (Macozoma, 2002):

- Reuse of the whole building or the building system in cases requiring renovasyon, relocation, adaptation in the same location

- Reuse of a building element or component in the same place for similar/ different purposes, in a different location for similar/ different purposes, at high/low value
- The reuse of the building materials that make up the building element in the same place for similar / different purposes, in different places for similar / different purposes, at high / low value
- Downcycling, recycling, upcycling recycling of building materials

Building parts lose their re-use capacity in cases where maintenance, repair and improvement to be applied again after a while is insufficient. In this case, the building parts must have a recycling capacity so that the parts are not demolished and sent to waste areas. A component that has reached the end of its service life and cannot be reused may not always be recycled at the same value. Three different strategies are applied for recycling: Upcycling, Recycling and Downcycling. (Macozoma, 2002).

- Upcycling is the conversion of building parts separated from the building system into a new part of better quality or less harmful to the environment. An example of such a transformation is the recycling of the wood used under the coating in the building system and using it as furniture.
- Recycling can be defined as the use of building parts separated from the building system into a new part of the same value as their main material.
- Downcycling can be explained as the separation of the parts that make up the building system and using them in a new low quality part. An example can be given to the use of concrete precast flooring as a landfill after being decomposed and converted into aggregate.

The Design for Disassembly principles, which offer high-value recovery to building parts in the circular building design process, are explained in Table 1.

Table 1. Design for Disassembly (DfD) Principles, (Guy and Ciarimboli, 2005)

Design for Disassembly (DfD) Principles	
Management of Assembly and Disassembly Documents of Construction Parts	Drawings, labels, specifications, methods to be used, teams to take charge of the assembly, disassembly, recycling and demolition processes of building parts should be created, distributed, stored and managed.
Use of Recovery Components	Components that can be recovery (reused and recycled) must be used.
Providing Easy Access to Assemblies of Components	It should be created in such a way that easy access to the carrier, installation and hardware systems of the building is required in cases where intervention is required.
Minimizing/Eliminating the Use of Materials Containing Chemicals and Hazardous Substances	Materials containing harmful chemicals (composite, asbestos, lead, cadmium, etc.) that will adversely affect human and environmental health should not be used.
Use of Easily Disassemble Connections in Joining Components:	Mechanical connections (bolted, screwed and nailed connections) should be used instead of wet connections in the joints of building parts.
Independent Design of Mechanical, Electrical and Installation Systems	For an easy and undamaged disassembly process, the mechanical, electrical and plumbing systems should be independent of each other in the building system.
Use of Standard Dimensions in Components	Standard dimensions should be used during the design phase in order to provide ease of transportation, assembly and disassembly during the application phases in the field.

Simplicity in Structure and Form	The structure and form of the building should be clear and readable from the outside, and confusion should be avoided. For this, building parts and combinations consisting of repeating geometries should be used in the building.
Possibility of Interchangeability of Components	Reusable, modular, standard and independent building systems, products and materials should be used.
Safe Disassembly and Assembly	The workers who will take part in the disassembly and assembly stages should be planned to work safely.

Design for Disassembly: Design for adaptability is based on the hypothesis that product lifespan ends due to inability to adapt to change. It aims to transform inflexible products into active, adaptable systems. Adaptive building design is a strategy used to avoid obsolescence, natural resource consumption and material waste (Moffatt and Russell, 2001).

The theoretical basis of design for adaptability should be understood as a dynamic system built with layers with different lifetimes rather than a static object. This design approach aims that the building can be modified to meet the time requirement and have a longer useful life (Kasarda and diğlerleri, 2007).

Contributing Design for Adaptability principles in the circular building design process are described in Table 2.

Table 2. Design for Adaptability Principles (Moffatt and Russell, 2001)

(Design for Adaptability (DfA) Principles	
Durability	The life span of the structural system and shell layers of the building should be longer. Building layers should be selected from products with low need for repair, maintenance and replacement.
Flexible Design	Spaces should be designed to meet alternative usage needs as a result of different needs and changes.
Building Components Development	Depending on the needs, components must increase their performance.
Ease of Access to Service Staff	Solutions that will provide easy access to suspended ceilings, raised floors, pipes, cables, ducts and other equipment (easily accessible central shafts, cores... etc.) should be produced.
Independent Intervention of Building Parts	It must be ensured that a component can be manipulated without affecting other components with which that component is related.
Complexity Level of Building Parts	Building parts should be designed in a simple, understandable and clutter-free manner.
Type and Number of Building Parts Used	A small number of components of the same type and variety should be used as much as possible in the building system.
Creating Building Information	In case of renovation or improvement, all necessary information for the future scenario (analysis, drawings, properties of building parts ... etc.) should be documented.

CONCLUSION and RECOMMENDATIONS

The concept of circularity is effective in many fields, especially in architecture. In addition to the benefits of the concept in the building design phase, it has been determined that there are some obstacles in its

implementation. If the benefits (Table 3) and obstacles (Table 4) obtained within the scope of the study are analyzed well, the concept can be used without any problems in the design phase. For this reason, in the conclusion part of the study, the benefits of the concept and the obstacles in front of it are explained.

In order to examine the positive aspects of the circular building design approach; we need to consider many different areas together such as energy, material and structure, qualified personnel, and capital resources. With this multi-perspective, the concept of circularity will provide a sustainable perspective in line with its goals and strategies. Then, the use of renewable resources will be increased and a more environmentally friendly system will be formed in which the use of natural resources becomes more important.

Table 3. Benefits of Circular Building Design

Benefits of Circular Building Design	
Education Factors	<ul style="list-style-type: none"> - Gaining a new perspective to the work to be done -Increasing the number of educated people, bringing the concept to the literature and creating new fields of study
Economic Factors	<ul style="list-style-type: none"> - With the introduction of the concept to the market understanding in our country, the use of local, natural materials and systems has become widespread, and as a result, the costs have decreased. -Strengthening the local market and thus reducing the demand for foreign trade networks - Reducing expenditure and material procurement costs with the understanding of recycling and reuse
Social Factors	<ul style="list-style-type: none"> -Better quality of living standards with the change of social perception -Developing a perspective towards the natural environment and renewable resources - Providing more job opportunities
Legal Factors	<ul style="list-style-type: none"> - The application of the perspective provided by Circular Building Design to government policies and as a result, the correct and effective use of resources

Table 4. Obstacle of Using Circular Building Design

Obstacle of Using Circular Building Design	
Education Factors	<ul style="list-style-type: none"> - Lack of necessary resources and technical equipment for training - Insufficient number of qualified personnel and experts - Lack of sufficient literature on the concept -The difference between the concept of Circular Building Design and other concepts and ways of thinking is not presented effectively.
Economic Factors	<ul style="list-style-type: none"> -Excessive costs in the building implementation process as there is no market understanding for the concept - People stay away from the concept due to the large number of items such as materials and labor to be purchased from other countries.
Social Factors	<ul style="list-style-type: none"> -Failure to carry out community-oriented activities -Failure to gain the concept of Circular Building Design in the perception of society -It is difficult to break the perceptions of the society for architecture
Legal Factors	<ul style="list-style-type: none"> -Lack of adequate studies on the concept in state policies - Failure to provide various incentives and supports to people who take an active role in the building design and implementation process by the state.

Each of the building design, application, use and demolition processes covers different time periods in itself and these processes are of different lengths. However, each of them includes a formation at the base and the transition of the structure to a different stage at the end of this formation. From this point of view, each process feeds each other naturally. The understanding of circularity in building design aims at the development of sustainable, long-lasting and flexible ideas and practices for each of these processes. It increases the life expectancy of the buildings obtained in the studies carried out in line with this goal and ensures that they are used longer than the planned life span (Lee ve Mitchell, 2020).

The circular economy and the circular building are basically formed around the same idea. It is very important to support these two concepts, especially with government policies. In the circular economy, buildings must be designed for an entire life cycle, not just for a single use. For this reason, structures should be carefully considered from the design stages to the stages of destruction or re-functioning. This should be fueled by performance-based contracts and holistic lifecycle certification and rewards for companies. People and companies should be made aware and encouraged to use circularity principles in their designs (ARUP, 2016).

In line with the literature studies; It has been observed that design decisions such as disassemble and reuse have significant effects on the implementation, renewal and reuse of the building system and its components. It has been determined that in circular studies where these design decisions are integrated, such as building construction circular, buildings should not be considered only in terms of construction or design, but also industrial resource and material use processes. In addition, under the perspective of building construction circularity; By increasing the use of renewable resources and the use of local materials as much as possible in buildings, it can be ensured that the buildings have a more flexible design. Thus, the risks posed by the structures for the investors are reduced (ARUP, 2016).

When resources begin to decrease in terms of material type and amount over time, significant restrictions will arise in the use of materials for building designs. Therefore, the considerations of modularity and adaptability, which form the basis of circular designs, should already be effective on structures. The structures designed under these considerations; Sustainable biomaterial usage areas can be expanded by building from reusable, durable and flexible elements. These situations will directly contribute to the country's economy and at the same time increase the sustainability of the materials (ARUP, 2016).

It is important in many ways to provide feedback for each parameter of the design under the circular view. For example, thanks to the recycling of the materials used in the production process, the creation of new business lines in the society is supported. This situation increases the

level of social welfare, decreases the unemployment rate and facilitates individuals to adopt the circular economy and design headings.

Today, building design and applications are static. However, with the developing technological activities and changing human psychologies, the functions of the structures and the demands of the structures are also different. Structures designed with the idea of building construction circularity have the opportunity to provide more adaptability and flexibility and enable them to create a dynamic platform. For example, façade systems that can be disassembled and reconfigured to suit the building function can be renewed as the building function changes and rearranged in an integrated manner with the function. This will reduce the time and cost to be spent for the renovation of the structures, and will eliminate waste and other negative parameters (ARUP, 2016).

Today, the importance of issues such as climate change, natural environmental pollution and global warming in human life leads to the emergence of new concepts and understandings that are sustainable, socially oriented and beneficial to the natural environment. The circular building design approach not only develops ideas about building design, but also affects the view of the natural environment, the use of renewable resources and the lifestyle of the society. From this point of view, circular building design is in close relationship with many areas of life. As in every field, in addition to the benefits provided in this concept, there are also negative situations. In this part of the study, the circular building design approach, the obstacles to its development and use will be explained.

The concept of circularity, which entered our lives with the constantly developing and changing world order, actually entered our lives with the concept of circular economy before the concept of building construction circularity. Since this concept of circularity, which is not fundamentally far from our lifestyle, enters our lives with the concept of circular economy, the obstacles that arise in terms of both concepts can be common. When we look at the obstacles to the development of the circular building design approach, we first encounter the lack of information in the literature. Lack of competent and effective literature, field and laboratory studies on the concept in the working environment

where developing technologies facilitate data supply and flow; It causes a weakening of the development and recognition of the concept in the working world and in the perception of society (Rahla vd., 2019).

Studies on the concept are very few. At the same time, the number of people who have received training on the concept and who are experts in both practice and theory is quite low. Especially for this concept, which starts from the field of architecture and spreads throughout the society, the education system and work areas to be put forward with a correct and effective planning will be important for the development of the concept. While mentioning the inadequacy of relevant trainings and knowledge on circular building design, it also mentions the weakness of its effect on people's thoughts. This weakness, on the other hand, can be attributed to the lack of effective studies on concepts with the process that started with the circular economy, and the presence of many complex ideas and concept definitions.

The aforementioned complex ideas and concepts can be addressed through the building construction circularity or the building life cycle. Basically, these two concepts have emerged as a combination of many understandings such as the effective use of natural resources, the effectiveness of renewable energy resources and sustainability. For this reason, in studies on building construction cyclicity; The understanding and development of building construction circularity is also slow, as the differences from the ever-expanding concepts such as building life cycle and sustainability, and the benefits it provides for other concepts cannot be expressed effectively (Rahla vd., 2019)

The understanding of architecture, which has been going on since the existence of mankind, has taken its current form by being affected by the developing technology and social changes over time. When we look at our country, it is seen that there are long-established understandings of architecture, especially the construction site setup and the response it finds in practice. Many of these understandings are works that are closed to development and change, that only reflect the characteristics of the time period in which they emerged, and whose benefits to architecture and society are decreasing day by day. These understandings of

society and architecture make it difficult for emerging concepts such as cyclical building design to find a response.

The fact that the idea that dominates the understanding of the market in our country today is in high demand both in the society and in the implementation of the building prevents the development of emerging concepts. It will take time for positive economic conditions to emerge in our country for new understandings. Foreign-related equipment and qualified personnel will be used for the building designs and studies to be carried out during this process. In this case, it naturally increases costs and causes people to stay away from new concepts and ideas. Thus, the implementation time of new concepts and ideas such as circular building design is prolonged.

It is seen that the government policies implemented in our country are aimed at the protection of the natural environment, reconstruction and use over time. However, the fact that this understanding is not established for every unit of the state causes the studies on circular building design not to be carried out in state policies. For this reason, for a concept that has not been reflected in the policies, it cannot be improved in the negative situations that arise economically. There are no incentives or support activities to improve adverse situations and adopt a circular building design approach. The absence of these studies causes a weakening of the relationship between building construction cyclicity and community life.

Records of building system parts are kept during the building design, implementation and use processes. Documentation of all processes from building design to waste generation, especially in cyclical flow; It makes the use of natural resources and renewable energy resources effective. Thanks to this cycle, a design that is beneficial to the natural environment and ecosystem, and the amount of waste is kept to a minimum, emerges.

The information of the building and all its subsystems are recorded using a comprehensive and effective information network such as Building Information Model (BIM). Thus, all decision makers can easily access the information about where and how they will be used as a result

of the interventions of all parts in a building through the BIM system. By integrating the circular building design approach into a cloud system such as BIM, the processes involved in the concept will be better managed. In addition, the entire life span of the building, such as the building design, application, use and usage process, will be systematically controlled. Thanks to the BIM system, the amount, type, combinations, future uses, and the amount of waste and recycling of the building parts to be used in the construction of the building will be recorded and monitored and controlled easily. In addition, all application stages, cost and time management, risks that may occur, environmental impacts that will take place throughout the life of the building can be determined in advance and preventive measures can be taken.

In the light of the data revealed within the scope of the study, it is possible to create an evaluation model for the effective and systematic use of the concept of circularity in building construction in the future. For the widespread use of the model on an international scale, various incentives and supports should be provided at the national and international level according to points, scores or degrees, as in building certification systems. In addition, integration with BIM should be ensured in order to create and manage buildings in a controlled manner through the evaluation model to be obtained.

REFERENCES

Arup Group Limited, (2016), *The Circular Economy In The Built Environment*. Retrieved from <https://www.arup.com/perspectives/publications/research/section/circular-economy-in-the-built-environment> (Erişim tarihi 28.07.2021)

Brand, S. (1994). *How Buildings Learn, What Happens After They're Built*. London: Viking.

Durmisevic, E. and Brouwer, P. J. (2006). *Design Aspects of Decomposable Building Structures*. Building.

Ellen MacArthur Foundation,(2012),*Towards the circular economy: economic and business rationale for an accelerated transition*. Ellen MacArthur Foundation. <https://doi.org/10.1162/108819806775545321>.

Ellen MacArthur Foundation. (2013). Towards the Circular Economy - Part 1; Economic and business rationale for an accelerated transition. *Journal of Industrial Ecology*, 1(1), 4-8. <http://doi.org/10.1162/108819806775545321>

Ellen MacArthur Foundation, Granta and LIFE (2015), *Circularity Indicators; An Approach to Measuring Circularity; Project Overview*.

Geldermans, R.J. (2016), *Design for change and circularity - accommodating circular material and product flows in construction*, *Energy Procedia* (96)

Guy B., Ciarimboli N., (2007). *Design for Disassembly in the Built Environment: a guide to closed-loop design and building*, Pennsylvania State University.

Kasarda, M. E., Terpenney, J. P., Inman, D., Precoda, K. R., Jelesko, J., Sahin, A., & Park, J. (2007). Design for adaptability (DFAD)-a new concept for achieving sustainable design. *Robotics and Computer-Integrated Manufacturing*, 23(6), 727-734.

Linder, M., Sarasini, S. and Loon, P. van (2017), *A Metric for Quantifying Product-Level Circularity*, *Journal of Industrial Ecology*.

Loppies, W. (2015), *Bouwen aan de Circulaire Economie*, Technische Universiteit Delft, Delft.

Macozoma, D.S. (2002). *Understanding the Concept of Flexibility in Design for Deconstruction*, Proceedings of the CIB Task Group 39, CIB Publication 272, Karlsruhe, Germany.

McDonough, W. and Braungart, M. (2002). *Design for the Triple Top Line: New Tools for Sustainable Commerce*, Corporate Environmental Strategy, Vol. 9, No. 3, 251-258.

Moffatt, S., & Russell, P. (2001). *Adaptability of Buildings*. IEA Annex 31 Energy-Related Environmental Impacts of Buildings.

Morgan, C. and Stevenson, F. (2005). *Design and detailing for deconstruction*. Scotland Environmental Design Association, SEDA Design Guides for Scotland: No:1, Scotland.

Pomponi, F. and Moncaster, A. (2017), Circular Economy for the built environment: a research framework, *Journal of Cleaner Production* (143)

Rahla, K. M., Brangança, L. and Mateus, R., (2019), Obstacles and barriers for measuring building's circularity, *IOP Conf. Series: Earth and Environmental Science* (225)

Saidani, M., Yannou, B., Leroy, Y. and Cluzel, F. (2017), How to Assess Product Performance in the Circular Economy? Proposed Requirements for the Design of a Circularity Measurement Framework, *Recycling* (2, 6), Paris.

SenterNovem. (2007). *Industrieel, flexibel en demontabel bouwen* (IFD).

INTERNET RESOURCES

MyLIFEteam, (2021). Towards a circular economy <https://my-life.lu/en/towards-a-circular-economy-30514/> (E.T. 07.08.2021)

Metabolic, (2019). The Seven Pillars of the Circular Economy <https://www.metabolic.nl/news/the-seven-pillars-of-the-circular-economy/> (E.T. 07.08.2021)

Lee, G., & Mitchell, H. A. (2020). Circularity Advantages The Built Environment <https://www.circularatharvard.org/articles/circularity-advantages-the-built-environment>, (E.T. 15.07.2021)

HVAC PRACTICES FOR DATA CENTERS

Kaan YILMAZKARASU¹, Ayhan ONAT²

Abstract: Today, energy consumption accounts for the majority of the import costs of developing countries. This necessitates examining all factors that may affect energy consumption amounts. It is necessary to interpret such factors with an engineering perspective and a mental filter. The electronic conversion of data has been a necessity in any business. Large servers and network equipment are needed to perform the instantaneous transmission request of digital information. These aggregated results and associated equipment are stored in multiple rooms throughout an entire building. Today's data centers are composed of thousands of high-powered and too-small servers running 24/7. Data centers are among the facilities with very high electricity consumption. This kind of consumption reveals too much potential for saving studies. This study is aimed to compare heat loss/gain software for heating, ventilation, and air conditioning engineering designs and to scrutinize the possible differences from an engineering and academic perspective. For a sample data center, a 3D model of the building is created using Trace 700, Carrier Hourly Analysis Program (HAP), Revit and Cypetherm Loads software, and thermal-load calculations are made on this model. The first step of efficiency studies in a mechanical system is the accuracy of calculations. Although the gained loads with the help of environmental conditions for the data centers are too small compared to the device loads, the calculation method or the software used in the thermal calculations in the study shows that the volumes with large outer wall and roof area affect the accuracy of the results.

1 Marmara University, Faculty of Technology, Mechanical Engineering, İstanbul / Türkiye
k.yilmazkarasu@gmail.com, Orcid No: 0000-0002-4399-8662

2 Marmara University, Faculty of Technology, Mechanical Engineering, İstanbul / Türkiye,
onattayhan@gmail.com, Orcid No: 0000-0001-9737-6300

Keywords: Data Center Cooling, Cooling Load Calculations, Thermal Load Calculation Softwares

INTRODUCTION

Today, project completion times are getting shorter and shorter in order to meet the sector's needs. For an energy efficient building, it is necessary to quickly calculate heat losses and gains. In a building where an air conditioning project is designed, heating or cooling calculations are a laborious and error-prone process due to the use of many tables and formulas. It has been determined that performing these operations with software will shorten the project period and minimize possible errors (Oranlier ve Eyriboyun, 2009).

The energy consumed in buildings in European countries is approximately 40% of the total energy consumed (Kürekci ve Kaplan, 2014). It is stated that it causes 30% of the total CO₂ emissions. It is a fact that Turkey is not rich in energy reserve areas. 76% of the total energy in Turkey is purchased from other countries. In addition, this demand increases by approximately 4% in 1 year. Optimization studies and economic savings are important (Alkan ve ark., 2017).

Today, energy efficiency has become a focus for data centers as in all sectors. Energy efficiency in data centers, which are exposed to high-density electrical loads, is much more important than other buildings. Most data centers are designed for the highest load density, cooling loads are not associated with the time parameter. In addition, it is known that mechanical equipment is chosen with more capacity than normal, which will increase both investment and operating costs. Energy efficiency as well as reliability should be considered in data center infrastructure design studies. Since most of the energy consumption for data centers is caused by mechanical cooling systems, strategies should be developed to increase the energy efficiency of cooling systems (Türkmen, 2019).

The software makes calculations with many different engineering assumptions, and the mathematical models used in the background of the assumptions affect the accuracy of the calculation results. In addition, each software uses internationally standards accepted by different coun-

ries. In this study, besides the software results, the difference in results that may occur from the calculation methods and standards will be examined and more accurate conclusions will be reached about the results.

There have been previous studies on different or similar software in the literature, and in addition to these, this study includes basic usage information about four different software. This study has been a guide study about software. The analysis of the standards used and the differences in calculation methods constituted the original value of the study. In addition, due to the limited number of studies on data centers in the literature, it is thought that this study will benefit the literature and related sectors. In addition, the number of alternative software to be used is important in terms of more accurate comparison of the results. In order to make the results more meaningful, the software that is known to be used the most in industry and academic studies was preferred.

Due to both commercial concerns and some mathematical processing difficulties, commercial software works with assumptions and estimations. In line with sectoral and academic experiences, these softwares, which have wide use in the field of engineering, as it is necessary for every study, should be verified by independent studies to be done.

In this study, the calculation methods of the software and which standards they use are examined. An existing data center building was selected and cooling loads were calculated with four different software. Simultaneously with the calculations, basic information about the use of the software is given. Finally, possible computational differences based on these results are interpreted.

The results calculated with the software will determine the capacity of the equipment that will consume energy throughout the year. The equipments will cause an energy and cost proportional to its capacity. The accuracy of the calculations means an energy to be saved and the cost of this energy. When these account values, which seem insignificant on a small scale, are considered on a large scale, they mean very large savings values throughout the country and economic gains to be obtained from these savings.

It is predicted that the data obtained from the study will allow the design of more efficient cooling systems for data centers. It is expected to prevent energy consumption and to reduce investment and operating costs on a small scale. When considered on a large scale, it is expected that the amount of imported energy will decrease and space will be opened for new investments.

HVAC Practices for Data Centers

Digital Transformation

Digitalization is a general term for the 'Digital Transformation' of society and the economy. It describes the transition from the industrial age characterized by analog technologies to the information and creativity age characterized by digital technologies and digital business innovations. Digital transformation provides many advantages, from efficiency to security, from spreading a collaborative culture to cost advantages.

It can be said that this transformation is the result of humanity's endless search for improvement. The part of the transformation is the result of productivity works. However, this definition only is insufficient. Similar to many developments in human history, not all of this transformation took place in a controlled manner. With the integration of technology into our lives, most companies and/or people have been forced into this transformation in some way. Figure 1 shows an image of digitalization.



Figure 1. Digitalization

Data Centers

Data Centers are areas where equipment is gathered in a single center for the purpose of obtaining, storing, processing, and transmitting very large data. There is a high density of computer and network equipment in these areas. They can be on a small or large scale, depending on their intended use and capacity. Although data centers are referred to by a single name, they include routers, switches, security devices, storage systems, servers, controllers and more. These are the IT components needed to store and manage the most critical systems that are vital to a company's continued operation. Therefore, the efficiency, security, reliability and continuous improvement of data centers should be a priority for organizations. Figure 2 shows an example of data center interior design.



Figure 2. Data Centers

Why We Need Data Centers?

The growth in the number of users connected to the Internet and the increase in data has led companies to invest in data centers that are growing and have more energy density per m².

There are various levels of "Data Center" needs, including government agencies, educational institutions, telecommunications companies, financial institutions, healthcare institutions, retailers of all sizes, and online marketers providing information and social networking services such as Google and Facebook.

While data center designs are unique, they can often be classified as internet-connected or enterprise or internal data centers. Internet-connected data centers support relatively few applications and are generally

browser-based and often have unknown users. In contrast, enterprise data centers serve fewer users but host applications ranging from off-the-shelf to custom applications. Data centers in the world of corporate information technologies; It is designed to support business applications and activities such as e-mail and file sharing, productivity applications, customer relationship management (CRM) and enterprise resource planning (ERP), big data, artificial intelligence and machine learning, communication and collaboration services.

Why are Data Centers so Important?

With digitalization, the developing internet technologies and the increasing number of web pages have become more than the number of people in the world. This means more bandwidth requirement and hence more disk space requirement. Increases in the speed of access had similar results and led to the enrichment of information resources. This situation has revealed the importance of storing and processing big data. An institution must have a data center for all kinds of data it produces or uses. There are various levels of “Data Center” needs, including government agencies, educational institutions, telecommunications companies, financial institutions, healthcare institutions, retailers of all sizes, and online marketers providing services via internet technologies such as Google and Facebook.

A slow and insecure access to data can cause serious disruption of services. This situation indirectly leads to loss of customers and it is inevitable for companies to experience financial losses. To avoid this loss, many businesses prefer to keep their data in data centers to both reduce costs and benefit from cloud services, rather than the structures created by their own computer networks and servers. The growth in the number of people connected to the Internet and the increase in data sizes have prompted companies to invest in data centers that can store and process more data per m². Selection and design of an efficient cooling system is very important as these cost savings will contribute greatly to the expense and income balance of a data center. Data centers are areas where temperature and humidity need to be controlled, the electricity supply is stabilized, continuous electricity supply is provided and spe-

cially air-conditioned. In addition to these, there are cable infrastructure systems, supervised access, security systems and fire detection and extinguishing systems. Thus, this center contains all of an organization's computing (IT) systems and hardware.

Data Center Equipments

In any structure used for data center and similar purposes, it is necessary to make a large number of cable connections. In data centers, certain rack structures are used that enable the equipment to be placed in an organized manner and to protect them against external factors. These structures also significantly reduce the residential area. Data center equipment is usually mounted in racks. But others are configured in prepackaged configurations as large, self-contained cabinets. Rack and cabinet dimensions are determined by the Electronic Industries Association (EIA). The vertical dimension is expressed in "unit" (U) (sometimes rack unit (RU)) and the overall height for a rack is 42U. A U stands for 44.45mm vertical height within the rack. The terms rack and cabinet are used interchangeably, although technically a rack is an open, two- or four-column structure used more for telecom and patch panels than servers; A cabin is a similar four-column frame equipped with side, top, front and rear doors. Examples of two column open rack and four column open rack are shown in Figure 3.

Rack technology should also be in a structure that will allow these equipment, which consumes high electricity, to transfer the heat produced by these equipment to the environment. In this way, the appropriate temperature for the operating conditions of the equipment can be provided by supporting it with cooling systems. Data center components (processors, memory, storage, input/output (I/O), power supplies) are packaged in data center equipment. These equipments mainly consist of servers (capacity, blade etc.), communication equipment (switches, routers etc.) and data storage devices (storage area network (SAN) etc.).

Data center equipment may be of the type that can operate with an air-cooled system or a liquid-cooled system. The critical condition for air-cooled equipment is air intake into the equipment. The important

point for liquid-cooled equipment is the fluid connection to the equipment or rack. Examples of air-cooled racks are shown in Figure 4 and liquid-cooled racks in Figure 5 (TTMD Issue 121).

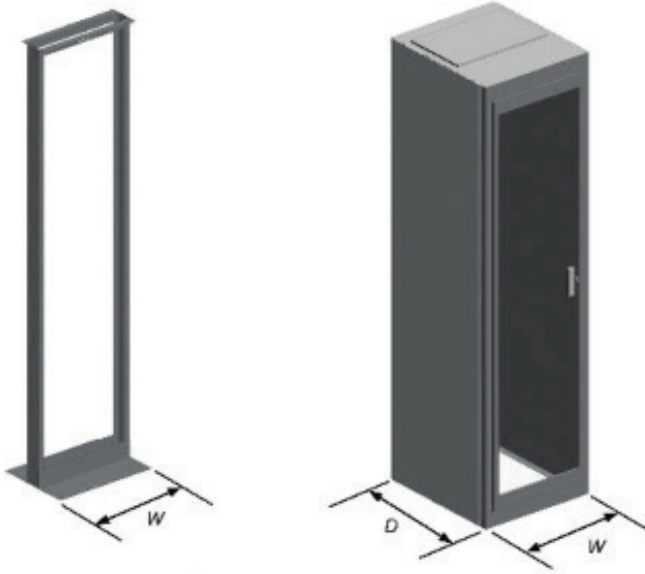


Figure 3. Examples of Two Column Open Rack and Four Column Open Rack

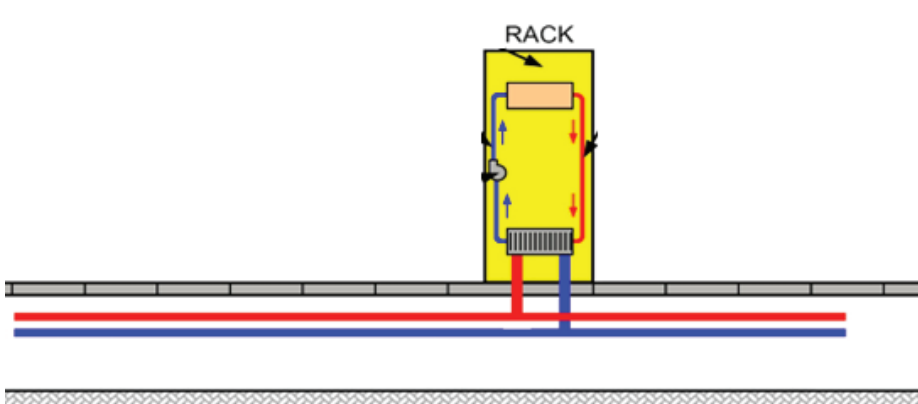


Figure 4. Equipment Air Flow

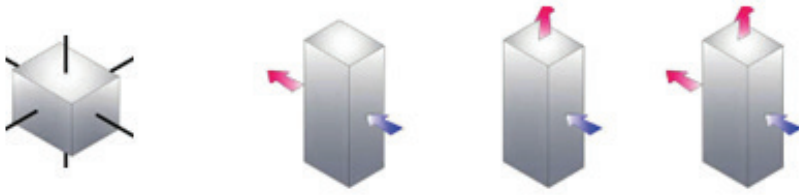


Figure 5. Equipment Air Flow

Work Load of Data Center Equipments

Data center equipment (hardware) has various workload states ranging from idle (not performing any useful work) to operating at its maximum performance. Hardware workload is managed by software. The number of applications available across all hardware types is certainly in the millions or more. Software can be added or upgraded in a variety of ways, often including remotely. This means that the workload can be very dynamic. Data center equipment lifecycles are much shorter than power and cooling infrastructure lifecycles. Application software lifecycles are even shorter. It is critical that power and cooling infrastructure planning considers the lifecycles of hardware and software.

How to Determine Data Center Size Scales

For a data center power and cooling infrastructure planning of U-type cabinets, two common metrics are watts per square meter and kW per rack. The data center industry sometimes uses the average item size (granularity) to define unit sizes. The general consensus in the data center industry is that kilowatts per rack are superior to watts per square metre. However, at the start of a project, there may not be enough information about the amount of racks making the metric multi-particle (granular). Professional calculation is critical for deciding which maximum load characterization to use. It is equally important to characterize the load variation as well as the minimum load. The time step for the load change can be too short (eg seconds, minutes) or too long. It is important to define or develop a detailed load profile, including future possibilities.

Data Center Components

Active Infrastructure Systems and Components

- *Application Software and Geographical Information Systems*
- *Server and Computer Systems*
- *Virtualization and Cloud Systems*
- *Crypto Security*
- *Network and Communication Systems*
- *Data Center Management Systems*
- *Secure Information Sharing and Cryptographic Communication Solutions*

Passive Infrastructure Systems and Components

- *Air Conditioning Systems*
- *Energy Systems (UPS, Generator)*
- *Fire Alarm and Suppression Systems*
- *Cabling, Floor Covering and Furniture*

Energy Efficiency in Data Centers

The Green Grid (TGG) is a joint institution of government agencies and educational institutes. Data centers support energy efficiency. TGG has developed a new measure in addition to many studies. PUE value; It is the ratio of the total energy consumed in the data center (including the energy used for IT equipment) divided by the energy consumed on the IT equipment. PUE is given in Equation 1.

$$\text{PUE} = \text{Total Facility Power} / \text{IT Equipment Power} \quad (1)$$

Data Center Infrastructure Efficiency (DCiE) is defined as the opposite of PUE. This measurement is made annually in order not to be affected by the effects of climate changes in different seasons of the year on energy consumption. For example: In summer, cooling devices for some

regions operate less efficiently and consume more energy to achieve the same cooling load. With the use of advanced air handling units (AHU), PUE values can reach as low as 1.06. In Table 1, the efficiency table determined by The Green Grid is given. In addition, in Table 2, the PUE values estimation table made by EPA for 2011 is given. DCiE is given in Equation 2.

$$\text{DCiE} = \text{IT Equipment Power} / \text{Total Facility Power} \quad (2)$$

Table 1. The Green Grid Efficiency Table

PUE	DCiE(%)	Verimlilik Durumu
3,0	33	Very Inefficient
2,5	40	Inefficient
2,0	50	Average
1,5	67	Efficient
1,2	83	Very Efficient

Table 2. EPA Estimated PUE Values in 2011

Scenarios	PUE
Current Trends	1,9
Improved Operations	1,7
Best Practices	1,3
State-of-the-Art	1,2

Parameters Affecting Thermal Loads in Data Centers

The purpose of the cooling design, as in all cooling designs, is to balance the cooling capacity with the actual thermal load. This requires being able to accurately analyze and understand the thermal release of equipment in the designed data center. Even if all equipment is known, system design is wrong if all parameters affecting the design

are not handled correctly. The cooling design should be able to stabilize the temperatures of all equipment components (processors, memories, storage, I/Q, power supplies) within the data center within their specific operating temperature ranges. This range is generally below the high temperature limit and above the low temperature limit. The designed system should be able to take the necessary measures to balance the conditions. This ensures smooth operation of the system and data integrity. A well-designed system balances component temperatures, data center equipment performance, noise level, and power consumption. Conventional cooling designs are developed over the loads of all factors that can thermally affect the environment. If these factors are considered from the classical point of view, it can be said that the sun (radiation), walls, windows and roofs, air leaks (infiltration), people, lighting and heat emitted by devices. The power distribution ratios for the data center are given in Table 3.

Table 3. Plant Power (The Green Grid)

Electrical Loads	IT Loads	Air Conditioning	Others
Circuit	Telco Equipments	CRAC	Lightings
Distrubution	Network	Chiller	Heating
UPS	Servers	Condensers	BMS
Generator	Storage	Cooling Towers	Security
Battery		DX Systems	Fire F.
Backup Systems		Pumps	
% 10	% 50	% 36	% 4

In data center cooling calculations, most of the factors above have very minor effects besides the thermal loads, which we define as loads from devices. Since these places are designed in isolation for the purpose of use, they are almost not exposed to sun loads. The human and lighting factor in the environment is also effective only in exceptional cases. As can be seen from the table below, IT loads correspond to a 50% part in the evaluation made over the plant power. While classical cooling optimizations are developed based on hourly analysis and calculation of

different cooling needs according to time intervals, such an optimization study is not available for data centers. For example, when calculating the thermal loads for a public building, the time when the density of people in the environment is the highest (peak point) and the moment when the lighting loads are at the highest are not the same. In this case, these two loads are not added linearly when developing the cooling system. Because at the same time, these cooling loads will never overlap.

Considering this, design engineering has become more important than the development of calculations for data centers. It is not possible to predict the minimum demand and maximum demand points, even if the equipment loads vary in direct proportion to the operations performed. For this reason, the missing part in the system is that the cooling process can be carried out in a near-perfect manner rather than the correct calculation of the thermal loads. The fact that IT loads correspond to half of the facility power also supports this situation. The literature has also developed in this direction. Cooling system designs have changed and developed many times until today. The sensitivity of the equipment and the process-specific conditions have been influential in the development.

Environmental Factors

Temperature, Relative Humidity and Dew Point

The temperature parameter has a direct and indirect effect on the ambient internal temperature. In the indoor environment, solar radiation has a direct effect on thermal gains caused by conduction and convection. In addition, it has an indirect effect on the efficiency and cost of indoor cooling, as it will also be effective on the efficiency of systems that use air cooling. Moisture is the least noticeable and overlooked element in a data center that threatens the operation of hardware. Even some of the traditional managers prefer not to consider this element. Humidity, which is a measure of water vapor in the air, can be explained in two ways: absolute or relative humidity. Relative humidity is the actual amount of water vapor in the air. At the same time, it is the percentage ratio between the amount of water vapor that must be present in order for the air to be saturated with moisture at the same reference

temperature. For example, a relative humidity of 40% means that at this temperature, the air contains 40% of the maximum water vapor that it can saturate. Another concept is the dew point or dew point, which is the temperature at which the water vapor in the air transitions from the gaseous state to the liquid state, when the relative humidity is one hundred percent. In this case, the air is considered saturated. In a data center, relative humidity can affect devices in two ways. The first danger is the discharges experienced as a result of the formation of electrostatic differences. The possibility of electrostatic discharge occurs when humidity is at very low levels. In addition, this probability increases with lower temperatures. Electrostatic discharge is difficult for humans to understand and does not have major effects such as injury. But a difference of 10V is enough to damage the hardware. Another dangerous situation is corrosion. This can occur as a result of an electronic device getting wet and some form of condensation of water vapor in the air. For example: In a location with high humidity, the electronic components inside the data center elements may be damaged and data loss may occur. The main thing for data center air conditioning is to ensure that the devices operate at a humidity level where there is no possibility of electrostatic discharge and corrosion. For this, the optimal relative humidity range is between 40% and 55% (This value is also recommended by the TIA/EIA 942 standard.

Design Parameters

Location of Data Center

Although the design parameters appear in different ways, as an example, the world giant Apple has established a data center in the city of Prineville in the state of Oregon. The temperature hovers with an average below 10 degrees in half of the year. In the remaining half, average temperatures not exceeding 20 degrees significantly reduced data center cooling costs. Since the outside air temperatures are quite low in this region, cooling was carried out with free cooling. Apple has realized a solution by planning the plant power and cooling needs based on location. It will not be possible to change the power consumed by the equipment, factors such as human or lighting loads. For the plant, these conditions

will remain constant. However, by developing a design based on external weather conditions, it has achieved a suitable environment and low cost result.

Hardware Layout, Cabinet Number and Density, Hot-Cold Aisle Applications

The temperature of the air entering the IT equipment is an important criterion for the cooling process. From this point of view, various methods have been tried to obtain the desired air temperature.

Hot-Cold Corridor Design Using Raised Flooring

At first the units were designed to face in different directions, and it was soon realized that this was an inefficient design, mixing hot and cold air together. This has resulted in the operating cooling machine set-point being greatly reduced and cooling costs increasing disproportionately. Subsequently, all units were designed to face the same direction (Figure 6).

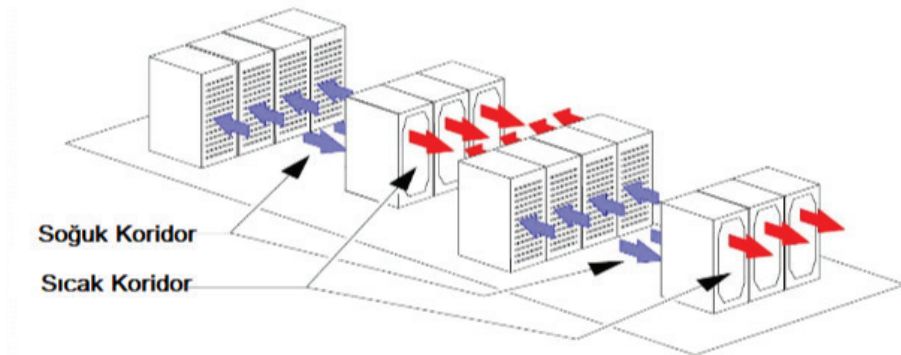


Figure 6. Application of Unit Facing the Same Direction

Although it is efficient compared to the previous settlement, similarly, the cold air supplied to the environment by the grills under the floor is mixed with the hot air to be expelled. In this case, the cold air warmed up before the floor cooling process could be completed. The

desired homogeneous temperature distribution could not be achieved at every point and malfunctions occurred in the servers.

As a solution to this situation, a hot and cold corridor design has been developed (Figure 7). Cold and hot corridors are formed by making the sides of the units to be kept cold facing each other. In this case, the cold air coming out of the grilles performed the necessary cooling process and this heated air was evacuated from where it rose. This situation increased the efficiency considerably, but it was not enough to achieve the desired cooling completely. There is still some mixing of hot and cold weather. A homogeneous separation has been achieved by the method of completely separating the hot and cold corridors by using the physical barrier, which is also frequently used today (Figure 8). Comparisons made in this section are based on cooling with precision control units (CRAC).

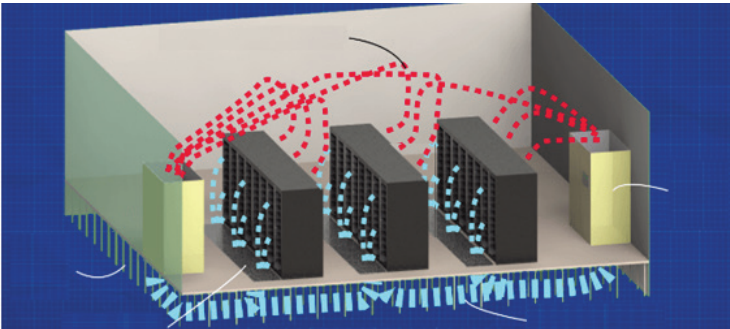


Figure 7. Hot Cold Corridor Application

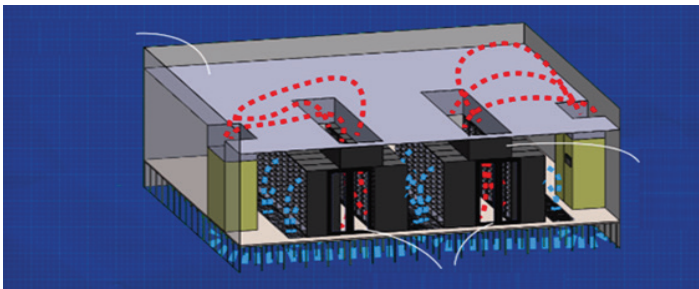


Figure 8. Physical Barrier Application

Cooling Close to the Heat Source

In the classical hot aisle/cold aisle design in the data center, the cooler loses energy until it reaches the source server cabinets. In close-coupled cooling, the chilled water or the refrigerant itself is provided as close as possible to the section where the cooling source is located, without leaving it into the environment until the racks where the servers are located. It is mounted very close to server cabinets. Air is blown directly into the rack without the cooling source air mixing with the air of the data center.

Insulation

Insulation is one of the important factors for the environment to be heated or cooled to maintain the current thermal situation for a longer period of time. If the data center is in an area with a very high outdoor temperature, insulating it from the outside environment will positively affect the efficiency. Today, rather than large data centers, small-scale institutions have data centers created to meet their own system requirements. By evaluating the operating temperature conditions of these centers, which are designed as a separate room in the building, it can be determined whether insulation is required between them and other spaces.

For data centers, insulation is made so that the system can work equally and correctly at every point in the section where the cooling process is performed. In addition, this system has a positive effect on efficiency. In order to prevent the possibility of mixing hot and cold air masses, the idea of separating hot and cold corridors from each other has emerged.

Cooling System Selection

The chosen cooling system can directly or indirectly affect the cooling process. Each cabinet can be cooled separately or the data center volume can be cooled completely. In this case, it will be more difficult to provide homogeneous cooling. A possible problem in the system may damage all hardware.

Air Flow Rate

Data centers vary in size and cooling loads. Based on the system cooling density (W/m^2), an optimum airflow rate must be determined for an accurate cooling design. The velocity of the cold air directly affects the cooling process. It leaves the environment in a cold way again, before it can leave the air temperature enough to the system faster than necessary. A slow air, on the other hand, may not provide the required cooling load at the appropriate speed and rate, and may cause hot air to accumulate near the equipment. Optimum velocities for the design are determined by examining the effects of air velocities on ambient temperature with computational fluid dynamics analyses. ASHRAE and various institutions have studies and standards on airspeeds. Air speed is determined to provide more comfort in room climates. Some definitions are used to set standards.

- *DR (Draught Rating): Percentage of people who are disturbed by drafts.*
- *PMV (Predicted Mean Vote): The estimated value showing how a defined thermal environment will be perceived by the majority of users according to the specified scale.*
- *PPD (Predicted Percentage of Dissatisfied): Estimated percentage of dissatisfied with indoor air conditioning*

The ASHRAE 55 Standard is based on the $-0.5 < PMV < +0.5$ requirement. According to this standard, it is seen that at least 5% of a group in an environment is not satisfied with the thermal aspect. As can be seen from Figure 9, this limit allows a maximum of 10% dissatisfaction. Therefore, if the PMV value is between the recommended -0.5 and $+0.5$, the PPD will be less than 10%.

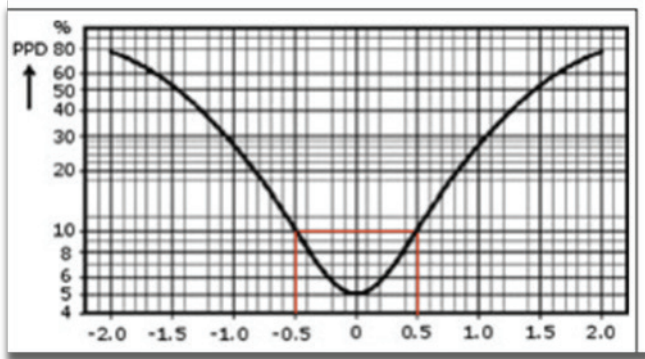


Figure 9. Thermal Sensation and Dissatisfaction Graph

The air velocity that will provide thermal comfort is found according to the NEN-EN-ISO 7730 standard. This standard allows a maximum DR value of 15%. It is essential that the turbulence intensity of the air velocity be measured to calculate the value of DR. Turbulence intensity is the bandwidth of true airspeed relative to the measured average airspeed. The allowable average air velocity is determined by the air temperature and turbulence density in Figure 10. The basic assumption is based on the assumption that 15% of those in the room may be disturbed. For example, in a room with a temperature of 25°C and a turbulence density of 10%, the allowable air velocity according to Figure 10 is 0.28 m/s; 0.23 m/s at 20% turbulence intensity; It is 0.18 m/s at 40% turbulence intensity and 0.16 m/s at 60% turbulence intensity. In the design for data centers, the healthy operation of the devices should be taken into consideration instead of comfort. This means the air velocity required to provide the set humidity value and the set temperature value. In air flow simulations, air velocities that can provide the appropriate temperature and humidity value for the data center area should be determined and the design should be carried out accordingly.

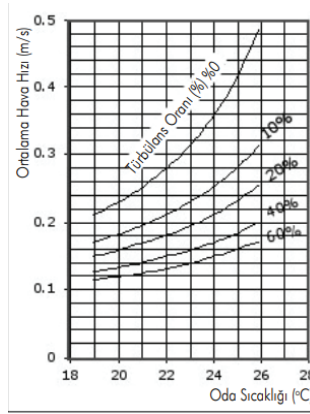


Figure 10. Room Temperature, Turbulence Rate and Average Air Velocity Graph

Pollution

The data center facility is generally well-designed and geographically designed in regions with relatively clean environments. Therefore, there are no concerns about contamination. However, the overall cleanliness of the environment is only one of the criteria for the location of a data center facility. This is usually not considered one of the most important issues. Some data center facilities may have harmful environments from the ingress of outdoor particulate and/or gas contamination. In some rare cases, contamination can also occur within the data center facility itself.

Air Conditioning Systems Used in Data Centers

It is possible to classify the systems used for data centers in various ways. These can be the heat transfer type, system of the indoor unit, the type of fluid used, or the heat transfer type and system of the outdoor unit.

Chilled Water System

Chiller and CRAH units work in this system. Computer Room Air Handling Unit (CRAH) unit works on a different principle with a Com-

puter Room Air Conditioning Unit (CRAC). It uses fans and chilled water coils to reject heat. Figure 11 shows the chiller and CRAH system.

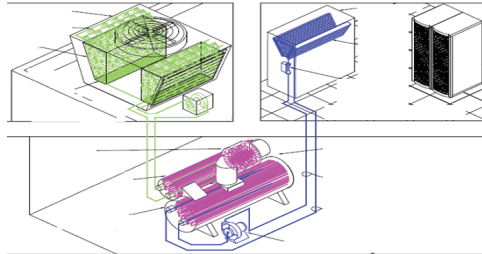


Figure 11. Chiller - CRAH Combined System

Pumped Refrigerant for Chilled Water Systems

There are 2 different liquid cycles in the system. The water cycle works between the chiller and the heat exchanger. The glycol cycle works between the cooler and the heat exchanger. The cooler in the room is glycol cooled. The glycol cycle is separated from the water cycle by a heat exchanger. The cycle runs continuously using pumps. Figure 12 shows how this system works.

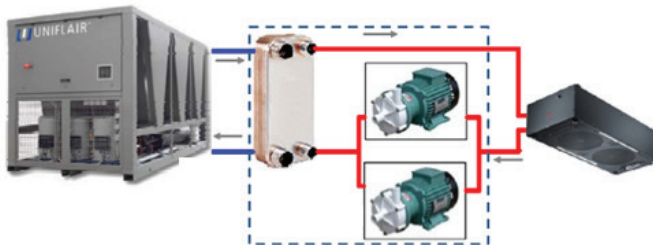


Figure 12. Chiller and Cooling Cycle Combined System Schematic Illustration

Air Cooled System (2-Piece)

The CRAC system works similarly to split air conditioners. Unlike the split system, the compressor is inside the CRAC unit. The CRAC unit transfers the heat from the room air to the refrigerant in the pipes. This

refrigerant discharges the heat to the outside with the condenser. The system show in Figure 13.

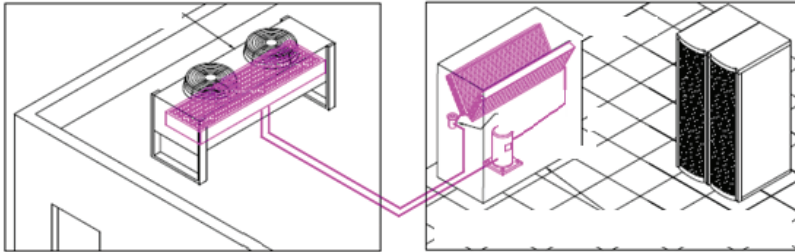


Figure 13. Schematic of Air-Cooled Condenser-CRAC Combined System

Glycol Cooled System

It is very similar to the air-cooled CRAC system. A small heat exchanger is used instead of large condenser coils. The heat exchangers and glycol pipes are quite small compared to the air-cooled system. Because glycol can transfer more heat than air. A pump is used to circulate the glycol. Figure 14 shows the glycol-cooled CRAC and dry cooler combined system.

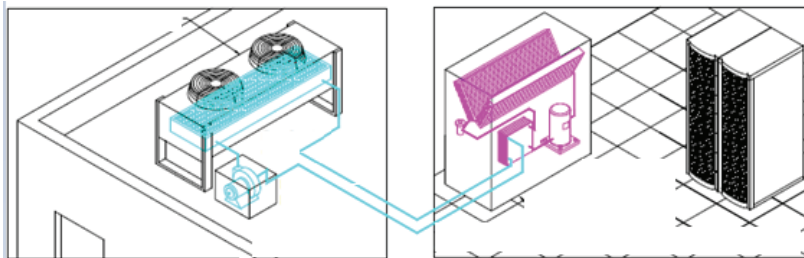


Figure 14. Demonstration of Glycol Cooled CRAC-Dry Cooler Combined System

Water Cooled System

If the CRAC unit is water-cooled and a cooling tower is added to the system, this system is called a water-cooled system. It is very similar to glycol cooled systems as all cooling components are contained within the CRAC unit.

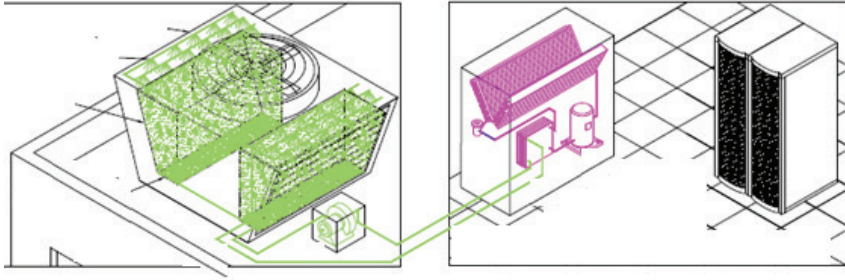


Figure 15. Demonstration Of Water-Cooled CRAC-Dry Cooler Combined System

Air Cooled Self Contained System (1-Piece)

The heat is transferred to the air and is removed directly from the IT room with ductwork. In case the system does not work, the backup system should be designed to cool this removed additional heat. Exhaust air should also be supplied from outside the computer room. This will prevent vacuum in the room. These systems are generally limited to 15 kW capacity. Air cooled self contained system is shown in Figure 16. Figure 17 shows an example of an air-cooled stand-alone system.

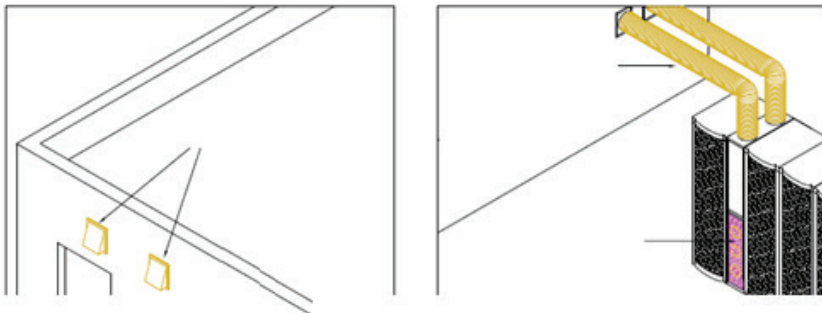


Figure 16. Schematic Illustration of Self-Running System with Air-Cooled Ducts



Figure 17. Air Cooled Self Contained & Portable Self Contained Cooling Unit

Direct Fresh Air Evaporative Cooling System

Direct fresh air evaporative cooling system is a system created with an evaporative cooler and duct system. The cooling system can be operated in two different ways as economizer and free cooling mode. In general, the DX air-cooled system is preferred for backup cooling systems in data centers. Evaporative system is most beneficial in dry climates. Figure 18 shows an example of a direct fresh air evaporative cooling system.

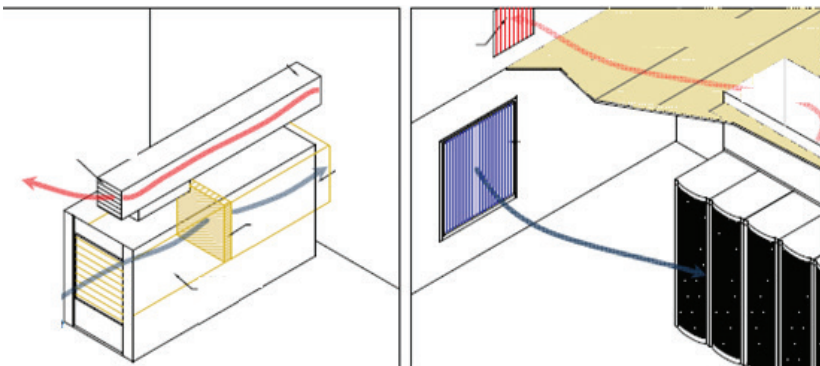


Figure 18. Types of Direct Fresh Air Evaporative Cooling System Equipment

Indirect Air Evaporative Cooling System

Indirect fresh air evaporative cooling system is a system created with an evaporative cooler and duct system. In this system, outside air is used for cooling. By using a heat exchanger, heat is transferred out

between the outdoor air and the air to be cooled in the data center. The heat exchanger separates the IT room. Evaporation support is also used in the system. Water is sprayed into the heat exchanger. An exemplary representation of an indirect air evaporator is shown in Figure 19. An example of a complete cooling system with this type of heat removal method is shown in Figure 20.

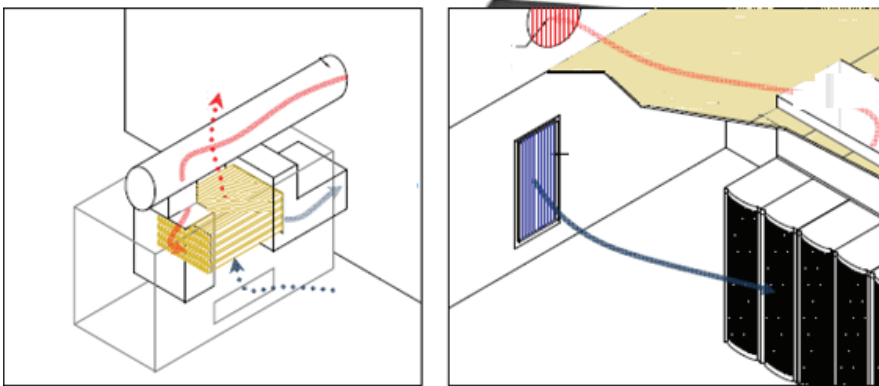


Figure 19. An Indirect Air Evaporator

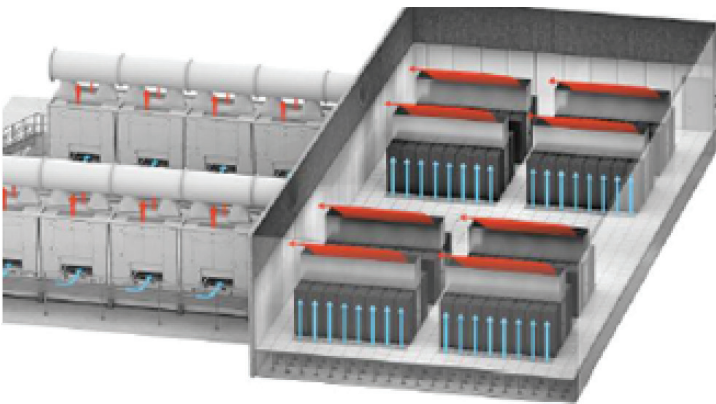


Figure 20. A Data Center Cooled by An Indirect Air Evaporator

Self Contained Rooftop System

It is a system installed with a package type rooftop unit and ductwork. Rooftop system is not traditional cooling system for new data centers. Figure 21 shows an example of a rooftop unit.



Figure 21. Rooftop Unit

Immersion Cooling

Servers or other IT components are immersed in a special liquid with a low boiling point, thermal conductivity but not electrical conductivity. Figure 22 shows the working principle of the 2-phase system. The boiling point of the Novec 7100 liquid used here is 61°C. The main reason for choosing a fluid with a low boiling point is to be able to boil at operating temperatures of the equipment without any problems. When the liquid surface layer reaches the boiling temperature, the vapor bubbles rise. With the help of the condenser placed at the top of the system, the excess heat in the rising steam bubbles is transferred to the fluid in the condenser. As a result, the vapor bubbles become liquid again and drip down with the help of gravity. The cycle continues like this. The immersed liquid can transfer its heat to another cycle with the help of a pump without any evaporation process. These types of systems are called single-phase systems (Liu and Yu, 2021).

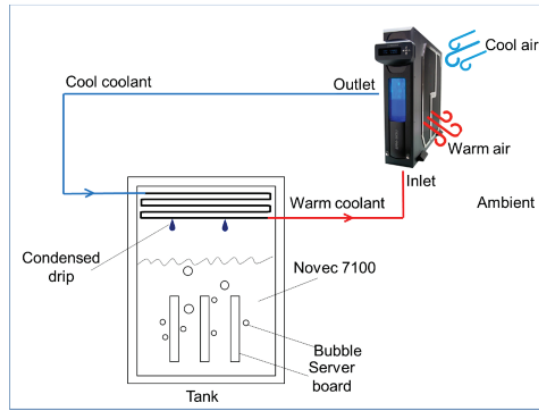


Figure 22. The Schematic of Immersion Cooling System

Carbon Emissions in Data Centers

In 2012, the electricity consumption of all data centers around the world was calculated as approximately 270 TWh. This rate corresponds to 1.4% of the total world electricity consumption. Considering the increasing need for data centers day by day; It is predicted that the energy consumption of data centers in 2030 will be 13% of the world's total energy consumption. Considering these analyzes and forecasts, it is an inevitable fact that energy consumption in data centers will create a big problem for the next 20 years (Sen, 2019). This consumption also reveals the importance of carbon emission rates for data centers. Figure 23 shows the carbon emission percentages by industry.

Figure 24 shows the comparison of carbon emission rates in data centers with the carbon emissions of some countries. Worldwide, the annual carbon emission value is approximately 30 billion tons, based on 2015 data.



Figure 23. Sector-Based Carbon Emission Percentages

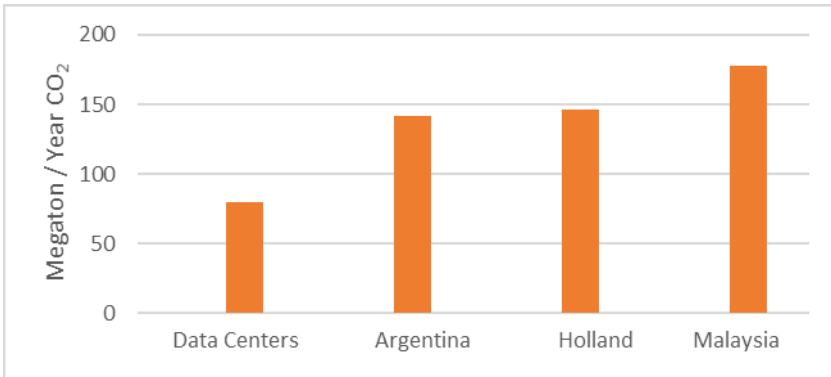


Figure 24. Country-Based Carbon Emission Percentages

In addition, according to the study conducted in 2007, the annual carbon emission amount, which was 80 million tons for the same year, is predicted to be 340 million tons for 2020 with a growth rate of 11% (Forrest et al., 2008).

EXAMPLE APPLICATION

Example Data Center Features

Figure 25 shows sample data center floor plan.

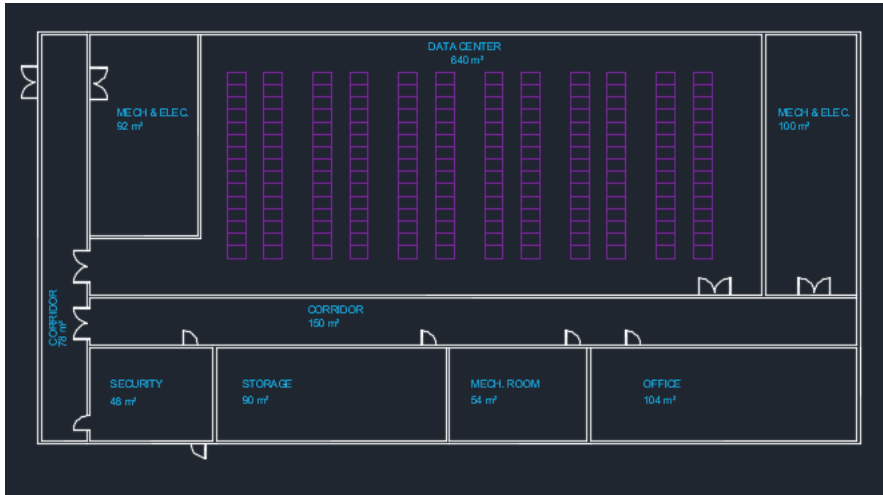


Figure 25. Sample Data Center Floor Plan

Table 4. Design Conditions for Data Center

Province	Adana
Summer Design KT Temperature	35,9°
Summer Design YT Temperature	23,8°
Winter Design KT Temperature	1°
Elevation	39m
Latitude, Longitude	37,00, 35,42
Floor Height	4,6m
Number of Cabins	180 units of 20 kW 42U Cabinet
Hourly Air Exchange Rate	0,1
Surface Absorption Ratio	0,45

Table 5. Cooling Setpoint Temperatures on Design

Location Name	Temperature [°C]	Moisture
Data Center	18-27	5.5°C DP with %60 RH and 15°C ÇN
Office Space	Summer Set Temperature:20°C Winter Set Temperature:24°C	%60
Security Room	Summer Set Temperature:20°C Winter Set Temperature:24°C	%60

Table 6. Total Heat Transfer Coefficients

Structural Element	U (W/m ² K)	SHGC
Earth Contact Flooring	0,6278	-
Roof	0,45	-
Interior Wall	0,37	-
Outer wall	0,38	-
Window	1,8927	0,65

Cooling Load Analysis

Loads from the External Walls

External wall cooling loads of the data center volume were calculated using 4 different software. The heat gain values provided from the south facade are given in Figure 26. It has been observed that the calculation values vary for the outer walls. In addition, additional loads from thermal bridges can be calculated with the Cypetherm Loads software. For this study, this value was calculated as 327 W. The external wall cooling loads comparison chart is given in Figure 26.

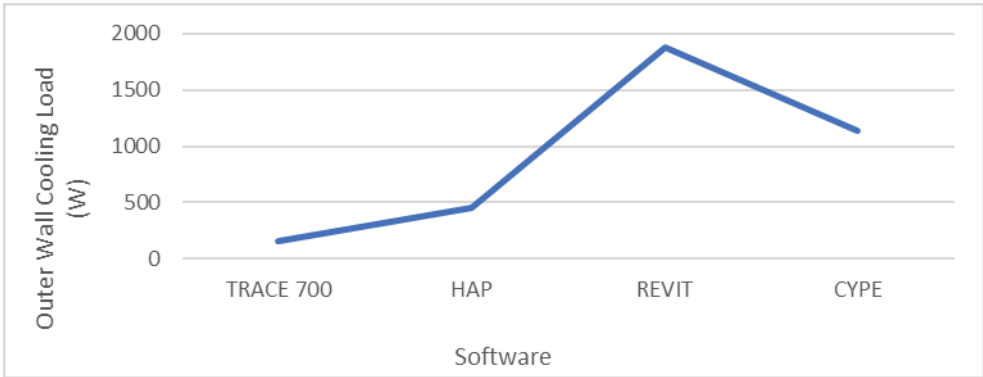


Figure 26. Comparison of Cooling Loads

Loads From the Interior Walls

The thermal loads gained from the interior are calculated and shown in Figure 27. It has been observed that the inner wall calculation values are more stable for all four software compared to the outer wall values. The internal wall cooling loads comparison chart is given in Figure 27.

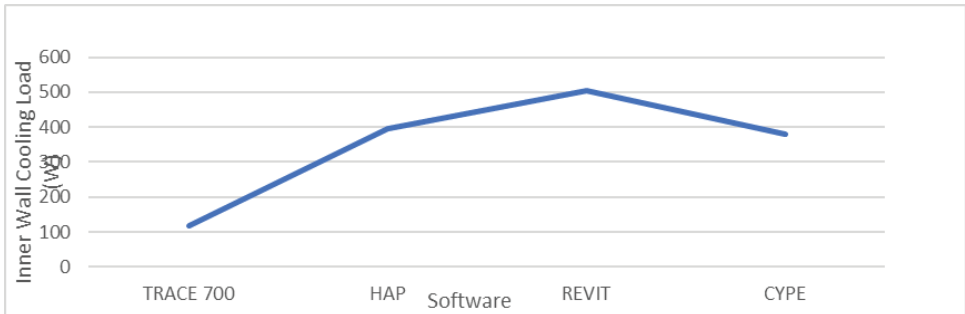


Figure 27. Loads from the Interior Walls

Loads From the Roofs

The thermal loads gained from the roofs are calculated and shown in Figure 28. It has been observed that the cooling value calculated as 670 W in the Trace 700 software is lower than the other 3 software. In addition, it has been observed that the loads for the other 3 software are calculated close to each other.

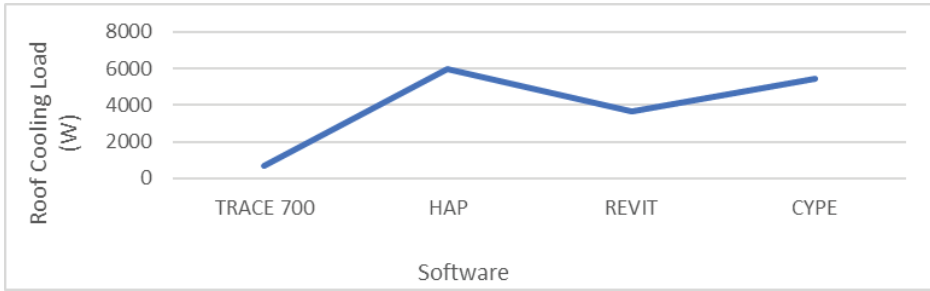


Figure 28. Loads From the Roofs

Standard Analysis

Revit and Cyptherm Loads software use RTS method, HAP, Transfer Function method, Trace 700 software uses TETD-TA1 method. In line with the results obtained, it has been observed that the values are closer to each other among the software using the same calculation methods, and the values diverge as different standards and methods are used. Data center total cooling load calculations according to calculation methods are shown in Figure 29.

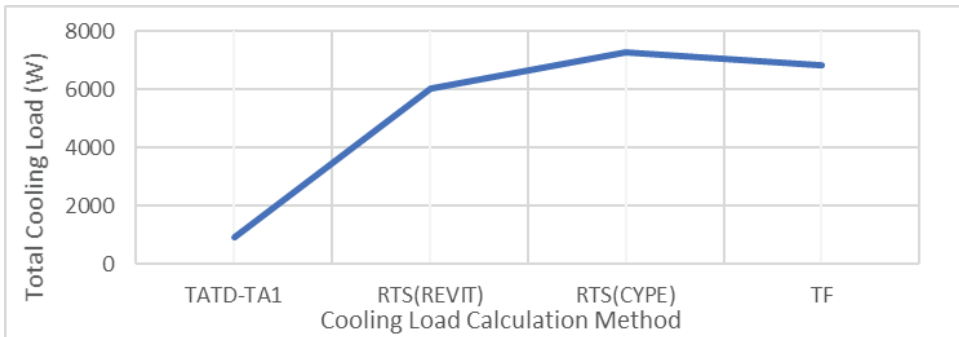


Figure 29. Average Cooling Loads According to Mathematical Methods

Comparison of Device Loads and Other Thermal Loads

The cooling of data centers is the volume where the cooling need is too high considering the cooling per square meter compared to the comfort cooling process. 180 units of 20kW 42U cabinets created a total cooling load of 3.6 MW. The unit cooling load per square meter for the data center, which is considered to be 640 m² for the project, is 5625 W. When

the other thermal loads are averaged across all software, it has been observed that only 10.3 W per square meter of cooling load is created.

BIM Based Softwares

It has been observed that when BIM-based software is used, it is not necessary to define the relations of the spaces with each other separately. In addition to the physical model, the software was able to calculate these relationships with the help of the information built on the physical model and used them in cooling load calculations. For example, in an account to be made with HAP, the user must enter the outer wall area of a place. However, when BIM-based software such as Cypetherm Loads or Revit is used, the necessary information is processed on this wall while creating the architectural model. If the concept of information modeling is considered for any wall object, it means creating a meaningful physical model by processing some information into it. The software will obtain the outer wall area from the created physical model and continue the calculations. It will also be able to do this for all other objects that will affect the calculation. Since the physical state of the architectural model can be followed instantly by the user, a possible error can be easily noticed. In this case, the number of data to be entered will be much less. However, this situation reveals the necessity of making the right definitions while creating the model. A wall that is not defined as an external wall will cause the heat loss calculation to be less than the actual calculation value. All the observations here support the previous studies in the literature on the concept of BIM. The observed data are presented in Figure 8 and Figure 9.

BIM provides very serious reductions in construction costs and durations, although it causes small increases in project costs and durations. The graphical representation between the effort spent and the accuracy of the process for BIM-based software is given in Figure 30. The graphical representation between the effort spent and the accuracy of the process for non-BIM-based software is given in Figure 31.

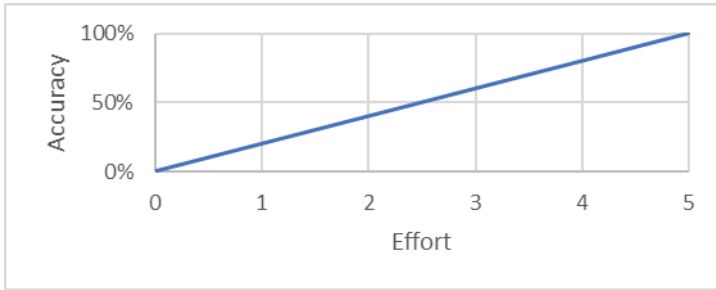


Figure 30. Accuracy in BIM-Based Software

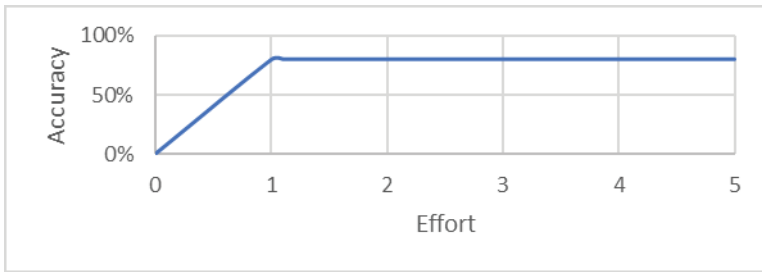


Figure 31. Accuracy in Non-BIM Software

Carbon Footprint

For the data center we have designed, it is calculated that 4093 tons of carbon dioxide gas will be released annually by accepting the PUE efficiency value of 2, and an IT hardware power of approximately 400 kW. By accepting the same efficiency rates, it has been calculated that approximately 716,219 tons of carbon dioxide emissions are made annually for the data centers in Turkey, taking into account the critical IT power of the data centers established in 2015. Comparing the carbon emission values of the existing installed data center in Turkey with the carbon emission values throughout the country will not yield any significant results due to the low installed capacity in our country. For this reason, the comparison was made over the CO₂ emission values of Turkey and the emission values of all data centers in the world. The emission values of data centers in the world and Turkey's total emission values are compared in Figure 32.

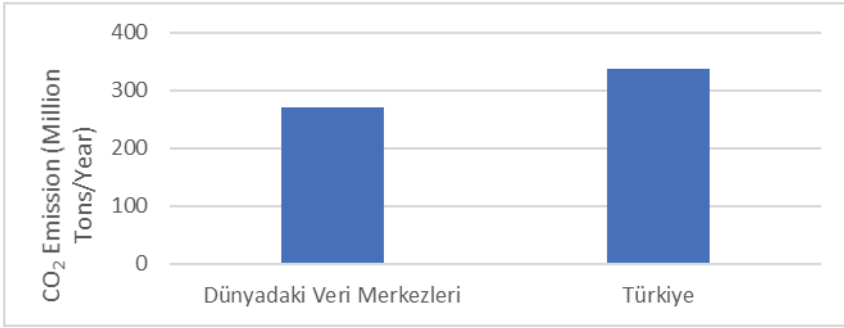


Figure 32. Turkey’s Carbon Emission Values and Data Centers in the World

While the electricity consumption of data centers all over the world was 203 TWh in 2007, the carbon emission value produced was 80 million tons. Annual electricity consumption values calculated with the assumption of 10.4% compound annual growth rate are given in Figure 33. The annual carbon emission values calculated by assuming a compound annual growth rate of 11% are given in Figure 34.

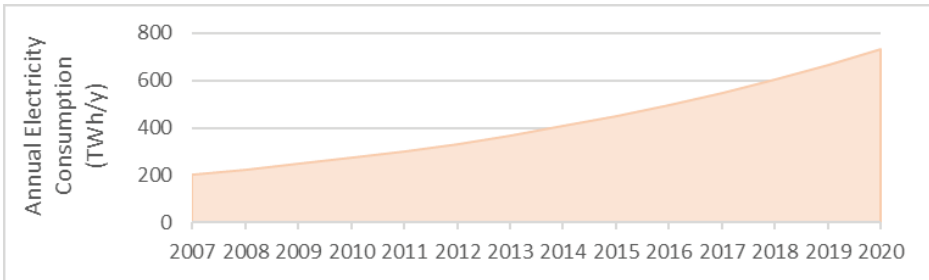


Figure 33. Electricity Consumption of Data Centers by Years

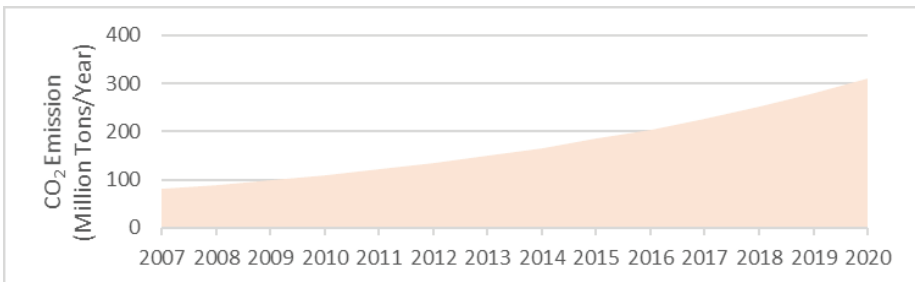


Figure 34. Carbon Emission Values of Data Centers by Years

The annual electricity consumption values and carbon emission values calculated for the next 5 years, assuming the same compound annual growth rates, are given in Figure 35 and Figure 36.

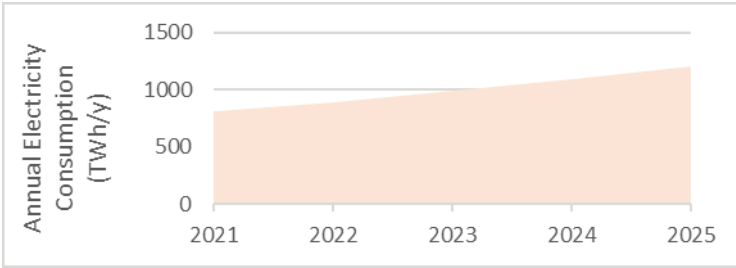


Figure 35. Estimated Electricity Consumption of Data Centers for the Next 5 Years

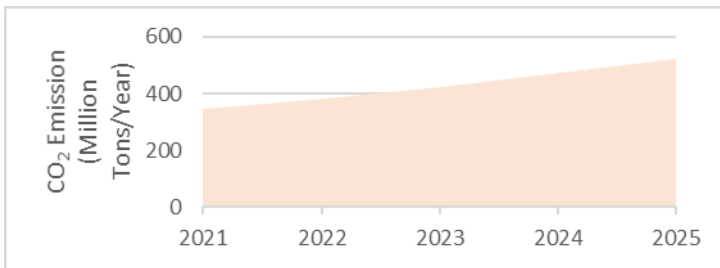


Figure 36. Estimated Carbon Emission Values of Data Centers for the Next 5 Years

RESULTS

In the study, it was predicted that a possible data center planned to be established for Turkey could be established in Ankara and Eskişehir provinces. Considering the electricity infrastructure, internet infrastructure and external weather conditions, installations can be made in cities similar to the ones foreseen.

It has been concluded that the necessity of making all data entries manually in non-BIM-based software for cooling calculations increases the margin of error. Working on the process data entry for a longer time may increase the accuracy of the calculations to some extent. In BIM-based software, the margin of error will be reduced to zero in direct pro-

portion to this effort. However, it has been concluded that this calculation process will take longer as the information modeling will be done in the building together with the physical model.

In the studies conducted for the data of 2015, it was concluded that the carbon emission rates of the data centers have a very serious effect on the total carbon emission rates in the world, and this effect will be much greater in the coming years with the ever-increasing demands.

It has been calculated that the total amount of carbon emissions from the data centers in Turkey is 0.22% of the total amount of carbon emissions in the country. Although this value may seem low, the main reason is that the total installed data center capacity in our country is much less than the total data center capacity worldwide. When this comparison is made for the 2015 data worldwide, it has been determined that this rate is around 1%. Compared to the world average, our country has 1/5 less data center installed capacity.

Calculations on data center electricity consumption values and carbon emission values, based on annual growth rates for the past ten years, have revealed the importance of efficiency studies to be carried out.

REFERENCES

AlHarbi, F., AlRomaih, A., AlHudaithi, S., AlHusayyani, A., AlQadhi, T., Alsagri, A.S., Alateyah, A.R., Basha, M.S., (2019). Comparison of Cooling Load Calculations by E20 and HAP Software. *Universal Journal of Mechanical Engineering*, 7(5), 285-298. <https://doi.org/10.13189/ujme.2019.070505>

Alkan, F., Kürekci, N.A., Çubuk, H. (2017). Comparison of Heating-Cooling Systems for a Sample Building. *MMO Journal of Plumbing Engineering*, 162, 5-19.

Crawley, D. B., Hand, J. W., Kummert, M., Griffith, B. T. (2008). Contrasting the Capabilities of Building Energy Performance Simulation Programs. *Building and Environment*, 43(4), 661-673. <https://doi.org/10.1016/j.buildenv.2006.10.027>

Erden, H.S. (2013). Experimental and Analytical Investigation of the Transient Thermal Response of Air Cooled Data Centers, MSc Thesis, Syracuse University, Syracuse, NY, U.S.A, 1-3.

Forrest, W., Kaplan, J., Kindler, N., (2008). Data Centers: How to Cut Carbon Emissions and Costs. *McKinsey on Business Technology*, 14, 4-13.

Gözcü, O. (2019). Energy Savings and Economic Potential Assessment of Economizer Use for Cooling Data Centers in Turkey's Climate Conditions. MSc. Thesis, ITU Graduate School of Science Engineering and Technology, Istanbul, Turkey, 1-3.

Hassan, S.F., Ali, M., Sajid, A., Perwez, U., (2015). Free Cooling Investigation of SEECs Data Center. *Energy Procedia*, 75, 1406-1412. <https://doi.org/10.1016/j.egypro.2015.07.233>

Huang, J., Chen, C., Guo, G., Zhang, Z., Li, Z., A (2019). Calculation Model for Typical Data Center Cooling System. *Journal of Physics: Conference Series*, 1304, 012022. <https://doi.org/10.1088/1742-6596/1304/1/012022>

Kanbur, B.B., Wu, C., Fan, S., Tong, W., Duan, F. (2020) Two-phase Liquid-immersion Data Center Cooling System: Experimental Performance and Thermo-economic Analysis. *International Journal of Refrigeration*, 118, 290-301. <https://doi.org/10.1016/j.ijrefrig.2020.05.026>

Kang, T.W., Choi, H.S. (2018). BIM-based Data Mining Method considering Data Integration and Function Extension. *KSCE Journal of Civil Engineering*, 22(5), 1523-1534. <https://doi.org/10.1007/s12205-017-0561-6>

Kürekci, N.A., Kaplan, S. (2014). Heating-Cooling Calculations with HAP and Revit Softwares. *Journal of Plumbing Engineering*, 141, 5-15.

Ling, L., Zhang, Q., Zeng, L. (2017). Performance and Energy Efficiency Analysis of Data Center Cooling Plant by Using Lake Water Source. *Procedia Engineering*, 205, 3096-3103. <https://doi.org/10.1016/j.proeng.2017.10.313>

Liu, C., Yu, H. (2021). Evaluation and Optimization of a Two-Phase Liquid-Immersion Cooling System for Data Centers. *Energies*, 14, 1395. <https://doi.org/10.3390/en14051395>

Mok, S., Kumar, S., Hutchins, R.R., Joshi, Y.K. (2016). Impact of a Rotary Regenerative Heat Exchanger on Energy Efficiency of an Air Cooled Data Center, 15th IEEE Intersociety Conference on Thermal and Thermomechanical Phenomena in Electronic Systems (ITHERM), May31-Jun 03, San Diego, USA.

Oranlier, B., Eyriboyun, M. (2009). A Software for Calculating Heat Gain for Air Conditioning, IX. National Plumbing Engineering Congress, 6-9 Mayıs, Izmir, Turkey.

Pan, Y., Yin, R., Huang, Z., (2008). Energy Modeling of Two Office Buildings with Data Center for Green Building Design. *Energy and Buildings*, 40, 1145-1152. <https://doi.org/10.1016/j.enbuild.2007.10.008>

Rey, F. J., Velasco, E., Varela F. (2007). Building Energy Analysis (BEA): A Methodology to Assess Building Energy Labelling. *Energy and Buildings*, 39, 709-716. <https://doi.org/10.1016/j.enbuild.2006.07.009>

Şen, E. (2019). Methods For Improving Data Centers Energy Efficiency. MSc. Thesis, ITU Energy Institute, Istanbul, Turkey, 71-72. 43-44.

Türkmen, İ. (2019). Experimental Investigation of UHEM Data Center Termal Profile and CFD Analysis. MSc. Thesis, ITU Graduate School of Science Engineering and Technology, Istanbul, Turkey, 1-2.

VanGilder, J.W. and Zhang, X. (2014). Cooling Performance of Ceiling-Plenum-Ducted Containment Systems in Data Centers, 14th IEEE Intersociety Conference on Thermal and Thermomechanical Phenomena in Electronic Systems (ITHERM), 27-30 May, San Diego, USA.

Waddell, C., Kaserekar S., (2010). Solar Gain and Cooling Load Comparison Using Energy Modeling Software, Fourth National Conference of IBPSA-USA, 11 - 13 August, New York, USA.

Yavuz, H. (2010). The Comparison of CLTD/CLF and RTS Methods in Heat Gain Calculations. MSc. Thesis, ITU Graduate School of Science Engineering and Technology, Istanbul, Turkey, 111-113.

ASSESSMENT ON OPERATING INLET PRESSURE HEAD FOR IRRIGATION SUBMAINS INCORPORATING DIFFERENT TYPES OF PRESSURE PROFILES-II: DESIGN APPLICATIONS

Gürol YILDIRIM¹

Abstract: Operating inlet pressure head, H_{01} , is a major hydraulic parameter for hydraulically-efficient design and evaluation of pressure head distribution along the line. The energy-gradient ratio (EGR) approach is a useful tool to identify first which type of pressure profile occurs for a given uniform design slope with other hydraulic variables initially known; then, comprehensively evaluate its definite hydraulic characteristics along the line. Knowing the hydraulic properties for any type of pressure profile regarded enables to the design engineer to evaluate pressure parameters through the line sections in a simple way. The procedure is simplified by regarding the localized head loss along the pipe but neglecting the change in kinetic head. The present technique is simple, direct, and sufficiently accurate for a wide range of water application uniformity, and can be efficiently implemented for different types of pressure head profiles for different line slope situations, without requiring any additional hydraulic variables (pipe inner diameter, pipeline total inlet discharge, required average outflow, downstream end pressure head, total friction drop or outlet hydraulic characteristics).

Keywords: Design, Hydraulics, Inlet Pressure, Pressure Profiles, Uniformity

¹ Giresun University Rectorate, Engineering Faculty, Civil Eng. Dept., Head of Hydraulics Division, Giresun, Turkey. E-mail: gurol.yildirim@giresun.edu.tr; yildirimg3@itu.edu.tr, Orcid No: 0000-0003-1899-5379

INTRODUCTION

Practitioners are often faced with three types of problems in most usually design cases. In the first type of problem (pressure head profile determination), for a given design value of uniform pipe slope, S_0 and required average outlet pressure head, \bar{H} , unknown hydraulic characteristics along pressure head profile [operating inlet pressure head (H_{0I}), downstream closed end pressure head (H_d), extreme pressure heads (H_{max} and H_{min}) with their positions along the line (i_{max} , i_{min} ; i : percentage of length, l is a length from the inlet in m, and L is the total length of the submain line in m), and the total energy drop due to friction $h_{f(L)}$], can be determined ensuring the desired level of water application uniformity as well as allowable pressure head variation along submain line (Yıldırım 2007).

In the second type of problem (water application uniformity evaluation), when H_{0I} is given as an input parameter together with required average outlet pressure head (\bar{H}) and for a given design slope (S_0), the proper values of required uniformity patterns (U_C, D_U, CV_q, E_U) can be directly approximated (Yıldırım 2008). In the third type of problem (direct sizing procedure), required parameters are the pipe diameter (D) or length (L) for a given design slope (S_0), desired level of water application uniformity, and required average outlet pressure head (\bar{H}), with the remaining hydraulic parameters as design variables (Yıldırım 2006).

The main objective of this paper is to develop a procedure to solve the first and second types of design problems, based on improved Energy Gradient Ratio (EGR) approach which is an improvement on the previous mathematical development (Yıldırım 2008) utilizing analytical approaches (Yıldırım 2006, 2007) and which covers different types of pressure head profiles (Type-I, Type-II.a, Type-II.b, Type-II.c and Type-III) (Gillespie et al. 1979, Wu et al. 1983, Barragan and Wu 2005) under different uniform line slope situations, while determining values of pressure parameters ($H_{0I}, H_d, H_{max}, H_{min}, h_{f(L)}, \Delta H_{max}$).

The proposed procedure incorporates simple mathematical formulations encompassing different uniformity patterns for water

application, such as Christiansen's uniformity (U_C), lower-quarter distribution uniformity (D_U), coefficient of variation of outflows (CV_q), emission uniformity (E_U), and fraction of the required average pressure head (δ_H).

The procedure is simplified by regarding the localized head loss along the pipe line but neglecting the change in kinetic head. The proposed methodology is found to be simple, sufficiently accurate, and can be used efficiently for different types of pressure profiles in different line slope situations. It offers considerable flexibility by directly computing values of the required hydraulic variables along the energy profile, incorporating different uniformity patterns and without requiring any additional hydraulic variables, such as pipe diameter, total inlet discharge, required average outflow, downstream end pressure head, total friction drop or outlet characteristics.

STEPS of ALGORITHM

For the sake of comparison between the formulations derived for design parameters [the friction slope, S_f , fraction of the required average pressure head, δ_H , and multiplication factors (α and β^*) for operating pressure], regarding the five types of pressure profiles (*Type I, Types II.a, II.b, II.c* and *Type III*), all formulations are synthesized and are shown in Table 1. Before starting the present algorithm, the following input data for hydraulic variables are assigned in advance to finally evaluate the required pressure parameters along the profile.

Input (initially known) parameters: S_0 : pipe slope which is assumed to be uniform along the line (%), L : total length of the submain line (m), \bar{H} : required average pressure head (m), (U_C , CV_q , E_U or D_U): uniformity parameters for the desired level of water application uniformity (%), l_e : equivalent length (m) to determine the enlargement factor (F_s), s and x : outlet spacing (m) and outlet discharge exponent, respectively.

Output (required) parameters: S_f : the friction slope (or the slope of EGL) (%), $K_S = S_0/S_f$: the dimensionless "energy-gradient ratio", which primarily identifies the type of pressure profiles, $h_{f(L)} = S_f \times L$: the total friction drop at the end of line (m), H_{max} , H_{min} : the extreme pressure heads

(m) with their locations (i_{max} , i_{min}), ΔH_{max} : the maximum allowable pressure head difference along the line (m), $\delta_H = \Delta H_{max} / \bar{H}$: the fraction of the required average pressure head (%), $\phi_H = \Delta H_{max} / h_{f(L)}$: the relative maximum pressure variation (%), α and β^* : the multiplication factors to the operating inlet pressure (H_{0i}), H_{0i} and H_d : the operating inlet and downstream end pressure heads (m), respectively, and β : nonuniform outflow exponent to evaluate the nonuniform outflow distribution along the line. Based on the present improved EGR approach, the following calculation steps are implemented, respectively, using the related formulations for each type of pressure profile.

(a). For a desired value of the uniformity coefficient (U_C , CV_q , E_U or D_U), and the outlet discharge exponent (x), the related dimensionless physical numbers (λ_1 , λ_2 , λ_3 or λ_4) are computed from Eq. (9) in the companion paper; and for a given value of required average pressure head (\bar{H}) and the total length of submain line (L), the dimensionless physical number, λ_5 , is also computed (see, Table 1 in the companion paper).

(b). Select the proper formulation for S_f in accordance with the given design slope (S_0) condition [zero ($p = 0$), upslope ($p = 1$), or downslope ($p = -1$)]. Then S_f is evaluated, depending on dimensionless physical numbers (λ_1 , λ_2 , λ_3 , λ_4 and λ_5), and certain values of design coefficients (k_1 , k_2 , k_3 , k_4 and k_5).

(c). Compare the friction slope (S_f) to the uniform pipe slope (S_0) with respect to the design intervals of the energy-gradient ratio ($K_S = S_0/S_f$), and make a decision about the type of pressure profile depending on the K_S value assigned in **Step (b)**. It should be noted for downslope condition, as an initial computation, the S_f formulation given for the pressure profiles Type II.c and Type III is first used; then if a negative value of S_f is reached, this would indicate that S_f is greater than the pipe slope, S_0 ; that means the formulation for S_f deduced for Type II.a profile should be used (see, Table 1 in the companion paper).

(d). For the type of pressure profile assigned in **Step (c)**, select the proper formulation to evaluate the percentage of the required average pressure head (δ_H). Then, compute the total friction drop, $h_{f(L)}$.

(e). For the type of pressure profile decided on above, compute multiplication factors (α and β^*) for the operating inlet pressure head (H_{0i}), depending on the dimensionless physical numbers ($\lambda_1, \lambda_2, \lambda_3, \lambda_4$ and λ_5) and certain values of design coefficients ($c_1, k_1, k_2, k_3,$ and k_4) from Table 1. Then, evaluate the operating inlet pressure head (H_{0i}) from Eq. (22) (in the companion paper), for both the design cases (considering or neglecting local losses).

(f). For the above type of pressure profile, determine the extreme pressure heads (H_{max}, H_{min}) with their positions along the line (i_{max}, i_{min}), and evaluate the maximum allowable pressure head difference (ΔH_{max}) to check the value of δ_H computed from **Step (d)**. Then, determine the relative pressure variation ($\phi_H = \Delta H_{max} / h_{f(L)}$) (see, Table 1 in the companion paper).

(g). Compute the downstream end pressure head (H_d) from the conservation of energy principle or the related analytical equations derived for each type of profile. Then, set the order of operating inlet (H_{0i}), downstream end (H_d), extreme (H_{max}, H_{min}) and required average (\bar{H}) pressure heads to check the identity for the assigned type of pressure profile from **Step (c)**.

(h). Introduce the value of S_f previously determined in **Step (c)** into analytical Eq. (3a) or Eq. (3b) (in the companion paper) to reveal the certain form of the pressure head profile along the line. Then, check the identity of the specific hydraulic characteristics between the certain and assigned pressure profiles, with regard to Table 1 (in the companion paper).

. Note that if a higher precision is required, the nonuniform outflow distribution along the line should be taken into consideration. For this case the nonuniform outflow exponent, β is evaluated from Eq. (4) (in the companion paper) depending on the values, $S_0, x, L, \bar{H}, F_s,$ and S_f [determined from **Step (b)**]. Then substituting into Eqs. (3a) or (3b), **Steps (f)~(h)** are repeated to evaluate the nonuniform outflow distribution.

(i). For water application uniformity evaluation, Eqs. (35a)~(36b),

can be used. For Type I (upslope: $K_S < 0$), Type II.a (gentle downslope: $0 < K_S < 1$), Type II.c (nearly-steep downslope: $1 < K_S < 2.75$) and Type III (steep downslope: $K_S \geq 2.75$) profiles, use Eq. (32b); and for Type I (zero slope: $K_S = 0$), and Type II.b (efficient downslope: $K_S = 1$) profiles, use Eq. (33b) to compute dimensionless physical number, θ , then substitute the θ value into Eq. (32a), and finally evaluate the proper values of required uniformity parameters (U_C , D_U , CV_q , E_U or δ_H), respectively (please see in the companion paper).

DESIGN APPLICATIONS on DIFFERENT TYPES of PRESSURE HEAD PROFILES and VARIOUS DESIGN CONFIGURATIONS

In order to demonstrate the applicability of the proposed improved EGR approach to compute the required pressure parameters along the energy-grade line (EGL), the systematic comparative analysis (Tables 2, 3 and 4), covering various design configurations for a wide range of water application uniformity, U_C , and for a large range of uniform line slope situations regarding three outlet discharge exponents ($x = 0.2, 0.5$ and 1.0), the following simple data are originally selected, herein, from the literature (Hathoot et al. 1993), without needing further input data for the required hydraulic variables: The total length of the submain line is 151 m ($L = 151$ m), and the required average pressure head is 7.2 m ($\bar{H} = 7.2$ m), considering the turbulent flow condition through the pipeline (the velocity exponent, $m = 1.75$ for the DW equation). For simplification, the uniform outflow concept ($m_\beta = m$, $\beta = 1$) is considered, the kinetic head change ($H_{VI} \cong 0$), and the local head losses ($F_S = 1$) are neglected.

Application-I: Determination of Friction Slope (S_f), Type of Pressure Profile, and Related Pressure Parameters along Energy-Grade Line (EGL) for Various Line Slope Situations

Using the data presented above ($L = 151$ m, $\bar{H} = 7.2$ m), the required hydraulic characteristics along the energy-gradient line (EGL) [S_f , K_S , H_{0L} , H_d , H_{max} , H_{min} , $h_{f(L)}$, ϕ_H] for a large range of uniform line slope situations examined ($S_0 = 0, \pm 0.5, 1.0, 1.5, 2.0, 2.5, 3.0, 3.5, 4.0, 4.5$ and 5.0%), and for a wide range of water application uniformity coefficient, U_C , ranging from 67% to 99%, regarding three outlet discharge exponents ($x = 0.2, 0.5$

and 1.0), are computed and tabulated in Tables 2, 3 and 4, respectively.

As shown in Table 2, for zero and uphill slope situations examined, *Type I* profile is identified in which the maximum pressure head is always at the upstream end (inlet) ($H_{0l} = H_{\max}$) whereas the minimum pressure is located at the downstream closed end ($H_d = H_{\min}$). Note that for *Type I* profile ($K_S \leq 0$), multiplication factor, α , to compute the operating inlet pressure head (H_{0l}), yields greater values than 1.0, for all performed simulations.

As shown in Table 3, three types of pressure profiles (Types II.a, II.c and III) are clearly identified for various downhill slope cases examined ranging from -0.5% to -5%, depending on the design intervals of the energy-gradient ratio, K_S . For downslope values $S_0 = -0.5\%$, -1.5% , -2% , -2.5% and -3% , *Type II.c* profile ($1 < K_S < 2.75$) is observed, since α yields smaller values than 1.0. In this type of profile, for $S_0 = -0.5\%$, the operating inlet pressure head, H_{0l} is approximately equal to the required average pressure head ($H_{0l} \cong \bar{H} = 7.2m$), and proportionally decreases ($H_{0l} < \bar{H} = 7.2m$) as the α values decreases for $S_0 = -1.5\%$, -2% , -2.5% , -3% . The location of minimum pressure head (i_{\min}) is observed near the upstream section ($i_{\min} = 0.04 \sim 0.39$).

Similarly, for the downslope $S_0 = -1\%$, *Type II.a* profile ($0 < K_S < 1$) is observed. In this slope case ($S_0 = -1\%$), the operating inlet pressure head, H_{0l} is higher than the required average pressure head ($H_{0l} > \bar{H} = 7.2m$) since the α yields greater values than 1.0. The location of minimum pressure head (i_{\min}) is observed near the downstream section ($i_{\min} \cong 0.70$).

For the downslope values, $S_0 = -3.5\%$, -4% , -4.5% and -5% , *Type III* ($K_S \geq 2.75$) profile is observed since α yields smaller values than 1.0. The result practically means that the operating inlet pressure head, H_{0l} proportionally decreases with decreasing α , and reaches minimum values as the downslope increases from -3.5% to -5% . The minimum pressure head is located at the pipe inlet ($H_{0l} = H_{\min}$), whereas the maximum pressure head is located at the downstream closed end ($H_d = H_{\max}$). Note that the steps of the whole computation based on the EGR approach are illustrated on the sample design example, and

presented in *Appendix-I*.

Application-II: Determination of Energy Grade Line (EGL), Efficient Friction Slope (S_f) and Related Pressure Parameters to Achieve "Ideal Hydraulic Design" for Efficient Downslope (Type II.b Profile)

To achieve "the most efficient" pressure profile or "the ideal hydraulic design" case, using the data in Application-I ($L = 151$ m, $\bar{H} = 7.2$ m), the required hydraulic characteristics along the energy-gradient line (EGL) [$S_f, K_S, H_{0l}, H_d, H_{max}, H_{min}, h_{f(L)}, \phi_H$] for a large range of uniform efficient-downslope situations examined ranging from -0.4% to -2%, and for a wide range of water application uniformity coefficient, U_C , ranging from 81.0% to 99.3%, regarding three outlet discharge exponents ($x = 0.2, 0.5$ and 1.0), are computed, as presented in Table 4.

As shown in Table 4, *Type II.b* ($K_S \cong 1.0$) profile is clearly observed since the energy-gradient ratio is nearly equal to 1.0, that means the uniform pipe (S_0) slope is nearly equal to the friction slope (S_f). From the examination in this table, an important characteristic of Type II.b profile in which $S_0 = S_f$ is clearly proved for all performed simulations. The operating inlet pressure head is little higher than the required average pressure head, since the multiplication factor, α , to compute the operating inlet pressure head (H_{0i}), is little higher than 1.0. The location of minimum pressure head (i_{min}) is observed along the upstream section ($i_{min} \cong 0.43 \sim 0.45$), and the design parameter for maximum relative pressure variation, ϕ_H , yields minimum values than those of other pressure profiles ($\phi_H \cong 0.36 \sim 0.38$). Note that the steps of the whole computation based on the EGR approach are illustrated on the sample design example, and presented in *Appendix-II*.

Comparative Analysis, Discussion and Verification

To test the degree of accuracy and for the sake of comparison, the results for the required design variables ($S_f, K_S, H_{0l}, H_d, H_{max}, H_{min}, h_{f(L)}, \phi_H$) obtained from the proposed EGR approach are compared with those obtained from the previous analytical development (Yıldırım 2007), and the computer-aided step-by-step (SBS) procedure (Hathoot et al. 1993) and are synthesized in Table 5. For the solution of the SBS method, a

computer program, *Multi-flowCAD* developed in *Visual Basic. 6.0* (Yıldırım and Ağralıoğlu 2004) based on the flowchart presented earlier (Hathoot et al. 1993), was conducted. The computational time was negligible, less than a few minutes for actual calculations, for *Multi-flowCAD* implementation.

In order to do a detailed comparative analysis, some uniform uphill/downhill slope cases are selected, herein, ($S_0 = 0, -0.5\%, -1\%, \pm 2\%, \pm 5\%$) among various design configurations (*Applications I and II*), to demonstrate the specific hydraulic characteristics of each type of pressure profile, and complete results from three procedures are synthesized in Table 5. This table clearly shows that the results from the proposed EGR approach are in a good justification with those of the previous analytical (Yıldırım,2007) and computer-aided SBS procedure (Hathoot et al. 1993). For different design combinations, the maximum deviation between the results of the proposed technique and those of the other two available procedures is only about 3-5%.

As a useful reference, regarding three outlet discharge exponents ($x = 0.2, 0.5, 1.0$), various shapes of pressure head distributions [$H(l)$] versus the dimensionless distance ($i = l/L$) are observed for each type of pressure profiles, based on the results from the present EGR approach and the SBS procedure, and shown in Figs. 2, 3 and 4, respectively.

As shown in Fig. 2, three pressure head distributions for *Type-I* profile are demonstrated for zero-slope case, $S_0 = 0$ from Fig. (2a), for uniform upslope case with $S_0 = 2\%$ from Fig. (2b), and for uniform steep-upslope case with $S_0 = 5\%$ by Fig. (2c), respectively. Fig. 2 reveals that typical hydraulic characteristics of *Type-I* profile are clearly observed in these three figures in which the pressure head exponentially decreases with respect to the line starting from inlet, and reaches a minimum value at the downstream closed end ($H_{0l} = H_{\max} > \bar{H} > H_d = H_{\min}$).

The maximum pressure head, H_{\max} , is at the inlet of the line and is equal to the operating inlet pressure, H_{0l} ($H_{0l} = H_{\max}$); the minimum pressure head, H_{\min} , is at the closed end of line, and is equal to the downstream pressure head ($H_d = H_{\min}$). The value of the pressure head roughly intersects to the required average pressure head value in the

middle section of the line. As shown in Fig. 2, ($S_0 = 0, 2\%, 5\%$), the pressure head is approximately equal to the average value ($H = \bar{H} = 7.2m$) for the interval of dimensionless distance at about $i = 0.40 \sim 0.45$ through the upstream section.

As shown in Fig. (3a), the pressure distribution for *Type-II.a* profile is demonstrated for gentle-downslope case $S_0 = 1\%$. As a typical hydraulic characteristic of *Type II.a* profile, the pressure head decreases from the upstream end with respect to the line, reaches a minimum point (i_{min}), and then increases with respect to the line. However, the downstream end pressure head (H_d) is still less than the operating inlet pressure (H_{0l}). The maximum pressure head is at the inlet ($H_{max} = H_{0l}$); and the minimum pressure head is located at about $i_{min} = 0.70$, through the downstream section ($H_{0l} = H_{max} > \bar{H} > H_d > H_{min}$). In this type of pressure profile, the value of the pressure head roughly intersects the required average pressure head value at about $i = 0.35$ through the upstream section.

As shown in Fig. (3b), the pressure distribution for *Type-II.b* profile is demonstrated for efficient-downslope case, $S_0 = 0.5\%$. As a typical hydraulic characteristic of *Type II.b* profile, the operating inlet pressure head is equal to the downstream closed end pressure head ($H_{0l} = H_d$); the maximum pressure is at the inlet ($H_{max} = H_{0l}$) as well as at the closed end of the line ($H_{max} = H_d$). The pressure head is equal to the average pressure head at two points, $i = 0.15$ along upstream and $i = 0.70$ along downstream section. The minimum pressure is located near the middle section of the line, $i_{min} = 0.44$, for all performed simulations.

As shown in Fig. (4a), the pressure distribution for *Type-II.c* profile is presented for nearly-steep downslope situation, $S_0 = 2\%$. This type of pressure profile occurs when the line slope is even steeper, so the pressure at the end of line is higher than the operating inlet pressure. In this condition, the maximum pressure is at the downstream closed end of line ($H_{max} = H_d$), which exponentially decreases along the line, and reaches the minimum pressure, located somewhere along the upstream segment of the line, then increases toward the upstream end ($H_d = H_{max} > \bar{H} > H_{0l} > H_{min}$ or $H_d = H_{max} > H_{0l} \geq \bar{H} > H_{min}$). In this type of pressure

profile, the value of the pressure head roughly intersects the required average pressure head value at two points, $i = 0.05$, near the pipe inlet, and $i = 0.65$ along downstream section for the SBS method, whereas the pressure head is equal to the average pressure head at one point, $i = 0.60$, along downstream segment for the EGR approach. The location of minimum pressure is observed near the upstream end, $i_{min} = 0.2$, for the EGR approach, whereas $i_{min} = 0.3$ for the SBS procedure.

As shown in Fig. (4b), the pressure head distribution for *Type-III* profile is demonstrated for steep-downslope case, $S_0 = 5\%$ in which the submain line is on a steep downslope, where the total energy gain due to the uniform downslope is larger than the total energy drop due to friction for all sections along the line. In this case, the pressure head increases with respect to the line length. In this condition the maximum pressure is at the downstream closed end of the line ($H_{max} = H_d$), and the minimum pressure head is at the pipe inlet and equal to the operating pressure head ($H_{min} = H_{0l}$) [$H_d = H_{max} > \bar{H} > H_{0l} = H_{min}$]. The value of the pressure head roughly intersects the required average pressure head value at the middle section of the line, $i = 0.5$, regarding both procedures.

As concluded from Figs, 2, 3 and 4, among all types of pressure profiles, the *Type-II* profile is considered as the optimal (or ideal) pressure profile which can produce the minimum pressure head difference when the total energy loss due to friction is just balanced by the total energy gain due to uniform downslope (Profile II-b), as shown in Fig. (3b) or Fig. (2b).

Summary and Concluding Remarks

Determination of the proper operating inlet pressure head is important for hydraulic design of multi-outlet pipelines in submain lines. This paper presents an analytical energy-gradient ratio (EGR) approach which offers simple, direct but sufficiently accurate relationships to determine the operating inlet pressure head and the the required pressure parameters, incorporating different uniformity patterns for water application. For this purpose, some mathematical expressions are initially deduced to relate water application uniformity parameters; such as Christiansen uniformity coefficient, lower-quarter distribution

uniformity, coefficient of variation of outlet discharge, emission uniformity and allowable pressure head variation. Hence, the operating inlet pressure head is reformulated by incorporating different uniformity patterns, and setting a multiplication factor, α , and the required average outlet pressure head, and β^* , for the change in potential energy head due to the uniform line slope. The present formulations can be efficiently used for a wide range of water application uniformity, and for different types of pressure profiles in different line slope situations, without requiring any additional hydraulic variables.

The resulting influence of different uniform pipe slopes on the water application uniformity as well as the operating inlet pressure head for various outlet models is graphically evaluated. Based on the proposed EGR approach, for all uniform slope situations, each type of pressure profiles is identified with its specific hydraulic characteristics along the line regarding various design configurations. Practical results for an extensive comparison test covering different uniform pipe slopes and outlet discharge exponents indicate that the performance of the proposed technique is sufficient in comparison with those of the previous analytical and computer-aided SBS design procedures.

Based on the present EGR approach, the following conclusions can be underlined:

1. Analysis of results obtained from the EGR approach shows that for given values of the uniform pipe slope, S_0 , the required average outlet pressure head, \bar{H} , and the outlet discharge exponent, x , as the operating inlet pressure head, H_{0I} increases the fraction of the required average pressure head, δ_H , and the coefficient of variation of outlet discharge, CV_q increase, whereas other uniformity parameters (U_C , D_U and E_U) decrease, for all types of pressure profiles.

2. To evaluate the influence of different uniform pipe slopes on the U_C values, as the upslope increases the U_C values linearly decrease; hence a large decrease in the U_C values is observed for the highest upslope range, $S_0 = 0.05$ ($U_C = 0.70$). For a given upslope range, the U_C values rapidly decrease as the x value increases. For instance, for $S_0 = 0.05$, the smallest value of $U_C = 0.70$ is observed for the largest value of $x = 1.0$. For

the downhill slope case, the U_C profile has a curve form, even for different x values. In this situation, peak points of the U_C profiles approximately occur around the downslope range, $S_0 = 1\%$.

3. To conclude the influence of different uniform pipe slopes on the H_{0I} values; the H_{0I} values increase with increasing upslope whereas decrease with increasing downslope.

4. For all uniform line slope combinations regarded, the water application uniformity gives smaller values with the increase in the outlet discharge exponent, x , generally; for instance for a value of $x = 0.2$, the uniformity coefficient has highest values, whereas for the laminar flow outlets ($x = 1.0$), it has smaller values.

5. The pressure head profiles for different uniform line slope situations reveal that the value of the pressure head roughly intersects the required average pressure head value near the middle section of the line. For instance, for *Type I* profile ($S_0 = 0, 2\%, 5\%$), the pressure head is approximately equal to the average value ($H = \bar{H} = 7.2m$) for the dimensionless distance, $i = 0.40 \sim 0.45$; for *Type II.a* profile ($S_0 = 1\%$), $i = 0.42$; for *Type II.b* profile ($S_0 = 0.5\%$), the pressure head is equal to the average pressure head at two upstream and downstream end points, $i = 0.15$ and $i = 0.70$; similarly, for *Type II.c* profile ($S_0 = 2\%$), $i = 0.05$ and $i = 0.60$ (for SBS) and $i = 0.55$ (for EGR); for *Type III* profile ($S_0 = 5\%$), $i = 0.50$.

6. Examination results shows that for the efficient-downslope case (*Type II.b* profile), the minimum pressure head nearly occurs at the point, $i_{\min} = 0.44$, through the upstream section, for all performed simulations.

Acknowledgment

The Scientific and Technological Research Council of Turkey (TUBITAK) is acknowledged for supporting the senior author through the fellowships and grant program (2219) at Texas A&M University/BAEN.

Appendix-I: Calculation Steps for Sample Example-I for Steep Downslope" (Type III Profile)

Based on the original data presented in Design Application-I, determine the energy-gradient line (EGL) with the corresponding

hydraulic variables for the steep-downslope situation, $S_0 = 0.05$, and for the desired level of water application uniformity, $U_C = 90.5\%$, based on the nonuniform outflow concept ($m_\beta = \beta \times m$, $\beta \neq 1$), and neglecting the change in the kinetic energy head ($H_{VI} \cong 0$) and local head losses ($F_S = 1$).

a. For $U_C = 0.905$, $\bar{H} = 7.2$ m, $L = 151$ m and $x = 0.5$, dimensionless physical numbers, λ_1 and λ_5 are already computed in Sample Example I, as follows: $\lambda_1 = 0.19$ and $\lambda_5 = 0.048$

b., c. The friction slope, S_f is directly computed from Eq. (53a) or Table 2 ($k_1 = 4.357$):

$$S_f = S_0 - k_1 \times \lambda_1 \times \lambda_5 = 0.05 - 4.357 \times 0.19 \times 0.048 = 0.0105, \quad S_f = 1.05\%$$

$$\text{The dimensionless energy-gradient ratio, } K_S = \frac{S_0}{S_f} = \frac{0.05}{0.0105} = 4.75$$

$K_S = 4.75 > 2.75$ (Table 1), therefore **Type-III** profile is observed along the line.

$$\text{Total friction drop, } h_{f(L)} = S_f \times L = 0.0105 \times 151 = 1.586 \cong 1.59 \text{ m.}$$

Total energy gain due to steep-downslope situation, $\Delta S = S_0 \times L = 0.05 \times 151 = 7.55$ m.

For the nonuniform outflow distribution along the line, the nonuniform outflow exponent, β is evaluated from Eq. (4), depending on the values of S_0 , x , L , \bar{H} , F_S , and S_f , as follows:

$$\beta = 1 - 3.322x \log \left[1 + \frac{H_{VI}}{\bar{H}} + \frac{h_{f(L)}}{\bar{H}} \left[\left(\frac{m+3-0.5^{m+1}}{m+2} \right) - F_S \right] + \frac{1}{4\bar{H}} (p\Delta S) \right]$$

$$\beta = 1 - 3.322 \times 0.5 \times \log \left[1 + 0 + \frac{1.59}{7.2} \times \left[\left(\frac{4.75 - 0.5^{2.75}}{3.75} \right) - 1 \right] + \frac{1}{4 \times 7.2} \times (-1) \times 7.55 \right]$$

$\beta = 1.172$, therefore the improved value of velocity exponent, m_β :
 $m_\beta = \beta \times m = 1.172 \times 1.75 = 2.05$

d. For **Type III** profile, δ_H can be directly determined from Table 2 ($k_1 = 4.357$):

$$\delta_H = k_1 \times \lambda_1 = 4.357 \times 0.19 = 0.828, \quad \delta_H = 83\%$$

e. For *Type III* profile, multiplication factors (α and β^*) are computed from Eq. (54a) or Eq. (54b) [see Table 2.]

$$k_1 = 4.357, c_1 = -0.75 \text{ for } F_S = 1]:$$

$$\alpha = 1 + c_1 \times \delta_H = 1 - 0.75 \times 0.828 = 0.379$$

$$\alpha = 1 + c_1 \times k_1 \times \lambda_1 = 1 - 0.75 \times 4.357 \times 0.19 = 0.379, \text{ and } \beta^* = 0.25 \text{ (for } F_S = 1).$$

The operating inlet pressure head (H_{0l}) is directly computed from Eq. (50):

$$H_{0l} = \alpha \times \bar{H} + \beta^* \times (S_0 \times L)$$

$$H_{0l} = 0.379 \times 7.2 + 0.25 \times (0.05 \times 151) = 4.617 \cong 4.62 \text{ m.}$$

Check the value of H_{0l} , for $i = 0$, from Eq. (3b) for $S_f = 0.0105$ and $m_\beta = 2.05$:

$$H_{0l} = H(l = 0, i = 0) = \bar{H} + H_{VI}[1 - (1 - i)^2] + h_{f(L)} \left[F_S[(1 - i)^{m_\beta + 1} - 1] + \frac{m_\beta + 1}{m_\beta + 2} \right] - p\Delta S \left(i - \frac{1}{2} \right)$$

$$= 7.2 + 0 + 1.59 \times \left[1 \times [(1 - 0)^{2.05 + 1} - 1] + \frac{2.05 + 1}{2.05 + 2} \right] - (-1) \times 7.55 \times \left(0 - \frac{1}{2} \right) = 4.62 \text{ m.}$$

The downstream end pressure head, H_d , can be directly evaluated from the conservation of energy principle:

$$H_d = H_{0l} + L \times (S_0 - S_f) = 4.62 + 151 \times (0.05 - 0.0105) = 10.585 \cong 10.59 \text{ m.}$$

Check the value of H_d , for $i = 1$, from analytical Eq. (3b) for $S_f = 0.0105$ and $m_\beta = 2.05$:

$$H_d = H(l = L, i = 1) = 7.2 + 0 + 1.59 \times \left[1 \times [(1 - 1)^{2.05 + 1} - 1] + \frac{2.05 + 1}{2.05 + 2} \right] - (-1) \times 7.55 \times \left(1 - \frac{1}{2} \right) = 10.582 \cong 10.58$$

m.

f., g., h. The location of minimum pressure head (i_{min}) can be evaluated from Eq. (32a):

$$i_{min(DW)} = \frac{l_{min}}{L} = 1 - 0.561 \times \left(\frac{K_S}{F_S} \right)^{0.57} = 1 - 0.561 \times \left(\frac{4.75}{1} \right)^{0.57} = -0.36,$$

Minus sign indicates the minimum outflow just occurs at the upstream pipe inlet point ($i_{min} = 0$), therefore the operating pressure head at the pipe inlet is just identical to the minimum pressure head along the

line ($H_{0l} = H_{min} = 4.62$ m), and the maximum pressure head occurs at the downstream closed end ($H_{max} = H_d = 10.58$ m)

The maximum pressure head difference, $\Delta H_{max} = H_{max} - H_{min} = 10.58 - 4.62 = 5.96$ m.

Check the value of δ_H from: $\delta_H = \frac{\Delta H_{max}}{\bar{H}} = \frac{5.96}{7.2} = 0.828$, ($\delta_H = 83\%$)

Compute parameter, ϕ_H , to evaluate the pressure variation:

$\phi_H = \frac{\Delta H_{max}}{h_{f(L)}} = \frac{5.96}{1.59} = 3.75$ means the excessive level for the pressure variation along the line for a given steep downslope situation (for $K_s = 4.75 > 2.75$)

Check the pressure orders for *Type- III* profile:

$$H_d = H_{max} = 10.6 > \bar{H} = 7.2 > H_{0l} = H_{min} = 4.6 \text{ m.}$$

The distribution of pressure parameters evaluated based on the EGR approach is verified by the *Type- III* profile as demonstrated in Fig. 3 (e).

1. For water application uniformity evaluation, Eq. (35a) and (35b) are used. For *Type III* profile ($c_1 = -0.75$, $k_1 = 4.357$ and $\beta^* = 0.25$), regarding the design value of operating pressure head, $H_{0l} = 4.62$ m, and $\lambda_5 = \bar{H}/L = 7.2/151 = 0.048$, the uniformity parameters are evaluated as follows:

$$\theta = \frac{H_{0l}}{\bar{H}} - \beta^* \times \frac{S_0}{\lambda_5} - 1 = \frac{4.62}{7.2} - 0.25 \times \frac{0.05}{0.048} - 1 = -0.61875$$

$$\delta_H = \frac{\theta}{c_1} = -\frac{0.61875}{-0.75} = 0.825 \cong 83\% \quad \lambda_1 = \frac{(1-U_C)}{x} = \frac{\theta}{c_1 \times k_1} =$$

$$\frac{-0.61875}{-0.75 \times 4.357} = 0.1894$$

$$U_C = 1 - \lambda_1 \times x = 1 - 0.1894 \times 0.5 = 0.905 \cong 90.5\%$$

Appendix-II: Calculation Steps for Sample Example-II for "Ideal Hydraulic Design" (Type II.b Profile)

In order to show the applicability of the present EGR approach on the design examples, a sample solution is presented for the desired value of the water application uniformity, $U_C = 90.5\%$, based on the following calculation steps (also see Table 4):

a. Dimensionless physical numbers, λ_1 and λ_5 from Eq. (37) [or directly from Table 1]:

$$\lambda_1 = \frac{(1-U_C)}{x} = \frac{(1-0.905)}{0.5} = 0.19 \quad \text{and} \quad \lambda_5 = \frac{\bar{H}}{L} = \frac{7.2}{151} = 0.048$$

b., c. The friction slope, S_f , which must be equal to the uniform pipe slope (S_0) for “the most efficient” design case (**Type II.b** pressure profile: $K_S = S_0/S_f = 1$), is directly computed from Eq. (56a) or Table 1 (for **Type II.b** profile: $k_1 = 2.178$):

$$S_0 = S_f = k_1 \times \lambda_1 \times \lambda_5 = 2.178 \times 0.19 \times 0.048 = 0.0198 \cong 0.02, \quad S_0 = S_f = 2\%$$

d. For the desired **Type II.b** profile, δ_H can be determined by two alternative ways:

From Eq. (31a), simplifying $F_S = 1$ (neglecting local losses):

$$\delta_H = 0.357 \times F_S^{-0.57} \times S_f \times \frac{L}{H} \cong 0.36 \times S_f \times \frac{L}{H} = 0.36 \times 0.02 \times \frac{151}{7.2} = 0.148 \quad (\delta_H \cong 15\%)$$

Alternatively, directly from Table 2 ($k_1 = 0.778$):

$$\delta_H = k_1 \times \lambda_1 = 0.778 \times 0.19 = 0.148, \quad \delta_H \cong 15\%$$

Total friction drop, $h_{f(L)} = S_f \times L = 0.02 \times 151 = 3.02$ m

$$(\Delta S = S_0 \times L = 0.02 \times 151 = 3.02 \text{ m})$$

e. For the desired **Type II.b** profile, multiplication factors (α and β^*) are computed from Eq. (58a) or Eq. (58b)

[or directly from Table 2] [$k_1 = 0.778$, $c_1 = 0.70$ for $F_S = 1$]:

$$\alpha = 1 + c_1 \times \delta_H = 1 + 0.70 \times 0.148 = 1.104$$

$$\alpha = 1 + c_1 \times k_1 \times \lambda_1 = 1 + 0.70 \times 0.778 \times 0.19 = 1.104$$

$$\beta^* = 0 \quad (\text{from Table 2}).$$

The operating inlet pressure head (H_{0I}) is directly computed from Eq. (50):

$$H_{0I} = \alpha \times \bar{H} + \beta^* \times (S_0 \times L)$$

$$H_{0I} = 1.104 \times 7.2 + 0 \times (0.02 \times 151) = 7.949 \cong 7.95 \text{ m}.$$

Check the value of H_{0I} ($H_{0I} = H_d$) from Eq. (20) or Eq. (21) for $S_f = 0.0197$ [$\Delta S = h_{f(L)} = 3.02$ m]:

$$H_{\max} = H_{0l} = H_{(l=0, i_{\max}=0)} = \bar{H} + \left(\frac{m+1}{m+2}\right) \times h_{f(L)} - \frac{\Delta S}{2} = 7.2 + \frac{2.75}{3.75} \times 3.02 - \frac{3.02}{2} = 7.905 \cong 7.91$$

m;

$$H_{\max} = H_d = H_{(l=L, i_{\max}=1)} = \bar{H} + \left(\frac{m+1}{m+2} - F_S\right) \times h_{f(L)} + \frac{\Delta S}{2} = 7.2 + \left(\frac{2.75}{3.75} - 1\right) \times 3.02 + \frac{3.02}{2} = 7.905 \cong 7.91$$

m.

f., g., h. The location of minimum pressure head (i_{\min}) can be evaluated from Eq. (32a) as:

$$i_{\min(DW)} = \frac{l_{\min}}{L} = 1 - 0.561 \times \left(\frac{K_S}{F_S}\right)^{0.57} = 1 - 0.561 \times \left(\frac{1}{1}\right)^{0.57} \cong 0.44$$

The minimum pressure head (H_{\min}) is directly computed from Eq. (3b) for $i = i_{\min} = 0.44$:

$$H_{\min} = H_{(i_{\min}=0.44)} = \bar{H} + H_{VI} [1 - (1 - i_{\min})^2] + h_{f(L)} \left[F_S [(1 - i_{\min})^{m_\beta + 1} - 1] + \frac{m_\beta + 1}{m_\beta + 2} \right] - p \Delta S \left(i_{\min} - \frac{1}{2} \right)$$

$$= 7.2 + 0 + 3.02 \times \left[1 \times [(1 - 0.44)^{2.75} - 1] + \frac{2.75}{3.75} \right] - (-1) \times 3.02 \times \left(0.44 - \frac{1}{2} \right) = 6.826 \cong 6.83 \text{ m.}$$

Alternatively, for the Type-II.b profile, one can use simple relationships given by Eq. (34c) which evaluates H_{\min} ,

in terms of H_{\max} and \bar{H} :

$$H_{\min} = f[H_{\max}, \bar{H}]: \quad H_{\min} = \frac{1}{2} \times (3 \times \bar{H} - H_{\max}) = \frac{1}{2} \times (3 \times 7.2 - 7.95) = 6.825 \cong 6.83$$

m.

Therefore, the maximum pressure head difference, $\Delta H_{\max} = H_{\max} - H_{\min} = 7.95 - 6.83 = 1.12 \text{ m.}$

$$\text{Check the value of } \delta_H \text{ from: } \delta_H = \frac{\Delta H_{\max}}{\bar{H}} = \frac{1.12}{7.2} = 0.15, \quad (\delta_H = 15\%)$$

Compute parameter, ϕ_H , to evaluate the pressure variation for “ideal hydraulic design” case:

$$\phi_H = \frac{\Delta H_{\max}}{h_{f(L)}} = \frac{1.12}{2.98} \cong 0.37 \text{ (acceptable critical level for the minimum}$$

pressure variation for ideal hydraulic design)

Check the pressure orders for **Type- II. b** profile:

$$H_{0I} = H_d = H_{\max} = 7.95 > \bar{H} = 7.2 > H_{\min} = 6.83 \text{ m.}$$

The distribution of pressure parameters, assigned based on the EGR approach, is verified by the *Type- II. b* profile, as shown in Fig. 2 (c).

1. From Eq. (36a), for the pressure profile Type II.b ($c_1 = 0.70$, $k_1 = 0.778$ and $\beta^* = 0$), regarding the design value of operating pressure head, $H_{0I} = 7.95$ m, and $\lambda_5 = \bar{H}/L = 7.2/151 = 0.048$, uniformity parameters are evaluated as follows:

$$\alpha_{(K_S=1, \beta^*=0)} = \frac{H_{0I}}{H} = \frac{7.95}{7.2} = 1.104$$

Using Eq. (36b) for θ one can yield:

$$\theta_{(K_S=1, \beta^*=0)} = \alpha_{(K_S=1, \beta^*=0)} - 1 = \frac{H_{0I}}{H} - 1 = 1.104 - 1 = 0.104$$

$$\delta_H = \frac{\theta}{c_1} = \frac{0.104}{0.70} = 0.149 \cong 15\% \quad \lambda_1 = \frac{(1-U_C)}{x} = \frac{\theta}{c_1 \times k_1} = \frac{0.104}{0.70 \times 0.778} = 0.191$$

$$U_C = 1 - \lambda_1 \times x = 1 - 0.191 \times 0.5 = 0.905 \cong 90.5\%$$

Notation

The following symbols with dimensions are used in this paper:

- \bar{H} = required average outlet pressure head [L];
- $H(l)$ = pressure head at a given length l from the pipeline inlet [L];
- H_{0I} = pressure head at the pipeline inlet [L];
- H_d = downstream pressure head at the first outlet from the closed end of the pipeline [L];
- H_{\max} = maximum operating outlet pressure head [L];
- H_{\min} = minimum operating outlet pressure head [L];
- $h_{f(L)}$ = total friction drop at the downstream closed end for the entire length of the pipeline [L];
- I = dimensionless variable of the original distance l which is measured from the pipeline inlet, $i = l/L$;
- i_{\max} = dimensionless distance where the maximum pressure head (or outflow) occurs, $i_{\max} = l_{\max} / L$;

- i_{min} = dimensionless distance where the minimum pressure head (or outflow) occurs, $i_{min} = l_{min} / L$;
- L = original distance which is measured from the multiple outlets pipeline inlet [L];
- l_{max} = location where the maximum pressure head (or outflow) occurs [L];
- l_{min} = location where the minimum pressure head (or outflow) occurs [L];
- M = velocity (or flow rate) exponent for the particular friction head loss formula used;
- m_{β} = improved value of the velocity exponent for the nonuniform outflow;
- N = total number of equally spaced operating outlets for the entire pipeline;
- P = slope indicator takes value 1 for uphill slope, -1 for downhill slope and 0 for zero slope;
- Q_t = total inflow rate for the entire length of the pipeline, $Q_t = N\bar{q}$ [L^3T^{-1}];
- $Q(l)$ = total flow rate that passes through the pipe section located at any distance l from the pipeline inlet [L^3T^{-1}];
- Q = discharge through the individual outlet [L^3T^{-1}];
- \bar{q} = required average outlet discharge [L^3T^{-1}];
- R = Reynolds number for pipe flow;
- S = common spacing between consecutive operating outlets [L];
- $S_f(l)$ = friction slope or the slope of the energy grade line at any distance l from the pipeline inlet;
- S_0 = uniform slope along the pipeline;
- U_C = Christiansen's uniformity coefficient (%);
- x = outlet discharge exponent;
- ΔH_{max} = maximum allowable difference in the outlet operating pressure heads along the pipeline [L];

- ΔS = total head loss or gain due to elevation at the closed end of the pipeline, $\Delta S = S_0 L$ [L];
- δ_H = percentage of the maximum allowable difference in outlet pressure heads to the average value (%);
- ν = kinematic viscosity of water [L^2T^{-1}];
- β = nonuniform outflow exponent;

Abbreviations

The following abbreviations are used in this paper:

- BSP = Back-Step Procedure
- DW = Darcy-Weisbach
- EGR = Energy-Gradient Ratio
- EGL = Energy-Gradient Line
- FSP = Forward-Step Procedure
- HW = Hazen Williams
- LATC = Lateral Computer Aided Design
AD
- RSBS = Revised Step-by-Step
- REGL = Revised energy-Gradient-Line
- SBS = Step-by- Step

REFERENCES

Anyoji, H., and Wu, I. P. (1987). "Statistical approach for drip lateral design." *Trans. ASAE*, 30(1), 187-192.

Barragan, J. and Wu, I.P. (2005). "Simple pressure parameters for micro-irrigation design" **Biosystems Eng.** 90(4): 463-475.

Christiansen, J. E. (1942). "*Irrigation by sprinkling.*" California Agricultural Experimental Station Bulletin 670, Univ. of California, Davis, California.

Cuenca, R.H. (1989). "*Irrigation systems design: an engineering approach*". Prentice Hall, New Jersey.

Hathoot, H. M., Al-Amoud, A. I., and Mohammad, F. S. (1993). "Analysis and design of trickle irrigation laterals." *J. Irrig. and Drain. Eng.*, 119(5), 756-767.

Hathoot, H. M., Al-Amoud, A. I., and Mohammad, F. S. (1994). "Analysis and design of sprinkler irrigation laterals." *J. Irrig. and Drain. Eng.*, 120(3), 534-549.

Hathoot, H. M., Al-Amoud, A. I., and Al-Mesned, A. S. (2000). "Design of trickle irrigation laterals considering emitter losses." *ICID Journal*, 49(2): 1-14.

Juana, L., Rodriguez-Sinobas, L., Losada, A. (2002). "Determining minor head losses in drip irrigation laterals. II: experimental study and validation." *J. Irrig. and Drain. Eng.* 128(6): 385-396.

Juana, L., Losada, A., Rodriguez-Sinobas, L., and Sanchez, R. (2004). "Analytical relationships for designing rectangular drip irrigation units." *J. Irrig. and Drain. Eng.*, 130(1), 47-59.

Kang, Y., and Nishiyama, S. (1996). "Analysis and design of microirrigation laterals." *J. Irrig. and Drain. Eng.*, 122(2), 75-82.

Kang, Y. (2000). "Effect of operating pressures on microirrigation uniformity." *Irrig. Sci.* 20: 23-27.

Keller, J., and Karmelli, D. (1974). "Trickle irrigation design parameters." *Trans. ASAE*, 17(4), 678-684.

Keller, J., and Bliesner, r. D. (1990). *Sprinkler and trickle irrigation*, Van

Nostrand Reinhold, New York.

Mahar, P. S., and Singh, R. P. (2003). "Computing inlet pressure head of multioutlet pipeline." *J. Irrig. and Drain. Eng.*, 129(6), 464-467.

Perold, R. P. (1977). "Design of irrigation pipe laterals with multiple outlets." *J. Irrig. and Drain. Eng.*, 103(2): 170-195.

Warrick, A.W. (1983). "Interrelationships of irrigation uniformity terms." *J. Irrig. and Drain. Eng.*, 109(3), 317-332.

Warrick, A.W., and Yitayew, M. (1988). "Trickle lateral hydraulics. I: analytical solution." *J. Irrig. and Drain. Eng.*, 114(2), 281-288.

Wu, I. P. (1992). "Energy gradient line approach for direct hydraulic calculation in drip irrigation design." *Irrig. Sci.*, 13, 21-29.

Wu, I. P. (1997). "An assessment of hydraulic design of micro-irrigation systems." *Agric. Water Manage.*, 32, 275-284.

Wu, I. P., and Yue, R. (1993). "Drip lateral design using energy gradient line approach." *Trans. ASAE*, 36(2), 389-394.

Valiantzas, J. D. (1998). "Analytical approach for direct drip lateral hydraulic calculation." *J. Irrig. and Drain. Eng.*, 124(6), 300-305.

Wu, I. P., and Gitlin, H. M. (1973). "Hydraulics and uniformity for drip irrigation." *J. Irrig. and Drain. Div., ASCE*, 99(IR2), Proc. Paper 9786, June, pp. 157-168.

Wu, I. P. and Gitlin, H. M. (1974). "Drip irrigation design based on uniformity." *Trans. ASAE*, 17(3), 429-432.

Wu, I. P. and Gitlin, H. M. (1975). "Energy gradient line for drip irrigation laterals." *J. Irrig. and Drain. Eng.*, 101(4), 323-326.

Yıldırım, G., and Ağralıoğlu, N. (2004). "Comparative analysis of hydraulic calculation methods in design of micro-irrigation laterals." *J. Irrig. and Drain. Eng.*, 130(3), 201-217.

Yıldırım, G. (2006). "Hydraulic analysis and direct design of multiple outlets pipelines laid on flat and sloping lands." *J. Irrig. Drain. Engrg., ASCE*, 132(6), 537-552.

Yıldırım, G. (2007a). "An Assessment of Hydraulic Design of Trickle Laterals Considering Effect of Minor Losses." *Irrig. and Drain. (ICID*

Journal) 56(4), 399-421.

Yıldırım, G. (2007b). "Analytical Relationships for designing multiple outlets pipelines." *J. Irrig. Drain. Engrg., ASCE*, 133(2), 140-154.

Yıldırım, G. (2008). "Determining inlet pressure head incorporating uniformity parameters for multioutlet plastic pipelines." *J. Irrig. Drain .Engrg., ASCE*, 134(3), 341-348.

Yıldırım, G. (2009). "Simplified procedure for hydraulic design of small-diameter plastic pipes." *Irrig. Drain. (ICID J.)* 58(3):209-233.

Yıldırım, G. (2010). "Total energy loss assessment for trickle lateral lines equipped with integrated in-line and on-line emitters" *Irrig. Science*, 28(4): 341-352.

ON THE VISCOELASTIC DYNAMICS AND STABILITY OF AXIALLY FUNCTIONALLY GRADED FLUID CONVEYING PIPES

Reza AGHAZADEH¹

Abstract: This study presents a novel modeling and analysis technique for viscoelastic dynamics of fluid conveying pipes (FCPs) composed of axially functionally graded materials (AFGMs). The model including equation of motion and boundary conditions governing the current fluid-solid interaction (FSI) problem is derived based on Euler-Bernoulli beam theory. The Kelvin-Voigt viscoelastic model is employed to take the effect of internal damping of the pipe material into account. The through-the-length variations of all material constants including internal damping coefficient are captured by a power law function which incorporates a parameter called functionally graded material (FGM) gradient index. The gradation index determines the distribution profile of material properties in axial direction. The system of partial differential equations are numerically solve through utilization of differential quadrature method (DQM). The procedures developed in the current study can be used to delineate the influences of material distribution patterns and internal damping upon the vibrational characteristics of axially functionally graded fluid contained pipes. As an important issue in FSI applications, determination of critical flow velocity in which instability of the pipe occurs is investigated in detail.

Keywords: Fluid Conveying Pipe, Axially Functionally Graded Material, Flutter, Critical Flow Velocity, Internal Damping

¹ Department of Aeronautical Engineering, University of Turkish Aeronautical Association, Ankara / Turkey, raghazadeh@thk.edu.tr, Orcid No: 0000-0003-4549-7068

INTRODUCTION

Due to the growing applications of fluid conveying pipes (FCPs) in various engineering fields such as oil exploitation, marine engineering, hydraulic pipelines and micro- and nano-fluidic devices (ElNajjar and Daneshmand, 2020; Sadeghi-Goughari et al., 2020;) the dynamics of these members has recently attracted a great deal of concern. In order to get over the possible leakage and explosion risks and fatigue failures caused by instability of pipes (Sadeghi and Karimi-Dona, 2011), thorough understanding of these fluid structure interaction (FSI) systems is indispensable. According to the types of boundary conditions used to support the pipe, two types of instabilities, namely divergence and flutter, may occur when the flow velocity reaches a certain critical value. Divergence or buckling is static form of instability which can be observed in conservative systems supported at both ends, whereas non-conservative systems, i.e. supported at one end, undergo flutter instability at which the FCP exhibits vibrations with large and uncontrollable amplitudes.

The study by Paidoussis (1998) is one of the first researches on the dynamics of FCPs which has been referenced by many papers. This work paved the way for other researchers to model and analyze various problems regarding flow-induced vibrations. In a number of studies mechanical responses of FCPs have been addressed within the scope of linear (Lee and Park, 2006; Xu et al., 2010) and nonlinear dynamics (Peng et al., 2018; Tang et al., 2018; Zhang et al., 2016). Dynamic analysis of Fluid contained pipes aims at computing natural frequencies in different flow velocities and hence determining the instability conditions. In order to improve the stability behavior of FCPs, some of the papers concerning dynamics of pipes with internal flow are devoted to assess the influences of adding concentrated masses and springs at various longitudinal positions (ElNajjar and Daneshmand, 2020), gravitational forces (Ebrahimi-Mamaghani et al., 2019; ElNajjar and Daneshmand, 2020; Ge et al., 2019) and types of supports (Dagli and Ergut, 2019; Liang et al., 2018) upon vibrational characteristics. In studies conducted by Abdollahi et al. (2021) and Jiang et al. (2020) dynamics of FCPs simultaneously subjected to internal and axial flows is examined. In a research work presented by Szmidt et al. (2019) experimental and theoretical effort is made to exa-

mine the effectiveness of using eddy-current damper to enhance stability characteristics of FCPs filled with fluid flowing with critical velocity within them.

In the recent years, due to their superior characteristics, functionally graded materials (FGMs) have become an excellent choice for technological and industrial applications. FGMs can be classified as novel composite materials in which the equivalent material properties vary spatially in a gradual and smooth manner. They combine the prominent properties of two or more constituents to put forward a medium with excellent performance in harsh and high temperature environments. Compared to conventional composites, high stress intensities, interfacial stresses and delamination are avoided in FGMs owing to smooth gradation of volume fractions of compositions. Consequently, in the recent years, FGMs have attracted a great deal of interest in different engineering fields such as aerospace industries and biomedical applications (Mahamood and Akinlabi, 2017; Petit et al., 2018). Along with rapidly growing applications of FGMs as structural components in piping industry, a large number of researches have been dedicated to modeling of functionally graded FCPs. A wide variety of studies on mechanics of fluid contained pipes made of FGM deal with pipes with through-the-thickness distribution of material properties, i.e. the equivalent value of mechanical constants are functions of radial direction (Dehrouyeh-Semnani et al., 2019; Deng et al., 2017; Khodabakhsh et al., 2020; Liu et al., 2019; Reddy et al., 2020; Tang and Yang, 2018; Zhu et al., 2021; Zhu et al., 2020). Axially functionally graded (AFG) materials are another type of FGMs which possess lengthwise variations in material properties. Although there is a large effort on pure structural analyses of AFG beams (Abo-bakr et al., 2021; Ghayesh, 2018; Li et al., 2017), the number of studies pertaining to FSI problem of AFG-FCPs seems to be insufficient in the technical literature. It is worth noting that, since material properties are varied in the same direction as fluid flows, pipes made of AFG materials possess more controllability and designability and hence they are more preferable than radial ones in fluid conveying applications. In some researches regarding mechanics of AFG-FCPs the focus have been on linear dynamics of these systems (An and Su, 2017; Zhou et al., 2018).

Taking the dynamic nonlinearities into account, Lu et al. (2020) investigated the fatigue life of AFG pipes with internal flow. In research works by Ebrahimi-Mamaghani et al. (2020) and Dai et al. (2019) the effort have been made on introducing thermal loads in modeling and analysis of AFG-FCPs. The vibration control and manufacturing problems of AFG fluid contained pipes are addressed in a paper by Mirtalebi et al. (2019). The dynamics of AFG-FCPs with conical form is examined by Zhao et al. (2021). Aghazadeh (2021) employed a higher order shear deformable pipe model for proper estimation of the through-the-thickness shear stress distribution in stability analysis of fluid conveying pipes made of AFG materials.

One of the significant features that should be considered when analyzing mechanics of pipes is internal energy dissipation or damping due to viscoelastic properties of materials. The internal damping effect is more pronounced when the pipe is made of a medium with high degree of viscoelasticity such as elastomer and rubber pipes. The well-known Kelvin-Voight model is prevalently used to model internal dissipation which incorporates viscosity or damping coefficient of material. In a number of studies available in the literature on the FSI problem of pipes, the viscoelasticity is considered in analyses of homogeneous pipes (Dagli and Ergut, 2019; Ghayesh et al., 2019; Ghayesh and Farokhi, 2018; Pisarski et al., 2018). By inspecting the technical literature it can be realized that there is no report on the dynamic behavior of axially functionally graded viscoelastic pipes conveying fluid. Note that, for a pipe with longitudinal gradation of material properties, similar to other properties, axial variation of internal damping coefficient should be taken into account. The current study seems to be the first effort dealing with the effects of viscosity on the stability of AFG-FCPs.

The current study aims at modeling and analysis of axially functionally graded fluid conveying pipes by taking the effects of internal damping into account. Consideration of through-the-length variation of damping coefficient, to the best of author's knowledge, is one of the significant novelties of the current study. The governing equations are established based on Euler-Bernoulli beam model and then solved by adopting differential quadrature method (DQM). The influences of ma-

terial distribution pattern, viscoelastic properties and flow velocity upon dynamics and critical flow velocities of fluid conveying AFG cantilever pipes are clearly demonstrated through provided numerical results.

FORMULATION

Figure 1 depicts the configuration of horizontally oriented axially functionally graded fluid conveying cantilevered pipe with length L , inner radius r_i , outer radius r_o , and containing a fluid with flow velocity Γ . In order to illustrate the smooth axial variation of pipe constituents, a gradient color scale is used. In absence of pressurization and external tension, the model for homogeneous FCP proposed by Paidoussis (1998) can be modified for AFG pipes with nonuniformity of material properties along x_1 -direction as follows

$$\begin{aligned}
 I \frac{\partial^2}{\partial x_1^2} \left(E(x_1) \frac{\partial^2 w}{\partial x_1^2} \right) + I \frac{\partial^2}{\partial x_1^2} \left(E^*(x_1) \frac{\partial^3 w}{\partial x_1^2 \partial t} \right) + m_f \Gamma^2 \frac{\partial^2 w}{\partial x_1^2} \\
 + \rho(x_1) A \frac{\partial^2 w}{\partial t^2} + m_f \frac{\partial^2 w}{\partial t^2} + 2m_f \Gamma \frac{\partial^2 w}{\partial x_1 \partial t} = 0
 \end{aligned} \tag{1}$$

In derivation of Eq. Kelvin-Voight model is used for dissipation. t here is the time and w designates the transverse displacement of pipe. The pipe material properties including modulus of elasticity, internal damping and density are denoted by E , E^* and ρ , respectively. ρ_f and A_f represent the fluid density and flow cross section, and $m_f = \rho_f A_f$ is the fluid mass per unit length. A and I stand respectively for cross sectional area and moment of inertia of the pipe. In addition, the cantilevered pipe is subjected to the following boundary conditions

$$\text{At } x_1 = 0 \quad w = \frac{\partial w}{\partial x_1} = 0, \tag{2.a}$$

$$\begin{aligned} \text{At } x_1 = L \quad I \frac{\partial}{\partial x_1} \left(E(x_1) \frac{\partial^2 w}{\partial x_1^2} \right) + I \frac{\partial}{\partial x_1} \left(E^*(x_1) \frac{\partial^3 w}{\partial x_1^2 \partial t} \right) &= 0, \\ IE(x_1) \frac{\partial^2 w}{\partial x_1^2} + IE^*(x_1) \frac{\partial^3 w}{\partial x_1^2 \partial t} &= 0. \end{aligned} \tag{2.b}$$

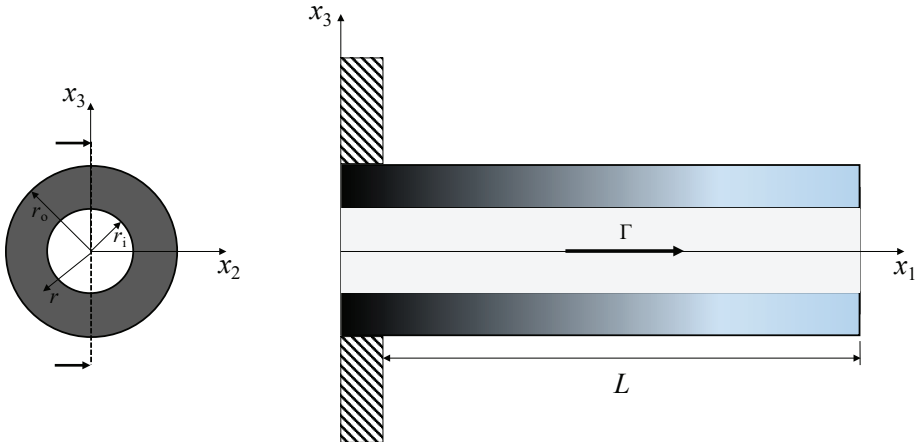


Figure 1. Schematic of Axially Functionally Graded Fluid Conveying Cantilevered Pipe

The dimensionless form of Eq. can be obtained by introducing the following dimensionless quantities

$$\begin{aligned} \xi = \frac{x_1}{L}, \quad \eta = \frac{w}{L}, \quad \tau = \left[\frac{E_0 I}{m_f + \rho_0 A} \right]^{1/2} \frac{t}{L^2}, \quad \alpha_v = \left[\frac{I}{E_0 (m_f + \rho_0 A)} \right]^{1/2} \frac{E_0^*}{L^2}, \\ \bar{E}(\xi) = \frac{E(\xi)}{E_0}, \quad \bar{E}^*(\xi) = \frac{E^*(\xi)}{E_0^*}, \quad \bar{\rho}(\xi) = \frac{\rho(\xi)}{\rho_0}, \quad u = \left(\frac{m_f}{E_0 I} \right)^{1/2} L \Gamma, \\ \beta_p = \frac{\rho_0 A}{m_f + \rho_0 A}, \quad \beta_f = \frac{m_f}{m_f + \rho_0 A}. \end{aligned} \tag{3}$$

where subscript '0' indicates the material at the left end of pipe, $x_1 = 0$. By substituting Eq. into Eq. , governing equation recast into dimensionless form as follows

$$\begin{aligned} & \frac{\partial^2}{\partial \xi^2} \left(\bar{E}(\xi) \frac{\partial^2 \eta}{\partial \xi^2} \right) + \alpha_v \frac{\partial^2}{\partial \xi^2} \left(\bar{E}^*(\xi) \frac{\partial^3 \eta}{\partial \xi^2 \partial \tau} \right) + u^2 \frac{\partial^2 \eta}{\partial \xi^2} \\ & + \beta_p \bar{\rho}(\xi) \frac{\partial^2 \eta}{\partial \tau^2} + \beta_f \frac{\partial^2 \eta}{\partial \tau^2} + 2u\sqrt{\beta_f} \frac{\partial^2 \eta}{\partial \xi \partial \tau} = 0. \end{aligned} \quad (4)$$

NUMERICAL SOLUTION

In the current study, a numerical solution procedure is developed based on differential quadrature method (DQM). A system of partial differential equations can be converted to system of linear algebraic equations by employing DQM. In this method it is postulated that the m^{th} derivative of a function $z(x, t)$ defined over spatial domain $0 \leq x \leq L$ with respect to x can be written as

$$\frac{\partial^m z(x, t)}{\partial x^m} \Big|_{x=x_i} = \sum_{j=1}^N c_{ij}^{(m)} z(x_j, t), \quad i = 1, 2, \dots, N \quad (5)$$

where N is the number of nodes utilized for discretizing problem domain. $c_{ij}^{(m)}$ represent DQM weighting coefficients for m^{th} derivative.

Utilization of Eq. converts the equation of motion and boundary conditions into the following system of linear algebraic equations form:

$$\mathbf{M}\ddot{\mathbf{d}} + \mathbf{C}\dot{\mathbf{d}} + \mathbf{K}\mathbf{d} = \mathbf{0} \quad (6)$$

\mathbf{K} , \mathbf{C} , and \mathbf{M} here are respectively stiffness, damping, and mass matrices. For a self-excited motion the displacement vector $\mathbf{d} = \{\eta\}$ can be given as

$$\{\eta\} = \{\eta^*\} e^{i\omega\tau} = \{\eta^*\} e^{\lambda\tau}, \quad (7)$$

where ω and λ designate eigenfrequencies and eigenvalues, respectively, and $\{\eta^*\}$ denotes corresponding eigenvectors. Substituting Eq. into Eq. , one can obtain following standard generalized eigenvalue problem

$$\{\mathbf{K} + \lambda\mathbf{C} + \lambda^2\mathbf{M}\} \{\eta^*\} = \mathbf{0}. \quad (8)$$

The nontrivial solution of Eq. can be achieved by equating determinant of the coefficient matrix to zero

$$\det\{\mathbf{K} + \lambda\mathbf{C} + \lambda^2\mathbf{M}\} = 0. \quad (9)$$

The eigenfrequencies computed by using the abovementioned procedures, determine the vibrational and stability characteristics of the dynamic system. $\text{Re}(\omega)$ represents oscillation frequency whereas $\text{Im}(\omega)$ designates decaying rate. The FCP loses its stability in critical flow velocity at which $\text{Im}(\omega) < 0$.

NUMERICAL RESULTS

In this section, on the basis of DQM solution technique, numerical results regarding dynamics of a metal-ceramic AFG fluid conveying cantilevered pipe are reported. In order to prescribe through-the-length phase distribution profile, the pipe is considered to be made of stainless steel SUS304 and silicon nitride Si_3N_4 at the left and right hand sides, respectively; material properties regarding these phases are as follows: $E_0 = 201$ GPa, $\rho_0 = 8166$ kg/m³, $E_L = 348$ GPa, $\rho_L = 2370$ kg/m³, where subscripts '0' and 'L' refer to $x_1 = 0$ and $x_1 = L$, respectively. A typical pipe material property designated by Z , including E , E^* and ρ change smoothly according to the following power-law function

$$Z(x_1) = Z_0 \left(1 + \left(\frac{Z_L}{Z_0} - 1 \right) \left(\frac{x_1}{L} \right)^\alpha \right) \quad (10)$$

The non-negative power-law index a delineates through-the-axis material variation pattern; $a = 0$ implies a fully ceramic pipe whereas a linear metal-to-ceramic profile can be achieved by letting $a = 1$. A desired nonlinear property variation can also be assigned by taking an appropriate power-law index as a value other than 0 and 1. Note that dimensionless parameters in the form $\bar{Z}(\xi)$ appeared in Eq. can be expressed as follows

$$\bar{Z}(\xi) = 1 + \left(\frac{Z_L}{Z_0} - 1 \right) \xi^a \quad (11)$$

Figure 2 illustrates the variation of dimensionless critical flow velocity u_{cr} with respect to dimensionless parameter β_f for different values of AFG power law indices. In the current non-conservative cantilevered system, the flutter type of instability occurs. It is worth mentioning that different industrial piping systems are characterized by their β_f -values. For example, homogeneous carbon steel pipe system which are used in drilling rigs can be represented by $\beta_f \approx 0.275$ (ElNajjar and Daneshmand, 2020). Also, it should be noted that, in the results provided in Figure 2, the internal dissipation is neglected by letting $a_v = 0$. From Figure 2, it is clearly observed that higher values of β_f yields a FCP with enhanced stability, i.e. with larger values of u_{cr} . This fact is more pronounced in pipes made of purely metal or ceramic. Another conclusion that can be drawn from Figure 2 is that the influence of power-law index on the stability features of AFG-FCPs depends on β_f -values. Due to the high rigidity of homogeneous ceramic material, the highest values of critical velocities are seen at $a = 0$ at almost all values of β_f . For non-homogeneous AFG pipe, the larger the power-law index gets, the smaller the u_{cr} becomes. A pure metal pipe destabilizes in lower values of u_{cr} compared to other AFG pipes, when β_f is small, however, at $\beta_f \approx 0.3$ it starts to exhibit more stabilized performance with respect to AFG pipes. Further to above-mentioned findings, one can observe that the u_{cr} - β_f curve belonging to homogeneous metal and ceramic pipes contain S-shaped segments whereas the curves for other values of a are free of such segments. The S-shaped segments imply destabilization-restabilization-destabilization

behavior such that, at a certain value of β_f at velocities higher than the smallest u_{cr} , the system gains stability, and by further increasing velocity the pipe destabilizes again.

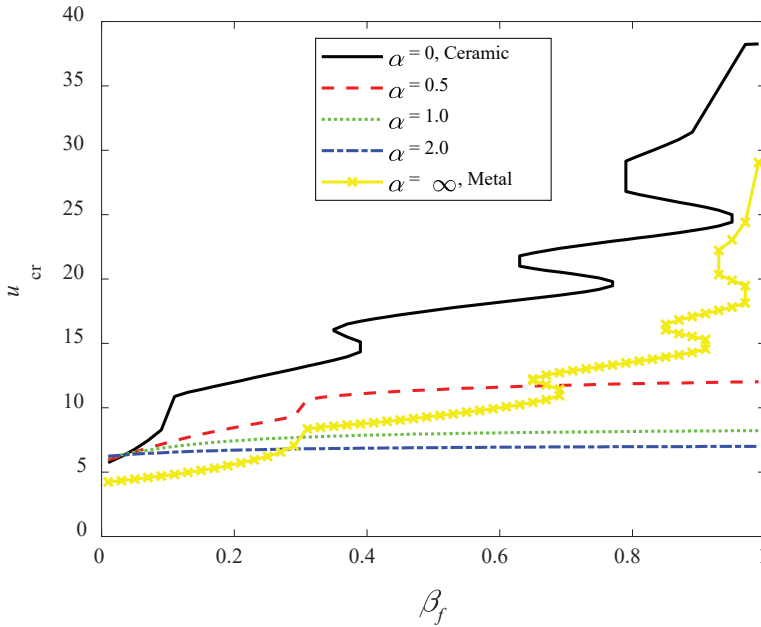


Figure 2. Critical Flow Velocity of Axially Functionally Graded Fluid Conveying Cantilevered Pipe, $\alpha_v = 0$

In order to delineate the influence of velocity on the eigenfrequencies of AFG-FCPs, Argand diagrams for internally undamped system, $a_v = 0$, and internally damped systems $a_v = 0.0005$ and 0.005 , are provided in Figures 3-5, respectively. The plots are generated for $\beta_f = 0.67$ and $a = 2$ and the axial variation of viscosity coefficient is neglected by taking $E_L^* / E_0^* = 1$. For undamped case, the velocity values corresponding to each data point are also inserted on the plot and since the damped cases display similar manner, to prevent complexity, the velocity values are not provided on them. The flutter instability occurs when $\text{Im}(\omega)$ gets negative. From Figure 3 it can be observed that the system first loses its stability at $u_{cr} = 6.95$ in its first mode. In the second mode, the instability exists approximately at dimensionless flow velocity equal to

15. Inspecting Eq. it is clear that two types of damping appears in equation of motion: internal damping of pipe material and Coriolis term $2u\sqrt{\beta_f}\partial^2\eta/\partial\xi\partial\tau$ due to flow. It is worth mentioning that for undamped system in absence of flow, $u = 0$, $\text{Im}(\omega) = 0$ and therefore the Argand curves start from $\text{Re}(\omega)$ axis. However, for a system with nonzero a_v -value, since internal damping exists even when flow velocity is zero, the Argand curves start from $\text{Im}(\omega) \neq 0$. Moreover, comparing Figure 4 and Figure 5, it can be found that at $u = 0$, $\text{Im}(\omega)$ is larger for a pipe with higher a_v . The influence of internal damping upon stability of an AFG-FCP cannot be clearly drawn from Figures 3-5. To justify this fact, it should be mentioned that for the current steel-silicon nitride pipe, both of which possess low viscosity constants, a_v can be estimated as 0.0005 which is small to have tangible effect on critical flow velocity values. In order to investigate the variation of u_{cr} with regard to internal damping and its distribution along the pipe length, dimensionless critical flow velocities at different values of E_L^*/E_0^* and at gradient index value of $a = 2$ are given in Table 1. $E_L^* = E_0^* = 0$ represents a pipe with internal dissipation neglected. According to Eq. a higher right-to-left internal damping ratio yields a larger equivalent damping coefficient. Increase in internal damping leads to a corresponding decrease in critical flow velocity and hence destabilization of the system. Although the effect of dissipation on u_{cr} is not numerically significant for the composition utilized to generate Table 1, drastic differences can be observed for elastomeric and rubber-like materials which possess higher a_v .

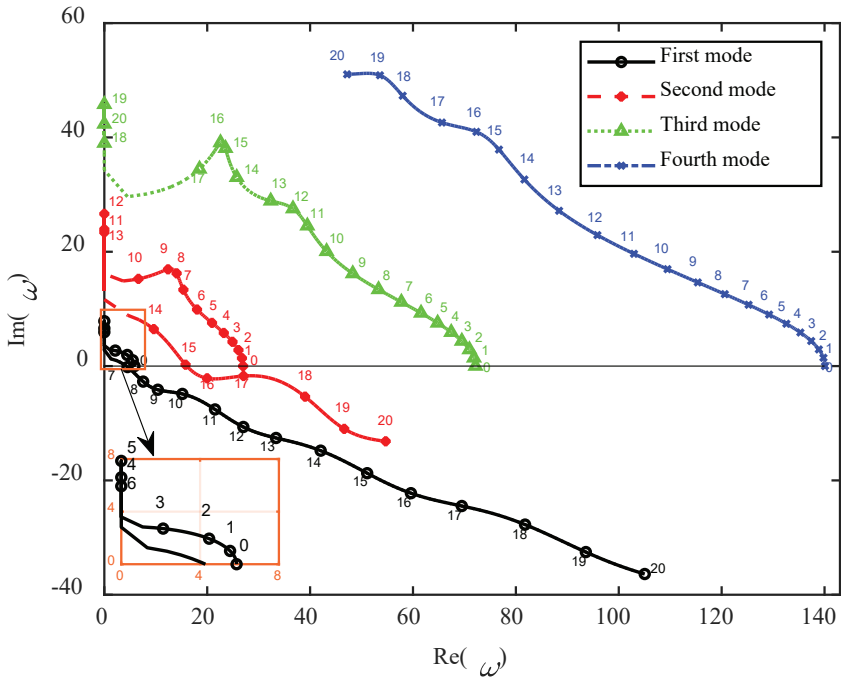


Figure 3. Argand Diagram for an Axially Functionally Graded Fluid Conveying Cantilevered Pipe, $\beta_f = 0.67, \alpha_v = 0, \alpha = 2$

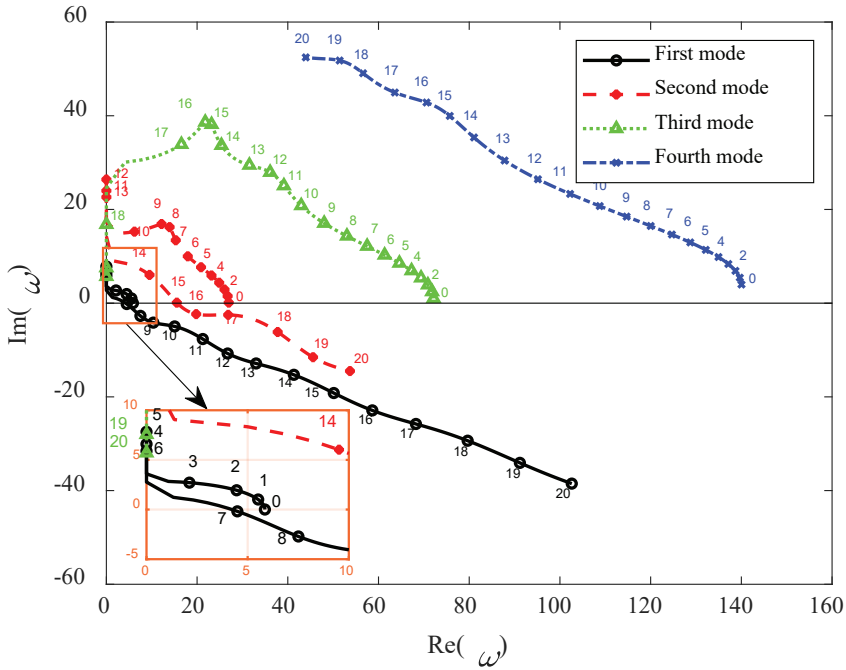


Figure 4. Argand Diagram for an Axially Functionally Graded Fluid Conveying Cantilevered Pipe, $\beta_f = 0.67$, $\alpha_v = 0.0005$, $\alpha = 2$, $E_L^* / E_0^* = 1$

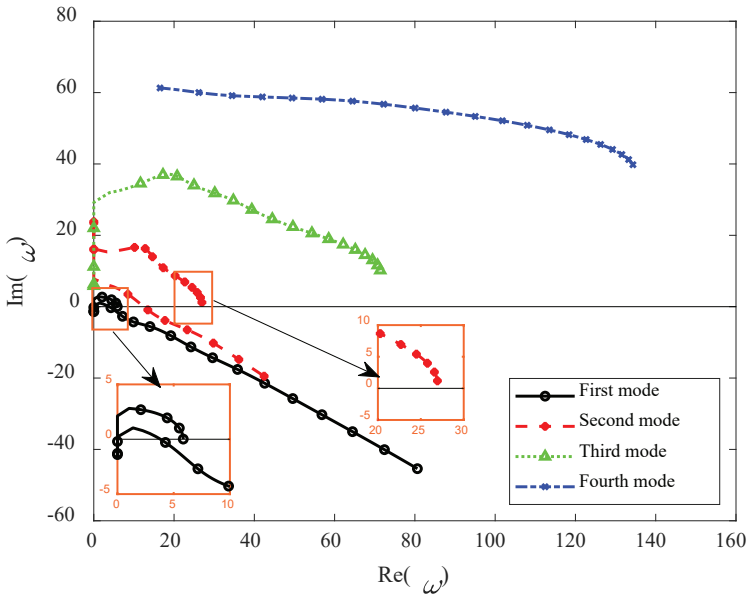


Figure 5. Argand Diagram for an Axially Functionally Graded Fluid Conveying Cantilevered Pipe, $\beta_f = 0.67, \alpha_v = 0.005, \alpha = 2, E_L^* / E_0^* = 1$

Table 1. Critical Flow Velocity of Axially Functionally Graded Fluid Conveying Cantilevered Pipe, $\beta_f = 0.5, \alpha = 2, \alpha_v = 0.005$

$E_L^* = E_0^* = 0$	$E_L^* / E_0^* = 1/2$	$E_L^* / E_0^* = 1$	$E_L^* / E_0^* = 2$
6.90	6.88	6.85	6.79

CONCLUSION

In this study, a model based on Euler-Bernoulli beam theory and Kelvin-Voight viscoelasticity scheme is proposed for stability and dynamic analyses of axially functionally graded cantilevered pipes conveying fluid. The developed procedures allow generating numerical results regarding pipes with different lengthwise phase distribution pattern and various flow velocities. A solution technique to solve governing equations is established on the basis of differential quadrature method.

The influences of power-law index, flow velocity, internal damping and dimensionless parameter β_f upon eigenfrequencies and stability characteristics of AFG-FCPs are investigated in detail through provided parametric analyses.

Power-law index a determines the material distribution profile along pipe length and is observed to have significant effect on dynamics of AFG-FCPs. In the metal-ceramic AFG pipe considered in the current study, the variation trend of critical flow velocity with respect to a is different depending on β_f -value. Generally, increase in β_f results in an increase in u_{cr} . This fact for homogeneous pipes is more evident. Further, higher values of u_{cr} are seen for the pipes with smaller a since the pipe composition becomes ceramic-dominant. The exception for this trend occurs at a certain value of β_f at which metal pipe starts to show more stabilized behavior than AFG ones.

The effects of internal damping and its through-the-length variation are captured by parameters, a_v and E_L^* / E_0^* , respectively. For a nonzero a_v , unlike undamped pipe, the system also exhibits damped behavior with $\text{Im}(\omega) > 0$ at zero flow velocity. Moreover, it can be seen that u_{cr} is a decreasing function of a_v . Increasing E_L^* / E_0^* yields a drop in stability performance of the metal-ceramic AFG cantilever pipe. The effect of viscoelastic parameters are more pronounced for pipes made of viscous materials with higher values of damping coefficients.

REFERENCES

- Abdollahi, R., Dehghani Firouz-abadi, R., and Rahmanian, M. (2021). On the stability of rotating pipes conveying fluid in annular liquid medium. *Journal of Sound and Vibration*, 494, 115891. <https://doi.org/10.1016/j.jsv.2020.115891>
- Abo-bakr, H. M., Abo-bakr, R. M., Mohamed, S. A., and Eltahir, M. A. (2021). Multi-objective shape optimization for axially functionally graded microbeams. *Composite Structures*, 258, 113370. <https://doi.org/10.1016/j.compstruct.2020.113370>
- Aghazadeh, R. (2021). Dynamics of axially functionally graded pipes conveying fluid using a higher order shear deformation theory. *Interna-*

tional Advanced Researches and Engineering Journal, 5(2), 209-217. <https://doi.org/10.35860/iarej.878194>

An, C., and Su, J. (2017). Dynamic Behavior of Axially Functionally Graded Pipes Conveying Fluid. *Mathematical Problems in Engineering*, 2017, 6789634. <https://doi.org/10.1155/2017/6789634>

Dagli, B. Y., and Ergut, A. (2019). Dynamics of fluid conveying pipes using Rayleigh theory under non-classical boundary conditions. *European Journal of Mechanics - B/Fluids*, 77, 125-134. <https://doi.org/10.1016/j.euromechflu.2019.05.001>

Dai, J., Liu, Y., Liu, H., Miao, C., and Tong, G. (2019). A parametric study on thermo-mechanical vibration of axially functionally graded material pipe conveying fluid. *International Journal of Mechanics and Materials in Design*, 15(4), 715-726. [10.1007/s10999-018-09439-5](https://doi.org/10.1007/s10999-018-09439-5)

Dehrouyeh-Semnani, A. M., Dehdashti, E., Yazdi, M. R. H., and Nikkhah-Bahrami, M. (2019). Nonlinear thermo-resonant behavior of fluid-conveying FG pipes. *International Journal of Engineering Science*, 144, 103141. <https://doi.org/10.1016/j.ijengsci.2019.103141>

Deng, J., Liu, Y., Zhang, Z., and Liu, W. (2017). Stability analysis of multi-span viscoelastic functionally graded material pipes conveying fluid using a hybrid method. *European Journal of Mechanics - A/Solids*, 65, 257-270. <https://doi.org/10.1016/j.euromechsol.2017.04.003>

Ebrahimi-Mamaghani, A., Sotudeh-Gharebagh, R., Zarghami, R., and Mostoufi, N. (2019). Dynamics of two-phase flow in vertical pipes. *Journal of Fluids and Structures*, 87, 150-173. <https://doi.org/10.1016/j.jfluidstructs.2019.03.010>

Ebrahimi-Mamaghani, A., Sotudeh-Gharebagh, R., Zarghami, R., and Mostoufi, N. (2020). Thermo-mechanical stability of axially graded Rayleigh pipes. *Mechanics Based Design of Structures and Machines*, 1-30. <https://doi.org/10.1080/15397734.2020.1717967>

ElNajjar, J., and Daneshmand, F. (2020). Stability of horizontal and vertical pipes conveying fluid under the effects of additional point masses and springs. *Ocean Engineering*, 206, 106943. <https://doi.org/10.1016/j.oceaneng.2020.106943>

Ge, X., Li, Y., Chen, X., et al. (2019). Dynamics of a Partially Confined, Vertical Upward-Fluid-Conveying, Slender Cantilever Pipe with Reverse External Flow. *Applied Sciences*, 9(7), 1425.

Ghayesh, M. H. (2018). Nonlinear vibration analysis of axially functionally graded shear-deformable tapered beams. *Applied Mathematical Modelling*, 59, 583-596. <https://doi.org/10.1016/j.apm.2018.02.017>

Ghayesh, M. H., Farajpour, A., and Farokhi, H. (2019). Viscoelastically coupled mechanics of fluid-conveying microtubes. *International Journal of Engineering Science*, 145, 103139. <https://doi.org/10.1016/j.ijengsci.2019.103139>

Ghayesh, M. H., and Farokhi, H. (2018). On the viscoelastic dynamics of fluid-conveying microtubes. *International Journal of Engineering Science*, 127, 186-200. <https://doi.org/10.1016/j.ijengsci.2018.02.010>

Jiang, T., Dai, H., and Wang, L. (2020). Three-dimensional dynamics of fluid-conveying pipe simultaneously subjected to external axial flow. *Ocean Engineering*, 217, 107970. <https://doi.org/10.1016/j.oceaneng.2020.107970>

Khodabakhsh, R., Saidi, A. R., and Bahaadini, R. (2020). An analytical solution for nonlinear vibration and post-buckling of functionally graded pipes conveying fluid considering the rotary inertia and shear deformation effects. *Applied Ocean Research*, 101, 102277. <https://doi.org/10.1016/j.apor.2020.102277>

Lee, U., and Park, J. (2006). Spectral element modelling and analysis of a pipeline conveying internal unsteady fluid. *Journal of Fluids and Structures*, 22(2), 273-292. <https://doi.org/10.1016/j.jfluidstructs.2005.09.003>

Li, X., Li, L., Hu, Y., Ding, Z., and Deng, W. (2017). Bending, buckling and vibration of axially functionally graded beams based on non-local strain gradient theory. *Composite Structures*, 165, 250-265. <https://doi.org/10.1016/j.compstruct.2017.01.032>

Liang, X., Zha, X., Jiang, X., Wang, L., Leng, J., and Cao, Z. (2018). Semi-analytical solution for dynamic behavior of a fluid-conveying pipe with different boundary conditions. *Ocean Engineering*, 163, 183-190. <https://doi.org/10.1016/j.oceaneng.2018.05.060>

Liu, H., Lv, Z., and Tang, H. (2019). Nonlinear vibration and instability of functionally graded nanopipes with initial imperfection conveying fluid. *Applied Mathematical Modelling*, 76, 133-150. <https://doi.org/10.1016/j.apm.2019.06.011>

Lu, Z.-Q., Zhang, K.-K., Ding, H., and Chen, L.-Q. (2020). Nonlinear vibration effects on the fatigue life of fluid-conveying pipes composed of axially functionally graded materials. *Nonlinear Dynamics*, 100(2), 1091-1104. <https://doi.org/10.1007/s11071-020-05577-8>

Mahamood, R. M., and Akinlabi, E. T. (2017) Types of Functionally Graded Materials and Their Areas of Application. *Functionally Graded Materials*. Springer International Publishing, Cham, pp. 9-21

Mirtalebi, S. H., Ebrahimi-Mamaghani, A., and Ahmadian, M. T. (2019). Vibration Control and Manufacturing of Intelligibly Designed Axially Functionally Graded Cantilevered Macro/Micro-tubes. *IFAC-PapersOnLine*, 52(10), 382-387. <https://doi.org/10.1016/j.ifacol.2019.10.061>

Paidoussis, M. P. (1998). *Fluid-Structure Interactions: Slender Structures and Axial Flow*. Academic Press, London

Peng, G., Xiong, Y., Gao, Y., Liu, L., Wang, M., and Zhang, Z. (2018). Non-linear dynamics of a simply supported fluid-conveying pipe subjected to motion-limiting constraints: Two-dimensional analysis. *Journal of Sound and Vibration*, 435, 192-204. <https://doi.org/10.1016/j.jsv.2018.08.018>

Petit, C., Montanaro, L., and Palmero, P. (2018). Functionally graded ceramics for biomedical application: Concept, manufacturing, and properties. *International Journal of Applied Ceramic Technology*, 15(4), 820-840. <https://doi.org/10.1111/ijac.12878>

Pisarski, D., Konowrocki, R., and Szmids, T. (2018). Dynamics and optimal control of an electromagnetically actuated cantilever pipe conveying fluid. *Journal of Sound and Vibration*, 432, 420-436. <https://doi.org/10.1016/j.jsv.2018.06.045>

Reddy, R. S., Panda, S., and Natarajan, G. (2020). Nonlinear dynamics of functionally graded pipes conveying hot fluid. *Nonlinear Dynamics*, 99(3), 1989-2010. <https://doi.org/10.1007/s11071-019-05426-3>

Sadeghi-Goughari, M., Jeon, S., and Kwon, H.-J. (2020). Fluid structure interaction of cantilever micro and nanotubes conveying magnetic fluid with small size effects under a transverse magnetic field. *Journal of Fluids and Structures*, 94, 102951. <https://doi.org/10.1016/j.jfluidstructs.2020.102951>

Sadeghi, M. H., and Karimi-Dona, M. H. (2011). Dynamic behavior of a fluid conveying pipe subjected to a moving sprung mass - An FEM-state space approach. *International Journal of Pressure Vessels and Piping*, 88(4), 123-131. <https://doi.org/10.1016/j.ijpvp.2011.02.004>

Schwengber, A., Prado, H. J., Zilli, D. A., Bonelli, P. R., and Cukierman, A. L. (2015). Carbon nanotubes buckypapers for potential transdermal drug delivery. *Materials Science and Engineering: C*, 57, 7-13. <https://doi.org/10.1016/j.msec.2015.07.030>

Szmidt, T., Pisarski, D., and Konowrocki, R. (2019). Semi-active stabilisation of a pipe conveying fluid using eddy-current dampers: state-feedback control design, experimental validation. *Meccanica*, 54(6), 761-777. [10.1007/s11012-019-00988-3](https://doi.org/10.1007/s11012-019-00988-3)

Tang, Y., and Yang, T. (2018). Post-buckling behavior and nonlinear vibration analysis of a fluid-conveying pipe composed of functionally graded material. *Composite Structures*, 185, 393-400. <https://doi.org/10.1016/j.compstruct.2017.11.032>

Tang, Y., Zhen, Y., and Fang, B. (2018). Nonlinear vibration analysis of a fractional dynamic model for the viscoelastic pipe conveying fluid. *Applied Mathematical Modelling*, 56, 123-136. <https://doi.org/10.1016/j.apm.2017.11.022>

Xu, M. R., Xu, S. P., and Guo, H. Y. (2010). Determination of natural frequencies of fluid-conveying pipes using homotopy perturbation method. *Computers & Mathematics with Applications*, 60(3), 520-527. <https://doi.org/10.1016/j.camwa.2010.04.049>

Zhang, T., Ouyang, H., Zhang, Y. O., and Lv, B. L. (2016). Nonlinear dynamics of straight fluid-conveying pipes with general boundary conditions and additional springs and masses. *Applied Mathematical Modelling*, 40(17), 7880-7900. <https://doi.org/10.1016/j.apm.2016.03.050>

Zhao, Y., Hu, D., Wu, S., Long, X., and Liu, Y. (2021). Dynamics of axially functionally graded conical pipes conveying fluid. *Journal of Mechanics*, 37, 318-326. [10.1093/jom/ufaa030](https://doi.org/10.1093/jom/ufaa030)

Zhou, X.-w., Dai, H.-L., and Wang, L. (2018). Dynamics of axially functionally graded cantilevered pipes conveying fluid. *Composite Structures*, 190, 112-118. <https://doi.org/10.1016/j.compstruct.2018.01.097>

Zhu, B., Chen, X.-C., Guo, Y., and Li, Y.-H. (2021). Static and dynamic characteristics of the post-buckling of fluid-conveying porous functionally graded pipes with geometric imperfections. *International Journal of Mechanical Sciences*, 189, 105947. <https://doi.org/10.1016/j.ijmecsci.2020.105947>

Zhu, B., Xu, Q., Li, M., and Li, Y. (2020). Nonlinear free and forced vibrations of porous functionally graded pipes conveying fluid and resting on nonlinear elastic foundation. *Composite Structures*, 252, 112672. <https://doi.org/10.1016/j.compstruct.2020.112672>

DESIGN AND ASSESSMENT OF A MATERIAL RECYCLING FACILITY IN THE MIDDLE-SCALE RESIDENTIAL AREA

Nesli AYDIN¹

Abstract: The use of recyclable materials has been increasing across the world due to economic, environmental, and technological developments. Mechanical separation of municipal waste is an efficient practice for increasing the quality of the recyclables in a concept of the circular economy. To maximise the quantity of recyclables and to produce the highest possible profits in the recyclables market, this separation could be conducted by a materials recycling facility, which accepts materials (wastes), separates and stores them for remanufacturing and reprocessing. This study aims to design a materials recycling facility to process recyclable household waste produced in the district of Corlu, Tekirdag and to assess the efficiency of this facility. The proposed facility was designed to operate on a two-shift basis, sixteen hours per day and five days per week to separate mixed green-bin-recyclable waste from households in Corlu, by particularly focusing on papers, textiles, cans and plastics. It was found that the compositional assay for many recyclables has a grade larger than 90%. However, the lowest grade is recorded for the mixed paper, as expected because of the nature of the product. It was also noted that the residue fraction consists of 61% of recyclable material, which means that the amount of waste sent to landfill could be reduced significantly by improving the reprocessing of this residual fraction. On the other hand, the recovery for news and magazine paper was found only 57.2%, which results in being put into the market as a product of lower quality and value.

¹ Namık Kemal University, Faculty of Engineering, Department of Environmental Engineering, Tekirdag / Turkey, naydin@nku.edu.tr, Orcid No: 0000-0002-7561-4280

Keywords: Compositional Assay, Efficiency, Grade, Recyclable Materials, Residual Fraction

INTRODUCTION

Currently, 2.01 billion tonnes of municipal waste are produced annually in the world, and this amount is expected to rise to 3.4 billion tonnes by 2050 (Kaza et al., 2018). Municipal solid waste management has, thus, become a concern for the municipal and environmental authorities worldwide (Ncube et al., 2017; Rahardyan et al., 2004; Chen et al., 2010). The problem of municipal waste management is considerably more complicated in developing countries due to the limited collection, ineffective treatment and inadequate disposal (Ciplak, 2015). Waste separation is, therefore, a significant element of a robust integrated waste management system by increasing the quality of produced compost and dry-recyclables (Bernstad, 2014; Stoeva and Alriksson, 2017). It also provides better financing of waste management activities and diminishes the energy and personnel inputs to any downstream processes (Ekere et al., 2009; Ghani et al., 2013).

This study aims to design a materials recycling facility to process recyclable household waste in the district of Corlu, Tekirdag, and assess the efficiency of the facility. The buildings of the facility were designed to comprise fully covered tipping and product storage areas within the main building with a sunken plate feed conveyor to permit the tipped waste to be pushed by a shovel loader into a reception hopper and conveyed into processing hall. The facility was designed to operate on a two-shift basis, sixteen hours per day, and five days per week.

MATERIAL and METHODOLOGY

Corlu is a middle-scale Turkish district in the eastern Thrace, under the administration of the province of Tekirdag (Corlu Municipality, 2020). It is predicted that 50 000 tonnes of mixed-green-bin-recyclable waste are produced annually from households in Corlu (Tinmaz and Demir, 2006). The composition of this waste is shown in Table 1.

The composition of the recyclable materials (waste) from the hand sorting sample was estimated from the reports and published documents (Bernache et al., 2001; Arkoc 2014; Sabiini and Rishmany, 2019; Dubanowitz, 2000; Vermont Department of Environmental Conservation, 2018) (Table 2). The methodological steps that were followed respectively as given below:

- An appropriate design feed rate (in tonnes per hour) of the facility was determined.
- Approximate dimensions were calculated for the tipping and product storage area.
- The recovery distributions of the green-bin-recyclables were determined.
- The effectiveness of the plant in terms of the quality of materials was assessed by using Equation 1; where R_x is the recovery of component x (%) and G_p is the grade of x in a feed (%).

$$\text{Efficiency } E = (R_x * G_p)^{1/2} \quad \text{Equation 1}$$

https://www.corlu.bel.tr/upload/tr/dosya/yayinlar/turkce_18112020145132.pdf (Access Date: 17.03.2021)

Table 1. Composition of Green-Bin-Recyclables in Corlu (Tınmaz and Demir, 2006)

Material category	Composition (%)
News and magazine paper	50
OCC - corrugated cards	5
Grey card (e.g cereal boxes)	5
Other papers (e.g. stationary)	5
Textiles	3
Ferrous cans	10
Aluminium cans	3
HDPE clear	5
HDPE coloured	5
PET	5
Residues / contaminants	4
Total	100

RESULTS

The amount of waste transferred to the facility was calculated as 192.31 tonnes/day by converting 50 000 tonnes/year into daily tonnages. This figure could vary seasonally for several reasons. The fluctuations are not expected to be very high, since only 'dry' waste is collected and sent to the proposed facility. Due to delays in changes between shifts, lunch breaks or reduced productivity at the end of each shift, the effective operating period per day was assumed to be 15 hours (93.75% efficiency). The design feed rate was determined as 12.8 tonnes/hour.

Table 2. Composition of the Materials from the Hand Sorting Sample (“N&M” Represents Newspaper and Magazines; “OCC” Stands for Corrugated Cards; “%” is a Percentage by Weight)

Flow Category	N&M		OCC		Mixed paper		Textiles		Fe cans		Al cans		HDPE clear		HDPE coloured		PET		Residue	
	kg	%	kg	%	kg	%	kg	%	kg	%	kg	%	kg	%	kg	%	kg	%	kg	%
N&M	214.32	91.2	2.6	2	90	60	1.5	3	1.11	3	0.5	2	0.3	1	0.22	1	0.25	1	8.75	25
OCC	2.35	1	120.9	93	7.5	5	0.25	0.5	0.037	0.1	0	0	0.03	0.1	0.022	0.1	0	0	1.05	3
Grey Card	5.875	2.5	3.25	2.5	18	12	0.05	0.1	0.111	0.3	0.075	0.3	0.03	0.1	0	0	0.025	0.1	0.7	2
Other Paper	9.4	4	1.95	1.5	19.5	13	0.05	0.1	0.037	0.1	0.125	0.5	0.09	0.3	0.044	0.2	0	0	4.2	12
Textiles	0.47	0.2	0.39	0.3	3	2	47.5	95	0.185	0.5	0.025	0.1	0	0	0.022	0.1	0	0	1.4	4
Fe cans	0.235	0.1	0.13	0.1	1.5	1	0.15	0.3	34.78	94	0.5	2	0	0	0.022	0.1	0	0	1.05	3
Al cans	0	0	0	0	0.75	0.5	0.05	0.1	0.074	0.2	22.275	89.1	0	0	0	0	0.025	0.1	1.75	5
HDPE clear	0.94	0.4	0.13	0.1	1.5	1	0.1	0.2	0.037	0.1	0.5	2	28.5	95	1.76	8	0.75	3	0.35	1
HDPE coloured	0.47	0.2	0	0	2.25	1.5	0	0	0	0	0.25	1	0.87	2.9	19.36	88	0.25	1	1.75	5
PET	0.235	0.1	0	0	1.5	1	0	0	0	0	0.25	1	0.12	0.4	0.44	2	23.65	94.6	0.35	1
Residue	0.705	0.3	0.65	0.5	4.5	3	0.35	0.7	0.629	1.7	0.5	2	0.06	0.2	0.11	0.5	0.05	0.2	13.65	39
Total	235	100	130	100	150	100	50	100	37	100	25	100	30	100	22	100	25	100	35	100

Design of the Tipping Area

When the materials are brought into the facility, they are deposited in a large hall called the tipping area. Tipping areas are designed to accommodate extra materials for at least two days. Therefore, tipping areas should be large enough to store these materials. It is important to ensure that the collection vehicles must have easy access to the tipping area, unload, and depart. In this study, a sunken plate feed conveyor was planned to be used to permit the tipped waste to be pushed by a shovel loader into the reception hopper and conveyed into the process hall. The conceptual layout of the tipping area is shown in Figure 1.

Since the material recycling facility is average in size, the tipping area of a two days capacity should prevent severe problems. During a two days breakdown, the collected amount should be 384.62 tonnes. On the third day, when delivery finishes, 126.6 tonnes of waste is expected to be processed when it is assumed that the facility operates 10 hours; effectively 9 hours on the third day. Therefore, the total amount of waste in the tipping area was planned to deal with a maximum of 450.27 tonnes.

By taking the compositional distribution of the waste (Table 1) into the account, the volume occupied for each category was calculated as approximately 5 267 m³ (Table 3). For the tipping area, it was assumed that the waste stock is 3 meters in height and rectangular in shape (corresponding to 1 756 m²).

DESIGN AND ASSESSMENT OF A MATERIAL RECYCLING FACILITY IN THE MIDDLE-SCALE RESIDENTIAL AREA

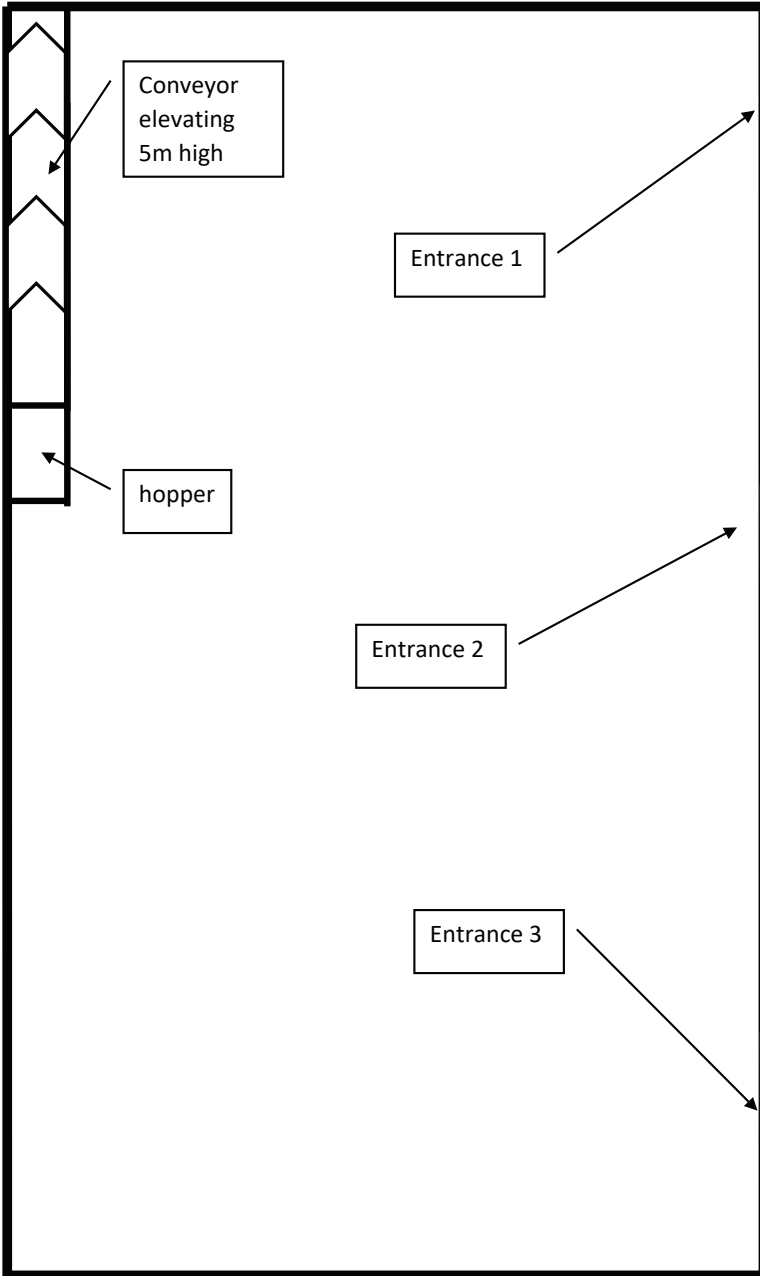


Figure 1. The Conceptual Layout of the Tipping Area

Table 3. The Volume of Materials in the Tipping Area

Category	Composition (%)	Received Waste (tonnes)	Bulk Density* (kg/m ³)	Volume Occupied (m ³)
N&M	50	225.14	310	726.26
OCC	5	22.51	60	375.17
Grey Card	5	22.51	110	204.64
Other Paper	5	22.51	178	126.46
Textiles	3	13.51	210	64.33
Fe cans	10	45.03	89	505.95
Al cans	3	13.51	40	337.75
HDPE clear	5	22.51	20	1 125.50
HDPE coloured	5	22.51	30	750.33
PET	5	22.51	25	900.4
Residue	4	18.01	120	150.08
Total	100	450.27		5 267

* Sayara et al. (2020), Fulford et al. (2018)

Design of the Product Storage Area

This area should provide protection from sun, moisture and degradation for the stored materials. When sizing the storage area, it should be taken into consideration that each truck carries a load of a single product. In practice, the loading pattern depends on the location of the recycling factories and the market. For instance, an industrial estate might include both an aluminium and paper factory, and thus aluminium and mixed paper products can be transferred on the same trip.

Table 4 shows the volume of each product category by assuming that the height of a pile is 3.5 meters.

Table 4. The Volume of Materials in the Product Storage Area

Product	Weight * (tonnes/day)	Bale density ** (kg/m ³)	Volume (m ³)	Area (m ²)
N&M	57.7	900	64.1	18.3
OCC	7.7	900	8.5	2.4
Mixed paper	53.8	900	59.8	17.1
Textile	5.0	900	5.5	1.6
Fe can	18.1	4 000	4.5	1.3
Aluminium can	3.8	1 750	2.2	0.6
HDPE clear	7.7	450	17.1	4.9
HDPE coloured	6.9	450	15.4	4.4
PET	7.7	450	17.1	4.9

* The weight of the processed waste at the proposed facility was estimated by assuming that the processed waste consists of almost 90% of the raw waste due to contamination, etc. (Sayara et al., 2020; Fulford et al., 2018)

** Baldasano et al. (2003); Palanivel et al. (2014)

Each of these products is stored for different periods. Some products are usually stored until they reach the full load of 20 tonnes (typical payload for vehicles taking baled products to the re-processors) and some of them are stored until the market prices are profitable. The areas in Table 4 are based on daily productions, therefore, the storage for a longer period needs more area depending on the recyclables market as explained below:

- Paper prices are very changeable. It is required to store them and send them to the market when it is profitable. Therefore the duration of paper storage was assumed 30 days (Li et al., 2020; Mansikkasalo et al., 2014, Angus, 2012)

- The textile market shows changes as well as paper. Therefore, the paper storage area was design for 30 days (Swinker and Hines, 2009; Grasso and McEnally, 2009; Angus, 2012)
- For aluminium and metals recyclables, there is generally stable demand in the market. They do not require a large area. Therefore, the storage area for aluminium and metals was design for 7 days (Sverdrup, and Ragnarsdottir, 2015; Frees, 2008; Angus, 2012)
- The price of recyclables plastics is also changeable, but not much as for paper. It was assumed that the facility should have a place for the storage of plastics for 14 days (Hopewell and Dvorak, 2009; Angus, 2012)

Table 5 shows the required areas for each type of products based on the assumptions above. It is also possible to discuss the compositional assays of the recyclable materials (grade of recyclables) by evaluating the underlined figures in Table 2 in Material and Methodology. It is seen that the grade of many products is about 90%. Especially, the quality of textile (%95), HDPE clear (%95) and PET (%94.6) is considerably high. Moreover, it is noticeable that the grade of residue is 39% (Table 2). The rest 61% of recyclables in the residue flow is not sorted during the process, which is sent to the landfill. It is, therefore, recommended to reprocess the residue flow to recover more recyclables, which also helps to decrease the amount of waste going to landfill.

Table 5. Required Areas for the Product Storage

MRF Product	Area (m ²)	Storage Period (day)	Required Area (m ²)
N&M	18.3	30	549
OCC card	2.4	30	72
Mixed paper (above materials and other paper)	17.1	30	513
Textile	1.6	30	48
Fe can	1.3	7	9.1
Aluminium can	0.6	7	4.2
HDPE clear	4.9	14	68.6
HDPE coloured	4.4	14	61.6
PET	4.9	14	68.6

Table 6 shows the unit weight of categories which were obtained by using the actual percentages of recyclables.

Table 6. Unit Weight of Categories (Tonnes)

Product	N&M	OCC	Grey card	Other paper	Textiles	Fe cans	Al cans	HDFE clear	HDFE coloured	PET	Residues	Total
N&M	13 680	150	375	600	30	15	0	60	30	15	45	15 000
OCC	40	1 860	50	30	6	2	0	2	0	0	10	2 000
Mixed paper	8 400	700	1 680	1 820	280	140	70	140	210	140	420	14 000
Textile	39	6.5	1.3	1.3	1 235	3.9	1.3	2.6	0	0	9.1	1 300
Fe can	141	4.7	14.1	4.7	23.5	4 418	9.4	4.7	0	0	79.9	4 700
Al can	20	0	3	5	1	20	891	20	10	10	20	1 000
Hdpe clear	20	2	2	6	0	0	0	1 900	58	8	4	2 000
Hdpe coloured	18	1.8	0	3.6	1.8	1.8	0	144	1 584	36	9	1 800
PET	20	0	2	0	0	0	2	60	20	1 892	4	2 000
Residues	1 550	186	124	744	248	186	310	62	310	62	2 418	6 200
Total	23 928	2 911	2 251.4	3 214.6	1 825.3	4 786.7	1 283.7	2 395.3	2 222	2 163	3 019	50 000

The figures in Table 7 show the recovery distributions in each category. For example, N&M has a 57.2 % recovery in the N&M product, but at the same time, 35.1% recovery in the mixed paper product and 0.2 % in OCC. It has a 92.5 % recovery in total which is a high rate. However; it is noticeable that textiles and Aluminium cans have only about % 68 recovery which is relatively low.

Table 7. Recovery Distributions (%)

Product	Recovery Distributions (%)											
	N&M	OCC	Grey cards	Other papers	Textiles	Fe cans	Al cans	HDPE clear	HDPE coloured	PET	Residues	
N&M	57.2	5.2	16.7	18.7	1.6	0.3	0	2.5	1.4	0.7	1.5	
OCC	0.2	63.9	2.2	0.9	0.3	0.0	0	0.1	0	0	0.3	
Mixed paper	35.1	24.0	74.6	56.6	15.3	2.9	5.5	5.8	9.5	6.5	13.9	
Textile	0.2	0.2	0.1	0.0	67.7	0.1	0.1	0.1	0	0	0.3	
Fe can	0.6	0.2	0.6	0.1	1.3	92.3	0.7	0.2	0	0	2.6	
Al can	0.1	0.0	0.1	0.2	0.1	0.4	69.4	0.8	0.5	0.5	0.7	
Hdpe clear	0.1	0.1	0.1	0.2	0.0	0	0.0	79.3	2.6	0.4	0.1	
Hdpe coloured	0.1	0.1	0.0	0.1	0.1	0.03	0.0	6.0	71.3	1.7	0.3	
PET	0.1	0.0	0.1	0.0	0.0	0	0.2	2.5	0.9	87.5	0.1	
Residues	6.5	6.4	5.5	23.1	13.6	3.9	24.1	2.6	14.0	2.9	80.1	
Total	100	100	100	100	100	100	100	100	100	100	100	

As a result, the efficiency of the products was calculated, by using Equation 1 in Materials and Methodology, as 72.2% for N&M, 93.14% for Fe cans, 78.57% for Al cans, 77.09% for OCC cards, and 79.2 for HDPE coloured. The least efficiency was recorded for N&M as expected because of the nature of the product.

The conceptual layout of the product storage area and the schematic diagram of the flow chart are given in Figure 2 and Figure 3 respectively.

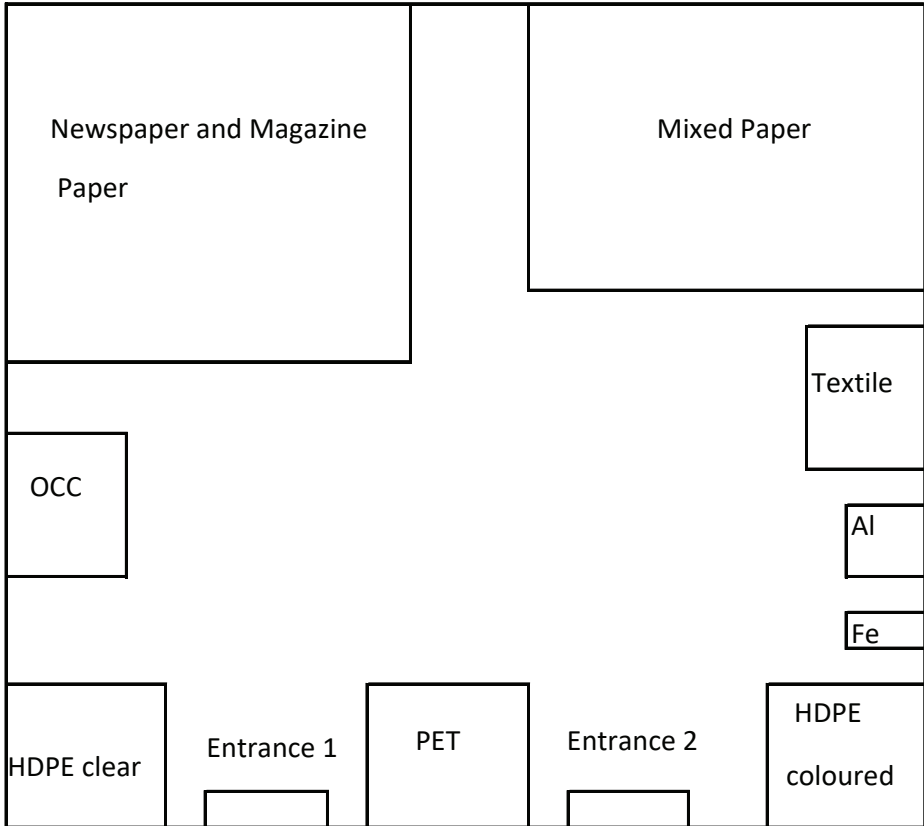


Figure 2. Conceptual Layout of the Product Storage Area

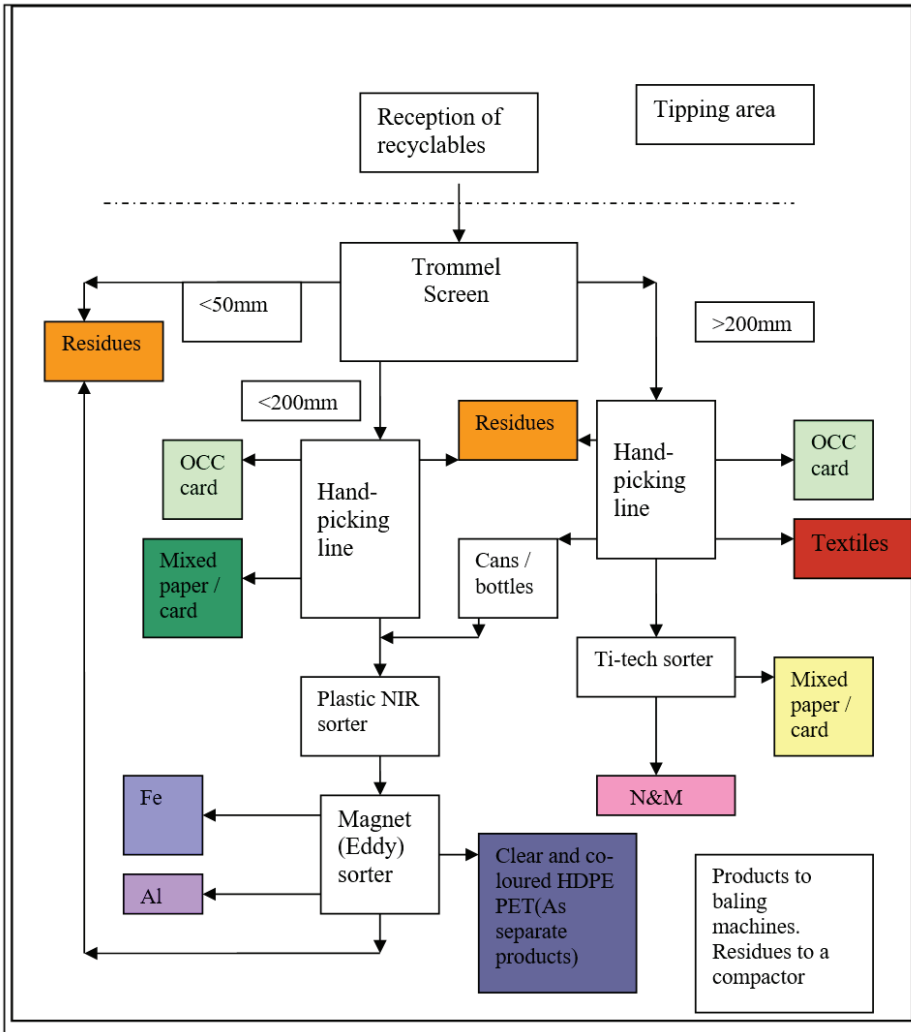


Figure 3. Flow Chart of the Facility

CONCLUSIONS

The composition of the materials from the hand sorting sample shows that the proposed facility manages to produce high-quality products as many of these recyclable materials have a grade larger than 90%, reaching up to 95% for textiles and HDPE clear. The lowest grade is recorded for the mixed papers, as expected due to the nature of the

product. It should also be pointed out that the residue fraction consists of 61% of recyclable material. This means that the amount sent to landfill (6 200 tonnes per year) can be reduced significantly by improving the reprocessing of this residual fraction, which also results in an increase in the recyclables feed.

On the other hand, the recovery of the components is relatively high, except for N&M, which is 57.2%. Additionally, 35.1% of N&M is diverted to the mixed paper category and eventually is put into the market as a product of lower-quality and value. This problem could be solved by improving the handpicking process for papers by training and/or increasing the number of personnel in handpicking line of the proposed facility.

ACKNOWLEDGEMENT

The author would like to thank Dr. Stephen Burnley from the Open University, the UK for his comments.

REFERENCES

- Angus, A., Rivas, M., Fitzsimons, C.D. (2012). Exploring the usefulness of a simple linear regression model for understanding price movements of selected recycled materials in the UK, *Resources, Conservation and Recycling*, 60, 10-19
- Arkoc, O. (2014). Municipal solid waste landfill site selection using geographical information systems: a case study from Çorlu, Turkey, *Arab J Geosci*, 7, 4975-4985, doi: 10.1007/s12517-013-1107-y
- Baldasano, J.M., Gassó, S., García-Pando, C.P. (2003). Baling-Wrapping Technology versus Conventional System, *Waste Management* 23(9):795-806, doi: 10.1016/S0956-053X(03)00087-4
- Bernache, G., Sanchez-Colon, S., Garmendia, A.M., Dávila-Villarreal, A. (2001). Solid waste characterisation study in the Guadalajara Metropolitan Zone, Mexico, *Waste Management & Research*, 19(5):413-24, doi: 10.1177/0734242X0101900506
- Bernstad, A., (2014), Household food waste separation behavior and the importance of convenience, *Waste Management* 34(7), 1317-1323

Chen, X., Geng, Y., Fujita, T. (2010). An overview of municipal solid waste management in China Waste Management, *Waste Management*, 30(4), 716-724

Ciplak, N. (2015). Assessing future scenarios for healthcare waste management using a multi- criteria decision analysis tool: A case study in the Turkish West Black-Sea Region, *The Journal of Air and Waste Management Association*, 65(8), 919-929

Dubanowitz, A. (2000). *Design of a Materials Recovery Facility (MRF) For Processing the Recyclable Materials of New York City's Municipal Solid Waste (Master Theses)*, <http://citeseerx.ist.psu.edu/viewdoc/download?doi=10.1.1.504.2477&rep=rep1&type=pdf>

Ekere, W., Mugisha, J., Drake, L. (2009). Factors influencing waste separation and utilization among households in the Lake Victoria crescent, Uganda, *Waste Management*, 29(12), 3047-3051

Frees, N. (2007). Crediting aluminium recycling in LCA by demand or by disposal. *The International Journal of Life Cycle Assessment*, 13, Article number: 212

Fulford, J., Slack, A., Gillies, R. (2018), Final Report for OPDC Waste Guidance for High Density Development, <https://www.london.gov.uk/sites/default/files/58.pdf> (Access Date:17.03.2021)

Ghani, W.A.W.Ab.K., Rusli, I.F., Biak, D.R.A., Idris, A. (2013). An application of the theory of planned behaviour to study the influencing factors of participation in source separation of food waste, *Waste Management*, 33(5), 1276-1281

Grasso, M.M., McEnally, M., Widdows, R., Herr, D.G. (2009). Consumer Behavior toward Recycled Textile Products. *The Journal of the Textile Institute*, 91, 94-106, <https://doi.org/10.1080/00405000008659530>

Hopewell, J., Dvorak, R., Kosior, E. (2009). Plastics recycling: challenges and opportunities. *The Royal Society Publishing*, 364(1526). <https://doi.org/10.1098/rstb.2008.0311>

Kaza, S., Yao, L.C., Bhada-Tata, P., Van Woerden, F., (2018). *What a Waste 2.0 : A Global Snapshot of Solid Waste Management to 2050*. Urban

Development, Washington, DC: World Bank, <https://openknowledge.worldbank.org/handle/10986/30317> (Access Date:17.03.2021)

Li, J., Mei, M., Han, Y., Hong, M., Man, Yi. (2020). Life cycle cost assessment of recycled paper manufacture in China. *Journal of Cleaner Production*, 252, 119868

Mansikkasalo, A., Lundmark, R., Söderholm, P. (2014). Market behavior and policy in the recycled paper industry: A critical survey of price elasticity research. *Forest Policy and Economics*, 38, 17-29

Ncube, F., Ncube, E.J., Voy, K. (2017). A systematic critical review of epidemiological studies on public health concerns of municipal solid waste handling, *Perspect Public Health*, 137(2):102-108. doi: 10.1177/1757913916639077

Palanivel, T.M., Sulaiman, H. (2014). Generation and Composition of Municipal Solid Waste (MSW) in Muscat, Sultanate of Oman, *APC-BEE Procedia*, 10, 96 – 102

Rahardyan, B., Matsuto, T., Kakuta, Y., Tanaka, N. (2004). Resident's concerns and attitudes towards Solid Waste Management facilities, *Waste Management*, 24(5); 437-451

Sabiini G., Rishmany, J. (2019). Sorting and Miniaturization of Household Waste, *European Journal of Scientific Research*, 153(3)

Sayara, T., Basheer-Salimia, R., Hawamde, F., Sánchez, A., (2020), Recycling of Organic Wastes through Composting: Process Performance and Compost Application in *Agriculture, Agronomy*, 10, 1838; doi:10.3390/agronomy10111838

Stoeva, K., Alriksson, S. (2017). Influence of recycling programmes on waste separation behaviour, *Waste Management*, 68, 732-741

Sverdrup, H.A., Ragnarsdottir, K.V. Koca, D. (2015). Aluminium for the future: Modelling the global production, market supply, demand, price and long term development of the global reserves. *Resources, Conservation and Recycling*, 103, 139-154

Swinker, M.E., Hines, J.D. (2009). Consumers' selection of textile products made from recycled fibres. *Journal of Consumer Studies & Home*

DESIGN AND ASSESSMENT OF A MATERIAL RECYCLING FACILITY IN THE
MIDDLE-SCALE RESIDENTIAL AREA

Economics, 21(3), 307-313. <https://doi.org/10.1111/j.1470-6431.1997.tb00290.x>

Tınmaz, E., Demir, I. (2006). Research on solid waste management system: To improve existing situation in Çorlu Town of Turkey, *Waste Management*, 26(3), 307-314

Vermont Department of Environmental Conservation, 2018, Vermont Department of Environmental Conservation, Solid Waste Program, Vermont Waste Characterization, <https://dec.vermont.gov/sites/dec/files/wmp/SolidWaste/Documents/2018-VT-Waste-Characterization.pdf> (Access Date:14.03.2021)

WEB SOURCES

Corlu Municipality, (2020). Publications Archive; Corlu Tourism Document, https://www.corlu.bel.tr/upload/tr/dosya/yayinlar/turkce_18112020145132.pdf (Access Date:17.03.2021)

NUMERICAL METHODS IN HEAT CONDUCTION AND PLOTTING THE TEMPERATURE DISTRIBUTION IN MATLAB PROGRAM

Abdull Ghafoor SHAIB¹, Senai YALÇINKAYA², Bahadır ALYAVUZ³

Abstract: Heat conduction is the motion of energy form high level thermal energy to adjacent low level internal energetic particle. Heat transfer and temperature are closely related although they are a different nature. Temperature doesn't have direction just has magnitude while heat transfer has direction as well as magnitude. Therefore, it is need to specify both direction and magnitude in order to describe heat transfer completely in a point. Heat transfer has three natures. Conduction heat transfer, convection heat transfer and radiation heat transfer. In this study work we only consider the conduction heat transfer nature only. In this study, it is purposed to examine the temperature distribution on the plate by the Finite Difference Method (Numerical Method). We can find the temperature distribution on the plate by creating an equation that is obtained by solving the heat conduction equation with Finite Difference Method and with using the Matlab program. The results of heat transferring heat steadily and unsteadily distribution are showed graphically.

Keywords: Numerical Methods, Heat Conduction, Analytical Solution, Matlab

1 Marmara University, Institute of Science and Technology, Istanbul / Turkey, abdullghafoorshaib@gmail.com, Orcid No: 0000-0002-6881-142X

2 Marmara University, Engineering Faculty, İstanbul / Turkey, yalcinkaya2012@gmail.com, Orcid No: 0000-0001-7076-7766

3 Gazi University, Faculty of Engineering, Ankara / Turkey, balyavuz@gazi.edu.tr, Orcid No. 0000-0003-4643-4368

HEAT CONDUCTION EQUATION

One Dimensional Heat Conduction Equation in a Large Plane Wall or Plate

In this study a thin plate of thickness Δx in a large plane wall is considered as shown in figure one. In the heat transfer calculation the density of the wall is ρ , the specific heat is C , and the area of the wall normal to the direction of heat transfer is A . The equation of energy balance on this thin element during a small time interval Δt can be taken as equation 1. The schematic of heat transfer in one dimension direction is shown in figure 1.

$$\left(\begin{array}{c} \text{Rate of heat conduction} \\ \text{in the } x \text{ direnction} \end{array} \right) - \left(\begin{array}{c} \text{Rate of heat conduction} \\ \text{in the } x + \Delta x \text{ direnction} \end{array} \right) + \left(\begin{array}{c} \text{Rate of heat} \\ \text{heat generation} \\ \text{inside the elemet} \end{array} \right) = \left(\begin{array}{c} \text{Rate of change of} \\ \text{the energy content of} \\ \text{the element} \end{array} \right) \quad (1)$$

$$\dot{Q}_x - \dot{Q}_{x+\Delta x} + \dot{E}_{gen.element} = \frac{\Delta E_{element}}{\Delta t} = 0 \quad \dots \dots \dots \text{ (steady sate)} \quad (2)$$

Fourier's law of Heat Conduction.

$$\dot{Q}_{cond.} = -KA \times \frac{dT}{dx} \quad \text{Or} \quad \dot{Q}_{cond.} = KA \times \frac{T_1 - T_2}{\Delta x} \quad (3)$$

$$\dot{Q}_x - \dot{Q}_{x+\Delta x} + \dot{e}_{gen.} A \Delta x = \rho c A \Delta x \frac{T_{t+\Delta t} - T_t}{\Delta t} \quad (4)$$

Dividing by $A \Delta x$ gives

$$-\frac{1}{A} \frac{\dot{Q}_{x+\Delta x} - \dot{Q}_x}{\Delta x} + \dot{e}_{gen.} = \rho c \frac{T_{t+\Delta t} - T_t}{\Delta t} \quad (5)$$

$$\frac{\partial}{\partial x} \left(K \frac{\partial T}{\partial x} \right) + \dot{e}_{gen.} = \rho c \frac{\partial T}{\partial t} \quad (6)$$

In the case of constant thermal conductivity, it reduces to

$$\frac{\partial T^2}{\partial x^2} + \frac{e_{gen.}}{K} = \frac{1}{\alpha} \frac{\partial T}{\partial t} \tag{7}$$

$\alpha = k/\rho c$ Is the thermal diffusivity

$$\frac{\partial T^2}{\partial x^2} + \frac{e_{gen.}}{K} = 0 \tag{8}$$

Steady state: $\partial/\partial t = 0$

Figure 1. The Heat Transfer in One Dimension Direction Schematic

Last equation indicates that the temperature is a function of \vec{x} direction or length of the wall. Equation 9 differential equation can be solved with boundary conditions and find a T(x) as a function of position. If the heat equation is write in the \vec{y} direction and \vec{z} direction the General Heat Conduction Equation is obtained. The schematic of heat transfer in two dimension is shown in figure 2.

$$\left(\begin{array}{l} \text{Rate of heat conduction} \\ \text{in the } x, y \text{ ve } z \text{ direnction} \end{array} \right) - \left(\begin{array}{l} \text{Rate of heat conduction} \\ \text{in the } x + \Delta x, yy + \Delta y \text{ ve } z + \Delta z \\ \text{direnction} \end{array} \right) + \left(\begin{array}{l} \text{Rate of heat} \\ \text{heat generation} \\ \text{inside the elemet} \end{array} \right) = \left(\begin{array}{l} \text{Rate of change of} \\ \text{the energy content of} \\ \text{the element} \end{array} \right) \tag{9}$$

$$\dot{Q}_x + \dot{Q}_y + \dot{Q}_z - \dot{Q}_{x+\Delta x} - \dot{Q}_{y+\Delta y} - \dot{Q}_{z+\Delta z} + \dot{E}_{gen.element} = \frac{\Delta E_{element}}{\Delta t} \tag{10}$$

Dividing by $\Delta x \Delta y \Delta z$ gives

$$-\frac{1}{\Delta y \Delta z} \frac{\dot{Q}_{x+\Delta x} - \dot{Q}_x}{\Delta x} - \frac{1}{\Delta x \Delta z} \frac{\dot{Q}_{y+\Delta y} - \dot{Q}_y}{\Delta y} - \frac{1}{\Delta x \Delta y} \frac{\dot{Q}_{z+\Delta z} - \dot{Q}_z}{\Delta z} + \dot{e}_{gen.} = \rho c \frac{T_{t+\Delta t} - T_t}{\Delta t} \quad (11)$$

$$\frac{\partial}{\partial x} \left(K \frac{\partial T}{\partial x} \right) + \frac{\partial}{\partial y} \left(K \frac{\partial T}{\partial y} \right) + \frac{\partial}{\partial z} \left(K \frac{\partial T}{\partial z} \right) + \dot{e}_{gen.} = \rho c \frac{\partial T}{\partial t} \quad (12)$$

In the case of constant thermal conductivity, it reduces to

$$\frac{\partial T^2}{\partial x^2} + \frac{\partial T^2}{\partial y^2} + \frac{\partial T^2}{\partial z^2} + \frac{e_{gen.}}{K} = \frac{1}{\alpha} \frac{\partial T}{\partial t} \quad (13)$$

$\alpha = k/\rho c$ Is the thermal diffusivity

$$\frac{\partial T^2}{\partial x^2} + \frac{\partial T^2}{\partial y^2} + \frac{\partial T^2}{\partial z^2} + \frac{e_{gen.}}{K} = 0 \quad (14)$$

Steady state: $\partial/\partial t = 0$

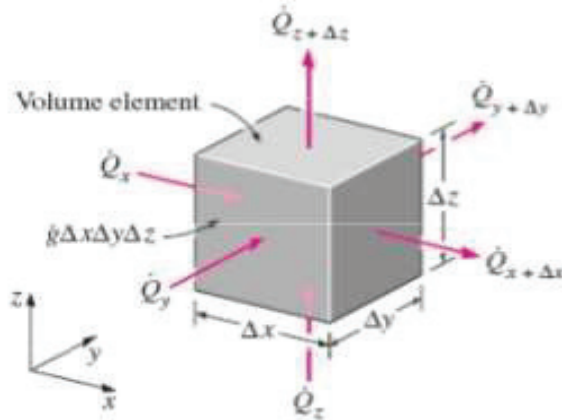


Figure 2. The Schematic of Heat Transfer in Two Dimension

NUMERICAL METHOD STEADY HEAT CONDUCTION EQUATION

One-Dimensional Steady Heat Conduction

So for it is derived relatively simple heat conduction involving simple geometry and it is used when the rate of heat conduction is desired to solve through a plate and distribution of temperature in difference point of the plate with a simple geometries of thickness L and with a simple boundary condition analytically, but many problems in real life or in phenomenon search involve complicated geometries with complex geometric boundary conditions and it is difficult to solve analytically. In such case, approximate solution can be obtained by computers using a numerical method. In this study, the Matlab program is used to approach the approximate solution of the heat conduction equations and plot the distribution temperature with Analytical Solution Method.

For improving the mathematical model, the finite difference formulation of heat conduction is developed in a plane wall using the general energy balance approach and discuss how to solve the resulting equation. To exhibit the approach once again steady one-dimensional heat transfer is considered in a plane wall of thickness L with heat generation $\dot{e}(x)$ and constant conductivity k. the wall is now subdivided into M equal regions of thickness $\Delta x = L/M$ in the x-direction. The schematic of heat transfer analyzing numerically is shown in figure 3.

$$\left(\begin{array}{c} \text{Rate of heat conduction} \\ \text{at the left surface} \end{array} \right) - \left(\begin{array}{c} \text{Rate of heat conduction} \\ \text{at the right surface} \end{array} \right) + \left(\begin{array}{c} \text{Rate of heat} \\ \text{generation} \\ \text{inside the element} \end{array} \right) = \left(\begin{array}{c} \text{Rate of change of} \\ \text{the energy content of} \\ \text{the element} \end{array} \right)$$

$$\dot{Q}_x - \dot{Q}_{x+\Delta x} + \dot{E}_{gen.element} = \frac{\Delta E_{element}}{\Delta t} = 0 \quad (15)$$

Steady state: $\partial/\partial t = 0$

Substituting the Fourier equation

$$\dot{Q}_{cond.} = KA \times \frac{T_1 - T_2}{\Delta x} \tag{16}$$

$$KA \frac{T_{m-1} - T_m}{\Delta x} + KA \frac{T_{m+1} - T_m}{\Delta x} + \dot{e}_{gen.} A \Delta x = 0$$

Which is simplify to

$$\frac{T_{m-1} - 2T_m + T_{m+1}}{\Delta x^2} + \frac{\dot{e}_{gen.}}{k} = 0 \tag{17}$$

For $m = 1, 2, 3, \dots, m - 1$

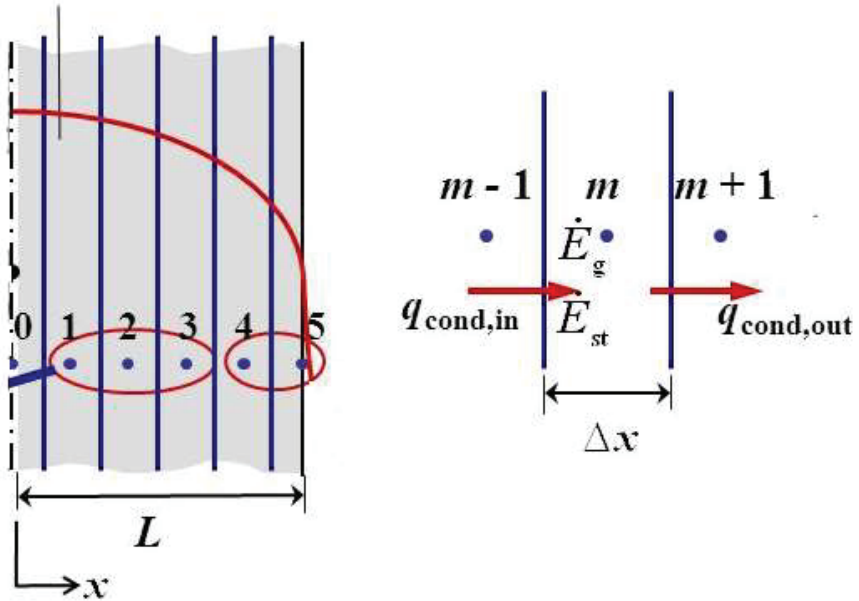


Figure 3. The Schematic of Heat Transfer Analyzing Numerically

Two-Dimensional Steady Heat Conduction Equation

In two dimensional steady heat conduction equation one-dimensional heat conduction is considered and assumed that heat

conduction in other direction to be negligible. Always it is need to consider heat transfer in other direction as well as when the variation of temperature in other direction is significant. To gain the two-dimensional heat conduction equation let's consider a rectangular region in which heat conduction is significant. The schematic numerically analyzing 2-D of the heat transfer is shown in figure 4.

$$\left(\begin{array}{c} \text{Rate of heat conduction at} \\ \text{the left, top, right, and} \\ \text{bottom surface} \end{array} \right) + \left(\begin{array}{c} \text{Rate of heat} \\ \text{heat generation} \\ \text{inside the element} \end{array} \right) = \left(\begin{array}{c} \text{Rate of change of} \\ \text{the energy content of} \\ \text{the element} \end{array} \right)$$

$$\dot{Q}_{cond.left} + \dot{Q}_{cond.top} + \dot{Q}_{cond.right} + \dot{Q}_{cond.bottom} + \dot{E}_{gen.element} = \frac{\Delta E_{element}}{\Delta t} = 0 \quad (18)$$

$$A_x = \Delta_y \times 1 = \Delta_y \quad (19)$$

$$A_y = \Delta_x \times 1 = \Delta_x \quad (20)$$

Fourier law of heat conduction.

$$\dot{Q}_{cond.} = -KA \times \frac{dT}{dX} \quad (21)$$

$$\dot{Q}_{cond.} = KA \times \frac{T_1 - T_2}{\Delta x} \quad (22)$$

$$K\Delta y \frac{T_{m-1,n} - T_{m,n}}{\Delta x} + K\Delta x \frac{T_{m,n+1} - T_{m,n}}{\Delta y} + K\Delta y \frac{T_{m+1,n} - T_{m,n}}{\Delta x} + K\Delta x \frac{T_{m,n-1} - T_{m,n}}{\Delta y} + \dot{e}_{gen.}\Delta x\Delta y = 0 \quad (23)$$

Dividing each term by $\Delta x\Delta y$ and simplifying gives

$$\frac{T_{m-1,n} - 2T_{m,n} + T_{m+1,n}}{\Delta x^2} + \frac{T_{m,n-1} - 2T_{m,n} + T_{m,n+1}}{\Delta y^2} + \frac{\dot{e}_{gen.}}{k} = 0 \quad (24)$$

If $\dot{e}_{gen.}$ is equal to zero and $\Delta x = \Delta y = l$

$$T_{m-1,n} - 2T_{m,n} + T_{m+1,n} + T_{m,n-1} - 2T_{m,n} + T_{m,n+1} = 0 \quad (25)$$

$$T_{m-1,n} + T_{m,n+1} + T_{m+1,n} + T_{m,n-1} - 4T_{m,n} = 0 \quad (26)$$

For $m = 1, 2, 3, \dots, m - 1$

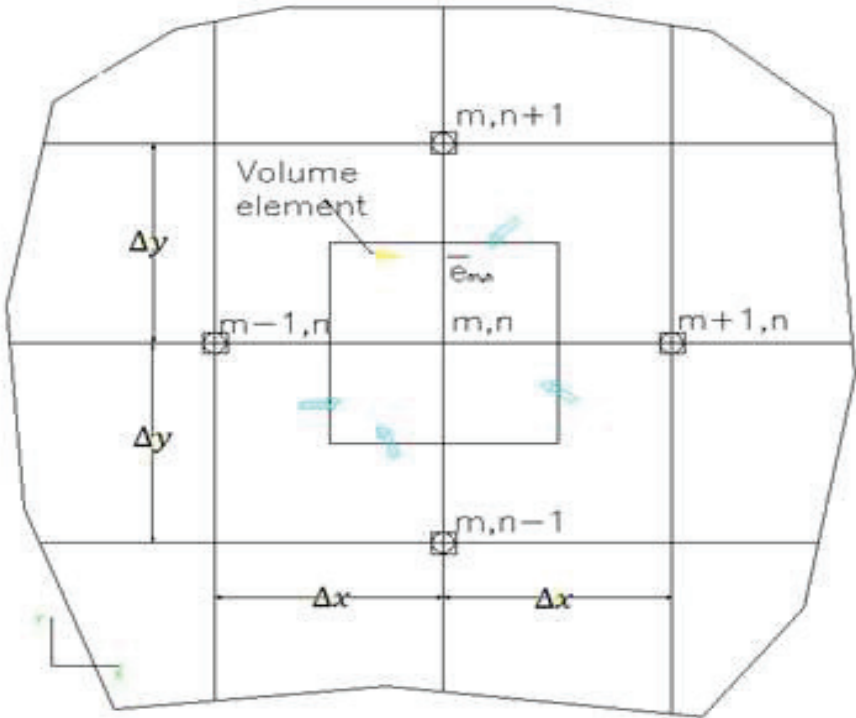


Figure 4. The Schematic Numerically Analyzing 2-D of the Heat Transfer

Mathematically Modeling of Steady Two-Dimensional Heat Conduction in L-Shaped plate

Steady heat transfers in a L-shaped which cross section is given in figure 5. is considered. Transfer of heat in the direction normal to the surface plane of the paper is negligible, so heat transfer in the plate is two-dimensional. The thermal conductivity of the solid plate is $k = 15 \text{ w / (m} \cdot \text{k)}$, and heat is generated in the body at a rate of $(\dot{e}) = 2 \times [10]$

6 W/m^3 . The left surface of the solid plate body is insulated, and the bottom surface is maintained at a uniform temperature of 90°C . The entire top surface is subjected to convection to ambient air at $T_\infty = 25^\circ\text{C}$ with a convection coefficient of $h = 80 \text{ W/(m}^2 \cdot \text{K)}$, and the right surface is subjected to heat flux at a uniform rate of $\dot{q}_R = 5000 \text{ W/m}^2$. The nodal network of this problem consists of 15 equally spaced nodes with $\Delta x = \Delta y = 1.2 \text{ cm}$, as shown in the figure 5. Five of the nodes are at the bottom surface, and thus their temperatures are known. Improving the finite difference equations at the remaining nine nodes and determine the nodal temperatures by solving them is need.

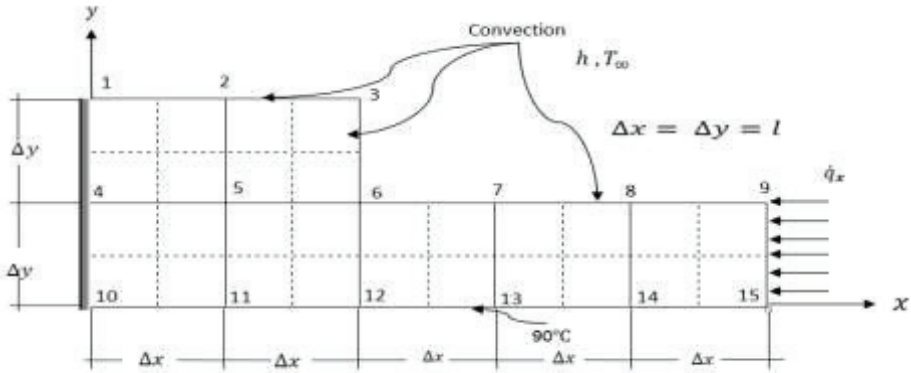


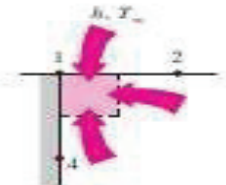
FIGURE 5-26

Figure 5. Steady State Heat Transfer in an L-Shaped Solid Body

NUMERICAL SOLUTION

$\Delta x = \Delta y = 1$

Node 1;



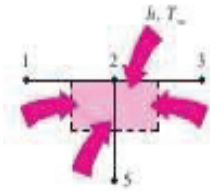
$$0 + h \frac{\Delta x}{2} (T_\infty - T_1) + k \frac{\Delta y}{2} \frac{T_2 - T_1}{\Delta x} + k \frac{\Delta x}{2} \frac{T_4 - T_1}{\Delta y} + \dot{e}_1 \frac{\Delta x \Delta y}{2} = 0$$

$$\Delta x = \Delta y = 1$$

$$-(2 + \frac{hl}{k}) T_1 + T_2 + T_4 = -\frac{hl}{k} T_\infty - \frac{\dot{e}_1 l^2}{2k} \tag{I}$$

NUMERICAL METHODS IN HEAT CONDUCTION AND PLOTTING THE TEMPERATURE DISTRIBUTION IN MATLAB PROGRAM

Node 2;

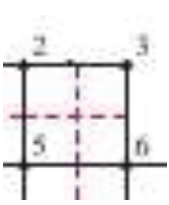


$$h\Delta x(T_\infty - T_2) + k \frac{\Delta y}{2} \frac{T_3 - T_2}{\Delta x} + k\Delta x \frac{T_5 - T_2}{\Delta y} + k \frac{\Delta y}{2} \frac{T_1 - T_2}{\Delta x} + \dot{e}_2 \Delta x \frac{\Delta y}{2} = 0 \quad \Delta x = \Delta y = 1$$

$$T_1 - (4 + \frac{2hl}{k}) T_2 + T_3 + 2T_5 = -\frac{2hl}{k} T_\infty - \frac{\dot{e}_2 l^2}{k}$$

(II)

Node 3;



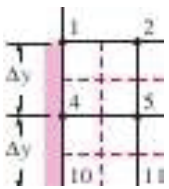
$$h(\frac{\Delta y}{2} + \frac{\Delta y}{2})(T_\infty - T_3) + k \frac{\Delta x}{2} \frac{T_6 - T_3}{\Delta y} + k \frac{\Delta y}{2} \frac{T_2 - T_3}{\Delta x} + \dot{e}_3 \frac{\Delta x \Delta y}{2} = 0$$

$$\Delta x = \Delta y = 1$$

$$T_2 - (2 + \frac{2hl}{k}) T_3 + T_6 = -\frac{2hl}{k} T_\infty - \frac{\dot{e}_3 l^2}{2k}$$

(III)

Node 4;



$$\Delta x = \Delta y = 1$$

$$T_5 + T_1 + T_5 + T_{10} - 4T_4 + \frac{\dot{e}_4 l^2}{k} = 0$$

noting $T_{10} = 90^\circ\text{C}$

$$T_1 - 4T_4 + 2T_5 = -90 - \frac{\dot{e}_4 l^2}{k}$$

(IV)

Node 5;



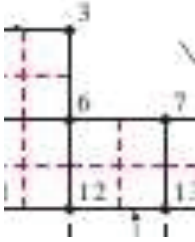
$$T_4 + T_2 + T_6 + T_{11} - 4T_5 + \frac{\dot{e}_5 l^2}{k} = 0$$

noting $T_{11} = 90^\circ\text{C}$

$$T_2 + T_4 - 4T_5 + T_6 = -90^\circ\text{C} + \frac{\dot{e}_5 l^2}{k}$$

(V)

Node 6;

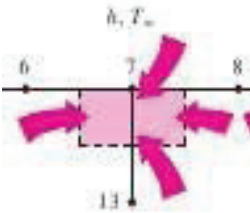


$$h\left(\frac{\Delta x}{2} + \frac{\Delta y}{2}\right)(T_{\infty} - T_3) + k\frac{\Delta y}{2}\frac{T_7 - T_6}{\Delta x} + k\Delta x\frac{T_{12} - T_6}{\Delta y} + k\Delta y\frac{T_5 - T_6}{\Delta x} + k\frac{\Delta x}{2}\frac{T_3 - T_6}{\Delta y} + e_6\frac{3\Delta x\Delta y}{2} = 0$$

$$\Delta x = \Delta y = 1$$

$$T_3 + 2T_5 - \left(6 + \frac{2hl}{k}\right)T_6 + T_7 = -180 - \frac{3\epsilon_6 l^2}{2k} \quad \text{(VI)}$$

Node 7;

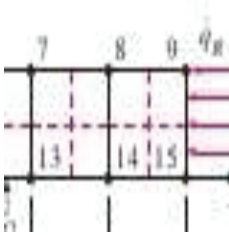


$$h\Delta x(T_{\infty} - T_7) + k\frac{\Delta y}{2}\frac{T_8 - T_7}{\Delta x} + k\Delta x\frac{T_{13} - T_7}{\Delta y} + k\frac{\Delta y}{2}\frac{T_6 - T_7}{\Delta x} + e_7\Delta x\frac{\Delta y}{2} = 0$$

$$\Delta x = \Delta y = 1$$

$$T_6 - \left(4 + \frac{2hl}{k}\right)T_7 + T_8 = -180 - \frac{2hl}{k}T_{\infty} - \frac{\epsilon_7 l^2}{k} \quad \text{(VII)}$$

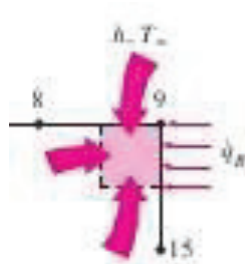
Node 8;



$$\Delta x = \Delta y = 1$$

$$T_7 - \left(4 + \frac{2hl}{k}\right)T_8 + T_9 = -180 - \frac{2hl}{k}T_{\infty} - \frac{\epsilon_8 l^2}{k} \quad \text{(VIII)}$$

Node 9;



$$h\frac{\Delta x}{2}(T_{\infty} - T_9) + q_R\frac{\Delta y}{2} + k\frac{\Delta x}{2}\frac{T_{15} - T_9}{\Delta y} + k\frac{\Delta y}{2}\frac{T_8 - T_9}{\Delta x} + e_9\frac{\Delta x\Delta y}{2} = 0$$

$$\Delta x = \Delta y = 1$$

$$T_8 - \left(2 + \frac{2hl}{k}\right)T_9 = -90 - \frac{q_R l}{k} - \frac{hl}{k}T_{\infty} - \frac{\epsilon_9 l^2}{2k} \quad \text{(IX)}$$

Nodes of 10, 11, 12, 13, 14, and 15 have the temperature of 90°C

To put the value of $h = 80 \text{ w / (m}^2 \cdot \text{k)}$, $k = 15 \text{ w / (m} \cdot \text{k)}$,

$(e) = 2 \times [10] \text{ }^6 \text{ w / m}^3$, $T_\infty = 25^\circ\text{C}$, $q_R = 5000 \text{ w / m}^2$ and $\Delta x = \Delta y = l = 1.2 \text{ cm} = 0.012\text{m}$.

And equations are simplified as,

$$-2.064T_1 + T_2 + T_4 = -11.2 \quad (1) \quad T_3 + 2T_5 - 6.128T_6 + T_7 = 212.0$$

$$T_1 - 4.128T_2 + T_3 + 2T_5 = -22.4 \quad (2) \quad T_6 - 4.128T_7 + T_8 = -202.4$$

$$T_2 - 2.128T_3 + T_6 = -12.8 \quad (3) \quad T_7 - 4.128T_8 + T_9 = -202.4$$

$$T_1 - 4T_4 + 2T_5 = -109.2 \quad (4) \quad T_8 - 2.064T_9 = -105.2$$

$$T_2 + T_4 - 4T_5 + T_6 = -109.2 \quad (5)$$

To solve the above equations therewithal it is need to create a matrix of the linear equations.

In table 1. A matrix of 9x9 is created and it is filled with variable of above equations.

Table 1. A Table Matrix for Solving Nine Linear First Order Equation

T1	T2	T3	T4	T5	T6	T7	T8T	T9	T	CONSTANT
-2.064	1	0	1	0	0	0	0	0	T1	-11.2
1	-4.128	1	0	2	0	0	0	0	T2	-22.4
0	1	-2.128	0	0	1	0	0	0	T3	-12.8
1	0	0	-4	2	0	0	0	0	T4	-109.2
0	1	0	1	-4	1	0	0	0	T5	-109.2
0	0	1	0	2	-6.128	1	0	0	T6	-212
0	0	0	0	0	1	-4.128	1	0	T7	-202.4
0	0	0	0	0	0	1	-4.128	1	T8	-202.4
0	0	0	0	0	0	0	1	-2.064	T9	-105.2

To solve this matrix in Matlab; firstly, it is need to create a zeros square matrix of 9x9 in the name of A. Then, it is time to substitute the values of matrix factor. Lately, a column vector of 9x1 in the name of B is created. In the last, the constant value multiplies to these matrices to give as the unknowns such as $C=A \setminus B$. The figure 6. Shows the coding to create matrix in Matlab program.

NUMERICAL METHODS IN HEAT CONDUCTION AND PLOTTING THE TEMPERATURE DISTRIBUTION IN MATLAB PROGRAM

```

1 % this program will solve the L shaped plate Steady state 2-D
2 % heat transfer
3 % the procedure: firstly create one 9x9 unite matrix then enter the value
4 % solving linear equation [A](B)-[C]----- [B]=[A]\[C]
5 A=eye(9);
6 A(1,2)=1;A(1,4)=1;A(2,1)=1;A(2,3)=1;A(3,2)=1;A(3,6)=1;A(4,1)=1;
7 A(5,2)=1;A(5,6)=1;A(6,3)=1;A(6,4)=1;A(6,7)=1;A(7,6)=1;A(7,8)=1;
8 A(8,7)=1;A(8,9)=1;A(9,8)=1;
9 n=[2,4,6];
10 A(n,5)=2;
11 A(4,4)=-4;A(5,5)=-4;A(1,1)=-2.064;A(9,9)=-2.064;
12 A(2,2)=-4.128;A(7,7)=-4.128;A(8,8)=-4.128;
13 A(3,3)=-2.128;A(6,6)=-6.128;
14 C=[-11.2,-22.4,-12.8,-109.2,-109.2,-212,-202.4,-202.4,-105.2]';
15 B=A\C;
16

```

Figure 6. Coding Matlab Program to Create Matrix

After creating the matrix then the matrix is solved with running the Matlab. Advantages of using Matlab in here is not only to solve multi numeric equation, this program utilize to show the graphic result of heat transfer steadily and unsteadily. The matrix of nine linear first order equation is shown in figure 7.

```

>> A
A =
-2.0640    1.0000         0    1.0000         0         0         0         0         0
 1.0000   -4.1280    1.0000         0    2.0000         0         0         0         0
         0    1.0000   -2.1280         0         0    1.0000         0         0         0
 1.0000         0         0   -4.0000    2.0000         0         0         0         0
         0    1.0000         0    1.0000   -4.0000    1.0000         0         0         0
         0         0    1.0000         0    2.0000   -6.1280    1.0000         0         0
         0         0         0         0         0    1.0000   -4.1280    1.0000         0
         0         0         0         0         0         0    1.0000   -4.1280    1.0000
         0         0         0         0         0         0         0    1.0000   -2.0640

```

Figure 7. A Matrix 9x9 is Filled With Coefficients of Linear Equations

Writing Cods in Matlab Program to Plot the Distribution of Temperature in Two-Dimensional Steady Heat Transfer Conduction

Considering steady heat transfer in an L-shaped solid body which cross section is given in figure 8. Heat transfer in the direction normal to the plane of the paper is negligible. The left, top, right surfaces of the body are maintained at a uniform temperature of 0°C, and the bottom surface is maintained at a uniform temperature of 90°C. The nodal network of problem consists of 33 equally spaced nodes with $\Delta x = \Delta y = 1$ unite, as shown in the figure. 27 of the nodes are at the middle surface that is unknown. Obtain finite difference equations at the remaining 27 nodes and determine the nodal temperatures by solving them then use a Matlab program to show the distribution of the temperature in this plate.

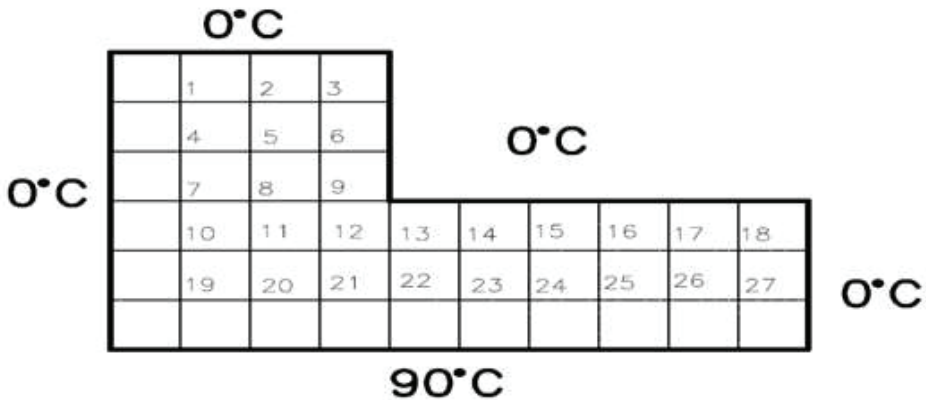


Figure 8. Steady Heat Transfer in an L-Shaped Solid Body

General numeric linear equations of heat transfer,

$$T_{m-1,n} + T_{m,n+1} + T_{m+1,n} + T_{m,n-1} - 4T_{m,n} = 0$$

$$T_1 = \frac{1}{4} \cdot (T_2 + T_4); \quad T_2 = \frac{1}{4} \cdot (T_1 + T_3 + T_5); \quad T_3 = \frac{1}{4} \cdot (T_2 + T_6);$$

$$T_4 = \frac{1}{4} \cdot (T_1 + T_5 + T_7)$$

$$T_5 = \frac{1}{4} \cdot (T_4 + T_2 + T_6 + T_8); \quad T_6 = \frac{1}{4} \cdot (T_5 + T_3 + T_9); \quad T_7 = \frac{1}{4} \cdot (T_4 + T_8 + T_{10})$$

Solving the matrix in excel to be sure that the Matlab program works truly then continuing to coding the Matlab program for solving this problem then obtain the results. The above linear equations of each nod is determined with solving the matrix in excel. The figure of 10 shows the excel screen which contains both the invers matrix and values of unknown temperatures.

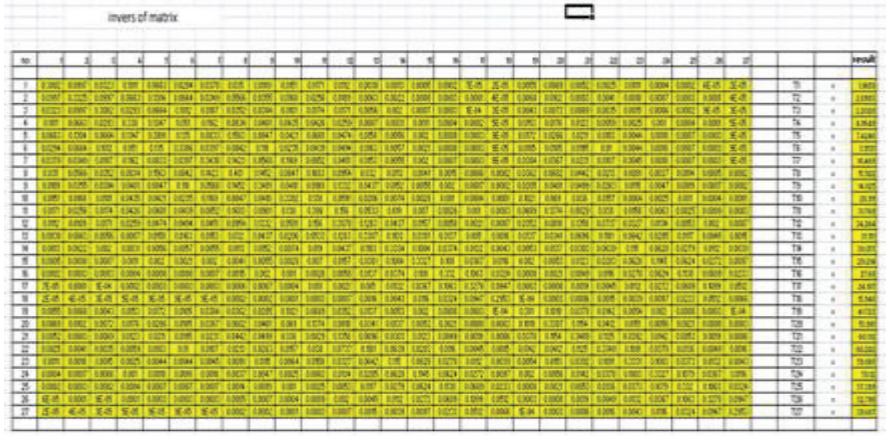


Figure 10. Invers Matrix of Linear Equations and Value of Each Unknown Temperature

MATLAB CODING

```
% in width 10m in high 6m
h=6;l=10; H=h+1; L=l+1;
% delta-x = n1 =1; delta-y =n2 =1;
U=zeros(H,L);
n1=7/H; n2=11/L
for i=1:H; j=1;
    U(i,j)=0;
end
for i=1:H; j=L;
    U(i,j)=0;
end
```

NUMERICAL METHODS IN HEAT CONDUCTION AND PLOTTING THE TEMPERATURE DISTRIBUTION IN MATLAB PROGRAM

```
    for i=1; j=2:L-1;
        U(i,j)=90;
    end
    for i=H; j=2:L-1;
        U(i,j)=0;
    end
    for i=2:H-1;
        for j=2:L-1;
            U(i,j)=(U(i-1,j)+U(i,j-1)+U(i+1,j)+U(i,j+1))/4;
        end
    end
    for i=4:7; j=1:7;
        U(i,j)=0;
    end
    T_now=U(2,2); epsilon=0.0001;Nmax=100; hata=0.01; n=0;
    while(hata>epsilon&& n<Nmax);
        for i=2:3
            for j=2:L-1
                U(i,j)=(U(i-1,j)+U(i,j-1)+U(i+1,j)+U(i,j+1))/4;
            end
        end
        T_later=U(2,2);
        hata=abs(T_later-T_now);
        n=n+1;
        T_now=T_later;
    end
    T_now=U(6,10); epsilon=0.0001;Nmax=100; hata=0.1; n=0;
    while(hata>epsilon&& n<Nmax);
        fori=4:H-1
```

```

for j=8:L-1
    U(i,j)=(U(i-1,j)+U(i,j-1)+U(i+1,j)+U(i,j+1))/4;
end
end
T_later=U(6,10);
hata=abs(T_later-T_now);
n=n+1;
T_now=T_later;
end
delta_x=n1; delta_y=n2 ;
for i=1:H;
    for j=1:L;
        T_2D(i,j)=U(i,j)
        x(j)=j*delta_x;
        y(i)=i*delta_y;
    end
end
surf(x,y,T_2D);

```

This Matlab cods are written for conduction heat transfer steadily. After t infinity time the temperature of nods become constant. Although the heat is transferring from hot nods through to cold nods the value of temperature does not change. The last distribution form of temperature in L shaped plate is shown in figure 11.

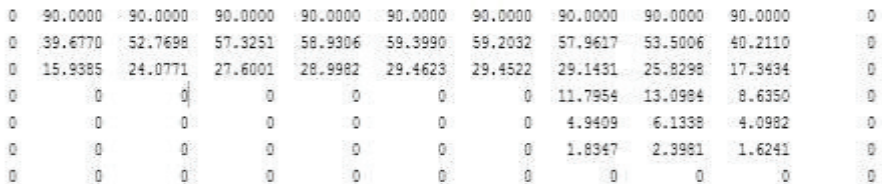


Figure 11. The Last Distribution Form of Temperature in L Shaped Plate

PLOTTING the DISTRIBUTION of TEMPERATURE

In herer a simple matrix is considered whit one row and one column. Many mathematical balances that work on arrays or matrices are create in to the Matlab environment. For instance, preparing determinants, dot-products, cross-products and inverse matrices. Vectorized operations adding two arrays together needs only one command, instead of a for or while loop. In Matlab the graphical output is optimized and plotting data is very easy. Changing colors, sizes, scales, etc, with using the graphical interactive tools is possible in Matlab. Matlab's workability can be greatly expanded by the addition of toolboxes. These are sets of specific functions that provided more specialized functionality. Ex: Excel link allows data to be written in a format recognized by Excel, Statistics Toolbox allows more specialized statistical manipulation of data. Matlab is not only a programming language, but a programming environment as well. Operations from the command line, as a sophisticated calculator can perform or can create programs and functions that perform repetitive tasks, just as any other computer language. The best advantages of Matlab is to distribute the numeric solutions graphically. In the figure 12. The distribution of temperature is plotted after the transferring conduction heat become steady.

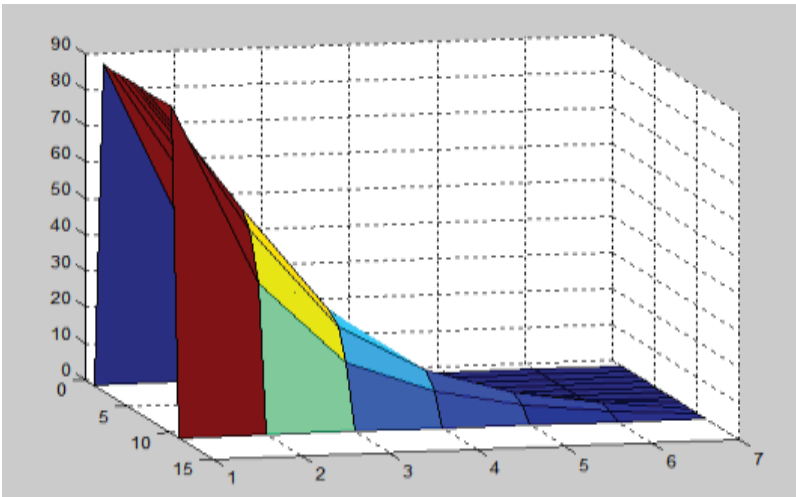


Figure 12. The Distribution of Temperature is Plotted After the Transferring Conduction Heat Becomes Steady

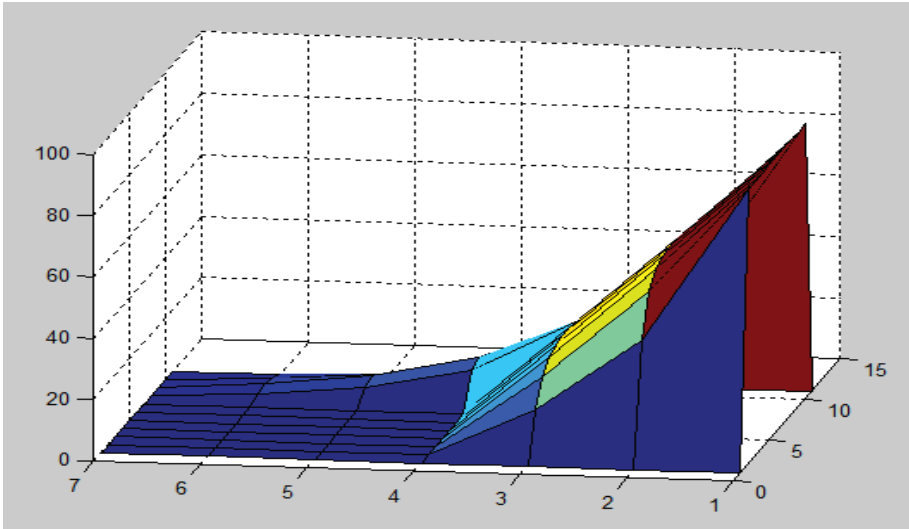


Figure 13. Perspective Plot View of Distribution of Temperature After the Transferring Conduction Heat Becomes Steady

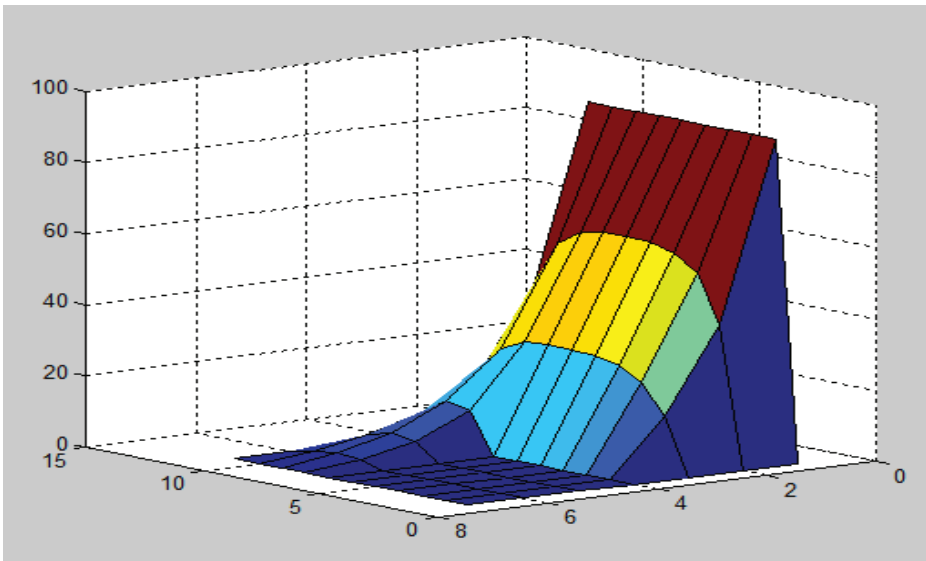


Figure 14. Perspective Plot View of Distribution of Temperature After the Transferring Conduction Heat Becomes Steady

CONCLUSION

In Heat and Mass Transfer knowledge many problems can be solved analytically. Such that, flow of heat from high temperature to low temperature as conduction, convection and radiation but many cases due to condition of shape of mold or condition of surrounding solving heat problems become more complex. So it is need to solve heat transfer phenomenon numerically. To keep time; while solving a problem numerically one of the useful computer programs should use. In this study to solve the heat conduction in two dimension numerically a L shape plate is considered as conductor. Because solving process of heat transfer and distribution temperature of this problem analytically takes to many time, by basic mathematic experience and writing cod in Matlab program is tried. In other word, the heat transfer and temperature distribution problem is solved in computer program to be fast and more correct. In the last; numerically computing programs especially Matlab program has many advantages to use for solving complex heat transfer phenomenon. Matlab program develops the computational codes easily creates simulation by using the graphical interactive tools.

REFERENCES

- Gates B., (2005). "In Proceedings of the 2005 ACM/IEEE Conference on Supercomputing", IEEE Computer Society, USA, 0., Doi: 10.5555/1105760.1116037.
- Trefethen L. N., (2015). "Computing Numerically with Functions Instead of Numbers. Commun". Doi: 10.1145/2814847.
- Wilkinson J. H. and Reinsch C., (1971), "Handbook for Automatic Computation", Volume II: Linear Algebra. Die Grundlehren der mathematischen Wissenschaften in Einzeldarstellungen, Vol. 186. Springer-Verlag, Berlin. Doi: 10.1007/978-3-642-86940-2.
- Richard L. Burden-J. Douglas Faires, (2011) "Numerical Analysis", Youngstown State University, 8th edition. ISBN-13: 978-0-538-73351-9.
- Steven C., Raymond C., and Canale P., (2005), "Numerical Method for Engineers", 6TH edition. ISBN: 9780071244299.
- James P. H., Young I. C., and Warren M. R., (1998) "Heat and Mass

Transfer Third edition", Handbook of heat transfer, ISBN: 0-07-053555-8.

Amos G., (2004), "Matlab An Introduction With Application" 4th edition, ISBN: 0471694207.

Pulkit S., Puneet T., Akash D. S. and Thakur H. C., (2017), "Heat Transfer analysis", Proc. 4 8565-8570.

THE HISTORIC CONCRETE: CONSTRUCTION AND ARCHITECTURE

*Hilal Tuğba ÖRMECİOĞLU*¹

Abstract: The invention of artificial building materials after the industrial revolution is a threshold in architectural history since they altered architecture irreversibly in terms of form, space, and structure. Among these artificial materials, reinforced concrete had the most widespread effects with its structural capabilities, plastic qualities, and constructional characteristics. The concrete, which was first introduced to the construction market with two different features as economy or durability, revolutionized the construction market offering both features at the same time. Over time, as the characteristics and capabilities of the material were understood by the architects, reinforced concrete would also revolutionize the architecture, which had been in a vicious circle throughout the 19th century. While the construction of reinforced concrete structures has been going on for more than a century, almost all of the formal and spatial features of modernist architecture of the 20th century were realized thanks to the material capacity of reinforced concrete. As a factor shaping the architecture of a whole century all over the world, reinforced concrete has become a historical construction system that has been built for more than 100 years. Meanwhile, the early examples of reinforced concrete buildings are shattered by time, climatic conditions, air pollution, and misuse problems. Besides, they are considered safe according to today's regulations since they did not build at the level of today's construction standards in terms of material class or construction techniques. As a sum of all these unfavorable conditions -climate, time, primitive construction conditions, low material class, etc.-, many deteriorations have occurred not only on surfaces but

¹ Akdeniz University, Faculty of Architecture, Department of Architecture, Antalya / Turkey, ormeციoglu@akdeniz.edu.tr, Orcid No: 0000-0002-0662-4178

also on structural members of these historic concrete structures which inevitably lead to the demolition of the building if not repaired. Under these circumstances, the aim of this paper is to convey the importance of historic concrete from a historical perspective and explain the conservation problems of assessment and repair of the historic concrete structures, which are the representatives of the architectural style and construction technique of their time. Although most of the sources of problems such as air pollution, climatic conditions, natural forces, etc. are similar in all conservation works, conservation the 20th-century architecture has become special expertise of restoration, since material characteristics of the period are totally different from previous centuries. It is important to preserve the document value of the historical reinforced concrete structures, reflecting our recent architectural history and the technical characteristics of their period, and to transfer them to future generations.

Keywords: Historic Concrete, History of Concrete, Conservation of Modern Architecture

INTRODUCTION

The invention of artificial building materials after the industrial revolution is a threshold in architectural history since they altered architecture irreversibly in terms of form, space, and structure. Before them, the concept of architecture was correlated with the material properties of the stone. Hence, heaviness and monumentality had been the main features of architecture until the 19th century, and these belong to the nature of stone and masonry (Gideon, 1995). The invention of industrial building materials such as the iron, steel, and concrete revolutionized the nature of architecture by creating a clear division between supporting and supported parts of a building with the help of the carcass structural system. The result was strikingly different in terms of not only aesthetics but also space. In this way, architects could make wider openings -even in ribbon form-, brighter interiors, dynamic and fluidic spatial organizations, and lighter buildings -even elevated from the ground-. This new architecture of the forthcoming century heralds a new world full of innovative possibilities with the help of the industrial revolution and developing technology. Among these artificial materials, reinforced concrete which had the most widespread effects is the most considerable.

HISTORY of CONCRETE as a BUILDING MATERIAL

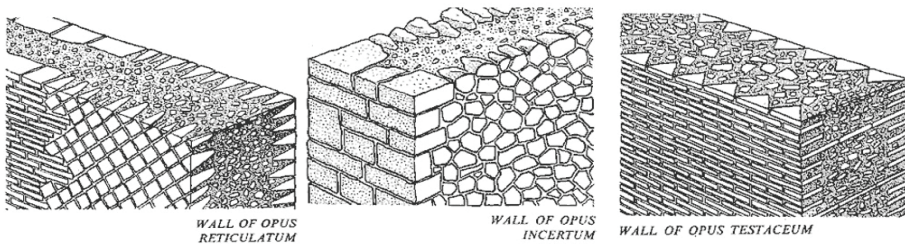


Figure 1. Drawing of Roman Wall Types Infilled With Roman Concrete²

Although concrete was a well-known and considerable material in Roman architecture its usage dates back to more ancient periods since first findings of concrete in construction were found at the foundations of houses in Lepenski Vir from 5600 BC, a Mesolithic site at Serbia on the Balkan Peninsula³. The usage of ancient concrete was a frequent practice in Egypt, Assyria, Babylon, and China from 3000 BC onwards. Nevertheless, the material became widespread in the Roman period as a filling within masonry and brick walls roman walls (fig 1). The usage of Roman concrete reached its climax especially with the construction of Villa Adriana and Pantheon in the second and sixth decades of the 2nd century AD. Meanwhile, the material developed significantly with the experiments adding several materials within the concrete mud such as Puzzolano volcanic ash, lime, brick parts, etc. This was a significant discovery on the way to the invention of concrete, as when mixed with water, they fuse and harden the materials it comes into contact with, hence, they were called hydraulic binders. Among them, the most significant was “the addition of lime to the ash initiated a complex hydration reaction to form calcium-silicate-hydrates which are the principal strength-giving hydrates in concrete” (Brueckner and Lambert, 2013). Despite all, the technique of concrete was completely forgotten in the Western world after the decline of the Roman Empire until the 18th century.

² <https://www.architettdigitale.it/la-struttura-portante-nel-progetto-di-una-casa/> (Date of access 10.16.2021)

³ <https://www.donsmaps.com/lepenski.html> (Date of Access 16.10.2021)

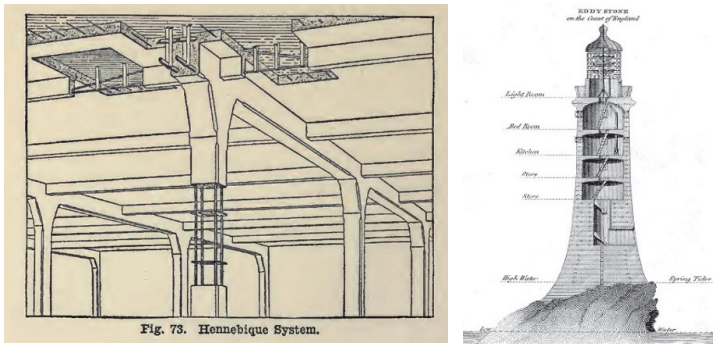


Figure 2. Left: Section Drawing of the Eddystone Lighthouse by John Smeaton, and Right: Drawing of the Hennebique System⁴

The first experiments after Romans were made in 1824 by the mason named Joseph Aspdin, who was engaged in brick making in Leeds, England. Aspdin observed that when water and sand were added to the powder obtained by cooking and grinding a fine-grained limestone and clay mixture, it hardened over time. He patented his invention under the name Portland Cement, as the final product was similar to the natural stones of Portland; and started production in the small factory he founded in 1825. However, this cement did not have the same properties as the Portland Cement used today, since the raw materials could not be fired at the required temperature during production. Later, in 1845, an Englishman named Isaac Johnson re-determined the appropriate proportions of raw materials and the firing temperature and determined the norms for Portland Cement used today (Erdoğan, 2021). It should be noted that Portland cement led concrete to re-emerge as a modern building material, largely due to the influence of John Smeaton who identified the compositional requirements of hydraulic cement for use in the construction of the Eddystone Lighthouse off the southwest coast of England in 1755 (Fig. 2)⁵.

4 https://en.wikipedia.org/wiki/John_Smeaton (Date of access 10.16.2021) and <https://www.jpconcrete.co.uk/francois-hennebique-a-pioneer-of-reinforced-concrete/> (Date of access 10.16.2021)

5 https://en.wikipedia.org/wiki/John_Smeaton (Date of access 10.16.2021)



Figure 3. Left: An Advertisement of Monier Reinforced Concrete Pipes he Patented in 1868, With the Background of a Plant Zigarettenfabrik Yramos-Dresden (Mistewicz, M. 2019), Right: Construction of Forth Bridge (1883) Upon Concrete Piers (Urquhart, 2013)

After the chemical experiments on the material by Aspdin in 1824, and Johnson's introduction of applicable cement norms in 1845, the vital development which changed the nature of the material was realized by Monier by laying the foundations of a tension-resistant reinforced concrete system in 1877. Joseph Monier, who was a gardener, aimed to find out a way for making more resistant pots for huge plants; but naturally, the tension on the surfaces of the pot increased as the dimensions enlarged, and cracks occurred. Concrete itself was better material than ceramic to make huge pots but it was still a very limited material due to its low tensile strength and ductility. With the addition of iron reinforcing to the concrete paste, Monier achieved preventing cracks at the certain regions subject to tensile stress. This can be listed as one of the most developments affecting the production of reinforced concrete structures. More persistently than his predecessors and contemporaries, such as Lambot (1854), Coignet (1861), and Hyatt (1877), Monier developed his system step by step and was successively awarded patents for pipes (Fig3), flat plates, bridges, and ladders; he built his first reinforced concrete footbridge in 1875 with a span of 16.5 m in the Marquise Tilière park in Chazelet, France (Mistewicz, M. 2019). However, never comprehended the revolutionary capacity of tension-resistant building material. It was first the German engineers who recognized reinforced concrete as a new building material in 1880. In 1879 G. A. Wayss, a German builder bought the patent rights of Monier's system, promoted it under the

name of Wayss-Monier system. He became successful in pioneering reinforced concrete construction in Germany, Austria, and even France at the end of the 19th century with this patent (Collins, 2004). But as Gideon (1995) states “the decisive step that would enable a new means of architectural design to arise from an ancillary material, from a construction detail, was taken by Francois Hennebique”.

Hennebique further developed the idea of using iron encased in concrete, which was up to that time used only for fireproof protection for wrought-iron beams, as a reinforcement of the concrete. Concrete can only resist compression, but together with iron, it became a super material that can both resist tension and compression without the danger of fire.

At first, Hennebique developed the idea for making prefabricated structural members or constructional components as Monier. In 1892 Hennebique took out a patent on reinforced concrete beams. But this system had problems in connection points between beams, ceiling, and vertical load-bearing elements. With an appropriate placement and bending of the reinforcing iron, Hennebique succeeded in bonding the ceiling, beams, and columns into one continuous unit and make the building as a monolith (Fig1). The invention of a unified frame structure had widened the limits of architectural imagination, and emancipated space from the load-bearing limits of the masonry structure.

EARLY REINFORCED CONCRETE in ARCHITECTURE

As Gideon expressed in amazement in 1928, “From slender iron rods, cement, sand, and gravel, from an “aggregate body,” vast building complexes can suddenly crystallize into a single stone monolith that like no previously known natural material is able to resist fire and a maximum load.” As he (1995) conveys that reinforced concrete was an accomplishment by which “the properties of ... almost worthless materials and through their combination increases their separate capacities many times over.” But in spite of persistent attempts of a small number of entrepreneurs the material did not gain commercial value in the construction sector for many decades.



Figure 4. Very First Reinforced Concrete Constructions in Architectural History. Left Coignet House⁶ in 1853; Right: Wilkons' Annex in 1854 (Fisher Cassie, 1955)

Except for the foundations of the Milbank prison built in 1817, the first concrete in architecture was the construction of a four-story house by Coignet in 1853 on Rue Charles Michels, Paris, and of two-story servants' cottage by Wilkinson in 1854 in Newcastle Upon Tyne, England (Fig4). These two buildings were structurally different, the first was built with rammed (mass) concrete, while the other was built with concrete iron reinforcements. Coignet, who was in the cement business, consider building a house with concrete will be good publicity for his business and constructed the building with rammed (mass) concrete despite all the negative reviews that it would not be safe, and patented the technique as *Béton Économique* in 1855. On the other hand, Wilkinson, preferred an advanced technique of reinforcement of slab with iron bars and wire rope, hence, the annex in Newcastle-upon-Tyne is often credited for being the first reinforced concrete building (Condit, 1968).

However, in both of the buildings, concrete was just a building material that was preferred only because it was more economical than its counterparts. The original characteristics of the material had no effect on either the construction or the architecture. Although the first applications of concrete in building construction were initiated in the 1850s,

⁶ <https://aehistory.wordpress.com/1853/10/05/1853-first-reinforced-concrete/coignet1/> (Date of access 10.16.2021)

the first patented on reinforcement of concrete was obtained in 1867 for Monier's reinforced concrete pots with iron wire reinforcement, the first commercial system and the first appreciation of reinforced concrete as a new building material was by Wayss in 1879, it was actually Hennebique who made the material accepted among architects (Collins, 2004). Throughout the late 19th century concrete was first used for its inherent compressive strength and setting capability as mass rammed concrete for floors, foundations, and engineering structures such as harbors and bridges. But Hennebique's reinforced concrete frame system patent discovered a spatial potential with the help of non-loadbearing walls in addition to materials economy and popularized its use outside of engineering structures.

However, Hennebique himself did not see architects as a target group of customers, rather focused on engineers and contractors. Even though he regarded his material as having architectural potential, there is no reference he collaborated with architects or involve in any aesthetic promotion of the material in 1900. As Cusack (1984) conveyed "Hennebique did not believe in imposing art in buildings and in particular scorned the methods of what he called puerile symmetry". By the end of the first decade of the 20th century, Hennebique's system was widespread all around the world through a network of agents, licensed contractors, and engineers, hence the number of applications reached to 19,000-20,000 buildings including nearly 1000 bridges and none of them were failed. This was a huge success of not only his patent but also his organizational network including 62 offices (43 of them in Europe, 12 in America, 4 in Asia, and 3 in Africa), a special training program, and a magazine, which publishes the constructed buildings with the Hennebique System, titled "Le Béton Armé" (Cusack, 1984).

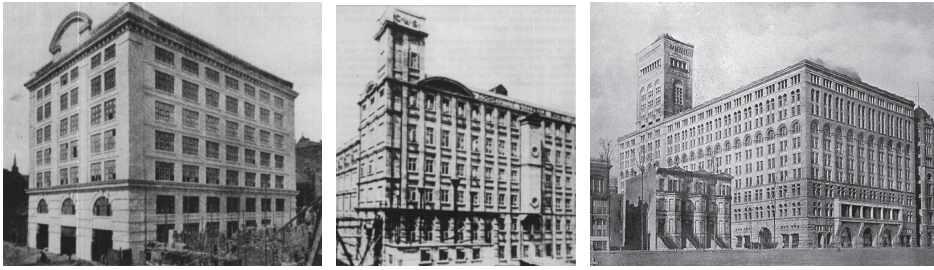


Figure 5. Left: Quayside Warehouse, Newcastle-Upon-Tyne, 1901; Middle: Grain Silo, Dunston, 1902, (Cusack, 1984); Right: Sullivan's Auditorium Building, Chicago, 1889

Not only Hennebique System but also the reinforced concrete frame structures gain general publicity along with the publication and distribution of “Le Béton Armé”. Architects were also interested. Perret Frères, the construction company of August Perret and his brother, was one of the licensed contractors of Hennebique System in France (Gökbayrak P., 2005). But unlike other licensees, Perret was not only a contractor but also an architect. As a licensed contractor-cum-architect Perret, was quite probably aware of the Hennebique-licensed structures published in the “Le Béton Armé” magazine such as warehouse at Newcastle and grain silo at Dunston (Fig5). Although these were industrial buildings which do not need so much daylight or modern façade, proportions of their mass and openings were precursors of new architectural configurations with the help of the monolithic frame structure (Cusack, 1984).

Concurrently Louis Sullivan was building similar façades in Chicago with the steel frame structure. The buildings which are considered as the first examples of high-rise architecture had façade liberated from the load-bearing system, hence had more openings than the traditional masonry architecture. These new generation of reinforced concrete industrial buildings have similar façade and mass propositions with Sullivan's steel-frame high-rise buildings.

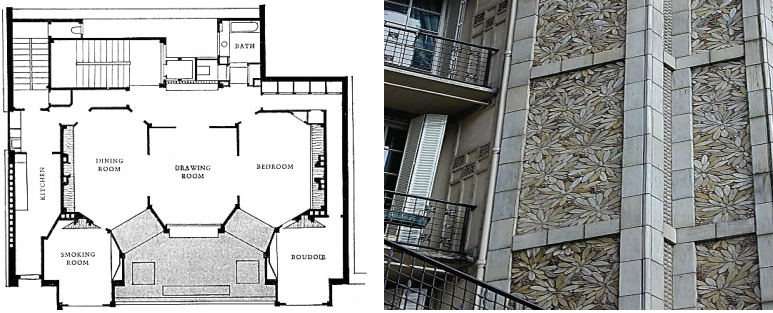


Figure 6. Left: Plan of 25b Rue Franklin⁷; Right: Ceramic Façade Detail of 25b Rue Franklin⁸

Soon after Perret would design a multi-story apartment building at 25b Rue Franklin, Paris (1903-1904) totally with the reinforced concrete frame structure. This was the very first use of reinforced concrete for architectural purposes. In order to underline the structural frame and get more aesthetic façades, the infill surfaces were covered with ceramic tiles in form of leaves (Fig6). The visible separation of structural and infill elements together with free interior space not limited with walls was the strikingly modern characteristic of the building. The construction of 25b Rue Franklin, opened the door to the possibility of making a new architecture in the new century. Therefore, unlike its industrial precursors, it became a symbol in architectural history. Perret continued experimenting with reinforced concrete in and outside France with his following designs such as the automobile garage on the rue de Ponthieu (1905), 51 Rue Raynour, Théâtre des Champs-Élysées (1911-1913), Wal-lut Docks, Casablanca (1914-1917), Cathedral of the Sacré-Coeur, Oran (1908-1912), etc.

⁷ <http://3.bp.blogspot.com/-zXWqSsDhuSo/VWnH3u7mLuI/AAAAAAAAACDo/p7Yp9ub2XTc/s1600/15108jpg> (Date of Access 19.10.2021)

⁸ <https://tr.pinterest.com/pin/364017582357457160/> (Date of Access 19.10.2021)

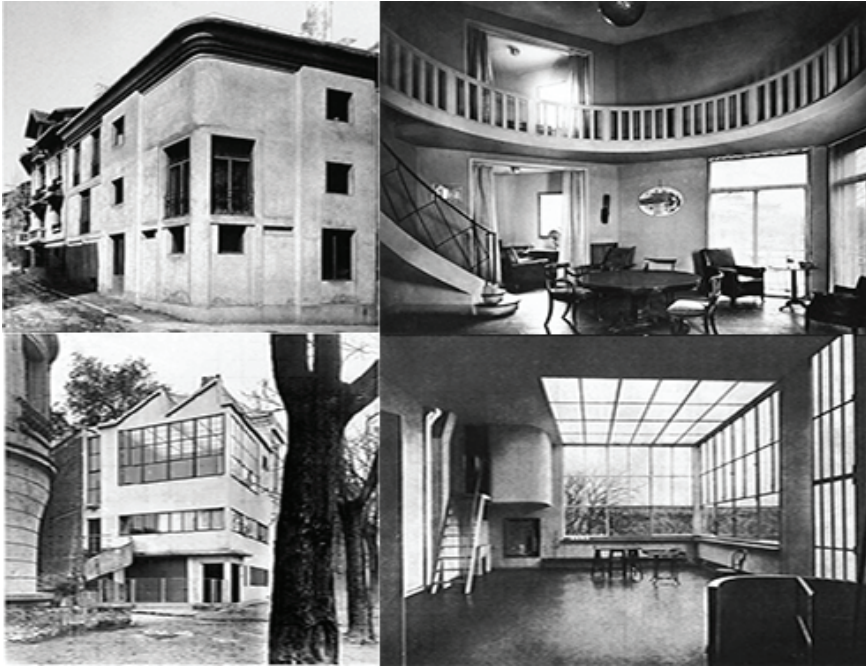


Figure 7. Above: Gaut House and Interior by Perret, 1923; Below: Ozefant House and Interior by Le Corbusier, 1923⁹ (Campell, 2014)

Nevertheless, Perret’s avantgarde position by offering a new architecture with reinforced concrete frame structure becomes controversial with the interest of other architects in the subject. Le Corbusier who got interested in the material while working in Perret’s studio sharply criticized Perret’s reinforced concrete architecture after the 1920s. In fact, he would add “the abolition of cornice” as the 6th point to his theory, which he conveyed as the “five points of modern architecture”, by despising Perret’s understanding of the façade, which is praised as structural rationalism. Gardner (1997) also believed that the perception of Perret’s reinforced concrete frame buildings as both monolithic and layered at the same time is already contradictory, but also the coexistence of linear openings and vertical windows slots on the façade are confusing.

⁹ https://64.media.tumblr.com/1b8578def8c72f75dec69126e7105ab5/tumblr_my2l03lxzJ1s6zot1o1_640.jpg (Date of Access 19.10.2021)

The two artist villas on the same street Gaut House and Ozenfant House, clearly reveal the difference in Perret's and Le Corbusier's view of the potentials of reinforced concrete. Unlike Gaut's, the Ozenfant's house had a concrete frame that produced an effect of weightlessness. The continuous corner openings of the building which reflect the lightness of the reinforced concrete frame structure created a brand-new aesthetics, in contrast to the solid corner of Gaut's house (Campell, 2014). In both houses, Perret and Le Corbusier enjoyed the structural potential of the material and created wide-span, double-height interior spaces. Nevertheless, the Ozenfant house has more luminous interiors with the help of wide windows continue in all three dimensions (Fig 7). As a result, although it was August Perret who introduced the reinforced concrete frame system to architecture, the five points of Le Corbusier's new architecture became more permanent when compared to Perret's confusing structural rationalism. Corbusier continued experimenting with reinforced concrete and discovered constructional potentials of the material and addition to his five points, the free plan, free facade, roof terrace, pilotis, and horizontal window.

During the first half of the 20th century, Europe had to cope with the destructions of the World Wars, one of the most urgent was housing for the accommodation deficit of millions of Europeans. Under these circumstances, reinforced concrete appeared as a solution which can respond to the problem and offer an advanced construction system that could decrease construction costs and offered by reputed architects such as Gropius, Taut, etc. Prefabrication as a building technique allowed architects to design and construct structures more quickly, at a larger scale, was also an option due to its ability to reduce construction costs and increase efficiency. Le Corbusier was also interested in the topic and proposed several projects with reinforced concrete. However, until then, prefabrication had been done with cast iron or steel material and prefabrication potential of the reinforced concrete frame has not been discovered.

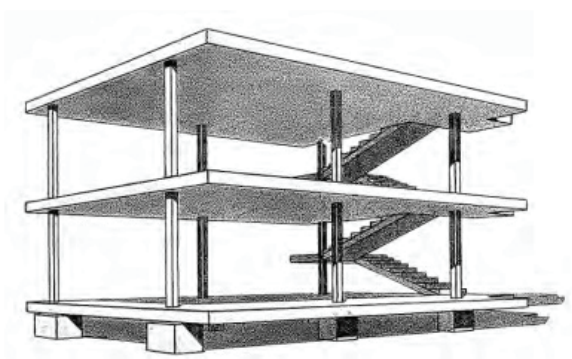


Figure 8. Maison Dom-ino by Le Corbusier, 1914 (Le Corbusier, 2006)

Le Corbusier with his Dom-ino House project developed the structural frame system of Hennebique which frees interior space from load-bearing walls to a further level (Fig8). He uses reinforced concrete slab as a structural element and designs a high-strength slab on slender columns that does not require additional beams. In this way, he achieved to free space not only from walls but from the exposed beams and “liberated design from all the structural constraints”. In the end, he prepared a flexible, durable, and economic construction system and wanted to patent it along with his other patented inventions. But as Vogt (1998) conveyed his attempt was failed because it is a masterpiece of analysis of reinforced concrete frame system rather than one of the invention (İskenderoğlu, 2009).

EARLY REINFORCED CONCRETE CONSTRUCTION

As mentioned above concrete is an ancient material that dates back to the Mesolithic age. But it was reinvented with the material advancements after the industrial revolution and combined with steel and became reinforced concrete. In the second half of the 20th century reinforced concrete the production of its components and procedure of application was standardized under strict design and engineering codes. The concrete prior to these advancements after the mid-century is referred to as historic concrete. Modern concrete is a combination of portland

cement, coarse and fine aggregates of stone and sand, and water along with some chemicals added to the concrete mix to control its setting properties under extreme environments, such as high or low temperatures, underwater moldings, windy conditions, etc. Besides modern concrete is classified according to its compression strength under several concrete classes. Concrete whether ancient, historic, or modern is a composite of a cementing material or binder (natural cement in the form of hydraulic lime or Portland cement), aggregate, and water. As the combination of concrete mixture has advanced, the qualifications of the reinforcement have advanced. Modern concrete is reinforced with ribbed steel bars while historic concrete with plain iron bars which has less coherence with concrete



Figure 9. Left: Construction of Weaver's Mill, Victoria Wharf With Wooden Formwork, 1899 (Cusack, 1984); Middle: Workers Pouring Concrete Foundation in a Housing Construction in the Netherlands, 1920s¹⁰; Right: A Concrete Mixer From 1930s¹¹

Moreover, construction with historic concrete was not similar today not only in terms of material quality of cement and steel but also the level of construction technology. As the historic concrete buildings are the products of a transition and exploration period of architecture and construction history, they were constructed under conventional construction techniques based on labor power with primitive equipment, and inexperienced workmanship (Okumuş, 2021; Urquhart, 2013). While timber elements made by carpenters, were used for formworks; mixing

¹⁰<https://dissolve.com/video/1920s-Workers-pouring-concrete-foundation-drilling-into-royalty-free-stock-video-footage/001-D378-81-741> (Date of Access 19.10.2021)

¹¹https://tractors.fandom.com/wiki/Liner_Concrete_Machinery_Company?file=A_1930s_LINER_Cement_Mixer.jpg (Date of Access 19.10.2021)

and pouring of concrete were made by using primitive equipment such as a concrete mixer (Fig8).

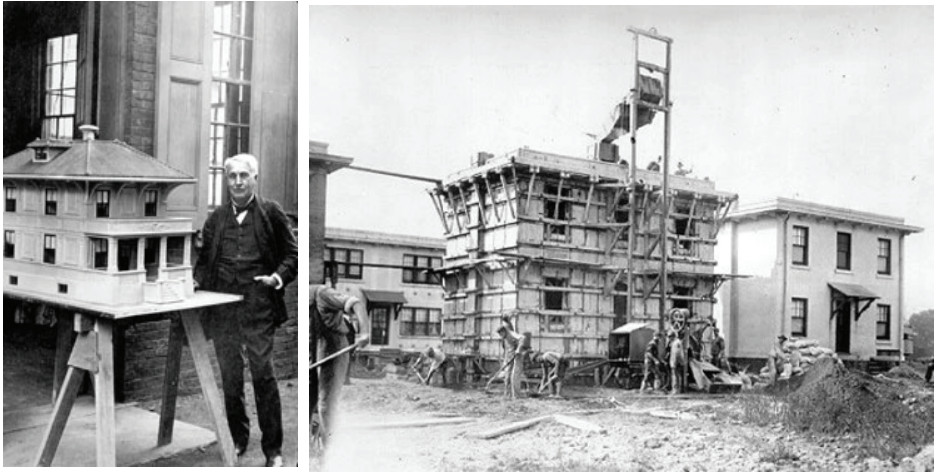


Figure 10. Left: Thomas Edison With A Model of a Concrete House, Circa 1910¹²; Right: One of Edison’s Concrete Houses Under Construction in 1919¹³

Apart from the unique material and construction features of historical concrete, there are also various types of construction -some of which are patented- that are no longer used today. Rammed or mass concrete is one of these. Rammed concrete is a technique that was first used for building elements -especially foundations and retaining walls- rather than the structure itself. It is a cast in situ (on-site) technique using formwork. There is no reinforcement in mass concrete, therefore it cannot be classified as reinforced concrete. It was mainly used for engineering structures where mass was required -such as dams, reservoirs, maritime structures- and there is a lack of stone resources, but also for the advantage of the speed of building with mass concrete (Urquhart, 2013). It was Thomas Edison who patented the mass concrete system for building (Fig10). Edison built a few fireproof, insect-proof, easy to clean houses with his patent around New Jersey with mass concrete; but he did not

¹²[https://www.cement.org/cement-concrete/paving/buildings-structures/concrete-homes/building-systems-for-every-need/removable-forms-\(cast-in-place\)](https://www.cement.org/cement-concrete/paving/buildings-structures/concrete-homes/building-systems-for-every-need/removable-forms-(cast-in-place)) (Date of Access 19.10.2021)

¹³https://en.wikipedia.org/wiki/Edison_Portland_Cement_Company#/media/File:Thomas_Edison_concrete_house.jpg (Date of Access 19.10.2021)

succeed to solve the complicated application problems of reusable formwork molds¹⁴.

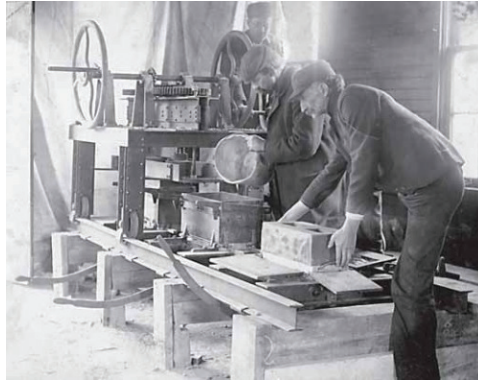


Figure 11. Concrete Block Manufacturing, Circa 1900¹⁵

The second type of historic concrete is precast concrete, which consists of concrete components poured and formed out of the building site, such as concrete blocks (Fig11). This type is the precursor of prefabrication with concrete in the construction sector. But the precast concrete is not reinforced, hence building components such as beams, or staircase could not be produced with this technique. Precast concrete blocks were used as masonry blocks, mostly painted or decorated to imitate natural stone.

The third type of historic concrete is reinforced with embedded metal to increase its tensile strength. Wrought iron was initially used but was generally replaced by iron after 1890 (Urquhart, 2013). These historic reinforced concrete buildings are framed with brick or stone infill which gave them extreme rigidity. All the trusted patented systems of reinforced concrete -Wayss-Monier, Hennebique, etc.- assumed that embedding the reinforcement into the concrete would protect iron bars against corrosion as it did for fire. But later its discovered that corrosion in reinforcement is a vital problem for historic reinforced concrete bu-

¹⁴<https://www.atlasobscura.com/places/thomas-edisons-concrete-houses> (Date of Access 19.10.2021)

¹⁵https://www.concrete.org/Portals/0/Files/PDF/ACI_History_Book.pdf (Date of Access 19.10.2021)

ildings because iron was not as corrosion resistant as steel. Besides, the amount of the water in concrete mixture and compaction process affects corrosion.

CONCLUSIONS

While Monier's invention paved the way for the development of concrete as a super-material with great resistance in both compression and tensile at the same time, Asbdin's invention solved the problem of limited production of concrete due to natural resources and opened up the opportunity to meet the rapidly increasing demand of construction sector after 19th century industrially. Hence, these two features make reinforced concrete an innovation equivalent to iron structurally, its monolithic structure, ease of application, and, of course, its aesthetic material qualities which are not indifferent from the aesthetics of traditional masonry has made this material much more acceptable than iron, in 19th-century architecture. The reinforced concrete technique was a great convenience compared to the traditional construction system, with the freedom in architecture and practicality in construction it offered.

However, due to material qualities, conventional construction techniques, inexperienced labor, and inadequacy of patent systems, historic concrete buildings - whether reinforced or not- are more delicate than other historic buildings although they were way too young when compared to them. Therefore, as Urquhart (2013) advised while working on historic concrete buildings, it should be recognized that compared with the modern concrete of today, "the early concrete has significantly less compressive strength and greater permeability". In addition, the lack of knowledge and understanding of the properties and performance of the components, together with mixing, pouring, and curing procedures, has had a negative impact on the durability of historic concrete. Therefore, before any cleaning, restoration, or conservation work is done on a historic concrete structure it is necessary to comprehend the characteristics of the material and not to compare it with modern concrete structures.

REFERENCES

Brueckner, R. and Lambert, P. (2013), *Assessment of Historic Concrete Structures*, Structural Studies, Repairs and Maintenance of Heritage Architecture XIII, WIT Transactions on The Built Environment, WIT Press Vol 131, 75-86.

Campell, (2014), Perret versus Le Corbusier Building for Art in the 1920s, *Kunst Og Kultur*, 4(97), 206-215.

Collins, P. (2004), *Concrete: The Vision of a New Architecture*, McGill-Queen's University Press.

Condit, W. C. (1968) *A Technological History: American Building: Materials and Techniques from the First Colonial Settlements to the Present*, Chicago: University of Chicago Press.

Cusack, P. (1984) François Hennebique: The Specialist Organization and the Success of Ferroconcrete: 1892-1909, *Transactions of the Newcomen Society*, 56(1), 71-86. doi:10.1179/tns.1984.004

Erdoğan, T. Y. (2021), *Beton*, Ankara: ODTÜ Yayıncılık.

Fisher Cassie, W., (1955), Early reinforced concrete in Newcastle upon Tyne, *Magazine of Concrete Research*, 7(19), 25-30.

Gardner, A. (1997), Auguste Perret: Invention in Convention, Convention in Invention, *Journal of Architectural Education*, 50/3, 140-155.

Gideon S. (1995), *Building in France, Building in Iron, Building in Ferroconcrete*, (trans. J. Duncan Berry), Los Angeles: Getty Research Institute Press.

Gökbayrak P., (2005), *Auguste Perret*, <https://v3.arkitera.com/h6320-auguste-perret.html>, (Date of Access 19.10.2021)

Le Corbusier, (2006) *Les Maisons Dom-ino, Oeuvre Complete*, Volume 1, 1910-29, edited by W. Boesiger and O. Stonorov, Berlin: Birkhauser Publishers.

İskenderoğlu, Y. (2009), *An Inquiry into The Design Potentials of Le Corbusier's Dom-Ino Clusters*, Y. Lisans Tezi, FBE ODTU, Ankara.

Mistewicz, M. (2019), The First Monier Arch Bridges in the Kingdom of Poland Constructed by Engineer Arnold Bronikowski, *Kwartalnik Historii Nauki I Techniki*, 64(1), 39-55, doi:10.4467/0023589xkhnt.19.002.10110

Okumuş, M. (2021), *Brüt Beton Yapılardaki Bozulma Tiplerinin Tahribatsız Muayene Yöntemleri ile Tespiti ve Onarım Yöntemleri: Ankara Örneği*, Y. Lisans Tezi, Çankaya Üniversitesi FBE, Ankara

Urquhart, D. (2013), *Historic Concrete in Scotland Part 1: History and Development*, Edinburg: National Conservation Center Pub. (<https://www.historicenvironment.scot/archives-and-research/publications/publication/?publicationid=c2a38944-eb81-44e8-bd5e-a59100f-b611a>, Date of Access 19.10.2021)

Vogt A. M. (1998), *Le Corbusier: The Noble Savage*, Cambridge: The MIT Press.

INTERNET SOURCES

<https://www.architettodigitale.it/la-struttura-portante-nel-progetto-di-una-casa/> (Date of access 10.16.2021)

<https://www.donsmaps.com/lepenski.html> (Date of Access 16.10.2021)

https://en.wikipedia.org/wiki/John_Smeaton (Date of access 10.16.2021)

<https://www.jpconcrete.co.uk/francois-hennebique-a-pioneer-of-reinforced-concrete/> (Date of access 10.16.2021)

<https://aehistory.wordpress.com/1853/10/05/1853-first-reinforced-concrete/coignet1/> (Date of access 16.10.2021)

<http://3.bp.blogspot.com/-zXWqSsDhuSo/VWnH3u7mLuI/AAAAAAAAACDo/p7Yp9ub2XTc/s1600/15108jpg> (Date of Access 19.10.2021)

<https://tr.pinterest.com/pin/364017582357457160/> (Date of Access 19.10.2021)

<https://dissolve.com/video/1920s-Workers-pouring-concrete-foundation-drilling-into-royalty-free-stock-video-footage/001-D378-81-741> (Date of Access 19.10.2021)

https://tractors.fandom.com/wiki/Liner_Concrete_Machinery_Company?file=A_1930s_LINER_Cement_Mixer.jpg (Date of Access 19.10.2021)

REACTION DIFFUSION EQUATION IN ENGINEERING

Esen HANAÇ¹

Abstract: Reaction diffusion equations have an outstanding role in variety of sciences areas for instances mathematical chemistry, mathematical physics, mathematical biology, and also practicable in genetic diffusion, traffic flow, chemical reactions, random progresses et cetera. Specifically, the solitary wave solutions to the nonlinear partial differential equations enable to this equation to be practicable in above mentioned areas. Yet, the solitary wave solution has not been elementary to acquire, for this reason multiple techniques has been improved. The tanh technique is one of these techniques. The tanh technique has been widely used to figure out innumerable partial differential equations much the same the reduced form of them. The solitary wave solutions of reaction diffusion model and the extension form of the model is easily established by the ability of tanh technique. The tanh method is substantial and direct solution practice to obtain closed form, exact representations for solitary waves of the reaction diffusion equations. In especial, the tanh technique is fitted well with problems which arises in pattern, convection and reaction diffusion phenomena. A strong nominal software package, that is useful for engineering to apply, has been formulated to ease finding the exact solutions of wider nonlinear partial differential equations. First, the reaction diffusion form equation and its practicability in the field of sciences are mentioned. Thereafter, the technique is summarized for demonstrating the alternative form of the exact solutions for nonlinear partial differential models and ordinary differential models. A modified reaction diffusion equation and its extension form, which do not have an alternative tanh form solutions, are examined. The acquired solutions of both equations are

¹ Adıyaman Üniversitesi, Fen Edebiyat Fakültesi, Adıyaman / Türkiye, ehanac@adiyaman.edu.tr, Orcid No: 0000-0001-5561-7495

exhibited in the $u(x,t)$ - x graph. On the basis of the chosen parameters, the aspect of wave velocity is alternated that exhibits in the first two graphs. The situation for the extension formed equation is vice versa. Even though the signs of parameters are changed, the aspect of wave velocity is remained. Thus and so, an alternative tanh polynomial form solutions of selected equations, which have a significant role in variety of areas such nonlinear dynamics, fluid flows, genetics et cetera, are established by the effort of tanh technique.

Keywords: Reaction Diffusion Equation, Tanh Method, Solitary Wave Solution

INTRODUCTION

A differential equation is a mathematical model that associates some functions with its derived form. In practice, functions usually symbolize physical quantities, derivative forms symbolize their rate of change, and equations represent the relationship between the two. Since the relations are highly common, differential equations play a significant role in various fields containing engineering, physics, economics, and biology. A partial differential equation (Pde) is formed by a dependant parameter and various distinct parameters. The linear and nonlinear Pdes arise in varied practices and play a significant role in the area of engineering and applied sciences. Almost all continua and occasion in sciences and engineering are naturally nonlinear of which they are determined by nonlinear partial differential equations (Npde) with many conditions and parameters. Npdes' research has been extensively improved in almost all fields of science and engineering. Nevertheless, mathematicians and searchers are conducting relative searches in multiple fields of science and engineering, and have produced new favorable results. Npdes have been extremely examined by several scientists throughout the years and has occurred omnipresent in universe, those equations can be categorized into integrable and nonintegrable. The behavior of integrable functions is represented by their initial conditions. Even though several methods have been used to determine exact solutions of Npdes, it is hard to say there is only one best method for a problem. A method is chosen depending on the fast overlap to exact solutions, computational stress and plainness of the method. Therefore, the performance of the solutions

to the problems is better than others depending on the radius of overlap of methods by methods. So many integrable equations can be counted such as the Benjamin-Ono equation is for internal waves, the Schrödinger equation which is practicable in shallow waves, Kadomtsev-Petviashvili equation is for shallow water waves, Korteweg-de-Vries equation (Ma, 1993), the Sine-Gordon equation which is used in quantum field theory, quantum field theory and so on (Baseilhac and Koizumi, 2003 and Caudrey, 1975).

Conversely, nonintegrable equations, for instance, the Ginzburg-Landau equation performed in conductivity, Fisher's equation performed (Conte and Mussette 1992) in genetic extension, Burger Huxley model practicable in advection transmission style et cetera. Countless methods have been used to get their exact solutions.

As known, those nonintegrable equations have few or no analytical solutions.

Even so, obtaining of analytic solutions to nonintegrable partial differential equations is possible with some countless noticeable techniques exactly like the integrable ones. The Jacobi elliptic function method, Darboux transformation, the tanh-function method (Al-Shaer, 2013), Weierstrass elliptic function method, Hirota bilinear method can be counted as the most noticeable ones.

The existence of exact solutions for nonlinear differential equation is mostly rare and as a consequence of this, so many distinctive methods, namely, Taylor collocation method (Jin, 2009, and Deniz and Bildik, 2017, Deniz, 2013), Euler collocation methods (Elzaki, 2018), wavelet collocation methods (Aziz et al, 2017, and Kumbinarasaiah, 2019), iterative differential quadrature method, variational iteration method (Elzaki, 2018), homotopy perturbation method (HPM) (Jin, 2009), perturbation iteration method (Bildik, 2017 and Bildik et al, 2017), Adomian decomposition method, new iterative method (Jena and Chakraverty, 2019), homotopy analysis method (Jin, 2009), reduced differential transform method (Mittal and Rajni, 2017), and residual power series method (Ren and Vong 2019), have been used to solve them in building numerical means, schemes or algorithms by mathematicians throughout the years. Evolution

of travelling wave solution takes a significant role in nonlinear scientific discipline so that several scientists make an effort to obtain the travelling wave solution of diverse equations embodying the Fishers equation.

Recently some of mathematicians have searched to get the exact solutions of nonlinear equations by using combination of two distinct methods, for example, Sumudu decomposi-

tion method, homotopy perturbation transformation (HPTM) method, homotopy-variational iteration method, Elzaki differential transform, Elzaki projected differential transform (Alderrem et. al, 2019), Elzaki homotopy transformation perturbation method (EHTPM), Laplace-Adomian decomposition method (Wazwaz, 2004), Elzaki iterative method (Alderrem et. al, 2019), Laplace-variational iteration method (Matinfar and Ghanbari, 2009), new iterative transform method (Mittal and Rajni, 2017)., and homotopy analysis transform methods (Elzaki and Chamekh, 2018).

A regular form of reaction diffusion equation is namely,

$$u_t = Mu_{xx} + h(u) \quad (1)$$

$u = u(x, t)$ is a state variable and depicts compactness of a material, a population and so on with x defines distance and t is time. The first term on the right hand side represents the diffusion with the diffusion constant M . The second term $h(u)$ defines changes of the processes, in short it is reaction part. In this chapter we will touch on such reaction diffusion equation to discover applications of the equation with tanh method.

Hereby, we have examined the Fishers equation in the case where $h(u) = u^2(1 - u)$ by applying tanh method.

Firstly, the tanh form of the solution of the equation is obtained. Then the obtained form of the equation can be identified numerically via computer softwair such as Matlab, Maple and so forth.

Previous to this several numeric, stationary, analytical and soliton solution of the Fishers equation has been exhibited in lettrures.

Equation (1) when $h(u)=u(1-u)$ was observed analtically (Wazwaz, 2009) and in addition to analytical methods, numerical, semianalytical methods have been established and applied throughout the years on the equation.(Wazwaz, 2002)

There is not only one method for an equation based upon the nonlinearity of partial differential equations. Methods by methods the speed of the convergence to analytic solution on some problems displays differences. Some methods can not even work for analytic solution of problems. For this reason nonlinear problems need new methods to develop the convergence of the solutions analtically. Therefore this became the main goal for observing this research.

The tanh method is a strong sloution method for exact solutions to nonlinear partial differential equations. Over the years, the tanh method is one of the most frank and effectual developed method (Khater, 2002) to obtain exact solutions of nonlinear diffusion equations.

Latterly, researchers put a lot of effort into finding diverse extended tanh method. The tanh method was represented as a new scale while all derivatives of a tanh presented by tanh itself. (Malfliet, 1992) Thus, the method will become more practicable to large class of equations. Afterwards, the generalized tanh method has been evolved to get more than one solitary solutions. (Fan, 2002)

A large classes of evolution equations has been analyzed by applying a new developed modified parameter. (Parkers, 1996)

The following structure of this chapter is designed as follows: First, we give a detail definition and practicality of the Fishers equation. Later, definition of the proposed method (tanh method) is represented. Then, the practicabilty of the tanh technique is exhibited on the specified Fishers euqation and its extension formed. In addition to this, the acquired solutions of both equations are exhibited in the $u(x,t)-x$ graph. Based upon the signs of the parameters, the aspects of the wave velocity is demonstrated in the graphs. Consequently, we summarized our work

by mentioning the sketch of the selected problems and their solutions, which are identified by the chosen technique.

The Fishers Equation

A common form of the Fishers equation is given as

$$u_t = u_{xx} + g(u)$$

$$g(u) = u(1 - u). \quad (2)$$

In 1937, Fisher, Kolmogorov, Petrovsky, and Piscunov examined the equation (2) separately and after that it was named as the Fishers equation. It is a significant model in population dynamics, which basically depicts the propagation of populations in space.

The several forms of the above equation (2) with some other factors were observed by scientists. For instance, a nonlinear evolution model of the equation (2) practicable in biology, which defines one dimensional model for animal dispersion and occupation has the form

$$u_t = (u^m_x)_x + u^\beta(1 - u^\gamma)$$

where x, t represents distance, time respectively, $u(x, t)$ is the density of the population and parameters m, β, γ are positive. The part $u^\beta(1 - u^\gamma)$ is presented as the change of the population when u^m is defined as the diffusion process based on the density of the population $u(x, t)$. The presence of various forms of the Fishers equation enables it exciting problem to seek.

When the part $g(u)$ in equation (2) is given as,

$$g(u) = \rho u(1 - u^\gamma)(u - b)$$

we have the Fishers equation with no dimension namely,

$$u_t = u_{xx} + \rho u(1 - u^\gamma)(u - b) \quad (3)$$

where ρ and γ are constants.

This nonlinear model is applicable in physical system which includes linear diffusion and nonlinear growth. While ρ is counted as 1, $\gamma=1$ and $b=0$ in equation (3), we get the Fishers equation as in (Ronald Fisher 1937). This model form equation (2) depicts a notable role in a nuclear reactor for the development of a neutron population. Consequently, the equation turned into one of the most distinguished types of nonlinear differential equations due to their practicable in chemical kinetics, neurophysiology, nuclear reactor theory, the diffuse of early farming in Europe and so forth.

The Tanh Method

In this section we use a regular form of the tanh method is presented in (Maliet, 1996). The tanh method plays a vital role for expression of the travelling wave solutions in terms of the tanh function. It is noteful to give main points about the tanh method:

- *At first, we search the general form of nonlinear equation*

$$S(u, u_t, u_x, u_{xx}, \dots) = 0. \quad (4)$$

- *A new transformation $V = c(x - vt)$ is given to obtain travelling wave solutions of the equation (4)*

$$u(x, t) = U(V) \quad (5)$$

with speed v . Depending on the transformation given in (5), the equation (4) is modified into

$$\frac{\partial}{\partial t} = -cv \frac{d}{dV}, \quad \frac{\partial}{\partial x} = c \frac{d}{dV}, \quad \frac{\partial^2}{\partial x^2} = c^2 \frac{d^2}{dV^2}. \quad (6)$$

- Substituting above changes into the partial differential equation (4) to reduce ordinary differential equation and we get that

$$S(U, U', U'', \dots) = 0. \tag{7}$$

- If all parameters of reduce ordinary differential equation comprise derivatives in V then by integrating this equation we conclude with an abbreviated ordinary differential equation.

- We now determine a new variable

$$Y = \tanh(V), \tag{8}$$

which leads the change of derivatives:

$$\begin{aligned} \frac{d}{dV} &= (1 - Y^2) \frac{d}{dY} \\ \frac{d^2}{dV^2} &= (1 - Y^2) \left(-2Y \frac{d}{dY} + (1 - Y^2) \frac{d^2}{dY^2} \right). \end{aligned} \tag{9}$$

- The ansatz is given as

$$U(V) = S(Y) = \sum_{l=0}^T c_l Y^l \tag{10}$$

where $T > 0$ is a constant. On substitution (9) and (10) into the reduced equation (7) generates an equation based on Y .

- We define the coefficient T via balancing the linear terms of the highest order into reduced equation with the highest order in nonlinear terms. Later a system of algebraic equation which involves $c_l, l = (0, \dots, T)$, c and v will be determined with equating indexes of powers of Y in the reduced equation by using the determined T .

- After all those parameters are indicated, we establish an analytic solution in a tanh form.

In the undermentioned, the tanh method is clarified via presenting exemplificative equation.

The Modified Fishers Equation

Herein we observe the following Fishers equation to exhibit the power of the tanh method,

$$u_t = u_{xx} + u^2(1 - u) \quad (11)$$

with x defines distance and t is time. Implementing (5) and (6) into equation (11) then we get

$$cv \frac{dU(V)}{dV} + c^2 \frac{d^2 U(V)}{dV^2} + U(V)^2(1 - U(V)) = 0. \quad (12)$$

We define the coefficient T via balancing the linear terms of the highest order into reduced equation (12) with the highest order in nonlinear terms. Hence we obtain

$$3T=T+2$$

since therefore $T=1$. We presume that $U(V), U'(V) \rightarrow 0$ as $Y \rightarrow 1$. Thus the tanh form of the solution becomes

$$S(Y) = c_0(1 - Y). \quad (13)$$

We establish the system of algebraic equation for c_0 , c and v by applying $S(Y), S'(Y), S''(Y)$ from (13) into the reduced equation (12):

$$Y^0: -c_0cv + c_0^2 - c_0^3 = 0$$

$$Y: 2c^2c_0 - 2c_0^2 + 3c_0^3 = 0$$

$$Y^2: c_0cv + c_0^2 - 3c_0^3 = 0$$

$$Y^3: c_0^3 - 2c^2c_0 = 0.$$

We fix the speed v , after some calculations:

$$v = 2c.$$

Later the undermentioned values of the other variables c_0 , c and v are found:

$$c_0 = \frac{1}{2}, c = \frac{1}{2\sqrt{2}}, \text{ and } v = \frac{1}{\sqrt{2}}$$

or

$$c_0 = -\frac{1}{2}, c = -\frac{1}{2\sqrt{2}}, \text{ and } v = -\frac{1}{\sqrt{2}} \tag{14}$$

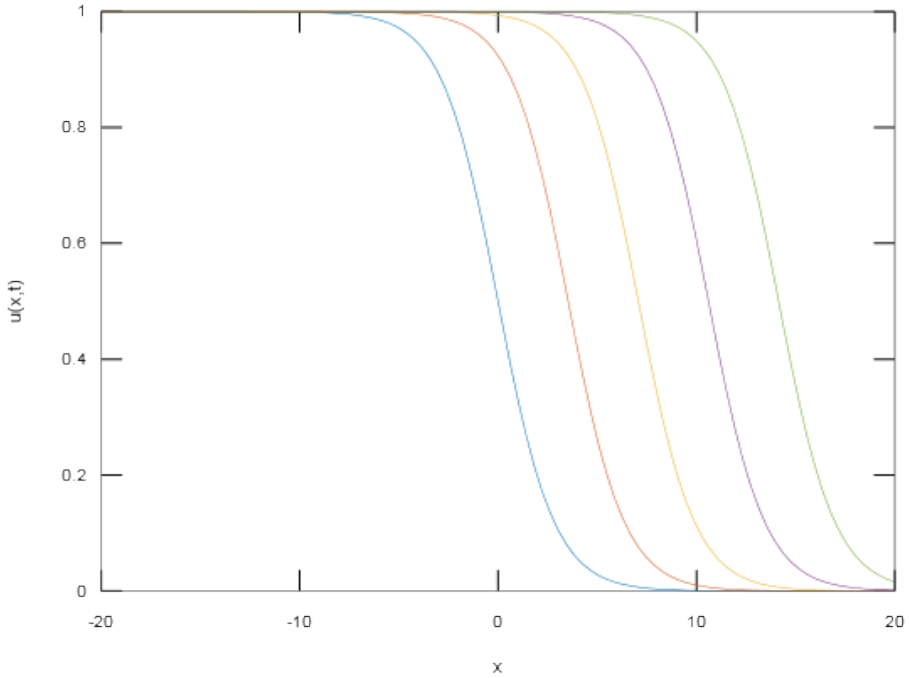
under the consideration of only positive and negative values of c and v . On the basis of values in (14) we have the final form solutions of the Fisher equation (11)

$$\begin{aligned} u(x, t) &= \frac{1}{2} - \frac{1}{2} \tanh\left(\frac{1}{2\sqrt{2}}\left(x - \frac{1}{\sqrt{2}}t\right)\right) \\ u(x, t) &= -\frac{1}{2} + \frac{1}{2} \tanh\left(-\frac{1}{2\sqrt{2}}\left(x + \frac{1}{\sqrt{2}}t\right)\right) \end{aligned} \tag{15}$$

which are in the solitary wave forms. In a similar manner, we also find the following solutions th the Fisher equation (11)

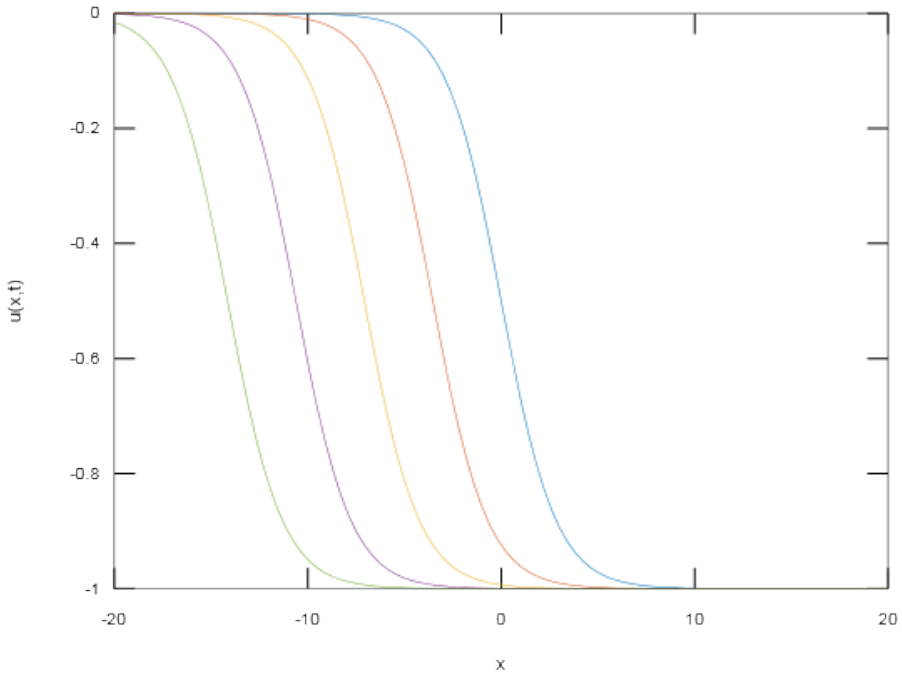
$$\begin{aligned} u(x, t) &= \frac{1}{2} - \frac{1}{2} \coth\left(\frac{1}{2\sqrt{2}}\left(x - \frac{1}{\sqrt{2}}t\right)\right) \\ u(x, t) &= -\frac{1}{2} + \frac{1}{2} \coth\left(-\frac{1}{2\sqrt{2}}\left(x + \frac{1}{\sqrt{2}}t\right)\right) \end{aligned} \tag{16}$$

Now we numerically examine the solitary wave form solutions given in (15) for same time ranges, respectively:



Graph 1. Graph of the First Solitary Wave Solution Given in (15) for the Time $t=0$ (Blue) $t=5$ (red), $t=10$ (Yellow), $t=15$ (Purple) and $t=20$ (Green)

In the first graph, the solitary wave solution of the Fisher equation (11) for positive values of c and v is considered in domain $x = [-20, 20]$



Graph 2. Graph of the Second Solitary Wave Solution Given in (15) for the Time $t=0$ (Blue), $t=5$ (Red), $t=10$ (Yellow), $t=15$ (Purple) and $t=20$ (Green)

In the second graph, the solitary wave solution of the Fisher equation (11) for positive values of c and v is considered in domain $x = [-20, 20]$ with same time range $t = [0: 5: 20]$.

Comparing graph 1 and graph 2, it is clearly seen when the solitary wave solution has as the first structure in given (15) the aspect of wave speed v is in positive x direction however, on the other side when the solitary wave solution has as the second structure in given (15) the aspect of wave speed v is vice versa.

Above analysis proves the tanh method with positive integer T practices efficaciously and so a closed form of the exact solution can be established.

The Extension Form of the Modified Fishers Equation

We examine the following Fishers equation to exhibit the power of the tanh method

$$u_t = u_{xx} + u^p(1 - u) \quad (17)$$

where $p > 0$. Progressing as in above analysis, T is chosen as $\frac{2}{p}$ when $p=1,2$. We apply the variable to accomplish our purpose

$$u(x, t) = w^{\frac{2}{p}} \quad (18)$$

Implementing the variable in (18) into the equation (17) we find that

$$ww_t = ww_{xx} + \left(\frac{2}{p} - 1\right)(w_x)^2 + \frac{p}{2}w^2(1 - w^{\frac{2}{p}}). \quad (19)$$

Later on we get the new form of the equation (19) with substituting the new scale $w(x, t) = U(K)$ and (6) into above expansion

$$cvU \frac{dU(K)}{dK} + c^2U \frac{d^2U(K)}{dK^2} + \left(\frac{2}{p} - 1\right) \left(\frac{dU(K)}{dK}\right)^2 + \frac{p}{2}U(K)^2(1 - U(K)^2) = 0. \quad (20)$$

After some computations, the coefficient T with $p=1,2$ via balancing the linear terms of the highest order into reduced equation (20) with the highest order in nonlinear terms is determined as $T=1$.

Once again assuming that $U(V), U'(V) \rightarrow 0$ as $Y \rightarrow 1$.

Thence the tanh form of the solution is indicated as

$$S(Y) = c_0(1 - Y) \quad (21)$$

After following above steps are completed we affirm variables c_0 , c and v as

$$c_0 = \frac{1}{2}, c = \frac{p}{2\sqrt{2p+4}}, \text{ and } v = \frac{p+4}{\sqrt{2p+4}} \tag{22}$$

under the consideration of only positive values of c and v . The final form solution of the Fisher equation (17) is demonstrated on the basis of v :

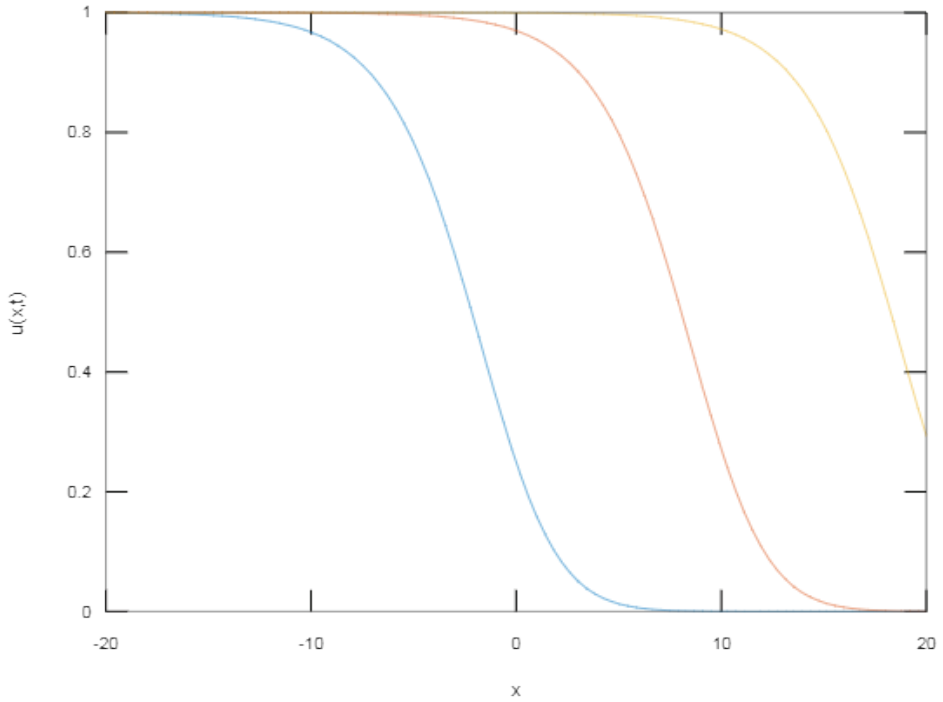
$$w(x, t) = \frac{1}{2} - \frac{1}{2} \tanh\left(\frac{p}{2\sqrt{2p+4}}\left(x - \frac{p+4}{\sqrt{2p+4}}t\right)\right) \tag{23}$$

since therefore the solution of the extension form of the modified Fishers equation (17) is obtained

$$u(x, t) = \left(\frac{1}{2} - \frac{1}{2} \tanh\left(\frac{p}{2\sqrt{2p+4}}\left(x - \frac{p+4}{\sqrt{2p+4}}t\right)\right)\right)^{\frac{2}{p}} \tag{24}$$

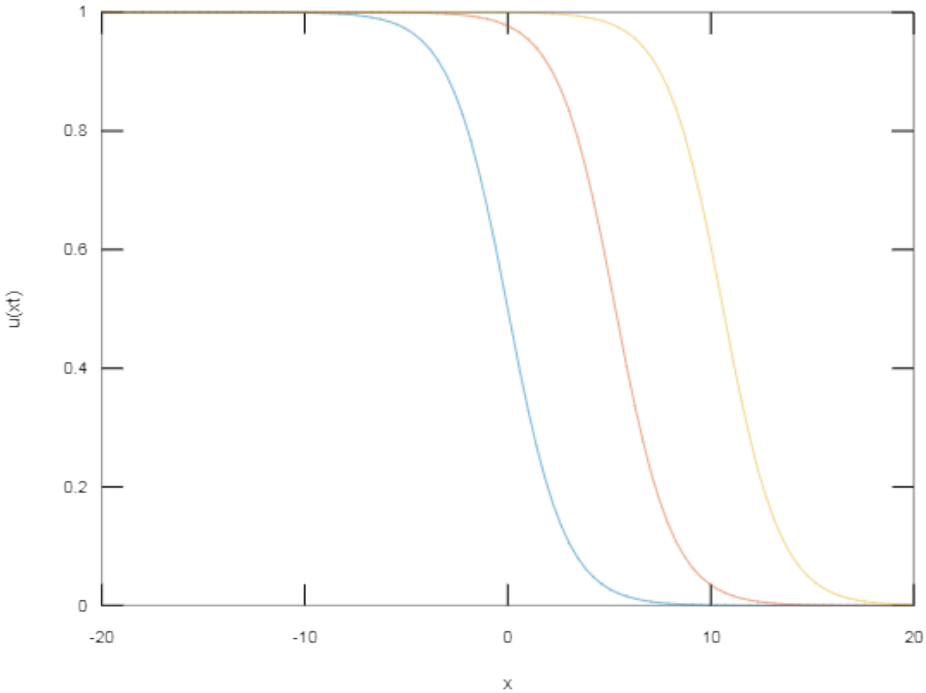
Finally, an extension form of the modified Fishers equation is successfully completed by the power of the tanh method.

Now, the solitary wave form solutions given in (24) is numerically examined for $p=1,2$ separately.



Graph 3. Graph of the Solitary Wave Solution Given in (24) for the time $t=0$ (Blue), $t=5$ (Red), $t=10$ (Yellow)

In graph 3 the solitary wave form of extensive modified Fisher equation has ben exhibited for the case of $p=1$.



Graph 4. Graph of the Solitary Wave Solution Given in (24) for the Time $t=0$ (Blue), $t=5$ (Red), $t=10$ (Yellow)

The solitary wave form of extensive modified Fisher equation has been exhibited for the case of $p=1$ in graph 4.

When the solitary wave solution has as the structure in given (24), the aspect of wave speed v is in same positive x direction in both above graphs.

CONCLUSION

In this chapter, the tanh technique has performed on a significant form and an extensive form of a reaction diffusion equation. This reaction diffusion model is well-known mathematical model in a variety of areas for instance genetic generation, population vitality and stochastic transactions.

A closed form solutions at the risk of painful algebra is established on the basis of the achievement of the tanh technique. Above represented equations and the results of them certified that the tanh method is substantial and direct solution practice to obtain closed form, exact representations for solitary waves of the reaction diffusion equations.

Additionally, two different cases of the reaction diffusion equation are considered. The results in graph 1 and graph 2 are diagrammatically demonstrated to analyze how a solitary wave generates with the change of time ranges and the aspect of wave speed v changes on the basis of parameters c_0 , c and v . In addition to those, graph 3 and graph 4 showed that solitary wave generates with the change of time ranges for two distinct values of p .

Eventually, the tanh technique enables to practice and guide to solitary wave profits. The tanh technique has been widely used to figure out innumerable partial differential equations much the same the reduced form of them.

Based upon the tanh technique, a strong nominal software package has been formulated (Baldwin et. al, 2004 and Baldwin et. al, 2004) to ease finding the exact solutions of wider nonlinear partial differential equations. It is useful package for engineering. Hereby, an easily found alternative form of the exact solutions to reaction diffusion equations has been a significant role in variety of areas such nonlinear dynamics, fluid flows, genetics et cetera.

REFERENCES

Alderremy, AA., Elzaki, TM., Chamekh M. (2019). Modified Adomian decomposition method to solve generalized Emden–Fowler systems for singular IVP. *Mathematic Problems in Engineering*, 6097095. <https://doi.org/10.1155/2019/6097095>.

Al-Shaer, MJARA. (2013). Solutions to nonlinear partial differential equations by Tan-Cot method. *IOSR Journal of Mathematics*, 5 (3),6-11. <https://doi.org/10.9790/5728-0530611>.

Aziz, I., Siraj-ul-Islam, I., Asif M. (2017). Haar wavelet collocation method for three-dimensional elliptic partial differential equations.

Computer and Mathematics with Applications, (73), 2023-2034. <https://doi.org/10.1016/j.camwa.2017.02.034>.

Baldwin, D., Göktaş, Ü., Hereman, W. et al., (2004). Symbolic computation of exact solutions expressible in hyperbolic and elliptic functions for nonlinear PDEs, *Journal of Symbolic Computation*, (37), 669-705. <https://doi.org/10.1016/j.jsc.2003.09.004>.

Baldwin, D., Göktaş, Ü., Hereman, W. (2004). Symbolic computation of hyperbolic tangent solutions for nonlinear differential-difference equations. *Computer Physics Communications*, (162), 203-217. <https://doi.org/10.1016/j.cpc.2004.07.002>.

Baseilhac, P., Koizumi, K. (2003). Sine-Gordon quantum field theory on the half-line with quantum boundary degrees of freedom. *Nuclear Physics B*, (649), 491-510. [https://doi.org/10.1016/S0550-3213\(02\)00980-X](https://doi.org/10.1016/S0550-3213(02)00980-X).

Bildik, N. (2017). General convergence analysis for the perturbation iteration technique. *Turkish Journal of Mathematics and Computer Science*, (6), 1-9. <https://dergipark.org.tr/en/pub/tjmcs/issue/30433/328709>, (04.12.2021).

Bildik, N., Tosun, M., Deniz, S. (2017). Euler matrix method for solving complex differential equations with variable coefficients in rectangular domains. *International Journal of Applied Physics and Mathematics*, 7(1), 69-78. <https://doi.org/10.17706/ijapm.2017.7.1.69-78>.

Caudrey, P. J., Eilbeck, J. C., Gibbon, J. D. (1975). The sine-Gordon equation as a model classical field theory. *Il Nuovo Cimento B*, 25(2), 497-512. <https://doi.org/10.1007/BF02724733>.

Conte, R., Mussette, M. (1992). Link between solitary waves and projective Riccati equations, *Journal of Physics A: Mathematical and General*, (25), 5609-5623. <https://doi.org/10.1088/0305-4470/25/21/019>.

Deniz, S. (2013). Applications of Taylor collocation method and Lambert W function to the systems of delay differential equations. *Turkish Journal of Mathematics and Computer Science*,(1),1-13.<https://dergipark.org.tr/tr/pub/tjmcs/issue/17532/183281>,(04.12.2021)

Deniz, S., Bildik, N. (2017). A note on stability analysis of Taylor collocation method. *Celal Bayar Üniversitesi Fen Bilimleri Dergisi*, (13), 149-153. <https://doi.org/10.18466/cbayarfbe.302660>.

Elzaki, TM. (2018). Solution to nonlinear partial differentials by new Laplace variational iteration method. *Intech Open*, (9), 153-171. <https://doi.org/10.5772/intechopen.7329>.

Elzaki, TM., Chamekh, M. (2018). Solving nonlinear fractional differential equations using a new decomposition method. *Universal Journal of Applied Mathematics & Computation*, (6), 27-35. <https://www.researchgate.net/publication/323846296>, (04.12.2021).

Fan, E., Hon, Y.C. (2002). Generalized tanh method extended to special types of nonlinear equations. *Zeitschrift für Naturforschung A*, 57(8), 692-700. <https://doi.org/10.1515/zna-2002-0809>.

Glasner, K. (2001). Nonlinear preconditioning for diffuse interfaces. *Journal of Computational Physics*, (174), 695-711. <https://doi.org/10.1006/jcph.2001.6933>.

Huubin, L., Kelin, W. (1990). Exact solutions for two nonlinear equations: I, *Journal of Physics A: Mathematical and General*, (23), 3923-3928.

Jena, RM., Chakraverty, S. (2019). A new iterative method based solution for fractional Black-Scholes option pricing equations (BSOPE). *SN Applied Science*, 1(1), 95. <https://doi.org/10.1007/s42452-018-0106-8>.

Jin, L. (2009). Application of variational iteration method and homotopy perturbation to the modified Kawahara equation. *Mathematical and Computer Modelling*, (49), 573-578. <https://doi.org/10.1016/j.mcm.2008.06.017>.

Kawahara, T., Tanaka, M. (1983). Interactions of traveling fronts: an exact solution of a nonlinear diffusion equation, *Physics Letters A*, (8), 311-314. [https://doi.org/10.1016/0375-9601\(83\)90648-5](https://doi.org/10.1016/0375-9601(83)90648-5).

Khater, A.H., Malfliet, W., Callebaut, D. K., Kamel, E.S. (2002). The tanh method, a simple transformation and exact analytical solutions for nonlinear reaction-diffusion equations. *Chaos Solitons and Fractals*, (14), 513-522. [https://doi.org/10.1016/S0960-0779\(01\)00247-8](https://doi.org/10.1016/S0960-0779(01)00247-8).

Kumbinarasaiah, S. (2019). Numerical solution of partial differential equations using Laguerre wavelets collocation method. *International Journal of Management, Technology And Engineering*, 9(1), 3635-3639. <https://www.researchgate.net/publication/331062529>, (04.12.2021).

Ma, W. (1993). Travelling wave solutions to a seventh order generalized KdV equation. *Physics Letters A*, (180), 221-224. [https://doi.org/10.1016/0375-9601\(93\)90699-z](https://doi.org/10.1016/0375-9601(93)90699-z).

Malfliet, W. (1992). Solitary wave solutions of nonlinear wave equations, *American Journal of Physics*, 60 (7), 650-654. <https://doi.org/10.1119/1.17120>.

Malfliet, W. (1996). The tanh method: I. Exact solutions of nonlinear evolution and wave equations, *Physica Scripta*, (54), 563-568. <https://doi.org/10.1088/0031-8949/54/6/003>.

Malfliet, W. (1996). The tanh method: II. Perturbation technique for conservative systems, *Physica Scripta*, (54), 569-575. <https://doi.org/10.1088/0031-8949/54/6/004>.

Matinfar, M., Ghanbari, M. (2009). Solving the Fisher's equation by means of variational iteration method. *International Journal of Contemporary Mathematical Sciences*, 4(7), 343-348. <http://www.m-hikari.com/ijcms-password2009/5-8-2009/matinfarIJCMS5-8-2009.pdf>, (04.12.2021)

Mittal, RC., Rajni, RR. (2017). A study of one dimensional nonlinear diffusion equations by Bernstein polynomial based differential quadrature method. *Journal of Mathematical Chemistry*, (55), 673-695. <https://doi.org/10.1007/s10910-016-0703-y>.

Parkes, E.J., Duffy, B.R. (1996). An automated tanh-function method for finding solitary wave solutions to non-linear evolution equations, *Computer Physics Communications*, (98), 288-300. [https://doi.org/10.1016/0010-4655\(96\)00104-X](https://doi.org/10.1016/0010-4655(96)00104-X).

Rajarama, J., Chakraverty, S. (2018). Residual power series method for solving time-fractional model of vibration equation of large membranes. *Journal of Applied and Computational Mechanics*, (5), 603-615. <https://doi.org/10.22055/jacm.2018.26668.1347>.

Ren, Shi J., Vong, DS. (2019). High accuracy error estimates of a Galerkin finite element method for nonlinear time fractional diffusion equation. *Numeical Methods for Partial Differential Equations*, 1-18. <https://doi.org/10.1002/num.22428>.

Wang, M. (1998). Exact solutions for a compound KdV-Burgers equation. *Physics Letters A* (213), 279-287. [http://doi.org/10.1016/0375-9601\(96\)00103-X](http://doi.org/10.1016/0375-9601(96)00103-X).

Wazwaz, A.M. (2002). *Partial Differential Equations: Methods and Applications*. The Netherlands, Balkema Publishers.

Wazwaz, A.M. (2009). *Partial Differential Equations and Solitary Waves Theory*. Berlin, Germany, Springer.

Wazwaz, A.M. (2004). An analytic study of Fisher's equation by using Adomian decomposition method. *Applied Mathematics and Computation*, (154), 609-620. [https://doi.org/10.1016/S0096-3003\(03\)00738-0](https://doi.org/10.1016/S0096-3003(03)00738-0).

SUSTAINABLE SMART CITY CONCEPT: DEVELOPMENT PROCESS OF KONYA¹

Nazmiye Nur ŞENYİL², Süheyla BÜYÜKŞAHİN³

Abstract: The city is the living spaces that have been shaped throughout history and have emerged as a result of the social relations that people have established in the places where they live as a result of the activities of living together. In the formation of cities, apart from these social relations it is important to produce solutions for the problems encountered in the process that created the city and brought it to the present. In this context, cities continued their existence by producing solutions suitable for the conditions of the period in line with the problems they faced in every period they passed. The global population growth throughout the history of humanity has affected cities, causing them to change, and has revealed smart cities with an innovative lifestyle. Smart cities are trying to find solutions to the problems that arise in the global sense, by approaching them with awareness and sustainable consciousness. In this process, it will be able to make cities more livable with the solutions it has developed by actively using information and communication technologies and will be able to bring cities to the future by means of sustainable methods. Especially in the last ten years, intensive studies have been carried out on smart cities in the global sense, but studies in this sense are insufficient in Turkey and smart city applications are not used widely except for some metropolitan cities. The city of Konya, which was chosen as case study,

1 This study was prepared by making use of the master's thesis titled "The Concept of Sustainable Smart City in Architecture and the Evaluation of the Development Process of Konya" completed by Nazmiye Nur ŞENYİL in Konya Technical University Graduate Education Institute, Department of Architecture under the supervision of Assoc. Prof. Süheyla BÜYÜKŞAHİN.

2 Master of Architect, Konya / Turkey, naz.mimar.94@gmail.com, Orcid No: 0000-0001-8874-6613

3 Necmettin Erbakan University, Faculty of Fine Arts and Architecture, Konya / Turkey, suheylabuyuksahin@gmail.com, Orcid No: 0000-0001-5869-3629

appears as a city that is advancing in the process of becoming a smart city throughout Turkey with its progress. In this sense, the current city features of Konya and the changes it has undergone are examined, and in order to determine its current position in the process of being a smart city, smart city applications in the city, smart environmental parameters and applications with sustainable features are explained. As a result, it is possible to say that Konya is a city that progresses and develops in the process of becoming a smart city with its smart applications and sustainable studies. This process will accelerate with the popularization and development of existing applications. In this context, in the future, a livable city with higher quality qualities will be created by means of the implementation and development of the city's existing smart applications with sustainable methods.

Keywords: City, Smart Environment, Smart City, Sustainability, Konya

INTRODUCTION

The city expresses the living spaces that have emerged as a result of people's coexistence and social relations throughout history. The concept of the city, rather than a spatial tangible area as a living space, expresses the changes and solutions in the process created by the problems and requirements that differ over time. Cities that brought solutions suitable for the conditions of the period in line with the needs that occurred, could continue to exist, and the cities that could not find a solution disappeared.

Considering the life line of humanity, it has been observed that the amount of population has constantly increased at regular intervals, except for unfortunate global events (pandemics, wars, etc.). This increase is especially an increase that has occurred globally after World War II. In addition, with this increase, the amount of global development, production and consumption has been added to the amount of increasing population after the Industrial Revolution, which occurred with technological developments and inventions. The developing world conditions in this location have affected the existing cities, causing them to change, develop and increase their attractiveness. With this development in cities, migration to cities has increased and the population has started to become crowded. With the ever-increasing urban density and global

pollution, which is the biggest problem of our age, new problems have arisen and started to transform cities into places that are difficult to live in. This situation has revealed the smart city approach, which is an innovative lifestyle that aims to find solutions to the problems that occur in cities with developing technology.

Smart cities are a way of life that emerged after the 2000s in order to produce innovative solutions by using information and communication technologies and to transform cities into livable conditions with awareness and consciousness against global problems and negative living conditions. With the use of developing technologies and the contribution of sustainability in every sense to this use, smart applications are developed and ease of use is provided by including these applications in urban life. Thanks to this concept, which consists of different sub-components, urban life, which creates crowded living spaces, becomes smart from their current situation and comes to a position that provides its own future.

In order to express the smart city approach, first it is necessary to understand the concept of sustainability. The concept of sustainability emerges as a concept that started to be used in the early 90s as a result of the worsening of current conditions in the changing, developing, exhausted and polluted world. This concept is the balancing of the production and consumption process, which expresses a transformation process based on efficiency in the way it operates. Sustainability emerges as a concept where the amount of consumption can be reduced by means of the balanced progress of the amount of production and the amount of consumption, and even the transformation practices it brings. The importance of the concept of sustainability has increased even more when it is understood that the amount of consumption should be reduced in today's cities where resource consumption has increased so much and that reaching the future can only be achieved with efficient uses. In this context, the smart city approach, which includes the concept of sustainability in every component, has been an important approach developed for reducing the amount of consumption, increasing efficiency, creating more livable cities and for these cities to exist in the future. In this sense, since the concept of smart city includes the changes and developments

in all areas of life, it has become a research topic for all kinds of science and new developments have emerged as a result of the researches.

Today's developing and changing urban life, while providing livable areas that are easy to use thanks to smart applications that use innovative methods created by the advancement of technology and science, also require the reduction of resource use with the support of sustainable methods. For this reason, within the scope of the study, the concept of sustainable smart city will be examined in detail and smart applications that will help cities in the process of reaching the future will be expressed in the light of the information obtained. In the case study, the process of becoming a sustainable smart city of Konya, which constantly advances itself with the developed strategies and carries out its activities similar to the smart applications used throughout the world, will be examined in detail.

City

Humans have felt the need to establish relationships and socialize since their existence. While continuing his life as a social and active being, he did not choose to be alone, but wanted to live together. The desire to live together arises from cooperation and social solidarity to act together in the face of life difficulties and overcome obstacles. While the reason for people to live together in prehistoric times was to ensure security, which is one of the biggest problems in the areas where they live, with the transition of people to settled life, the need to overcome the problems caused by social burdens has been added to the purpose of security. People living together started to fulfill the activities found in human nature such as production, solidarity, cooperation, sharing, etc. and they tended to establish cities in order to create unity and solidarity with the ease of living together (Gürsoy, 2019).

While the concept of the city is expressed by Aristotle as the common area where people come together to have better living standards, according to Simmel, the city is defined as the places where the society that comes together and shares the same city can provide the highest level of division of labor (Boy, 2020).

In his book "Image of the City"; Lynch (1960) expressed the city as common living spaces that can be created by using various symbols or summarized expressions by dealing with five different images: path, edge, district, node and landmarks (Ocakçı, 2018).

Williams (1973) in his book "The Country and The City" states that "City, as a word, is a time, place and phenomenon that contains very strong emotions that society has achieved by coming together over time. The society has achieved these successes on cities and it will be understood how important these strong meanings that emerged on the city are when we look at the past experiences of human communities." In short he described the city as a phenomenon created by the combination of humans living there and their achievements.

Tatlıdil (1994) first approached the city from a spatial point of view to define the city and expressed it as "common areas where people with different lifestyles accept their lifestyles by respecting other people living in a common area with defined boundaries".

In order to define the concept of the city, a visible physical city based on quantitative measurement and the amount of population defined by numerical data should not come to mind. Apart from these quantitative values, the concept of the city consists of deep-rooted structures that can be explained qualitatively over time, unwritten rules from culture and social life, historical accumulations and the foundations formed by many different disciplines. Thanks to the various disciplines that make up the city, the definition and researches of the city are studied in different fields (Hayta, 2016).

Regarding the concept of the city, based on the other definitions given above, if we need to create a current phenomenon, it is possible to express city as "settlement areas where people, who are loyal to the government and constitution of the country they inhabit, live together with an ethical understanding and respect each other regardless of language, religion, race and show a population density of various amounts, economic development is provided through the industry and service sector, and the form of government is the administrative organization determined in the constitution."

Smart City

If it is accepted as a general perception, cities are a center of attraction for people with the opportunities they provide in economic and social terms. This makes cities more successful than rural areas in terms of labor mobility. A similar situation is observed between large and small cities (Gürsoy, 2019). On the other hand, rapid population growth, especially in big cities, brings many problems of dissolution with it. These problems reduce the life quality of city residents, negatively affect the economic and social life in cities, and reduce the power of brand and competitiveness of cities (Örselli and Akbay, 2019).

The emergence of the negative effects of scientific developments as well as their positive effects caused it to be understood that the current state of the world could not handle these negative effects, and it did not leave the concept of “development” as a term on its own, but directed it to “smart development”. This smart development has not only been in science and technology, but also in cities that create dynamic environments in the world, where resource consumption is kept at maximum levels, and which are in the process of continuous planning and change. These smart development activities that took place on cities have turned into the concept of “Smart City” in order to express and define itself. The concept of smart city is a concept that has emerged with the aim of controlling the use of natural resources in increasingly crowded cities, preventing the destruction of natural environments due to density, and preventing random unplanned settlement and growth (Akkan, 2019).

While defining the concept of smart city, Totty (2017) mentions that every phenomenon that makes up the city should take on a participatory task by applying smart methods in the use of natural resources. In addition, by making a serious capital investment for these smart methods and creating a sustainable feature, it includes increasing the quality of life while making cities smart to the definition.

A smart city has been defined by Giffinger et al. (2007) as a city that has positive effects on life, environment and mobility by taking precautions for the future, while carrying out all kinds of activities of people

who live consciously under independent conditions on a certain piece of land, via developed smart solutions.

According to Sinmaz (2013), the smart city is “a new concept that aims to reduce the pressure on the city with the increasing amount of population, to reduce the negative effects of cities against both their natural environment and their users, and to create livable spaces with developed innovative solutions”.

The smart city approach aims to create livable spaces based on the concept of sustainability. While creating these living spaces, it is the basis of the smart city approach to ensure that the tools that both support and improve each other work together by meeting the quality and security needs in managerial and economic development by acting with the principles of open data, governance and efficiency (Gürsoy, 2019).

With the smart city approach created, it is important to absorb the negative effects in the city, to minimize the destruction on nature, to reduce the pressure on the city with the emerging population and crowd, to develop the efficient use with the principle of creating a livable city and to continue the urban life without interruption with the designed plans come into prominence. From the times when moving to cities was considered important in the 2000s, as the population of the city increased, smart city approach has been constantly expanding to increase the quality of life of the people living in the same city, to use the existing land capacity efficiently, to strengthen the economy on the basis of the city, to reduce the use of limited resources and to ensure that the people living in the city can live a quality life (Sinmaz, 2013).

The smart city approach, with the policies carried out in detail by the private institutions and organizations of the world countries, has become an approach that comes into prominence with its smart solutions to increasing demands, solving urban problems and carrying hope for the future. It is aimed to make human life easier while increasing the quality of life by making the energy, transportation, infrastructure, technological system and usage networks needed by the cities self-operating with the applications and methods developed without constant supervision (Elvan, 2017).

The transformation of cities into smart cities cannot be separated from the urban fabric created by the people living on it from past to present. Another issue that should be taken as a basis when starting the transformation is to act in accordance with the city's own infrastructure features and systems and to plan and implement it step by step. While starting the transformation, the problems of the city should be determined first, solutions should be found for these problems and the transformation should be done starting from the city center (Kayapınar, 2017; Özdil, 2017).

Some basic strategies should be included in the creation of the smart city concept. According to Sınmaz (2013), these strategies will enable cities to be made smart, and designs that support each other will emerge. The main strategies to consider in designing smart cities will be:

- Developing social, cultural, educational and health opportunities by strengthening the concept of security
- Creation of a city that competes and works in this context by removing the city mechanism from being fixed with the activities carried out.
- Generating more livable spaces on the common denominator by including public spaces in the lifeline
- Increasing cultural diversity with socio-cultural changes and developments
- Promoting co-decision making and execution
- Advancement of information and communication technologies with technological development and strengthening of integration with the city
- Bringing information and communication technologies together for equal and common use by users
- Replacing the resources required for energy needs with renewable ones
- Keeping factors such as waste, air, water, etc. under control to prevent pollution by respecting nature.

- Developing public transportation in vehicles used for transportation and making non-motorized use widespread in vehicles to be used.
- Applying natural air-conditioning methods to prevent excessive energy use in the settlement plan.
- Supporting the creation of smart buildings in order to minimize energy use in the structures to be designed (Sinmaz, 2013).

As with every concept that exists in a complex form in the world, the concept of smart city consists of sub-components that make up this concept when they come together. According to Kaygısız and Aydın (2017), if the components that make up the smart city are expressed with keywords it is possible to gather them under the titles such as smart person which includes creativity, education and socialization; smart economy that includes production, trade and entrepreneurship; smart management encompassing open data sharing, supply and service; smart mobility encompassing accessibility, access and compliance; smart life which includes safety, health and vitality, and finally smart environment which includes continuity, design and sustainability, and we architects will be most interested in and will work on. The components that make up smart cities do not have definite borders. In this context, the inclusion of urban people and the city administration, which takes the most active role in urban life, is the main reason why these boundaries cannot be clarified (Sinmaz, 2013). Smart cities are empowering themselves with a strategic approach to sustainable development and citizens' well-being through technology integration. Establishing sound strategic planning supports the development of infrastructure, innovation and technology (Luque Vega et al, 2020).

Globally accepted strategist Dr. Boyd Cohen's smart city circle has a methodology that can be used for smart cities with its easy-to-follow setup. This methodology, which has also been accepted by the European Union (EU), summarizes the components that make up smart cities through six basic parts. Cohen takes the concept of the smart city to the center of the circle. The function areas that make up this smart city are lined up around the center. The various foci of the components that make

up the smart city form the last part of the circle (Figure 1) (Anonymous, 2019a).



Figure 1. Dr. Boyd Cohen's Smart City Circle⁴

When the circle is looked at in general, it is seen that each component that makes up the circle plays an important role and these components should work in harmony with each other. In this study, in which the concept of sustainable smart city is discussed, the smart environment component and parameters will be examined in detail in the continuation of the study in order to ensure that the evaluations in the case study can be healthy.

Smart Environment and Sustainability Concept

Smart environment is a smart city component that includes the energy used, designed buildings and cities, which takes the concept of sustainability into its focus. It is possible to say that the most effective part of the architectural design process is the concept of the smart environment. The smart environment encourages the use of renewable energy resources together with the concept of sustainability in the city where it

⁴ <https://smartvillage.ca/2019/04/09/climateaction/>

will be designed. The use of renewable energy sources can help stop the ozone layer depletion brought about by global warming by reducing the amount of waste and preventing the formation of greenhouse gases. In this context, together with waste control, water consumption amounts will be regulated and resources will be used efficiently (Akkan, 2019; Çiftçi and Balyemez, 2019).

The aforementioned concept of “sustainability” was introduced for the first time in the world by Meadows et al. in the book “The Limits of Growth” written in 1972, and is a concept that has survived to the present day. The term sustainability emerged in the late 1970s and early 1980s as a clear social and economic idea (Caradonna, 2014). After emerging as a concept, it has become a term that has survived to the present day and is used more actively especially after the 21st century. In the book “The Limits of Growth”, it is explained that if global growth and consumption of ecological resources continue in the same way, with the beginning of the 2000s, global functioning and natural balance may collapse and world life may become impossible. In the book, it is explained that a solution to this problem can be created by establishing sustainable, ecological and economic conditions in a balanced way and ensuring sustainability (Meadows et al., 1972).

Thus, the concept of sustainability, which has entered our lives, draws a road map for the important problems that need to be addressed as a universal issue and for the general work carried out to solve these problems. It is also possible to express it with a concept that tries to produce solutions according to the ecological footprint data by examining the events such as carbon emission, greenhouse gas effect, events that occur as a result of global warming, consumption of water resources, melting of glaciers, etc. The concept of sustainability includes not only ecological practices created for the protection of the deteriorated natural balance, but also it is used to make activities with high resource usage such as ensuring efficiency in development activities, preventing the use of unnecessary information in technological developments, etc. (Terzi and Ocakçı, 2017).

The concept of “sustainability”, which is used to use the existing more effectively or to turn the negative effect into a positive, basically

means the transfer of an existing thing to new generations by transmitting it between generations. This concept, which is used to secure the future, has affected the phenomenon of urbanization and caused smart city development by aiming to protect and expand sustainable spatial areas with technology since the end of the 20th century (Gürsoy, 2019).

Among the smart city components where sustainability comes into play, perhaps the most related component with sustainability is the smart environment component with which the urban people will interact the most with its dynamic movement in smart cities. Within the scope of smart environment in smart city components, cities reveal the importance of sustainability with green solutions. The elements that we can call green sustainability designed in cities are parks, gardens, water resources, green areas, green energies used and green buildings. In order to create a smart environment, it should be planned to reduce the factors that will cause all kinds of pollution (light, air, noise, etc.) at the urban and regional scale for the use of sustainable settlements and buildings, efficiency-enhancing and renewable resources in resource use and should be applied to urban designs (Özdil, 2017).

In support of the concept of sustainability, information communication systems also come into play in the context of the smart environment. The use of these technological devices in accordance with the design objectives by providing the efficiency of the environmental sensors, meters and monitoring devices used in the city creates more livable environments by increasing efficiency (Akıncı and Pouya, 2019).

Apart from the sustainable information communication devices used, the use of environmentalist designs in fixed designs that make up the city has a significant effect on reaching the smart city. In this context, it is very important to make buildings and structures smart and to design environmentally friendly systems in buildings by producing effective solutions on site. (Çetin and Çiğdem, 2019).

To summarize the smart environment component; it is possible to express it as “a sustainable design that includes renewable energy sources, technology-supported energy networks, measurement, pollution control and monitoring, transformation of buildings and facilities, green

buildings, sustainable urban planning, as well as resource use efficiency and reuse” (Anonymous, 2019a).

In the smart city approach; sustainable technology and knowledge-based information management of the ecosystem should be focused in order to reduce and prevent negative economic effects in the urbanization process. Produced information and communication technologies can provide economic continuity by supporting sustainable development and by working to increase economic recycling and efficiency in smart cities (Kayapınar, 2017).

The essentials for sustainable design can be summarized as;

- Sustainable urban planning designed in detail,
- Transportation modes based on sustainability,
- Use of environmentally friendly green materials,
- Appropriate direction and aspect positioning for air conditioning,
- Use of clean energy for energy efficiency,
- The evaluation of rain water and wastewater (Aytis and Polatkan, 2009).

As a result, designing cities with the understanding of sustainability is at the center of smart city development strategies, identifying the issues that the city needs, planning every issue that needs solutions for every problem occurred (energy, pollution, infrastructure, transportation, building, etc.) and its organization constitutes the basic relationship between sustainability and the concept of smart city. (Terzi and Ocakçı, 2017).

Smart Environment Parameters

Smart environment parameters consist of three main headings: sustainable energy, sustainable building and sustainable city.

Sustainable Energy

With the industrial development in our age, the world’s cities needed raw materials and energy. The use of non-renewable energy resources despite the destruction it caused on the ecosystem until the near future has adversely affected the world’s health. It has caused the thinning

of the atmosphere layer, which creates a livable natural environment by surrounding the world, by being adversely affected by the carbon emission caused by the excessive use of fossil fuels, and global warming has started with the thinning atmosphere tissue passing the harmful rays from the sun and excess heat, causing the world's specific heat to increase. The occurrence of global warming has continued its existence in the polar circles, causing the reduction of the ice cover, which creates a climate effect on the earth's surface, and the faster deterioration of the living environment. In addition, global environmental pollution has occurred as a result of not only global warming but also the pollution caused by the use of fossil energy on nature. Realizing that the ecological balance has deteriorated as a result of the use of non-renewable energy, the people of the world started new researches to correct the disturbed balance in the early 1990s and the researches directed people to the use of changing energy sources (Aytıs and Polatkan, 2009; Şenel and Koç, 2015).

Sustainable energy, which has started to be used to prevent these damaging factors, is basically based on the use of self-renewable energy sources. In this use, which takes care of resource consumption by standing by the ecosystem, it can be seen as a goal that replacing non-renewable and endangered energy resources with renewable resources, reducing energy consumption, making it sustainable and using it without consuming resources, trying to minimize the negative effects that may occur on the environment of the wastes that will be created by the clean energy forms used (Arsan, 2008).

When it comes to renewable energy sources, the first source that will come to mind will be the sun that rises and sets every day and the high energy it contains. Thanks to the systems developed today, electricity can be produced from solar energy. The energy from the sun is converted into usable electrical energy by using collectors, photovoltaic (PV) solar panel cells (solar cells) and electricity storage (Figure 2). This application can be made to produce energy in all areas that consider the midrail countries with regular sun as a border. Except for the methods applied in open lands exposed to the sun, regardless of the intended use,

energy can also be provided by placing them on the surfaces of the shell, wall, roof, etc. of the designed structures (Uzun and Yeğın, 2017).



Figure 2. Solar Panel Tilt and Orientation (Uzun and Yeğın, 2017)

Another renewable energy source is wind. Throughout history, mankind has been aware of wind energy and used this energy for the purposes to extract the husks from the seeds, turn windmills, navigate in sailing ships, etc. Today, however, it has been learned that the wind provides more energy than is known, huge wind panels and tribunes which operate depending on electrical mechanisms and are positioned in windy areas have begun to be used.

Apart from solar and wind energy, the water stored in large volumes and produced energy thanks to the fluid movement, geothermal water and steam formed by the hot effect of the earth’s crust near the surface, biofuels to be produced from the organic waste of all kinds of living organisms and biodiesel that are formed through oilseed plants as a result of the reaction under suitable conditions etc. sources are other renewable energy sources used (Kılınçarslan et al, 2019; Uzun and Yeğın, 2017).

Architects have a great role in ensuring the sustainability of renewable energies. It is very important at this point to make designs that will ensure the on-site use of energy. Many energy sources such as ventilation, daylight and wind direction need to be positioned and shaped in the designed structures. In addition, not only the positioning of these renewable energy sources, but also the materials to be used in designs

are of great importance in terms of energy saving. It is also very important to choose natural materials that provide natural ventilation and create heat balance and do not harm the ecological environment, instead of artificially produced petroleum-derived unhealthy building materials. Purifying the waste water (tap water, rain water, etc.) generated as a result of use in the designs within the structure and making them suitable for reuse also ensures a decrease in energy consumption (Anonymous, 2018a; Elvan, 2017).

The concept of sustainable energy, which is one of the focal points of the smart environment, which is one of the smart city components, is a concept developed to create a solution to the problems caused by the excess energy consumption caused by the increase in the population as a result of migration to the cities, and it is planned to prevent the consumption of non-renewable energy resources by increasing its prevalence over time. Today, it is necessary to transfer the sustainability of water, air and soil resources to the city models to be designed by taking into account all environmental elements of the works carried out in urban areas, and to ensure the continuity of the resources while providing urban services. Smart cities, which are tried to be created in this context, are trying to produce sustainable solutions in energy use. Smart cities with the concept of sustainability aims to change the way of energy consumption, to keep energy efficiency at the maximum level, to reduce negative environmental reactions by providing energy saving in the city, to reduce or end the problems related to energy use in the future. (Kayapınar, 2017).

Sustainable Buildings

As a result of the complex structuring caused by urbanization, the buildings built for various uses have increased continuously since the 70s. The buildings, which serve the crowded population and form the fixed parts of the city, were designed and built quickly with the materials (cement, iron, brick, adobe, etc.) available in those years only to provide short-term solutions to the increasing population and to maintain order. These constructed buildings were generally high-rise buildings in city centers that met their energy needs by using fossil fuels. As time passed,

the methods to meet this energy need have changed. In the beginning, the coals with high carbon emissions were burned and the smoke was given from the building chimneys and the heating process was carried out. These black smokes coming out of the chimneys were observed until the 2000s in the recent past. Although various filtering methods have been tried to prevent the damage caused by chimney fumes, no solution has been found. In the continuation of the awareness movement in the world, the use of coal has been replaced by liquid fossil fuels such as petrol, fuel oil, etc. in order to prevent atmospheric pollution. However, the use of these liquid non-renewable energy sources for energy purposes for buildings has damaged the atmosphere just like the use of coal. In order to reduce the damage, natural gas, which is one of the non-renewable energy sources and which is discovered by the development of technology and the advancement of excavation systems, has begun to be used. Although natural gas seems to be more environmentally friendly than previous energy sources, since it is a non-renewable resource that conflicts with the principle of clean, sustainable and continuous energy resources, which is the common issue of every state today, it has become necessary to develop new methods in order to meet the energy needs in building designs. Thus, the idea of a sustainable building, which is transformed into smart with renewable energy sources and technology used in buildings, has emerged (Erten, 2017b).

Transforming the buildings used for the accommodation, housing, education, trade, public etc. purposes into sustainable buildings, which is one of the smart environmental focuses, will provide access to smart cities by providing efficient and smart use of resources. In this context, some of the applications to be made in order to make the buildings sustainable are as follows (Aytis and Polatkan, 2009):

- **Use of Solar Cells:** One of the sustainable applications that can be used in green building designs is solar panels/batteries, also called PV. It is possible to design solar energy by thinking that it is permanent and renewable, and to use solar energy by converting solar energy into electrical energy by positioning solar panels where the buildings can receive sunlight at an appropriate angle. Solar cells are used in terrace roofs, sloping roofs, entrance-eaves, parapet walls, facades with no

openings, sunshades, etc. in buildings. It converts solar energy into electrical energy by storing it in the areas where it will be placed. Solar cells are frequently used in sustainable building designs because they can produce energy independently in the area where they are installed, their maintenance costs are negligible, they are much more reliable among other energy production sources, they can be positioned as modular parts in desired areas and they can be placed without disturbing the aesthetics of the building (Uzun and Yeğın, 2017).

- **Waste Water-Rainwater Use:** One of the most wasted resources in its use is water resources. The temperature of the world is constantly increasing as a result of the melting of ice masses that occur with the temperature changes caused by global warming. As a result of this increasing temperature, the change in climatic conditions and the decrease in the amount of precipitation, the existing fresh water resources are depleted. The areas with the highest consumption are undoubtedly crowded urban systems. The rate of water consumption is increasing day by day as a result of the unconscious use of users, especially in buildings located in cities. Innovative as well as efficient methods are used in sustainable buildings designed to prevent these consumptions. Recycling tanks are among the applications designed to prevent water consumption. Water consumption levels can be reduced by using the waste water generated as a result of the use of tap water in wet areas of the buildings, after they are collected in the warehouses within the building and recycled, and used in areas such as landscape irrigation required for the building. Another system used to prevent water consumption is the creation of rainwater tanks. By the means of these tanks to be created in the building design, rain water, which is much cleaner than the used tap water, is collected and refined and used in the areas of the building that need water (Erten, 2017a).

- **Use of Green Walls and Roofs:** The crowded urban population has brought many problems with it. Natural air conditioning, which is one of these problems, is not possible in complex areas formed by high-rise buildings. The green spaces designed in the buildings that make up the city in order to provide natural air conditioning and support the creation of clean air help sustainability. Besides, thanks to the O₂ produ-

ced by the designed green landscape, the quality of the atmosphere can be increased. In addition, by the means of the green areas to be created in the areas such as roof, wall, etc. in sustainable buildings, spacious spaces can be produced for the building users to escape from the crowd of the city (Anonymous, 2018a).

- **Use of Natural Materials:** The materials used while constructing the buildings differ according to the designs. The use of this material, which has changed with the development of technology, has taken a different direction with the effectiveness of the concept of sustainability. The use of both sustainable and smart building materials, which emit low carbon emissions, provide air conditioning by passing heat and air through their porous structures, and provide information about the environment thanks to the nano technologies placed inside, has started to become widespread. These building materials affect the interior of the building, its immediate surroundings and the global environment throughout their life cycle. Solutions developed to prevent the negative effects on the environment, to minimize the damages and to ensure the sustainability of the environment gain importance. Sustainable natural materials are used as they do not leave negative effects on nature with their structures that can be dissolved with zero waste when necessary, increase efficiency by changing energy use, and can be selected correctly according to the environmental conditions used, and can provide on-site air conditioning and ventilation (Kılınçarslan et al., 2019).

The fact that the world's future is in danger has led the world's governments to develop certification methods that are used to establish legal institutions, to produce solutions against the problems that await the world in the future, to disseminate designs that meet their own needs with sustainable smart solutions (Erten, 2017a).

- **BREEAM Certificate:** It stands for "*Building Research Establishment Environmental Assessment Method*" and is one of the first applications developed by states on the concept of sustainability. The system, which was created in England in 1990, is a form of certification that evaluates the sustainability degrees of the designed buildings and gives the appropriate documents. It is an application that evaluates many different categories from low carbon emission to energy use, waste conversi-

on to material use and gives certificates at different degrees. The reason why this form of certification, which is widely known in the UK, could not spread to the whole world, is that approximately 500 of the more than 600,000 buildings it has certified are outside the UK, and all the remaining buildings were located within the country. Although BREAM continues to work over the years, it is not as well-known as the LEED certification known around the world⁵.

- **LEED Certification:** It stands for “*Leadership in Energy and Environmental Design*” and is a widely known practice around the world developed by the USGBC “*United States Green Building Council*”. Buildings that have been awarded the certificate show energy-efficient and green features, while using sustainable resources, they are graded according to their features that cause minimal damage to the nature and obtain the necessary LEED certificate. The purpose of the certificate is to develop and disseminate environmentally responsible design, practice and operating standards at the building and city scale. Sustainable buildings are scored according to their environmentally friendly features and are named with certificates of different degrees (Figure 3).



Figure 3. Types and Scores of LEED Certification⁶

- **ÇEDBİK:** It is an organization that continues to work with the same system established in Turkey as the green building rating methods used throughout the world. ÇEDBİK, which was established in 2007

⁵ <https://www.breem.com/>

⁶ <https://www.langschwander.com/news/2016/12/14/leed-certification-the-benefit-for-builders-designers-the-environment>

with 25 members in our country, which introduced itself as a member of WGBC, stands for Environment Friendly Green Buildings Association. It is an organization that works not only in our country but also around the world to create, develop and disseminate environmentally friendly sustainable buildings. The aim of the association is to determine the aspect and location of the buildings to be designed or designed, to determine the environmentally friendly building materials and appropriate techniques to be used, to work to create high-efficiency, economical buildings that aim to eliminate the effects that may adversely affect health in all aspects, by trying to create quality areas (Özdil, 2017).

As a result, designing and creating sustainable buildings does not only affect the quality of life, energy efficiency and environmentally friendly behavior of the designed building and its users. In addition, while the quality of life increases in sustainable cities formed by the combination of designed sustainable buildings, the sphere of influence of sustainability also expands (Öztopcu and Salman, 2019).

Sustainable City

The concept of sustainable city, known throughout the world, was developed at the beginning of the 21st century in order to prevent irregular and inefficient urbanization as a result of the increase in the urban population as a result of migration to the cities, resource and energy consumption and the deterioration of environmental factors. If we explain with a general definition over the concept of sustainability, sustainable cities are cities that develop themselves over time, make themselves smart at every scale by using information and communication technologies and ensure their continuity with the solutions they come up with (Dal and Özdemir, 2020; Öztopcu and Salman, 2019).

Sustainable city is a comprehensive system composed of not only administrative, social, economic, housing etc. buildings with identity characteristics, but also streets, avenues, roads that provide transportation between these buildings; parks, gardens, green areas that form resting and breathing areas, the units that work in a chain consisting of infrastructure services and systems that ensure the continuity of every

factor that exists on the ground, and the administrative management methods that work to protect and ensure the continuity of the historical and cultural heritage of the city, while doing all of these, it is the use of practices that will ensure the socio-economic integrity of the city. It is possible to clarify the basic principles necessary for sustainable urbanization as follows:

- Establishing a balance to ensure a natural balance in resource consumption,
- Producing solutions to reduce the effects of climate changes as a result of global warming,
- Use of renewable resources in energy consumption,
- Healthy, safe water supply and waste water evaluation,
- Recycling by providing waste recycling,
- Realization of innovations without ruining the local cultural heritage,
- Protection of the cultural assets of the city,
- Ensuring the continuity of urban development,
- Ensuring the continuity of the public and service sector with the principle of equality (Dal and Özdemir, 2020).

The basis of the measurable features that make up sustainable cities is to design and maintain the balance in nature by reducing the use of resources by controlling the carbon emissions with the ecological footprint. In order to prevent environmental pollution caused by urbanization, it is one of the important goals to prevent pollution by developing solutions to the problems that pollute the environment in sustainable cities. The standards that affect the ecological footprint of the sustainable city are:

- Green buildings,
- Environmentally friendly transportation systems,
- Clean-Renewable energy usage,
- Air-Water quality,

- Amount of green area-Healthy environment (Akıncı and Pouya, 2019).

INVESTIGATION of SMART ENVIRONMENT PARAMETERS of KONYA

Sustainable Energy Resources of Konya

Solar Panels

Konya, located in the Midrail and in the Central Anatolia region of Turkey, is located in a place where solar energy can be used efficiently due to its convenient location (Figure 4). In these lands, where it is known that high efficiency can be obtained from solar energy, efforts are being made to expand the use of this energy.

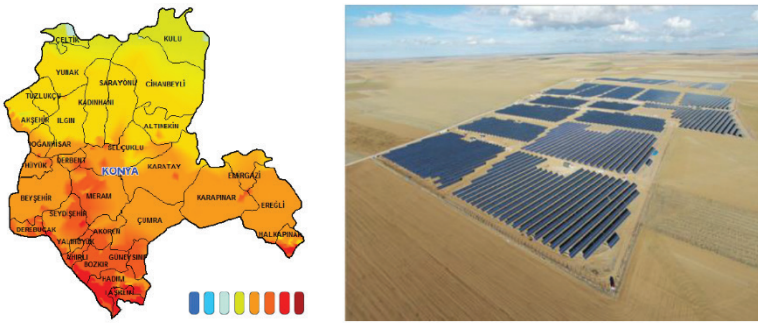


Figure 4. Konya Solar Energy Potential Map⁷ and Kızören Solar Power Plant⁸

Due to the fact that Konya is an efficient city in terms of the suitability of solar energy panels, solar power plants have been established at 45 different points in the city and electrical energy is produced. Especially Karapınar YEKA-1 solar power plant with a daily electricity production of 65 MW, and with other solar power plants such as Alibeyhöyük SPP, Karatay Kızören SPP, Apa SPP etc. a total of 600 MW of electrical energy is produced in the city during the day. In addition, five different solar power plants that are in the process of being built in Konya will start to

⁷ <https://www.enerjiatlas.com/gunes-enerjisi-haritasi/konya>

⁸ <https://www.memleket.com.tr/turkiyenin-en-buyuk-gunes-enerjisi-santrali-kizilorende-854410h.htm>

serve soon⁹. One of the smart applications used within the scope of these studies is the use of water wells with solar energy. In Konya, which is known as an agricultural city, the water pumps were connected to photovoltaic solar energy panels in order to reduce the use of electricity in water pumps and to provide efficiency with the application developed due to the high amount of electricity consumed for irrigation in water wells opened for irrigation purposes. Thanks to these photovoltaic batteries, which convert the energy from the sun into electrical energy with the devices in its system, water pumps that consume high energies in water use have turned into applications that operate in a sustainable way (Anonymous, 2019b).

Another sustainable solar panel application used in the city of Konya is the use of solar energy in parks, lighting signs, city lights and bus stops in the city. With photovoltaic solar energy panels, electricity is saved in urban lighting. Especially the 890 bus stops in the city, as well as the Urban Forest, Japanese Park, Birlik Park, Kozağaç Park, etc. in Konya. Renewable resource consumption is increased in energy use by using these solar energy panels in lighting poles, viewing terraces and camellias in many park areas (Anonymous, 2019b).

Another application where solar panels are used is to meet the required energy in meteorology stations located in the city. Solar energy panels placed around Gümüştepe and Tavus Baba in Konya and station systems that measure the city's temperature, sun exposure, humidity, wind speed and rain amount reduce electricity use.

Electricity Generation from Methane Gas in Solid Waste Facility

In order to provide a smart environment, it is necessary to integrate sustainable practices into urban life and to increase the quality of the city. One of the factors that arise at this point and reduce the quality of the city is the amount of waste. When the wastes are unconsciously stored in nature or tried to be destroyed, they cause air, environment and water pollution and eventually poisoning of the aged world. In order to

9 <https://www.enerjiatlasi.com/gunes-enerjisi-haritasi/konya>

prevent this situation that reduces the quality of life, Konya Metropolitan Municipality has started its works as of 2011¹⁰.

With the waste collection process, which has started to be implemented especially in the densely populated city center, the amount of garbage is brought under control. With the regular collection processes established in the city center, the wastes generated by the city users are collected and recycled, and the damage to the environment is reduced. During recycling, large amounts of methane gas are produced. The facilities that will enable the conversion of methane gas produced as a result of the transformation in the Aslm Solid Waste Landfill Site, where solid wastes are collected in Konya, started to serve in October 2011 (Figure 5). Electricity generation from the resulting methane gas is a sustainable practice that can be used for the city. The electrical energy produced at the facility, which operates at full capacity, is 5.6 MW per hour. In order to understand this amount, the amount of electricity generated by the converted methane gas meets the energy needs of 26.000 houses per day, allowing maximum efficiency with recycling (Anonymous, 2019b).



Figure 5. Electricity Generation Facility in Aslm Solid Waste Landfill Site¹¹

In addition, the heat energy generated during recycling at the facility was also wanted to be evaluated. In this context, annual regular tomato production is provided with the greenhouse effect in the city of

¹⁰<https://akillisehir.konya.bel.tr/>

¹¹<https://akillisehir.konya.bel.tr/uygulama/kati-atik-tesislerinde-elektrik-uretimi>

Konya, which has a continental climate, by using the heat energy generated by the transformation in the greenhouses designed to be close to the recycling facility. The size of the greenhouses is approximately 1,200 square meters and an average of 30 tons of tomatoes are produced and distributed annually (Anonymous, 2019b).

Sustainable Building Designs in Konya

Apart from the dynamic part that makes up a city, that is, the city users and the urban living environment, the part that occupies an important area is the buildings, which are fixed structures in the city. These living spaces, where urban users meet their housing, education, social activity needs and carry out other activities, should be designed in a planned manner. In this context, it is necessary to design smart buildings in order to create smart cities.

Smart building designs have recently started to gain importance in Turkey. As a result of the studies on it, the applications to be made in smart building designs are determined and used in the analysis. Konya has started to work by taking its own steps towards creating smart cities and smart buildings. Especially as of 2012, the importance given to smart building design has increased and in 2014, Unilever Tas Konya Ice Cream Factory, which is the first smart building in Konya, was built (Anonymous, 2018b).

One of the important criteria in smart building design is BREAM and LEED certificates, which are based on the registration and measurement of sustainable practices of smart buildings, as mentioned in the study. The importance of the LEED Certificate in our country has increased as a result of the fact that the BREAM certificate could not go far beyond the UK, where it was born. When smart building designs are to be realized in Turkey, they apply for this certificate and register themselves. In this context, in the process of becoming a smart city, Konya has given importance to LEED Certificate in smart building design and 8 certified and sustainable buildings (Table 1) have been designed throughout the city to date¹².

¹²<https://cedbik.org/>

Table 1. LEED Certified Buildings in Konya (Şenyıl and Büyüksahin, 2021)

Building Name	Date/Area	Points	Certificate
1 Unilever Tas Konya Ice Cream Factory	11.07.2014 49.143 m ²	54/110	LEED Silver
2 Konya Science Center	18.11.2014 25.010 m ²	66/110	LEED Gold
3 Konya Tropical Butterfly Garden	12.02.2015 6.899 m ²	55/110	LEED Silver
4 Konya Sports and Congress Center	13.01.2015 25.009 m ²	52/110	LEED Silver
5 Unilever Nestle Liquid Production Plant	09.06.2017 25.571 m ²	60/110	LEED Gold
6 Unilever Vector Repository	09.06.2017 18.104 m ²	61/110	LEED Gold
7 Unilever Vector Administration Building	09.06.2017 9.746 m ²	82/110	LEED Platinum
8 Metic Distribution Center	10.08.2018 325.348 m ²	59/110	LEED Silver



Leed certificate points of buildings

Unilever Tas Ice Cream Factory

Konya Science Center



Konya tropical Butterfly Garden

Konya Sports and Congress Center

Unilever Vector Repository

Sustainable Urban Characteristics of Konya

Sustainable solutions to be realized in cities in order to create smart cities are mentioned under the title of sustainable city, which is the third and last parameter of smart environment parameters, which is one of the smart city components. Sustainable solutions should be designed and implemented throughout the city in order to move cities to the future and ensure the quality of life. A general sustainable city can be created by spreading these smart sustainable practices to all areas that make up a city, instead of smart applications used in only one place in one area.

Creating sustainable cities ensures that the ecological footprints of cities are reduced and the damage they cause to the environment is reduced. It is necessary to develop clean energy systems in transportation networks in order to reduce the ecological footprint throughout the city, to prevent all kinds of pollution for the protection of urban health, and to protect and develop the natural environment, which is the most impor-

tant element that can fight with the ecological footprint. In the process of creating a sustainable city, Konya continues to progress towards becoming a smart city by developing smart applications and spreading these applications throughout the city.

Bicycle Routes and Smart Bicycle System

Konya is a city with suitable environmental conditions for bicycle use with its flat land structure, lack of slope, wide and long streets formed as a result of the drying up of an old lake bed (Great Konya Lake) in Central Anatolia. Special roads and applications are designed in the city in order to care about pedestrians and cyclists. Konya is at the forefront of the cities that work by supporting transportation with the use of bicycles, which is a sustainable use in Turkey.

550 kilometers of special roads designed in the city are reserved for cyclists only. The safety of cyclists in the city is ensured with the roads designed to be separated from the vehicle traffic. Bicycle lanes create sustainable urban life by providing sustainable transportation in the city, with the necessary slope and transition priorities given at the edges of the main roads and intersections in the city and with special traffic lights for bicycle traffic (Figure 6) (Mert and Öcalır, 2010).



Figure 6. Konya Bicycle Paths - Bench to Wait for Traffic Lights (left) and Konya Bike Rental Stations (Right)

Another smart application developed in the city and providing convenience for city users is bicycle rental points. The Konya Metropolitan Municipality provides the opportunity to rent bicycles at 80 different points in the city for the citizens who do not have personal bicycles but want to use bicycles for urban transportation. Rental transactions are

carried out at these points without the need for an officer, with individual handcards or bank cards. In this way, bicycle rental transactions can be rented and delivered every day and every hour without requiring a different process¹³.

Air-Water-Noise Quality

As a developed city, Konya has a large population and large industrial areas and factories with the requirements of development. These phenomena have a negative impact on the environmental health of the city. In order to prevent these negative effects, there are smart applications placed throughout the city.

One of the studies carried out to measure urban health is the determination and evaluation of air quality. In this context, the established air quality monitoring system continuously controls and analyzes the air quality for detailed analysis (Figure 7). With 4 different stations located in the city, the air quality, the amount of particles in the air and the carbon dioxide level are constantly measured. By the means of the measurements made in three main districts in the city center, instantaneous weather conditions are checked daily and hourly. In addition, when the recorded data goes out of the average values, it is kept under control with a system that gives a warning message (Anonymous, 2019b).



Figure 7. Air Quality Monitoring System (left), Noise Control System (Right)

¹³<https://akillisehir.konya.bel.tr/uygulama/bisiklet-yollari-ve-akilli-bisiklet-sistemi>

In order to prevent water pollution in Konya, 6 different water installation lines have been established. It is a first in Turkey in terms of quantity. In the studies carried out by the General Directorate of KOSKİ affiliated to Konya Metropolitan Municipality, there are city water, dirty water, fresh water, rain water, irrigation water and purple network line formed as a result of use in the city¹⁴. Thanks to the water installation networks used, the mixing of waters with different pollution levels is prevented. In this way, unconscious mixed use that creates water pollution is prevented, and pollution is prevented by ensuring efficiency in water use. In addition, thanks to the separated water installations, recycling and usage areas suitable for their structure and chemistry are determined for water that shows various differences, and it is recycled to the city. The purple grid in the city takes the most active step in the recycling process. By the means of the purple network, which can be considered as a recovery facility for treated wastewater in Konya, the lands that form green areas in the city have been irrigated since 2012. It is used as dripping in irrigation areas with 24 km long installations laid underground after the chlorination, filtering and disinfection process by taking the wastewater into a conversion system with the help of transmission pumps (Anonymous, 2019b).

Another environmental pollution that occurs in urban life and reduces the quality of life is noise pollution. Intense and busy city life causes involuntary decibel sounds and this affects the city users negatively. In this context, a Noise Control, Monitoring and Warning System has been developed by Konya Metropolitan Municipality in order to measure the amount of noise that occurs in cities and exceeds the limits of comfort conditions, especially in crowded areas. It works in order to take necessary measures by continuously recording and analyzing the sounds that occur in urban life with electronic devices that measure noise placed in the city. Thanks to the system;

- Identification of sound sources in the city,
- Calculating the daily average values of these sound sources by constantly listening in certain areas,

¹⁴<https://akillisehir.konya.bel.tr/uygulamalarimiz/11>

- Detection of measured sources when they pass the city sound barrier,
- Taking necessary measures by informing the authorities via SMS when necessary is provided (Anonymous, 2019b).

CONCLUSION

With the increase in the world's population and the increase in energy consumption, the importance of resource use on a global scale emerges. As a result of the use of fossil fuels and non-renewable resources over the years, these resources are faced with depletion in the future. This situation poses a danger in terms of cities that we can define as collective living spaces of today. Cities have turned to the use of renewable resources with new technological developments in order to reduce the use of lost non-renewable resources and to carry cities to the future. This orientation in cities also means making cities smart by using information and communication technologies and science. Cities that have been made smart will enable the use of only these renewable resources in the future by supporting and expanding the use of renewable resources that are constantly created as a result of the movement of our planet, instead of non-renewable resources in resource consumption.

Solar energy is at the forefront of renewable energy sources. In Konya, which is on the way to become a smart city for the purpose of generating electrical energy from solar energy, solar energy is converted into electrical energy by the use of photovoltaic batteries in the panels used by establishing solar energy fields with the studies carried out by the Konya Metropolitan Municipality. Innovative applications have been integrated into the city for the use of energy from the sun, apart from the solar power plants used. The most important of these is the use of solar energy panels in lighting elements that enable the regulation of urban mobility and making it more livable. Thanks to its large lands and mathematical location, Konya is one of the cities with high potential in terms of insolation and solar energy generation. It continues to work for clean energy production with solar power plants and panels, which it uses in the process of becoming a smart city by using its current potential. Alt-

though the number of solar power plants in the city will reach 49 with 4 power plants under construction, this number is insufficient to meet the daily electricity needs of the crowded city of Konya.

Another smart application that provides energy generation that will reduce the use of non-renewable resources used in Konya, while reducing the damage to the environment, is to collect the waste garbage generated in the city as a result of use and convert it into electrical energy in the recycling facility. Konya is a suitable city for generating electricity with waste recycling in terms of the large urban population and the high amount of waste material due to use. However, much less than the amount of waste generated in the city can be recycled.

As a result of the researches, it has been understood that the future will be in danger as a result of the continuation of the process in the buildings where the use of resources increases due to the increase in the amount of use. In order to prevent this danger, solutions have started to be found with smart and sustainable building designs for the problem encountered throughout history. Sustainable building designs are one of the applications that will help smart cities in protecting the future. With the understanding of the importance of these smart buildings in the way of building the smart cities of the future by meeting on a common denominator as a result of global urbanization, these structures have started to gain more importance today. Sustainable building designs and practices are tried to be made widespread in our country, especially in crowded and developed cities, designs are made with this understanding. In Konya, which is trying to improve itself in the process of becoming a smart city, it gives importance to sustainable building designs and carries out studies for the spread of these buildings in the city. Considering the population of the city and the number of buildings increasing in direct proportion, 8 certified sustainable buildings in the city are a situation that should be considered for the future of the city.

The use of bicycles placed in the city is of great importance in ensuring mobility and sustainability in smart cities, where sustainability gains importance and can reach the future. Making the use of bicycles widespread ensures the development of urban energy efficiency and environmentally friendly methods by keeping the transportation made with

non-renewable resources in the background. Konya is a suitable city for bicycle transportation thanks to its land structure and smooth roads. The planned settlement in the city, which is tried to be developed, and the bicycle transportation integrated into the city are tried to be expanded by showing parallelism to each other. The existing bicycle networks in the city today consist of divided roads on double-lane roads, specially paved on the sides of the road and painted on blue asphalt, which is clearly distinguished for cyclists. Since Alaaddin Hill and its surroundings, which make up the historical city center, and the Mevlana Museum and its surroundings have a congested city texture from the past and heavy vehicle traffic as well as pedestrian traffic, bicycle transportation becomes difficult in the city center. Since the existing bicycle paths in Konya are located on the main streets of the city, it is thought that there are many transportation opportunities by bicycle when looking at the city in general. However, the roads in the city are the developed continuation of the Konya city axes that have been shaped throughout history. For this reason, it is seen that the blue roads designed for bicycle transportation are not throughout the city. When it is desired to provide transportation by bicycle for every workplace or residence, it is seen that there are no suitable bicycle paths. Although Konya has given importance to bicycle networks and developed the use of bicycles in the city, as a result of the current situation in the city, bicycle users have to enter the roads with vehicle traffic along the way in order to reach their destination. In the city, where sustainability gains importance and is encouraged, it is predicted that the use of bicycles will increase in the coming years. In order to prevent the problems caused by the increased use of bicycles in the face of this situation, solutions should be developed that will integrate future cyclists on roads, avenues and streets and eliminate the difficulties in transportation by ensuring their safety.

As a result, the city of Konya emerges as a city that progresses and develops step by step in the process of becoming a smart city with its smart applications and sustainable studies. This process can be accelerated by increasing and disseminating the practices carried out in the city. By raising the awareness of city users and increasing the investments to be made in this area, it will be easier for all urban units to come together

on a common ground to transform the city into a smart city. In addition to the existing smart and sustainable applications, approaching the new methods to be developed on the basis of the user will be one of the basic methods that will ensure the use of new and successful applications in the city. This concept will gain even more value and help the formation of high quality, healthy and livable cities, with all units that make up the city adopting the smart city practices and sustainable methods created with the awareness of reaching the future in a healthy way. It should not be forgotten that the future will be a time that can be reached with smart cities where smart applications brought by information and communication technologies and sustainable methods with environmentally friendly resource use are used. Because the future; will come with green environment, sustainability and innovative friendly practices brought by technology.

REFERENCES

Akıncı, İ. and Pouya, S. (2019). The Eco-City Proposal As A Sustainable City Model. *Türkiye Peyzaj Araştırmaları Dergisi*, 96-107.

Akkan, M. M. (2019). *Akıllı Kent Uygulamaları Konya Örneği*. Necmettin Erbakan University Institute of Social Sciences, Konya.

Anonymous. (2018a). *Dünyada ve Türkiye’de Enerji Durumu*.

<https://www.gazbir.org.tr/uploads/page/Dunya-ve-Turkiye-Enerji-Gorunumu.pdf>

Anonymous. (2018b). *IGSC Uluslararası Yeşil Başkentler Kongresi (International Green Capital Congress)*. (A. Ötegen, Prof.Fikret Akınerdem, C. Kılıç, A. Öztürk ve S. Uçar, Ed.). KONYA.

Anonymous. (2019a). *Akıllı Şehirler Beyaz Bülteni*. T.C. Çevre ve Şehircilik Bakanlığı. https://webdosya.csb.gov.tr/db/cbs/menu/akilli-sehirlerkitap_20190311022214_20190313032959.pdf

Anonymous. (2019b). *Akıllı Şehir Konya Uygulamaları*. (B. İşlem D. Başkanlığı, Ed.) Konya.

Arsan, Z. D. (2008). Türkiye’de Sürdürülebilir Mimari. *Mimarlık* 340, Mart-Nisan, 21-30. https://www.researchgate.net/publication/333665786_Turkiye'de_Surdurulebilir_Mimari

Aytıs, Y. D. D. S. and Polatkan, I. (2009). Ekolojik Mimarlık Kavramı Temel İlkeler. Antalya: Uluslararası Ekolojik Mimarlık ve Planlama Sempozyumu. https://www.researchgate.net/publication/331211881_EKOLOJIK_MIMARLIK_KAVRAMI_VE_TEMEL_ILKELER

Boy, J. D. (2020). ‘The metropolis and the life of spirit’ by Georg Simmel: A new translation. *Journal of Classical Sociology*. doi:10.1177/1468795X20980638

Caradonna, J. L. (2014). *Sustainability: A History*. New York: Oxford University Press is the department of the University Oxford.

Çetin, M. and Çiğdem, Ç. (2019). Literatüre Göre Dünya ve Ülkemizden Örneklerle Akıllı Kent Kavramının İrdelenmesi. *Ulusal Çevre Bilimleri Araştırma Dergisi*, 2(3), 134-143.

Çiftçi, E. and Balyemez, S. (2019). Enerji Verimliliği Açısından Yüksek Yapılar ve Sürdürülebilirlik. *Anadolu Bil Meslek Yüksekokulu Dergisi*, 15(58), 127-141. doi:10.17932/IAU.ABMYOD.2006.005/abmyod

Dal, M. and Özdemir, Y. (2020). Dijital Çağda Neden Bir Kent Sürdürülebilir Akıllı Şehir Olmalıdır? *Uluslararası Doğu Anadolu Fen Mühendislik ve Tasarım Dergisi*, 2(2), 205-215. doi:10.47898/ijeased.728019

Elvan, Y. M. L. (2017). Akıllı Şehirler: Lüks Değil İhtiyaç. *İstanbul Teknik Üniversitesi Vakfı Dergisi*, 77, 6-10.

Erten, D. D. (2017a). *Yeşil Binalar*. Sürdürülebilir Üretim ve Tüketim Yayınları - V.

Erten, D. D. (2017b). Yeşil Bina ve Yerleşke Sertifikaları. *İstanbul Teknik Üniversitesi Vakfı Dergisi*, 77, 40-43.

Giffinger, R., Fertner, C., Kramar, H. and Kalasek, R. (2007). “Smart cities - Ranking of European medium-sized cities”. *Vienna University of Technology*.

Gürsoy, O. (2019). *Akıllı Kent Yaklaşımı Ve Türkiye’deki Büyükşehirler İçin Uygulama İmkânları*. <http://www.openaccess.hacettepe.edu.tr:8080/>

xmlui/bitstream/handle/11655/6037/10219043.pdf?sequence=1&isAllowed=y

Hayta, Y. (2016). Kent Kültürü Ve Değişen Kent Kavramı. *Bitlis Eren Üniversitesi Sosyal Bilimler Enstitüsü Dergisi*. <https://dergipark.org.tr/en/download/article-file/713306>

Kayapınar, Y. E. (2017). Akıllı Şehirler ve Uygulama Örnekleri. *İstanbul Teknik Üniversitesi Vakfı Dergisi*, 77, 14-19.

Kaygısız, Ü. and Aydın, S. Z. (2017). Yönetişimde Yeni Bir Ufuk Olarak Akıllı Kentler. *Mehmet Akif Ersoy Dergisi Sosyal Bilimler Enstitüsü Dergisi*, 18. doi:10.20875/makusobed.292381

Kılınçarslan, Ş., Şimşek, Y., Uygun, E., Akoğlu, M., Cesur, B., Tufan, M. Z. and Turan, U. (2019). Sürdürülebilir Yapı Malzemeleri Açısından Bina Sertifikasyon Sistemlerinin İncelenmesi. *Uluslararası Sürdürülebilir Mühendislik ve Teknoloji Dergisi*, 3(1), 1-14. <https://dergipark.org.tr/tr/pub/usmtd/issue/47222/445951>

Lynch, K. (1960). *The image of the city*. Cambridge: The MIT Press.

Luque Vega, L. F., Carlos Mancilla, M. A., Payan Q., V. G. ve Lopez Neri, E. (2020). Smart Cities Oriented Project Planning and Evaluation Methodology Driven by Citizen Perception-IoT Smart Mobility Case. *Centro de Investigación, Innovación y Desarrollo Tecnológico CIIDETEC-UV-M, Universidad del Valle de Mexico*. doi:10.3390/su12177088

Meadows, D. H., Meadows, D. L., Randers, J. and Behrens, W. W. (1972). *The Limits To A Report For The Club Of Rome's Project On The Predicament Of Mankind*. New York: Universe Book. <http://pinguet.free.fr/meadows72.pdf>

Mert, K. and Öcalır, E. V. (2010). Konya'da Bisiklet Ulaşımı: Planlama ve Uygulama Süreçlerinin Karşılaştırılması. *Metu Journal of the Faculty of Architecture*, 27(1), 223-240. doi:10.4305/METU.JFA.2010.1.12

Ocakçı, M. (2018). Sözlük'ten: Kent İmgesi-Kevin Lynch. *Kent Stratejileri Merkezi*. <https://kentstratejileri.com/tag/kevin-lynch/>

Örselli, E. and Akbay, C. (2019). Teknoloji ve Kent Yaşamında Dönüşüm: Akıllı Kentler. *Uluslararası Yönetim Akademisi Dergisi*, 228-241. doi:10.33712/mana.544549

Özdil, Y. M. S. (2017). Şehirlerimiz Nasıl Akıllanır? *İstanbul Teknik Üniversitesi Vakfı Dergisi*, 77, 20-23. https://www.ituvakif.org.tr/dergi/sayi_77.pdf

Öztopcu, A. and Salman, A. (2019). Sürdürülebilir Kalkınmada Akıllı Kentler. *Karadeniz Uluslararası Bilimsel Dergi*, (41), 167-188. doi:10.17498/kdeniz.476335

Sınmaz, S. (2013). Yeni Gelişen Planlama Yaklaşımları Çerçevesinde Akıllı Yerleşme Kavramı ve Temel İlkeleri. *Megaron Dergisi*, 8(2), 76-86. doi:10.5505/MEGARON.2013.35220

Şenel, M. C. and Koç, E. (2015). The State Of Wind Energy In The World And Turkey. *Mhendis ve Makina*, 56(663), 46-56.

Şenyıl, N. N. and Büyükaşahin, S. (2021). Akıllı Kentlerde Sürdürülebilir Binalar: Konya Örneği, Kongre Kitabı, pp 149-160. 5. Uluslararası Mimarlık ve Tasarım Kongresi, 26-27 May 2021, İstanbul.

Tatlıl, E. (1994). Türkiye’de Kentleşme ve Kentleşmede Kimlik Sorunu. *2000’li Yıllarda Türkiye’deki Toplumsal ve Kültürel Dönüşümler Sempozyumu* içinde . Abant: UNESCO Turkey National Commission.

Terzi, D. D. F. and Ocakçı, P. D. M. (2017). Kentlerin Geleceği: Akıllı Kentler. *İstanbul Teknik Üniversitesi Vakfı Dergisi*, 77, 10-13. https://www.ituvakif.org.tr/dergi/sayi_77.pdf

Totty, M. (2017). The Rise of the Smart City - WSJ. *The Wall Street Journal*. <https://www.wsj.com/articles/the-rise-of-the-smart-city-1492395120>

Uzun, Ö. G. T. and Yeğın, Y. D. D. M. (2017). Enerji Etkin Yapılarda Güneş Pili Uygulaması. *Yapılarda Performansı Arttırmak İçin Yeni Yöntemlerin Geliştirilmesi* içinde . Adana: Çukurova Teknokent.

Williams, R. (1973). *The Country And The City*. New York: Oxford University Press.

INFORMATION SECURITY WITH STEGANOGRAPHY

*İnan GÜLER*¹

Abstract: Today, with the increase in the use of the internet and computers, the information assets of institutions and organizations are constantly increasing. In the internet age we are in, the fact that public institutions, private organizations and people are in constant communication with the internet has become a big problem in order to ensure the security of this knowledge. All these reasons have led to the transfer of some long-standing security applications to computer science. Today, the content of these concepts is filled much faster than in the past. Data security is devoted to many different fields and disciplines such as cryptography, steganography and watermarking. Likewise, one of the most difficult tasks in today's modern communication systems is the successful transmission of confidential digital information over an unsecured channel with adequate and proper methods. Many encryption algorithms have been developed to hide confidential information. But over time, flaws have been discovered in even the most advanced encryption algorithms. Each encryption algorithm can be decrypted using sufficient time and sufficient resources. With the development of the processors of the computers and the increased speed and extensive data search, the probability of decryption has also increased. In this case, it has led to the development of steganography. Steganography is one of the methods used for the hidden exchange of information and it can be defined as the study of invisible communication that usually deals with the ways of hiding the existence of the communicated message. In this way, if successfully it is achieved, the message does not attract attention from eavesdroppers and attackers. Using steganography, information can be hidden in different embedding mediums,

¹ Prof. Dr. İnan Güler Gazi University, Faculty of Technology, Department of Electrical & Electronic Engineering, Ankara <https://orcid.org/0000-0002-5058-0846> iguler@gazi.edu.tr

known as carriers. These carriers can be images, audio files, video files, and text files. The focus in this paper is on the use of an image file as a carrier, and hence, the taxonomy of current steganographic techniques for image files has been presented. These techniques are analyzed and discussed not only in terms of their ability to hide information in image files but also according to how much information can be hidden, and the robustness to different image processing attacks.

Keywords: Information security, Cryptography, Steganography, Steganalysis.

INTRODUCTION

Superalloys Any confidential information sent through an unprotected communication channel must be protected against unauthorized access by third parties. An example diagram of confidential information between unprotected communication methods and between the sender and the receiver is given in Figure 1.

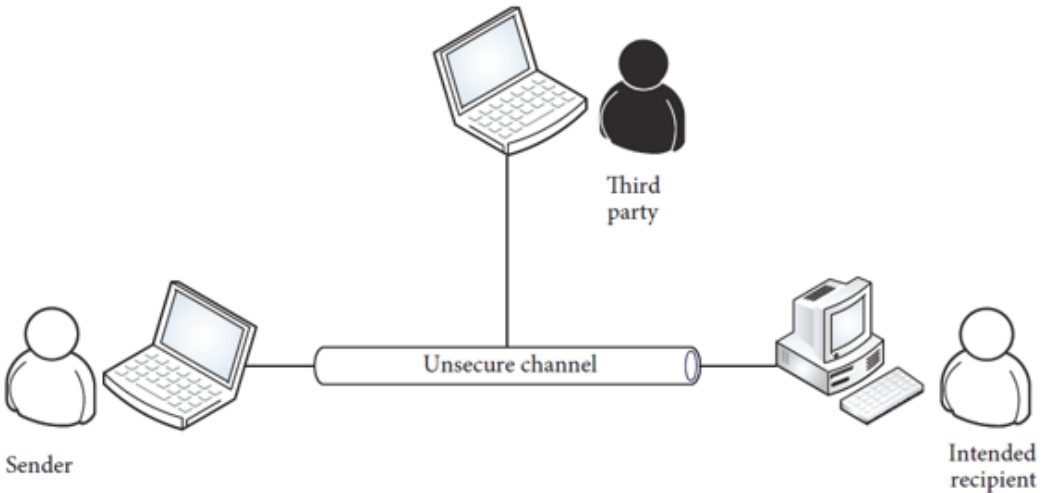


Figure 1. Unprotected Communication Channel

In the case of the presence of third parties, secure communication techniques are examined in the field of cryptography. Confidential information can be protected in encryption processes (Mirko Köhler, 2017). Confidential information is returned to an encrypted form with

appropriate encryption algorithm techniques. The content of encrypted information cannot be decrypted without the encryption key. But the important point here is that the encrypted information is not confidential. With sufficient time and computational resources, the encryption algorithm can be decrypted with a proper decryption algorithm and the content of confidential information can be revealed. Every newly developed encryption algorithm has some advantages, but every encryption algorithm can be decrypted in sufficient resources and sufficient time. The only exception to this situation is the “one full pad” algorithm, which destroys itself immediately after using a temporary card or pad.

Another approach to protecting confidential information is to hide the existence of information using steganography. Steganography is comprised by a set of techniques that allows one to write messages and hide them, for example, in images, in such a way that no one suspects of their existence. Steganography is a science of writing secrets. Therefore, no one other than the sender and receiver knows of the existence of the message. If the existence of hidden information is revealed in some steganography files, its content can be easily read. One advantage of steganography is that the hidden message does not attract attention. On the other hand, encrypted messages, although undecipherable, will arouse suspicion. Therefore, while cryptography protects the content of the message, steganography hides the message itself. The main property of a steganographic system is to be statistically undetectable (R. Karakış at all, 2015).

Presence of stego-images (embedded information within the picture) can be detected thanks to specialized algorithms called steganalysis. Some previous studies have shown that most steganographic algorithms can be detected by steganalysis algorithms. The important thing here is to protect the information by using proper protection approaches as a methodology.

In this chapter, encryption and steganography techniques were analyzed. The weaknesses and strengths of these techniques are explained. Moreover, the positive features of these techniques have been taken into account in order to better secure information over an insecure communication channel. In addition, a new method is proposed using substi-

tution encryption based encoding table and steganography. That is, this method called subcodstanoigraphy is presented and the features of this method are explained.

STEGANOGRAPHY AND INFORMATION SECURITY

Steganography is the art of sending a data containing a hidden message or information in a way that no one but the recipient can notice. The word 'steganos' in Latin means 'invisible' and steganography means 'hidden writing'. In short, steganography can be defined as the 'art of hiding data'. The aim is to hide the information that is wanted to be conveyed and the existence of this information well enough to prevent others from noticing it. In Steganography, even the person to whom information is sent can obtain confidential data only if he knows the key information (İ. Güler and R. Karakış, 2019).

Modern steganography takes advantage of digital technology and includes hidden message attachments to some multimedia files, such as pictures, audio or video files. These files are an integral part of normal communication and therefore do not attract attention. Steganography can be applied to various types of files. In the subject of this chapter, steganography application in digital pictures has been described. Other types of steganography (linguistic or audio file) are not analyzed in this chapter.

Image files often contain unused or less significant bits (LSB) that can be replaced by various steganography techniques or replaced with confidential information. Such files can be modified without raising doubt about the actual communication purpose. Unlike cryptography, encryption of information is not important in steganography. Cryptography is a science that takes its robustness from the encryption algorithm and does not hesitate to know the existence of the data to be transmitted. Therefore, in cryptography, it is not a matter of which channel the data will be transported, but no algorithm is unsolvable, no matter how robust it is. Unlike this, in steganography, how the data will be transported has to be stored.

The important point in steganography is to hide the existence of the data. The better the existence of the data can be concealed, the safer the data to be transferred. While an ordinary picture or music file does not arouse suspicion, it may contain very confidential information. No one, including the recipient, would suspect this without key information, without knowing where the data is stored. Therefore, in steganography, it is of no importance to transmit the data to the other party without the receiver's information on which channel the data will be transported and how the message can be deciphered.

Steganography Techniques

When examining a steganographic algorithm, three main features should be considered: inability to detect change, amount of data that can be stored, and robustness. In accordance with the principle of not detecting the change, the changes made on the cover data should not be in a position to be perceived by the human senses. In case of detection, confidential communication is revealed and the third party has the possibility to perform various operations on the file containing confidential data. Although the steganographic method has limitations, it is necessary to show a certain resistance against such attacks.

Various steganography techniques have been applied throughout history (Y. A. Fadil 2017). With the advancement of technology and computer power, new techniques have been created and introduced. The main categorization of steganographic techniques in digital images focuses on spatial domain methods, frequency domain methods and adaptive methods. List of steganographic methods and techniques classified as the following:

Histogram shifting method

Image Steganography Classification

Spatial domain (based) methods are as follows:

LSB Histogram shifting method

LSB replacement

LSB matching

- LSB matching revisited
- Pixel value differencing method
- Singular value decomposition method
- Histogram shifting method

Frequency domain methods are as follows:

- Discrete Fourier transform (DFT) method
- Discrete cosine transforms (DCT) method
- Discrete wavelet transforms (DWT) method
- Integer wavelet transform (IWT) method

Spatial domain techniques generally use the least significant bit (LSB) replacement method directly. This technique, although simpler, has greater impact compared to the other two techniques. Here, as additional information, BMP and GIF-based steganography apply LSB techniques. Although their resistance to statistical counterattacks and compression is reported to be weak, it is recommended to use BMP instead of JPEG images. Moreover, JPEG images are avoided as they can be detected with changes as small as changing the LSB of a pixel in a JPEG image.

Frequency domain-based techniques generally use a discrete cosine transform (DCT), DFT (Discrete Fourier Transform) and DWT (Discrete Wavelet Transform). Finally, adaptive techniques can be applied in either spatial or frequency domains. Data embedding can be examined under two subheadings by paying attention to the data used. The first of these is the Spatial / Image Domain Technique, and the second is the Frequency / Transform Domain Technique.

Spatial Field/Image Field Technique: The hiding method directly uses the data in the image file. The dataset in which the information is stored during the hiding process refers to the pixel values (R. Karakış at all, 2015). An example is Least Significant Bit Insertion (LSB).

Frequency Domain/Conversion Field Technique: The hiding method is applied on the changes in the original data. For this technique, the preferred algorithms for embedding data in JPEG type image files

can be given as an example. The mentioned algorithms store data on the preferred DCT coefficients during compression of JPEG image files. Preferred methods for storing data in image files are divided into three subheadings as the following: methods based on modification, methods based on signal processing, and methods based on spectrum spread. Among the steganographic algorithms that store data by applying the above methods, Data Storage in the Frequency Domain and LSB-Least Significant Bit Insertion method is used the most.

Substitution Method

The substitution method works to replace some or all of the unnecessary components in media files with confidential information. The purpose here is to replace the already encrypted information in the file with unnecessary components. To detect the secret message, the actual content of the file must be suspected first. A part of the media file where the real content is hidden and the distribution of bits of information in the encoded file should be determined. At this point, the decoding process can begin. To understand this principle, it is important to know the structure in steganography. For example, it is necessary to know the detailed information of the RGB (Red, Green, Blue) system of the Bitmap, the effect of adding more information to the visual information in the picture, and the details of the processes of the information added to the given BMP picture (M. E. Saleh, 2016).

A second security prevention method is described as the following: in simple terms, we can explain this method as a function that adds a string of bits from the first step (encryption) to the original file (carrier). For example, like a bitmap image. The original file can be selected from the multimedia database. The way these bit series are placed in the original file can be changed each time to hide a new information to avoid steganalysis methods. Steganalysis methods, the steganography method used and its key are explained in the next section.

Steganalysis Attacks and Countermeasures

The science of revealing data hidden by steganographic methods is called steganalysis. There is no general steganalysis method developed to reveal the data stored using steganographic methods. However, most steganalysis applications are based on mathematical - statistical analysis. The purpose of steganalysis is to identify and detect suspicious datasets. An example of this is the process of removing confidential information from a steganography file. Unlike cryptanalysis, cryptanalysis is the branch of cryptography that studies the decryption of encrypted texts; Steganalysis usually starts with a few questionable datasets that may contain a hidden message. Using advanced statistical analysis methods, the steganalist can reduce the suspicious dataset until the correct steganographic file is found. Information can be any publicly available source on the Internet, further complicating the steganalysis processes. steganalysis; analysis and detection of attacks, isolation, rendering unusable or deletion of confidential information. The attack type depends on the resources available to the steganist (S. Ansari, 2019).

The types of attacks used in steganalysis are as follows: only stego, known carrier, known message, selected stego, selected message and known stego attacks. Since only the name of known carrier attacks is mentioned in the article that is the subject of the homework here, its explanation is considered sufficient at this point.

In the known carrier attack, there is both the image before the message is hidden and the image after the message is hidden. By checking the patterns, the process of comparing the steganography file carrying confidential information with the original steganography carrier is done at this stage. In the article on the subject of homework, the following statements are made as a precaution for the known carrier. The original file used should be deleted after adding information. This prevents the second type of steganalytic attacks and provides the possibility of a third step in enhancing security processes. However, in addition to these, the following operation can be done. Confidential data can be encrypted before they are buried. Encryption of confidential data provides a definitive solution against active steganalysis methods; In other words, even if

the secret data can somehow be extracted from the embedded signal, the difficult cryptanalysis process must be successfully completed in order to obtain its content.

Cryptography and Steganography Interaction

The difference of steganography from cryptography is that the existence of the hidden message in steganography is hidden. In other words, the information that the hidden data is embedded in the cover data is known only to the receiver of the message, and someone else who has the cover data cannot notice the existence of the hidden data. In cryptography, everyone knows that the data sent is confidential. Its contents cannot be understood without the secret key, and it takes a great deal of effort and time to understand the secret data [9]. Due to the use of strong algorithms in cryptography, it is resistant to brute-force attacks and it is very difficult to obtain confidential data (Y. A. Fadil 2017).

In steganography, on the other hand, it is relatively easy to obtain confidential data when it is understood that the message is hidden in any object. In steganography systems, the information inside can be encrypted while the message is transmitted, so even if the presence of the message is detected by a third party, the message will still protect its confidentiality since there is no secret key.

Current steganographic methods rely on the secret key and robustness of the steganographic algorithm. However, no single steganalysis algorithm is superior or the best, as demonstrated in (N. Hamid, A.2012). Moreover, current steganographic techniques do not address the issue of encryption of payload before embedding. Various studies have been conducted in recent years covering the interaction between cryptography and steganography. For example, DWT (Discrete Wavelet Transforms) based steganography is used together with filter bank cipher to encrypt a secret text message.

SUBCODSTANOGRAPHY METHOD [1]

This section describes a new method that has emerged by integrating cryptography and steganography using an encoding table based on sub-

stitution encryption (Mirko Köhler, 2017). The features of the described approach are given as follows: First of all, the existence of confidential information obtained using steganography should be suspected. Next, the steganography method and key used must be discovered. Each new secret uses a new steganography key and a new steganography file. If the first two steps are detected and the secret message is read, a series of encrypted data is obtained as a result. In this step, the encryption algorithm that is different and used for each encryption should be determined. In the end, if the identification of an encryption algorithm is successful, the encryption key used must be found.

Here, it is assumed that each secret information has different steganography methods, steganography keys, encryption algorithms and encryption keys. If the suggested method is performed and a message is decrypted, only the information in that message can be read, but the confidential information in other messages cannot be accessed because all the steps mentioned above are different for each message. The information hiding process is presented step by step in the next section. In the example, a Bitmap image is selected for information insertion and an encoding table is used for encryption. This whole process is shown in Figure 2 and is called “subcodstanography”.

Encoding Table Structure for Substitution Encryption

In this step, encryption algorithm is used to protect the information for the purpose of initial security. At the same time, the encryption method proposed in this step uses an encoding table. The encoding table is hidden and is randomly generated for each new encryption. coding table; contains a string of bits used in place of letters, numbers, or other characters. Depending on how many bits are used to represent each symbol in the encoding table, there are several different sequences for each symbol (“A”, “j”, “”, “2”). There may be several different rankings for each symbol, so commonly used symbols cannot be found or searched with the aid of statistical value. After all symbols in the message have been replaced with a series of bits from the encoding tables, the first measure of security encryption is completed in this step.

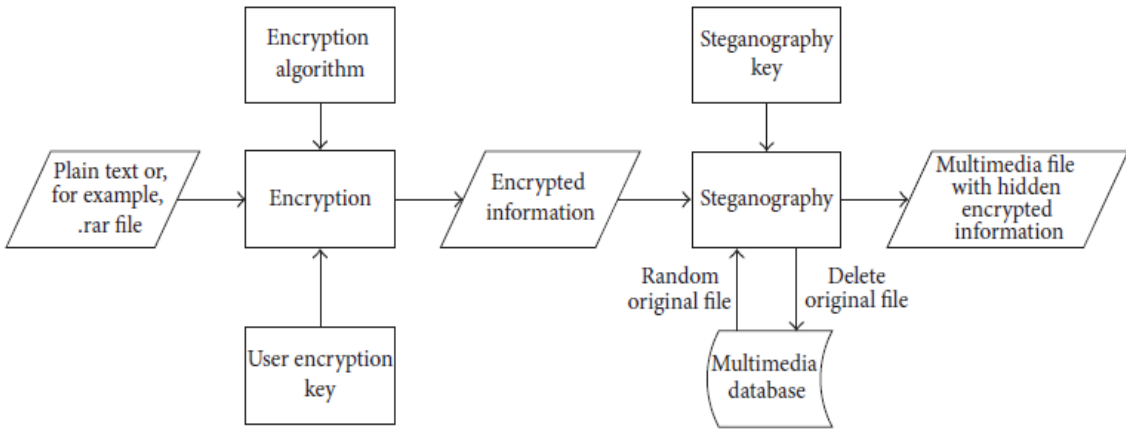


Figure 2. Process of hiding information

An encoding table consists of all possible ASCII symbols. As mentioned earlier, each symbol consists of several different sequences (orders) generated by a random function, depending on how many different bits are used to store a single symbol in the encoding table (Table 1). In the Table 1, four different bit combinations include the letter “A” and the rarely used “!” character, the first security encryption measure is completed in this step.

Table 1 uses a symmetric key cryptography where all symbols are represented by the same number of differently coded values. It was stated that this method was chosen in this application for reasons such as simplicity. From the example in Table 1, it can be seen that an ASCII symbol (letter “l”) is presented with different bit combinations at different places in the message. Using familiar values of the statistical occurrence of certain characters in a given language, attackers cannot find either patterns or the most frequently used characters.

Table 1: Encoding Table

Plain text: Hello world!

Encoding table

" "	0100001111	1000110010	1110001100	0011100101		
"A"	1010101010	0110000001	1000001101	0111011001		
		...				
"H"	1000111111	0111000011	0001111000	0000100000		
		...				
"d"	1010000110	1001001110	1000000111	1110000000		
"e"	0000011100	0000000001	1000001110	0111000100		
		...				
"l"	1100111001	0101011100	0001111100	1000000110		
"o"	0001111100	1000111010	1001010101	1010001011		
"p"	1111001111	0110011100	1110110000	1110010101		
"r"	1000101101	1111111100	1100000010	0000111100		
		...				
"w"	0011110001	1100111000	0011000111	0011111001		
		...				
"!"	0101101001	1110011111	1110011010	1001110100		
		...				
	"H"	"e"	"l"	"l"	"o"	" "
	0111000011	0000011100	0101011100	1100111001	0001111100	1000110010
	"w"	"o"	"r"	"l"	"d"	"!"
	0011110001	1001010101	1111111100	0001111100	1001001110	1110011111

Depending on the needs and the level of security that must be achieved, more combinations can be obtained for each symbol by increasing the number of bits in the encoding table. In this method, it is suggested to use an asymmetric coding table where the symbols that appear more frequently are coded with more mutually different combinations than the symbols that appear less frequently.

Another advantage of this encryption method is that for each new encryption, a new encoding table is used with new randomly generated bit sequences. Therefore, the secret message cannot be encrypted without the encoding table unless you have a lot of time and resources.

The sender and intended recipient do not know which encoding table is used in the encryption process. Only the computer encryption program knows which encoding table is used.

Adding Encrypted Information to a Picture

After encrypting the confidential information using an encoding table, the next step is to add the encrypted information to the BMP image. Here steganography is used to hide an encrypted message inside the media file. The selected container is the bitmap file in the example given. It is described that the bitmap file was chosen in this method because it allows a larger amount of data to be inserted. In the rest of the article, different algorithms for adding encrypted information are explained and their effects on the changes in the visual information of the bitmap file are explained. For each new information hiding process, various steganography methods and information insertion methods and a new bitmap file are used. Since the place where the information inside the media file is hidden is not predefined, the article mentions that this process increases the security.

To detect confidential information, either steganography and the original files or the steganography algorithm used must be known. The goal is to get in touch with any of these data. It is mentioned that the original file is deleted from the multimedia database after the hidden file is added. Therefore, it is difficult to find lice modified using the steganalysis method. Using extensive data search methods, one can try to find all possible combinations of bits added to the media file. This will produce a series of obscure bits. Of all the combinations, only one is the real message and cannot be deciphered because of the still encrypted message.

The size of the encrypted message (SEI); It is found by multiplying the number of symbols (NS) and the number of bits (NBCT) in the encoding table ($SEI = NS \times NBCT$). Here SEI is the size of the encoded information, NS represents the number of symbols and NBCT is the number of bits in the encoding Table 1. For example, to store the message "Hello World!," which uses a 10-bit symmetric encoding table. In this

case, the size of the encrypted information is 120 bits according to this calculation method.

The number of bits available for steganography (NSB) in the bitmap file can be calculated using the equation below.

$$\text{NSB} = (\text{height}) \times (\text{width}) \times (\text{color}) \times (\text{bits}),$$

where NSB represent the number of bits in steganography, (height) X (width) represents the bitmap dimensions, color represents the number of colors, and bits represents the number of bits useful for steganography. The total number of steganography combinations of the bitmap file can be calculated using the following equation.

where NSC represents the number of steganography combinations.

If the information is added to the 24-bit bitmap file size of 100×100 pixels, then according to the NSB formula, 120,000 bits is suitable for steganography manipulation, where the number of colors is 3 and the number of bits is 4 (İ. Güler, R. Karakış 2019). However, "Hello World!" Only 120 bits are required to add your message. According to the NSC formula, the encrypted message "HelloWorld!" Indicates that there are $4.47 * 10^{410}$ different combinations that can be added to the image. Therefore, $4.47 * 10^{410}$ different 120-bit encrypted messages should be analyzed using the general search method. For this analysis, each message must be decoded. But without the encoding table this task is almost impossible.

The inability to decrypt a message also means that the length of the message appended to a bitmap file is unknown. In this example, the message is 120 bits long; It was stated that the length of the message is unknown. Similarly, when a particular message is read, it is unknown how many bits are used in the message to present each ASCII symbol. Because the number of bits used in the encoding table is unknown. Therefore, the bit length variation in the encoding table must be taken into account. In this case, the message length is 120 bits, so 8, 10, and 12 bits (or any other number divisible by 120) must be assumed for encoding. This means that the number of encrypted messages is multiplied by three and the total number of combinations is $13.41 * 10^{410}$. It is stated in the article that for messages longer than 120 bits there are many sections

and hence the encoding table can use more than 12 bits to represent each ASCII symbol.

Encryption Process

It has already been mentioned that both the sender and receiver know neither the steganography method, nor the application key, nor the encryption key. As such, it reduces the possibility of others reading confidential information. It is understood that information about the encryption method should be placed in the steganography file next to the secret message. There are several ways this can be done. It is emphasized in the article that it is important that this information is hidden and not known by both the sender and the receiver.

One way to send a steganography key is to add data to the file header. The software solution of this method stores all possible keys for all algorithms used. These keys have their own code words applied in the header of the steganography file. When the steganography file is received, the decoding program first reads the steganography key from the file header and recognizes the algorithm used and the location of the bits in a file where the message is hidden. Therefore, the file header should not stand out. It is mentioned in the article that it is possible to hide the key in various places in the file to prevent manipulation of the steganography file header and ensure its consistency.

Besides the secret message, the code word for the encryption algorithm used is embedded in the steganography file. When this codeword is added to a steganography file, it must be sent to the recipient. When the receiver receives the sent file, the decoding program uses the program part for codeword recognition and finds the matching algorithm. The last step of the decryption process is to read the encrypted message. The decryption process is shown in Figure 3.

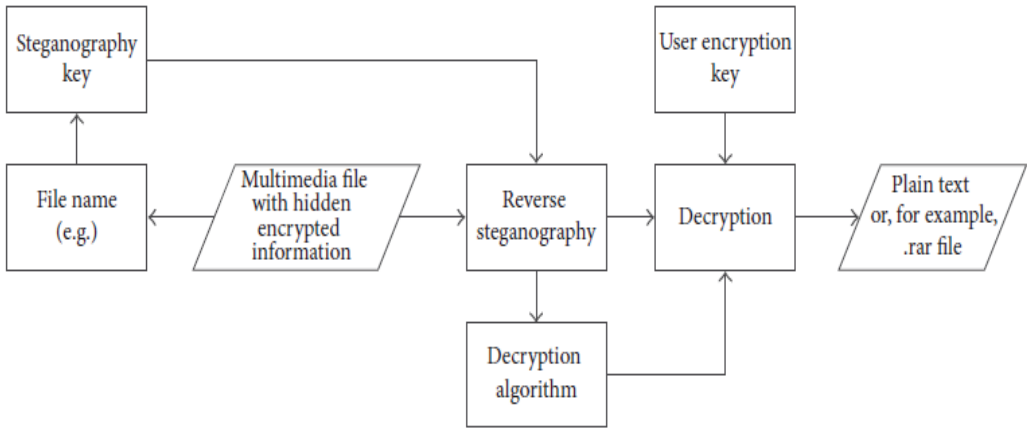


Figure 3. Decryption Process

When the media files are received by the recipients, they are uploaded to the decoding program that monitors the files containing the secret message. From now on; The program checks whether the steganography key appended to the filename matches the key in the image and finds the codeword of the encryption algorithm used. If the keys are equal and the tag of the algorithm is recognized, the secret message is read from the file. Confidential information is decrypted using the encryption algorithm and decryption key. This completes the process of transmitting confidential information and obtaining original information. Another advantage of this encryption method is that for each new encryption, a new encoding table is used with new randomly generated bit sequences. Therefore, the message cannot be decrypted without the encoding table.

RESULTS AND CONCLUSION

In this chapter, the idea of combining encryption and steganalysis methods is examined in such a way as to propose a method for securely transferring confidential information over an insecure communication channel called “subcodtanography”, taking advantage of the favorable features of both methods. Encryption method using coding table is also recommended in this context. In this method, the plaintext is encrypt-

ed with one of many possible codes which are changed with each new encoding. The advantage of the encoding table is based on the fact that different numbers of bits can be used to represent the same ASCII symbol. By increasing the number of bits, the encryption system increases the number of combinations that can be used in place of a separate ASCII symbol applied to the same character in the encrypted message.

In the described method, the next step in protecting confidential information is to add the encrypted message to the carrier file. Multimedia files have been used for the carrier file. Because they are widely used and have enough unobtrusive bits to add information on these files.

Steganography is a dynamic tool with a long history and the capability to adapt to new levels of technology. As the steganographic tools become more advanced, the steganalyst and the tools they use must also advance. Like any tool, steganography (and steganalysis) is neither inherently good nor evil, it is the manner in which it is used which will determine whether it is a benefit or a detriment to our society.

REFERENCES

İ. Güler, R. Karakiş (2019). Medical Data Security in Cryptographic and Information Security, *Cryptographic and Information Security Approaches for Images and Videos*, S. Ramakrishnan, Editör, Taylor e Bookstore, New York, ss.629-662,

M. E. Saleh, A. A. Aly, F. A. Omara, (2016). Data Security Using Cryptography and Steganography Techniques, *International Journal of Advanced Computer Science and Applications*, Vol. 7, No. 6, pp. 390-397,

Mirko Köhler, Ivica Lukic, and Višnja Krizanovic Cik., (2017). Protecting Information with Subcodstanoigraphy, *Security and Communication Networks*, Volume 2017, Article ID 9130683, 13 pages, doi.org/10.1155/2017/9130683.

N. Hamid, A. Yahya, R. B. Ahmad, O. M. Al-Qershi (2012). Image Steganography Techniques: An Overview, *International Journal of Computer Science and Security (IJCSS)*, Vol. 6, No: 3, pp. 168-187.

R. Karakış, İ. Guler, İ. Çapraz, E. Bilir (2015). A novel fuzzy logic-based image steganography method to ensure medical data security, *Computers in Biology and Medicine*, Vol.67, ss.172-183,

S. Ansari, M. S. Mohammadi, M. T. Par (2019). A Comparative Study of Recent Steganography Techniques for Multiple Image Formats, *International Journal Computer Network and Information Security*, Vol 1, pp.11-25.

Y. A. Fadil (2017). Security Analysis of Steganalyzers, Ph.D. Dissertation, *Cryptography and Security [cs.CR]*. Université Bourgogne Franche-Comté,

STRUCTURAL PROPERTIES OF THE SUPER ALLOYS AND THEIR MACHINABILITY

*Abdullah ALTIN*¹

Abstract: The skeletal system is the most important component of our body that gives shape to our body, keeps it alive, and protects our internal organs against external impacts. When skeletal system is damaged, it can regenerate itself, but if the damage is big and severe, it cannot be regenerated by normal physiological processes. Therefore, bone damage requires scaffolds to improve healing process. The purpose of bone tissue engineering is to restore, regenerate, improve and maintain the function of damaged bone tissue through a combination of cells, biomolecules, and scaffolds. In order to repair and functionalize the bone tissue, scaffolds that mimic the structure of bone mineral and adapt to the cell are prepared. Metals, ceramics, polymers, and composite materials are used as biomaterials in the production of scaffolds. Among these, bioactive glasses, which are in the class of biologically used ceramics (bioceramics), draw attention. Various biomaterials and manufacturing techniques for scaffold provide achievable advances in bone tissue regeneration. Bioactive glass (BG) can form a strong bond with bone by forming a layer of apatite on its surface. They have important properties such as bone conduction, bone inducibility, biocompatibility, and bioactivity. BG can stimulate gene expression that regulates bone formation by releasing ions from its surface. They are mainly composed of silicon, sodium, calcium and phosphate components. When transplanted into the human body, it binds to bone through the hydroxyapatite layer formed on the surface and reacts with surrounding tissues to form a strong mechanical interface bond

¹ Prof. Doktor Abdullah ALTIN Yuzuncu Yıl University, Van Vocational of Higher School, 65100 Van, Turkey <https://orcid.org/0000-0003-4372-8272>. aaltin@yyu.edu.tr

between the host tissue and the implant. These properties make BG an important potential material in bone tissue regeneration.

Keywords: Super alloys, Structural properties, Machinability, Manufacturing techniques,

INTRODUCTION

Superalloys are iron-nickel, nickel or cobalt-based alloys with high thermal resistance to severe mechanical stresses and surface structure changes at high temperatures unlike other alloys (Chouldhury, I. A., El-Baradie, M. A, 1997). Nickel-based superalloys are the most difficult-to-process materials in obtaining a quality surface (Field, M., 1968). These alloys are used in aircraft engines, industrial gas turbines, space vehicles, rocket engines, nuclear reactors, submarines, steam generating plants, petrochemical devices and other heat resistant applications (Warbuton, P., 1967). Due to the ability to operate at high temperatures in the engine, the amount of super alloys used has reached 60% of the total aircraft engine weight in the 1990s and shows a steady increase. These alloys have excellent oxidation strengths at the temperatures exceeding 650 °C and their resistance to phase boundaries are excellent. 45% of the amount of superalloys produced is forged and 25% is cast nickel based super alloy (Bartlay, E., 1988). Nickel-based superalloys contain at least 50% nickel (Loria, E. A., 1992). Nickel is the main component. Super alloys are grouped into forging, casting and powder metallurgy alloys. The Inconel 718 is the most widely used superalloy in the aircraft and aerospace industries. In the processing of nickel based superalloys, the short life of the tool and the frequent deterioration of the surface quality of the workpiece are considered as a subject to be investigated. (Chouldhury, I. A at all, 1996). The residual stresses occurring on the part surface can adversely affect the mechanical stress and corrosion properties of the treated material during the chip removal process (Şahin, Y., 2000). Super alloys are used at temperatures of 650 °C and above, where surface stability is required and high stresses are present. The term usable super alloy can be used for iron, nickel, cobalt and chrome combinations or for alloys of iron, nickel and cobalt. These alloys contain lower amounts of tungsten, molybdenum, tantalum, niobium and aluminum, as well

as various iron, nickel, cobalt and chromium elements (Ezugwu, E. O., 2003). To increase the creep-rupture life, nickel-based superalloys, low amounts of boron, zirconium and hafnium can be added. Carbon is present in all nickel and iron based super alloys up to about 0.03%. However, higher amounts of cobalt-based alloys may be present to cause the carbide phase to be strengthened. Superalloys include iron-nickel-chrome-cobalt alloys, cobalt-based alloys, cobalt-based carbide-reinforced alloys, nickel-based precipitation-reinforced alloys, and nickel-based oxide-dispersion-reinforced alloys. Considering the difficulties in terms of cost, processing and processing of the Inconel 718 material in the literature, it has been observed that there are few studies evaluating the machinability parameters of the Inconel 718 (AMS 5663) super alloy.

Super Alloys

Superalloy is an alloy developed to serve at high temperatures based on Group VIII B elements, where severe mechanical stresses and surface stability are often required. Super alloy is developed for use in aircraft turbine engines and turbochargers requiring high performance at high temperatures. It was used shortly after the World War II. The basis of the super alloys used today is the 20% chromium alloy with 80% nickel and has been developed for 50 years as an electrical resistance wire. Super alloy was first used in the 1940s due to its remarkable oxidation resistance due to creep rupture strength (low titanium and aluminum). The first produced super alloy is Nimonic 80. Shortly after this alloy was developed and Nimonic 80 A was produced. Afterwards, this was also improved by the addition of 20% cobalt, which provided an advantage of 50 °C, and which had a higher demand than Nimonic 80 A, and which would be required by turbine engine designers, to serve at high temperatures. By increasing the demand, molybdenum was added to titanium and aluminum to form alloys with solid solution tension by the development of Nimonic 105 and 115. At the end of the 1940s, Pratt and Whitney Aircraft and General Electric Company developed two important forged superalloys, Waspalloy and M 252. Forged alloys have an important place in aircraft engines. Following these alloys, solid solution and carbide form were further strengthened with the addition of molybdenum.

The developed Rene 45 and 95 are reinforced with high sedimentation and are often used in welding applications. The Inconel 718 super alloy based on nickel and iron provides high thermal stress and shows good resistance to cracking in welding processes. The Incoloy 901 is another durable and popular super alloy. The most demanding applications of these alloys, such as Waspalloy and Astroloy, are turbine discs. Programmatic progression in nickel-based superalloys has been achieved not only as a function of the composition in the composition, but also as a result of the melting method, hot work situation and optimization of heat treatments. Super alloys; They usually contain iron, nickel, cobalt and tungsten, molybdenum, tantalum, niobium, titanium and aluminum alloys in lesser amounts (Ezugwu, E. O., at all., 1998). The most important properties of super alloys; They are resistant to temperatures above 650 °C for long periods of time and resistance to corrosion and erosion. Nickel and cobalt-based superalloys have high strengths at high temperatures (1500-1650 °C). Nickel-based superalloys Rene 95, 760 °C at 1100 Mpa and Udimet 700, 870 °C at 635 Mpa yield strength and also have an extension rate of 15% and 27% respectively. The cobalt-based S-816 super alloy has a yield strength of 240 Mpa and an extension ratio of 16% at 870 °C. Therefore, superalloys have replaced many types of alloys. These include iron-based alloys containing chromium and nickel, iron, nickel, chrome, cobalt compounds, carbide-supported cobalt-based alloys, some solid-state-reinforced alloys, nickel-based alloys with precipitation and dispersion (Ezugwu, E. O. and Tang, S. H., 1992). Super alloys can be used by machining or casting. Generally, the strength of iron-based alloys, iron, nickel, chromium, cobalt compounds and nickel-based solid solution reinforced alloys at temperatures above 650 °C is significantly lower than that of nickel-based second phase and significantly lower than cobalt based alloys. Iron, nickel, chrome, cobalt alloys (Fe - 20Ni - 20Cr - 20Co) containing solid molybdenum with small amounts of tungsten and first iron-based super alloys such as 16-25-6 alloy containing 16% Cr, 25% Ni and 6% Mo solution is supplements. Iron-based alloys containing low amounts (2% to 3%) of aluminum and titanium exhibit greater resistance to high temperatures by precipitation of an aluminum-titanium strengthening phase. Due to the melting point

superiority, cobalt alloys are generally more resistant than nickel-based alloys at temperatures above 1100 °C. Cast cobalt-based alloys containing carbide compounds and characterized by a surface-centered cubic (fcc) solid solution matrix are used as airfoils in gas turbine engines. Nickel-based alloys which are reinforced by dispersions have high resistance at high temperatures. However, they show medium strength at medium temperatures. The second stage is in the structure of these alloys in the form of a solid curing mechanism until melting occurs. In contrast, precipitated reinforced alloys lose strength as a solid solution at temperatures below the melting point. Distributed alloyed alloys have been used in combustion applications of some gas turbine engines. Nickel-based super alloys, fortified with the second precipitation stage, are the most complex and most attractive among all super alloys. The physical metallurgy of these alloys is well understood, although the solution is difficult and complicated. The structure consists of a precipitated nickel-aluminum-titanium compound and a surface-centered-cubic (fcc) austenitic matrix in the initial strengthening step. Depending on the alloy compound and the temperature process, various carbides are present in the second precipitation stage. These alloys are used in the areas of tension and temperature in gas turbine engines (Bartley, E., 1988).

The Development Process of Super Alloys

Nimonic 80 A, developed after the first super alloy Nimonic, was melted in the air using high frequency melting in the 1940s (Ezugwu, E. O., 2003). In those years, the alloy produced by the incorporation of the curing elements in the melting was provided with a strengthening. But this was not enough to dissolve in the air. In the 1950s, there was a significant progress in the development of nickel-based superalloys, and the method of melting and thinning under vacuum was introduced. This method prevented the oxidation of reactive hard elements, thus allowing more titanium and aluminum to be added. In the production process, the vacuum-thinning method for the precipitation process also allowed the other elements to be removed (such as bismuth, tellurium). One benefit of reducing the amount of additive elements present in the raw metals which adversely affects the creep stress and facilitates the

forging of nickel-based superalloys is the substantial progress in hot workability. In this way, the vacuum melting method was achieved and the materials such as strong superalloys, Nimonic 115 and Udimet 700 were developed (Bartlay, E., 1988).

Since the late 1950s, the turbine hot blades have been pounded from the forged alloys with great difficulty. These were back then.

Metallurgy of Super Alloys

Super alloys are used at temperatures of 650 °C and above, where surface stability is required and high stresses are present. The term of super alloy can be used for iron, nickel, cobalt and chrome combinations or for alloys of iron, nickel and cobalt. These alloys contain lower amounts of tungsten, molybdenum, tantalum, niobium and aluminum in various forms of iron, nickel, cobalt and chromium (Ezugwu, E. O., 2003). Nickel-based superalloys may contain small amounts of boron, zirconium and hafnium to increase creep-breaking life. Carbon is present in all alloys, usually up to about 0.03% in nickel and iron based superalloys. However, higher amounts of cobalt-based alloys may be present to cause the carbide phase to be strengthened. Various types of superalloys include iron-nickel-chromium-cobalt compounds containing iron-based chromium and nickel, cobalt-based alloys with solid solution, cobalt-based carbide-reinforced alloys, nickel-based precipitation-reinforced alloys, and nickel-based oxide dispersion-reinforced alloys (Ezugwu, E. O., at all., 1998). In some examples, iron-nickel ratios require the nickel-based name of the alloys. Examples of this are 16% Fe and 49% Ni solids reinforced Hastelloy X and 28% Fe and 52% Ni reinforced γ solution reinforced Inconel 718. In these two examples, the alloys are classified as nickel based superalloys containing iron as an alloy admixture. Other alloys of this type are not fully defined. For example, the ir-reinforced INCOLOY 901 super alloy contains 42% Ni and 36% Fe. This alloy can be evaluated on a nickel basis or put into the iron-nickel-chromium category. As an example of a mixed compound solid solution reinforced alloy, Multimet can be given containing 21% Cr, 20% Ni, 20% Co, 32.5% Fe, 3% Mo, 2.5% W and 1% Nb. Another complex alloy of this class is Incoloy

903. In addition to high strength, this alloy is used in desired places with low constant thermal expansion coefficient (Bartlay, E., 1988).

Classification of Superalloys

Nickel-based precipitation-reinforced superalloys are used more and more in terms of their strength at high temperatures. It is a fact that at very high temperatures, oxide dispersion reinforced alloys and even some cobalt alloys show extreme resistance to precipitation reinforced nickel based superalloys. However, both of these alloy types are much weaker at lower temperatures than nickel based superalloys. Iron-based superalloys and solid solution-reinforced alloys are the weakest of the superalloys due to their low strength in high temperatures. Iron-based superalloys are less used in high temperature applications. This does not apply to the Inconel 718 alloy, which is a commonly used iron-containing nickel-based alloy. The primary advantage of iron-based superalloys has been lost. However, solid solution alloys have continued to be used where strength is not important. However, oxidation and hot corrosion resistance are required. Cobalt alloys such as MAR-M 509 have been widely used for aircraft engine turbine propeller castings, and cobalt-based Haynes 188 is a popular combustion material. Super alloys take different names according to their formation elements. The general classification of these alloys is shown in Table 2.1.

Table 1. Classification of Superalloys Super Alloys

Nickel based	Iron based	Cobalt based
Inconel (578, 597, 600, 601, 617, 625, 706, 718, x750)	Incoloy (800, 801, 802, 807, 825, 903, 907, 909)	Haynes188
		L-605
Nimonic (75, 80A, 90, 105, 115, 263, 942, PE.11, PE.16, PK.33)	A-286	MAR-M918
	Alloy 901	MP35N
Rene (45, 95)	Discaloy	MP159
Udimet (400, 500, 520, 630, 700, 710, 720)	Haynes 556	Stellite 6B
	H-155	Elligo
Pyromet 860		
Astroloy		
M-252		
Hastelloy (C-22, G-30, S, X)		
Waspaloy		
Unitemp AF2-IDA6		
Cabot 214		
V-57		

Nickel Based Super Alloys

Nickel-based superalloys have been identified as nickel-containing alloys with significant amounts of chromium. They may contain cobalt, iron, molybdenum, tungsten and tantalum as the basic alloying.

Table 2. Chemical Compositions of Nickel Based Superalloys

Alaşım adı	Ni	Cr	Co	Mo	W	Ta	Cb	Al	Ti	Mn	Si	C	B	Zr
Inconel 718	53	18.3	0.23	3.04		0.005	0.23	0.50	09	0.08	.08	0.04	0.004	
Alloy 713C	74	12.5	-	4.2	-	-	2.0	0.8	-	-	-	0.12	0.012	0.10
Alloy713LC	75	12.0	-	4.5	-	-	2.0	0.6	-	-	-	.05	0.010	0.10
B-1900	64	8.0	10.0	6.0	-	4.0	-	1.0	-	-	-	.10	0.015	0.10
FORT 406	60	6.0	10.0	1.0	8.5	6.0	2.0	2.0	-	-	-	.13	0.018	0.06
IN-100	60	10.0	15.0	3.0	-	-	-	4.7	-	-	-	.18	0.014	0.06
IN-162	73	10.0	-	4.0	2.0	2.0	1.0	1.0	-	-	-	.12	0.020	0.10
IN-731	67	9.5	10.0	2.5	-	-	-	4.6	-	-	-	.18	0.015	0.06
IN-738	61	16.0	8.5	1.7	2.6	1.7	0.9	3.4	-	-	-	0.17	0.010	0.10
IN-792	61	12.4	9.0	1.9	3.8	3.9	-	4.5	-	-	-	.12	0.020	0.10
M22	71	5.7	-	2.0	11.	3.0	-	-	-	-	-	.13	-	0.60
MAR-M200	60	9.0	10.0	-	12.	-	1.0	2.0	-	-	-	.15	0.15	0.05
MAR-M200(Ds)	60	9.0	10.0	-	12.	-	1.0	2.0	-	-	-	.13	0.15	0.05
MAR-M246	60	9.0	10.0	2.5	10.	1.5	-	1.5	-	-	-	.15	0.15	0.05
MAR-M421	61	15.8	9.5	2.0	3.8	-	2.0	1.8	-	-	-	.15	0.15	0.05
MAR-M432	50	15.5	20.0	-	3.0	2.0	2.0	4.3	-	-	-	.15	0.15	0.05
NX188(DS)	74	-	-	18.0	-	-	-	-	-	-	-	.04	-	-
Rene'77	58	14.6	15.0	4.2	-	-	-	3.3	-	-	-	.07	0.016	0.04
Rene'80	60	14.0	9.5	4.0	4.0	-	-	5.0	-	-	-	.17	0.015	0.03
Rene'100	60	9.5	15.0	3.0	-	-	-	4.2	-	-	-	.18	0.014	0.06
SEL	51	15.0	22.0	4.5	-	-	-	2.4	-	-	-	.08	0.015	-
SEL-15	58	11.0	14.5	6.5	1.5	-	0.5	2.5	-	-	-	.07	0.015	-
TAZ-8A	68	6.0	-	4.0	4.0	8.0	2.5	-	-	-	-	.12	0.004	1.00
TRW-NAZAVA	61	6.1	7.5	2.0	5.8	9.0	0.5	1.0	-	-	-	.13	0.020	0.13
UDIMET 500	52	18.0	19.0	4.2	-	-	-	3.0	-	-	-	.07	0.007	0.05
WAZ-20(DS)	72	-	-	-	20.	-	-	-	-	-	-	.20	-	1.50

element. They were fortified with solid solution and second stage intermetallic precipitation. Aluminum, titanium and niobium are the elements of intermetallic formation. Nickel-based superalloys contain 30% to 75% Ni and 30% Cr. In many Inconel, Nimonics and Hastelloy alloys, iron content is found in small amounts to vary by up to 35%. Many nickel-based alloys contain small amounts of aluminum, titanium, niobium, molybdenum and tungsten to increase strength or corrosion resistance.

The combination of nickel and chromium gives these alloys a significant degree of oxidation resistance. Nickel-based superalloys pass stainless steel as mechanical strength at temperatures exceeding 650 °C. Nickel-based superalloys; They are widely used in applications requiring oxidation and corrosion, high strength and resistance. Solid solution alloys such as Inconel 600, Inconel 601, and RA 333 are used in furnace parts and other temperature-related applications. These alloys are also used in high-temperature chemical processing equipment, such as hydrocarbon modifiers. Energy production is another area where nickel-based superalloys are widely used. In addition, they are used in nuclear power plants, steam generator installation and reactor structural parts. These alloys are used in fossil fuel plants, super heater installation, waste systems, gas storage units, parts requiring temperature or corrosion resistance (Bartley, E., 1988). Chemical compositions of nickel based superalloys are shown in Table 2.2.

Nickel Based Super Alloys and Their Properties

These alloys have a wide range of uses in the industry (Chouldhury, I. A., 1995);

- a) High thermal voltage
- b) High hardness
- c) High working strength and high working hardness.
- d) Low thermal conductivity causing high temperatures
- e) Existence of highly abrasive carbide particles
- f) Strong boiling tendency and pile sawdust (BUE) formation on the team

All of the above-mentioned properties make it extremely difficult to process the superalloys by causing high wear rate and high shear temperature on the cutting tools during machining. Nickel-based superalloys can be machined with tungsten-carbide-cobalt grades at a speed above 50 m / min. Chip control at this speed is weak. The chip type is continuous and has abrasive saw teeth. The combination of high temperatures is the main problem that causes high workpiece tension and

abrasive chips to be notched at the depth of cut. (Brandt, G. at all, 1990). Nickel based alloys; They are poorly processable materials in obtaining a satisfactory and quality surface and there are a number of reasons that undermine their workability. These;

- 1- It is difficult to process due to its high temperature resistance.
- 2- Work hardness during machining causes notch in depth and causes tool wear.
- 3- Hard abrasive carbides in super alloys significantly affect the cutting tool during cutting and accelerate wear.
- 4- Chemical reactions at high temperatures cause diffusion wear between the chips.
- 5- During adhesion, adhesion or welding occurs between sawdust and cutting tool.
- 6 - The presence of continuous and hard chips during the processing makes the control difficult to control, causing the chips to form a crater on the tool surface.
- 7- Due to its poor thermal conductivity, nickel-based superalloys often form high temperatures on the surface of the tool, resulting in high radial gradients in the cutting tool.

It is noteworthy that on the nickel-based superalloys, the tool life is short and the surface quality of the workpiece is very sensitive to processing. Residual voltage on the part surface, mechanical stress and corrosion of the workpiece during machining may adversely affect the characteristics. It requires extreme attention to ensure the surface balance and quality during processing. The tool gives a long service life with low cutting parameters (Ezugwu, E. O. at all, 1998). Parameters such as tool selection, tool geometry, machining method, cutting speed, feed, depth of cut need to be checked frequently during machining to achieve long tool life. With the operation of modern aircraft engines at high temperatures and the emergence of complex conditions, the superalloys were freed from the simple nickel chromium matrix and switched to the multi-element phase system (Goessler, F.W., 1985). Nickel-based super alloys, in addition to chromium, aluminum, titanium, cobalt, molybdenum and other elements, are added in different amounts to pro-

duce higher performance alloys (Groover, M. P., 1996). The shorter tool life and metallurgical damages with this shape composition of the material are the more common problems during the machining of the workpiece. Nickel-based superalloys, although not extremely high hardness (250-350 H. V.) is difficult to process due to high thermal stresses and thermal hardness. Work hardness trends cause high cutting forces and surface changes considerably.

Strengthening of Nickel-Based Superalloys

Strengthening mechanisms of nickel-based superalloys, strengthening with solid melt, strengthening with precipitation and strengthening with dispersion. The properties of the grain boundaries are largely controlled by these processes. Carbide shape, quantity and phase structures play an important role in gaining strength.

Strengthening With Solid Solution

Commercial austenitic superalloys always contain substantial alloy additions. In addition, they provide stronger alloy and elements to provide strength gain in the solid melt and to provide resistance to creep and surface defects. As a result of suitable heat treatment or thermo-mechanical processes, these elements are distributed in an intermetallic composition in the form of small harmonious particles. In addition, typical nickel-based alloys are converted into an austenitic nickel-chromium-tungsten (or molybdenum) matrix. In order to obtain a considerable solid melt strength gain, an alloying element must satisfy the following requirements.

- 1) Having a wide range of solid solubility in the matrix,
- 2) A large difference in atomic size with matrix,
- 3) Must have high melting point.

The solid melt elements are probably aluminum, chrome, iron, titanium, tungsten, vanadium, cobalt and molybdenum. The atomic diameter of the cobalt in the solution differs from the atomic diameter of nickel by + 1%, and the atomic diameter of the tungsten differs from the atomic diameter of nickel by + 13%.

Strengthening With Precipitation

The consolidation of nickel-based superalloys by precipitation is actually caused by precipitation. Small amounts of borides and carbides in the phase at low temperatures help to impart strength, because borides and carbides have low partial volumes, low creep rates and breakage lives. In strengthening nickel-based superalloys, the precipitation phase (') ada has a relationship with several factors. These factors

(1) Part volume of the existing (faz) phase,

(2) The size of (in) phase

(3) The phase boundary energy of the phase (d1r) (anti phase boundary (APB) energy), the volume of the phase (,) present at a given temperature is proportional to the amount of total strengthening elements present. Like aluminum, titanium and niobium. The volume of phase (er) directly affects the strengthening of nickel alloys at high temperatures. This effect is perhaps an important basis for alloy designers. The increase in the alloy strength gain is also related to the particle size of the phase (()). The purpose of heat treatment for commercial forged nickel-based superalloys is to obtain similar properties in the particle size and peak hardness of a (ve) phase (Ezugwu, E. O., at all. 1998)

Strengthening With Distribution

At high temperatures, the (different) phase enters the melt and exhibits a substantially stable dispersion which is essentially non-metallic and insoluble in the matrix. This is the most effective way to maintain strength. The best dispersion materials used to serve at high temperatures are oxides. Elements such as thorium, yttrium and lanthanum have high free energy. The distribution of the dispersion phase is characterized by its distribution as the effect of strengthening. The particles must be small and tidy. The level of achievable strength gain is limited by the low partial volume of the oxides (White, C. H., 1986). Developments in strengthening processes in nickel based alloys are as follows (Ezugwu, E. O., at all 1998)

1) Solid melt strength gain

- 2) (m) phase volume increase
- 3) (erj) increase of phase defect energy
- 4) Reduction of formation in the Ni₃Nb phase in strengthening with solid solution
- 5) M₂₃C₆ grain boundaries and control of carbide shape to prevent cellular structures
- 6) Increase of control carbides and fracture stress.

Alloying Elements in Nickel Based Super Alloys

Nickel alloys are inherently resistant to high thermal oxidation due to chromium in their structure. When heated in oxygen, Cr₂O₃ adheres as a protective layer on the material surface. The optimum oxidation resistance in the nickel chromium alloy is the time when the amount of chromium is kept at 15-30%. Chromium also forms chromium carbide form. This plays an important role in increasing the stress of the material at high temperatures. Aluminum, titanium and niobium are added to the material and Ni₃(Al, Ti) is formed in order to form the gamma phase and increase its tension. Niobium can replace some of titanium and aluminum. Or, if the amount of niobium is more than 4%, it forms a hard phase, Ni₃Nb. Titanium and niobium also form carbide. Aluminum has an important contribution to oxidation resistance. Al₂O₃ form occurs at high temperatures. The Al₂O₃ or Cr₂O₃ form depends on the amount of the two elements in the alloy. When developing high-temperature alloys, a lower amount of chromium is required in order to maintain stability in the microstructure. Elements such as aluminum, titanium and niobium are added to enhance creep properties. This can be compensated by increasing the amount of lower amounts of chromium and aluminum to reduce the oxidation resistance. Alloys such as Inconel 718 and Nimonic 901 contain 18-36% iron. Increased iron content causes a decrease in oxidation resistance of nickel-based alloys. The addition of a small amount of cobalt decreases the solubility in nickel-chromium austenitic surface centered cubic structure, whereas aluminum and titanium are in the positive direction. This increases the dissolution temperature. It also helps to maintain the voltage at high temperatures. The solubility of

cobalt in carbon is better than nickel. In this case, more carbon can be tolerated. Molybdenum, tungsten and tantalum increase the solid solution tension at high temperatures. The complex carbide form and tantalum are present in particular in solution.

Boron and zirconium are added elements to increase creep tension and flow. These elements serve well in separating the grain boundaries. However, the presence of boron and zirconium in the nickel alloy is not entirely useful. Because they reduce the ability to weld. Carbon can be added in a limited amount to increase the creep tension due to the carbide form. The other additive elements are to increase the workability and oxidation resistance. Calcium, magnesium and yttrium are added in small amounts in recent years. Hafnium is the major additive in cast alloys and is useful in both fluency and stress reduction. Hafnium helps to guide hot cropping resistance and solidification at medium temperatures. The effects of some elements in super alloys are shown in Table 2.3.

Table 3. Effects of Some Elements in Superalloys

Fe based	Ni based	Co based	Effect
Cr,Mo	Nb,Cr,Mo	Co,Cr,Fe,Mo	Solid solution boosters
	Ni,W,Ta	W,Ta	
C,Ni,Co	Ni	Co	Surface centered cubic matrix stabs
			Carbide form
Ti	Ti	W,Ta,Ti,- Mo,Nb	MC type
...	Cr	Cr	$M_7 C_3$ type
Cr	Mo,W	Cr,Mo,W	$M_{23} C_6$ type
Mo		Mo,W	$M_6 C$ type
			Nitrogenous carbon
C,N	C,N	C,N	M (CN) type
P	The progress of the general content of carbides

Al,Ti,Ni	...	Al,Ti	Forms γ^1 Ni ₃ (AL,Ti),
Al,Zr	Hexagonal μ (Ni ₃ Ti) de- celeration formation
...	...	Co	Rising solvus temperatu- re of γ^1
...	...	Cr	Decreasing solvus tem- perature of γ^1
Al,Ti,Nb	Al,Mo,Ti,W,- Ta	Al,Ti,Nb	The content of forced and / or intermetallics
Cr	Al,Cr,Ta	Al,Cr,Ta	Corrosion resistance
La,Y	La, Y,Th	La,Th	Increased corrosion resistance
Cr	Cr	Cr	Sulfide strength
B	B,Zr	B,Zr	Increasing the channel boundary properties with changes in cre- ep-break morphology
...	...	Hf	Increased moderate tem- perature softness
...	...	B,C,Zr	Boundary adjustment

Micro Structures of Nickel Based Super Alloys

Recognizing the microstructure of nickel-based super alloys has helped to develop these alloys. Nickel-based super alloys have been characterized and developed by some alloying elements. Microstructures and phase descriptions are shown below.

1-Alloy matrix: Continuous matrix, which is the surface centered cubic nickel based austenitic phase, contains a high proportion of cobalt-chromium-molybdenum and tungsten which are generally solid melt elements.

2-Gamma Phase 1: In the fraction of the high volume surface centered cubic structure, aluminum and titanium are added in the fractional

ratio to be a suitable precipitation process that does not change with Austenite.

3-Carbide form: 2% to 5% of the carbon formed by joining in this form, carbon is often in contact with the reactive and refractory elements and the first MC carbides are formed. During heat treatment, this is disturbed and the lower carbide M₂₃ changes to the grain boundaries, turning into the C₆ and M₆C form.

4-Grain boundaries phase (ane). Heat treatment techniques have been developed to form a film of phase (in) along grain boundaries to optimize creep properties for a number of alloys.

5-Indoor package topological phase: This phase, which is a flat circular type under certain conditions, offers low creep voltage and yield property.

Gamma 1st phase; A nickel-based super alloy requires a fcc crystal. To create the precipitation must be the 1st phase. Ni₃Al is the normal composition but is usually introduced as Ni₃(Al, Ti). Up to 65% of aluminum is replaced by titanium. Nickel can be replaced by a limited amount of chromium, cobalt, molybdenum and iron (White, C. H., 1986). During the partial melting operations applied to some alloys, or during aging processes applied at relatively high temperatures, second phase particles are formed between the surfaces. (Enebilir) phase can be formed at the boundaries. After the melting process, during the aging process, the nuclei initially collapse in a harmony. It grows in the form of crystal-line centered similar matrices and spherically, loses its cubic structure and develops in a way as fine and homogenous particles. (Ni₃Al) is an intermetallic phase. By influencing each other, it affects the antiphase limit and strengthens the phase (az) of the alloy. As the temperature increases, the phase force increases. It also helps to prevent the fluency and severe confusion inherent in the (help) phase. As with the carbides, the phase improves with a higher hardness and a different strength. In Ni (Al), most aluminum can be replaced by titanium, niobium or tantalum. By leaving the phase forming capability, titanium (is) phase can be transformed into a hexagonal closed package structure (Ni₃Ti) at 700 - 900 °C. Transformation produces an irregular precipitation from a reg-

ular shape and the ratio of titanium to aluminum increases. In addition, the stability of the alloy is reduced. With the transformation of (.) Phase, an undesirable drop in alloy strength occurs. In Inconel 718, when a niobium ratio is more than 4%, a similar transformation occurs in Ni_3Nb . Transformations are b Ni_3Nb return. It consists of a tetragonal centered structure. A circular and planar structure of small size is formed which is in conformity with this phase deposition matrix. The Ni_3Nb structure is an upright rhombic structure. When the structure becomes a large circular and planar structure, Ni_3Nb particles contribute positively to the creeping and breaking properties (Ezugwu, E. O., at all 1998)

Topological Closed Package Phase (TCP)

This phase is the result of stresses that occur at high temperatures in certain alloys. This phase can be precipitated at 650-925°C in chromium-nickel-based alloys. This phase is an intermetallic compound and exhibits a tetragonal structure between metal transition elements. It forms and grows as a result of nucleation. It can be seen in the form of needles or flat circular particles between the surfaces of borides and carbides in the grain boundaries. Mechanical formation and the TCP phase have an important effect on alloy properties. The compounds themselves are brittle and hard. The phase has more influence on the creep voltage, sometimes at high temperatures. The TCP phase contains elements that are difficult to process and can also open the matrix of the alloys and cause weakness in strength.

Carbides and Their Effects in Alloys

The role of carbides in superalloys is dynamic and complex. Many researchers believe that they have significant and beneficial effects on creep stress at high temperatures. In addition, the carbide morphology can affect fluidity and can also affect chemical stability by removing reagent elements from the matrix. Nickel-based superalloys contain three types of carbide. MC, M₂₃C₆, M₆C and rarely Cr₇C₃. MC carbides are the main source of carbon for alloys for later use in the case of chemical interaction. They have a fcc structure that should be considered as

the most stable elements in nature. The carbides are formed after the solidification process either at high temperatures or in the liquid state. Carbides appear along grain boundaries or within a block of grain. Titanium, tantalum, niobium and hafnium are the main components of MC form. Like the less reactive molybdenum and tungsten containing alloys, the $M_{23}C_6$ carbides generally dominate the alloy by forming at high temperatures (760-900°C) with high chromium content in the alloy. $M_{23}C_6$ carbides are shaped by the deterioration of MC carbides and the soluble carbon remaining in the alloy matrix, and have significant effects on the properties of nickel-based superalloys and have significant impacts on creep stresses such as carbides that are visible at grain boundaries. Due to the situation that does not leave grain boundaries, the properties are adversely affected. M_6C carbides are shaped as a result of high temperature heat treatment in alloys with high molybdenum content. They also occur as a result of the deterioration of MC. It can replace chromium, nickel and cobalt M in MC form. Molybdenum and tungsten are different and they are suitable for $M_{23}C_6$ and their composition is very wide. At high temperatures, M_6C carbides are more stable than $M_{23}C_6$ and are more useful in controlling grain size in forged alloys and in precipitation at grain boundaries (Ezugwu, E. O., at all 1998)

Boron Compounds and Their Effects on Alloys

Many nickel-based super alloys contain low amounts of boron. Normally boron is associated with type $M_{23}C_6$ carbides. However, if the boron amount is greater than 0.01%, M_3B_2 form is formed. M is usually molybdenum. But chromium, titanium and nickel may also replace M. The M_3B_2 form has a tetragonal lattice system and has a tendency to precipitate at grain boundaries.

Heat Treatments Applied to Nickel Based Super Alloys

The heat treatments applied to gain the required properties are evaluated in three stages.

Annealing/ Softening Processes

This type of process is only applicable for alloys subject to work hardness. In this case, a soft fluency is given at the end of production with both middle and final processes. Softening is often associated with recrystallization. However, it may cause some chromium carbides to dissolve. Annealing is usually required for solid-alloy reinforced alloys. Smoothing operations are also applied during the production of alloys which can be strengthened by precipitation. It is very important to know the time and temperature used in these processes in order to completely dissolve the collapsible reinforced phases.

Melting Operations

The main purpose of the melting process is to melt the precipitable phase. In general (tir) phase and some carbide formations, it is primarily to control precipitation during aging or cooling. The selection of the temperature of the melting processes depends on the melting temperatures of the various phases. It should be preferred to choose the temperature that will give the best roughness, best grain size, best grain size, best flow rate and fatigue properties. Creep breakage properties and roughened grains at high temperatures can be corrected by high solid melt processes.

Precipitation Operations

The main purpose of this process is to precipitate the strengthening phase to develop mechanical properties. For optimum strengthening, the strengthening event should be carried out at about 700 ° C for 128 hours or 650 hours at 500 hours. However, these periods are not considered commercially viable, and may not be considered the maximum strength. For this reason, more strengthening procedures are preferred in a more practical environment.

Nickel Alloys With Solid Solution

These alloys are generally used at temperatures between 870 and 980 °C to achieve high expansion and fatigue strength. At higher tempera-

tures between 1120 and 1200 °C, they exhibit higher expansion strength and creep-breaking properties at 600 °C. Some solid solution nickel alloys, especially Hastelloy X, Inconel 601, Inconel 617 and Inconel 626, are used in space studies. Hastelloy X, Inconel 601 are also used in jet engines, gas turbine parts and widely in turbine engines. Above 980 °C, the Inconel 617 is suitable for various parts of aircraft gas turbines that require high tensile and tensile strength. Inconel 625 is used in heat shields, aircraft systems, exhaust systems, thrusters, turbine coatings in fuel and hydraulic installations.

Nickel Alloys With Precipitation Reinforcement

These alloys contain aluminum, niobium or titanium to aid in the precipitation of the second phase during the appropriate hot-processing process. The precipitated phase Y1 or Yll increases the strength and hardness of the alloy. (Li, R. B., 2002). For example, the Inconel X-750 alloy, the precipitated version of Inconel 600, has three times the strength of the Inconel 600 at 540 °C. Nimonic 80 A, a precipitated reinforced alloy, has 3 times more strength than Nimonic 75, which is similar to its solid solution. If the temperature processes for precipitated reinforced alloys are generally more than 600 - 815 °C, then a solution treatment is required at 970 - 1175 °C. Aluminum and titanium are added to most of these alloys in order to increase the sedimentation strength by forming the Y Intermetallic Ni₃ (Al, Ti) phase. In niobium reinforced alloys such as Inconel 718, precipitation reacts to hardening temperatures. Such alloys are capable of welding significantly. Because the welding temperature does not reduce hardening and does not cause breakage after welding. Space work is one of the most common applications for precipitated reinforced superalloys (Hunn, J. D., 2001). These alloys are used in rocket engines and aircraft gas turbine parts. Other applications include bolts and springs in nuclear reactors. Applications of precipitated reinforced alloys include forgotten components. As a result, the mechanical properties of these alloys in forged and hot treatment situations are important. Due to the fact that castings are stronger than forging at high temperatures, cast superalloys are used for applications requiring high temperatures. For this reason, cast nickel alloys such as INCO

713, INCO 100, B-1900, MAR-M 147 and MAR-M 200 are used in the turbine nozzles. High-strength as B-1900, MAR-M 247 and MAR-M 200 A small amount of hafnium was added to improve the average working temperature of cast alloys (Ezugwu, E. O., 2003). Nickel-based superalloys are reinforced by both solid solution and precipitation. Hastelloy X, an example of a lower strength nickel based solid solution super alloy with 18.5% Fe, 22% Cr, 9% Mo, 1.5% Co and 0.6% W, is widely used in combustion and consumption applications in gas turbine engines. (2nd). These alloys combine with excellent processability and weldability to provide resistance to high temperature corrosion erosion. In applications requiring high temperature resistance, nickel-based alloys with precipitation reinforcement are generally selected. Reinforced by a second stage of precipitation, these alloys are the most complex and indeed the most popular among all superalloys. Although the physical metallurgy of these alloys is well known, sometimes it is difficult and complex to solve, depending on the properties of the microstructure. These alloys appear as metal with a surface-centered cubic (fcc) austenitic solid solution matrix or nickel-aluminum-titanium compound precipitated as the initial strengthening step. Ir Austenitic verilen is an expression given to the solid metal of a fcc crystalline structure, intermediate metals or metal. For example, each metal crystal is in the form of a cube with an atom at each corner, next to the center of each of the six cubic surfaces. Various carbides, depending on a particular alloy compound and heat treatment, are included in the second precipitation phases. Undoubtedly, Y1 reinforced superalloys are used in gas turbine engines, in many applications of stress and temperature. This developed alloy system has proven to have a considerable resistance even at the boundaries close to the melting point of the base metal. Another strengthening mechanism in nickel alloys is the presence of dispersed oxide particles in the structure. The alloys reinforced with this type of distribution show high strength at high temperatures. Cobalt alloys are more resistant than nickel-based alloys at very high temperatures (above 1905 ° C). They are characterized by a fcc austenitic solid solution matrix in cobalt based superalloys such as nickel based alloys. Cobalt-based superalloys contain significant

amounts of carbon to obtain complex carbides as second stage builders (Bartlay, E., 1988).

Iron-Based Superalloys

Generally, iron-based, iron-nickel-chromium-cobalt compounds and nickel-based solid solution-reinforced alloys have a higher temperature resistance than nickel-based precipitation above 650 °C and lower than that of cobalt-based carbide-reinforced alloys. The first iron-based superalloys are 16-25-6 alloys containing 16% Cr, 25% Ni, 6% Mo and equilibrium, and Multimeters containing 40% Fe, 20% Ni, 20% Cr, 20% Co, and small amounts of tungsten and molybdenum. Such as iron-nickel-chromium-cobalt alloys are essentially reinforced with solid solution. A solid solution occurs when two or more metals or intermediates are joined together as completely and homogeneous solids. A solid solution is the same homogeneous combination as a liquid solution, such as sugar in the coffee. The solutions differ from the mechanical mixtures, such as a mixture of dry flour and sugar, in which each part carries its properties. Strengthening occurs when a metal dissolves in another metal to form a new metal. Nickel, chromium, and iron-based alloys containing small amounts of aluminum and titanium have increased their resistance to high temperatures by precipitating a nickel-aluminum-titanium strengthening step. The presence of a second stage in the structure is more effective than strengthening the solid solution. The formation of the second phase is important, thin and more widespread, has more effective strength. In fact, high temperature exposure results in reduced strength. Iron-based alloys, the most important for application temperatures above 540 °C, have fcc (surface-centered cubic lattice) matrix. Because a closed cage is more resistant to time-dependent deformation processes. The iron-based superalloys reinforced by intermetallic compound precipitation have found use in gas turbine engines. For example, some gas turbine engines, turbine disks and joints and turbine housings A-286 are used. Many superalloys which do not fall into the iron-based superalloy category contain significant amounts of iron. Because, the compounds are complex combinations of molybdenum, tungsten or niobium compounds with lower amounts of iron, nickel, chromium and

possibly cobalt. These alloys are fortified with solid solution or intermetallic precipitation.

Cobalt Based Super Alloys

Cobalt-based superalloys are cobalt and basic amounts of chromium tungsten and lesser amounts of molybdenum, niobium, tantalum, titanium and iron. They were fortified with solid solution and carbide phases. They contain 0.4% to 0.85% carbon, depending on the strength of the carbide phase. Cobalt solid solution alloys are divided into three subgroups according to their application. (a) Alloys used from 650 to 1150 °C, including Haynes 25, Haynes 188, UMCo-50 and S-816; (b) Used in the vicinity of 650 °C and MP-35N and MP-259 binders, c) Abrasion resistant Stellite 6B alloys. All hot-processed alloys have fcc crystal structure. But; The MP-35N and MP-159 alloys develop closed hexagonal structures during the thermo-mechanical processing recommended before service applications. None of the cobalt-based superalloys is a complete solid solution alloy. Because they all contain a second carbide phase or intermetallic compounds. Aging causes an additional second phase precipitation, which usually leads to room temperature loss (Bartlay, E., 1988). Haynes 25 is a cobalt-based alloy that can be widely used in heat-exposed parts of gas turbine engines, nuclear reactor components and cold working conditions. Haynes 188 offers excellent quality as oxidation resistance at temperatures up to 110 ° C with its simple formation which can control the contents of lanthanum, silicon, aluminum and manganese, especially designed for sheet metal parts in gas turbines. The MP-35N and MP-159 are specifically designed for use as hardened, and both alloys have high resistance in difficult operating conditions. MP-35N and MP-159 were used for more bonds; The MP-159 has an upper working limit of 650 ° C. The final group of high temperature cobalt alloys, solid solution reinforced, contains a single alloy called Stellite 6B. This alloy exhibits high temperature hardness and relatively good resistance to oxidation. This property is derived from the high chromium content in which the temperature hardness is achieved by the complex carbide formations. Stellite 6B is widely used as a connection part in erosion shield in steam turbines, wear pads in gas turbines, particle systems

in particle carrying tube systems at high temperatures and high speeds. Superalloys reinforced with carbide phase, such as X-40, WI-52, MAR-M 302 and MAR-N509, are primarily used in turbine engine airfoils, mainly for static propeller applications. These alloys have high temperature resistance, oxidation and welding ability.

Castings and Forgeds

Castings are substantially more resistant to high temperatures than forgeds. Coarse particles of castings are more resistant at high temperatures than fine forging particles. Casting contents are very effective for high temperatures. For example, high strength at high temperatures, aluminum and titanium can be increased, and nickel based Y1 reinforced superalloys. Thus, Y1 volume percentage increases and chrome content decreases (Ezugwu, E. O., at all 1998). The reduction in the amount of chromium causes a reduction in hot corrosion and strength, so this grade of superalloys containing 8-12% Cr may require the use of coatings such as dissolved aluminum to meet the loss of hot corrosion resistance. The addition of small amounts of hafnium led to a significant improvement in nickel superalloy castings at average temperatures. Due to the superiority of high temperature resistance, many aircraft gas turbine engines use Y1 reinforced nickel based superalloy castings for high temperature applications. It is clear that superalloys are complex compound combinations and that various elements have significant effects (6). Alloying elements in superalloys (a) solid-solution builders affecting only the matrix; (b) elements that form carbides or intermediate metallic compounds within the particles or within the particle boundaries; (c) elements constituting a Y1 phase in nickel-based alloys; and (d) elements having various effects, such as improving the ambient temperature or reducing or raising the Y1 solid solubility temperature, improving the oxidation resistance. The largest structural difference between a cast product and a workable product is that the processed products have finer particles due to hot processing. Processed products have a better resistance than castings, from room temperature to 540 °C. Processed products generally have better breakage and fatigue properties than castings. Because

defects and large particles are broken and porosity has been improved during the hot processing processes (Bartlay, E., 1988).

Behavior of Super Alloys at High Temperatures

High temperature resistance behavior of metallic elements follows melting characteristics. For example, the higher the melting point, the higher the temperature resistance of the metal. Therefore, the melting points of the elements play an important role. Some elements, especially titanium, draw a different curve. However, this relationship should be closely examined. Creep / stress-breaking and metallurgical instability in the material determine the behavior of superalloys at high temperatures.

Creep / Strain-Stress

The life of a metal compound subjected to static or dynamic loading at high temperatures is limited. In contrast, in the case of low temperatures and no corrosive environment, the life of a part is unlimited under the static conditions if the working loads do not exceed the strength of the metal. To be defined, creep is time-dependent stress or deformation under high temperature. After a while, it disappears by a so-called "strain-break". As a result, errors due to high temperature occur in a wide temperature range. Creep usually allows the atomic structure to recover again depending on time (Bartlay, E., 1988).

Metallurgical Instability

Another feature of high temperature operation is that it contains metallurgical instability. Tension, duration, temperature and environment; changes the metallurgical structure during use. It should be noted that in some cases strength can be increased. These structural changes or metallurgical instabilities are best explained by their effects on tensile and tensile properties. A type of carbide was found in the superalloys. Temperature and stress affect both the carbides in the particles and the carbides in the grain boundaries, the effects on the carbides in the grain boundaries are often a more important factor in the change of creep and

break behavior. The particle boundary morphology is actually very important due to its high temperature properties. The presence of carbide solids at the grain boundary is necessary for optimum creep and shear life. However, changes in form and fracture to other carbide forms may cause grading. The best type of carbide formation in the grain boundaries for optimum strength are the individual block particles. Continuous carbide layers in the grain boundaries reduce the tensile-breaking life. Carbide formations in superalloys can be classified as MC, M₂₃C₆, M₆C and Cr₇C₃. The content of M in these carbides is generally titanium. However, elements such as molybdenum, niobium, vanadium, zirconium and tantalum may be included. Cr in Cr₇C₃ is chromium. In order to obtain the alloy at the appropriate tensile-breaking properties, the carbides must be obtained at the appropriate processing, temperature and particle boundaries. For optimum properties, continuous layer and fine cellular carbides should be avoided. In order to increase the creep rupture properties of nickel-based super alloys by strengthening the particle boundaries, small amounts of boron and zirconium must be added. The understanding of the presence of free elements in the nickel-based superalloys is necessary in order to fully reflect the nature of the compound in the properties of the superalloys. In the case of an instability, the presence of some elements can cause significant reductions in properties (Bartley, E., 1988).

Use of Superalloys in Powder Metallurgy

The use of metal powders is increasing in order to obtain aircraft and engine parts from a single type of chemical and metallurgical structure. Another important development regarding dust cleaning is the process in which dust production, collection and concentration are realized in an ineffective environment. High strength nickel based superalloys; they tend to have violent macro-cleavage that breaks into a bullion. Conceptually, powder metallurgy provides a method to overcome this problem. Because the material is divided into small droplets as a homogeneous liquid. The maximum separation distance is limited by the size of the solidified droplets. The production of superalloy powders using sudden solidification technologies has been a fundamental research topic.

Selection of Super Alloys by Place of Use

The use of superalloys has spread from aircraft gas turbine engines to many other industries. However, aircraft engines will continue to be the most important market for the use of superalloys for such applications. Inconel 718 alloy reinforced with intermetallic precipitation will continue to be the main working material in aircraft engines. Inconel 718, other than iron-containing nickel-based precipitation-reinforced superalloys are not used as non-ferrous alloys. The use of nickel-based and complex iron-nickel-chromium alloys with precipitation reinforced is decreasing. Nickel superalloys reinforced with solid solution containing chromium iron and molybdenum such as Hastelloy X are widely used. The use of cobalt-based superalloys is small. Cobalt alloys such as MAR-M 509 are used in aircraft turbine engine air foils, especially static propellers. Haynes 188 cobalt based alloy remains a popular burner alloy. Cobalt-based alloys are also used in the medical field. The products, which are the mechanical alloy of Inconel, which includes the oxide dispersion reinforcement, have gained some importance with the use of the MA754 alloy for military engine turbine propellers. The MERL 76 alloy of Pratt & Whitney, similar to the IN-100 alloy, has created new activities for new alloy compounds. This alloy of Pratt & Whitney is a new single-crystalline alloy containing 12% tantalum and does not contain carbon, boron, zirconium and hafnium. Superalloys are used in a variety of locations, such as aircraft parts, chemical factory equipment and petro-chemical equipment, working at high temperatures. Among the existing applications of superalloys:

- 1- Aircraft and industrial gas turbines: discs, bolts, nests, blades, valves, combustion chambers,
- 2- Steam turbine power plants: bolts, gas heaters, turbochargers, exhaust valves, hot plugs, valve-seats,
- 3- Medical applications: dentistry, prosthetic instruments,
- 4- Spacecraft: aerodynamically heated surfaces, rocket engine parts,
- 5- Temperature processing equipment: containers, mixtures, conveyor belts,

6- Nuclear Power Systems: Control Arm Drive Mechanisms, Springs, Channels

7 - Chemical and Petrochemical industries: bolts, valves, pipes, pumps etc. countable.

Iron-based, cobalt-based and nickel-based superalloys are conventionally produced with forged bars, sheets, ribbon cables and presses. Super alloys, also rod, sheet, sheet, strip tube, pipe etc. They are in such shapes. Pre-alloy superalloy powders with high purity are used in many places as isothermal forging, super-elastic forming or hot isostatic printing parts. Casting super alloys are widely used in turbine applications (Ezugwu, E. O., at all 1998).

New Approaches

New approaches, including powder metallurgy and thermo-mechanical processing, aim to significantly improve material resistance at moderate temperatures. In Y 'reinforced superalloys, the use of powder metallurgy to disperse oxide particles has improved the high temperature resistance. The combination of superalloy metallurgy and composite technology has provided the future for turbine materials.

WORKS MANUFACTURING and WORKING

Machining Mechanics and Chip Formation

Machining is one of the most important manufacturing methods. Casting, forging, rolling and other forming methods should be subjected to machining operations in order to make the materials ready for use. In order to bring the workpiece to the desired geometry in the machining process, the surpluses on it are removed by using suitable machine tools and cutting tools in the form of chips and the desired dimensions and surface quality is provided (Arunachalam, R., Mannan, M. A., 2000)

Increasing the workability of workpiece materials and cutting performance of cutting tools in machining has been the subject of many scientific researches. Machinability is the ability of the workpiece to be machined, the simplicity or difficulty of shaping the workpiece is called workability. Chemical composition of the workpiece, micro structure,

heat-treatment property, purity etc. all these variables affect the workability. When different processes are performed in practice, different processability criterion arises. When any kind of material has good workability according to a criterion, when different types of operations are performed, cutting speed, cutting depth, feed rate, cutting fluids, cooling type, stiffness, vibration, tool geometry and tool materials can show poor machinability when cutting materials are changed. (Shaw, M. C., 1989). The appropriate tool tip (factors to be considered in the selection of tool tips are shown in Figure 3.1) and if the cutting parameters are not selected, the workability is reduced and extreme difficulties are experienced. Mn, Ni, Co, Nb and W contribute positively while cutting tools Pb, S, P and C contribute negatively.

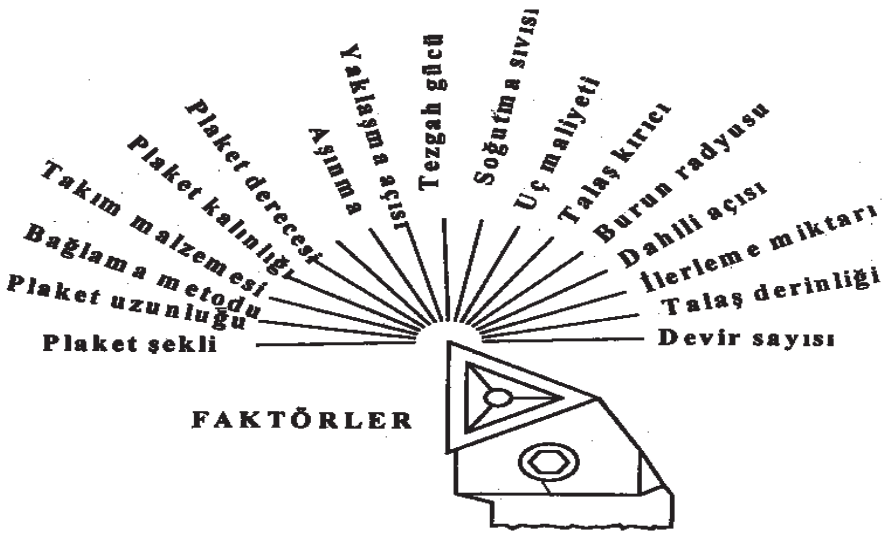


Figure 1. Factors to be Taken Into Account When Selecting a Tool Tip (Plaque)

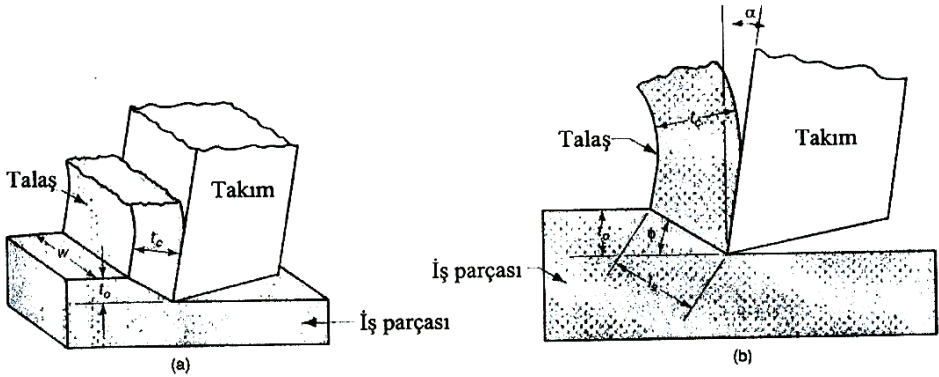
In the analysis made on the mechanics of the machining process and chip formation, metals were generally chosen as work pieces. However, these rules apply to non-metallic materials. Since the machining process is in fact three-dimensional and complex, a two-dimensional orthogonal model is used to define the mechanics of the machining process (Figure

3.2.). Two-dimensional vertical cutting model plays an important role in the machining process. According to this model, cutting of the workpiece by the force of the cutting tool occurs.

Criteria Based on Machinability

The workability of a material is evaluated according to one or more of the following criteria. These criteria are (a) tool life, (b) cutting speed, (c) chip removal amount, (d) cutting force and strength, (e) surface quality and chip shape (Şahin, Y., 2001). These criteria, such as the cutting speed or the tool life, the low cutting force or the low power, indicate that good workability is available (Arunachalam, R., Mannan, M. A., 2000).

However, the workability of the material is generally measured by comparing the cutting speeds of the materials for a given tool life, provided the cutting conditions remain constant. The workability of a workpiece can always be expressed as the number of parts produced per hour, the processing cost for each part, or the final surface quality of the part produced. Factors affecting the processing cost of a part In Figure 3.2, the parameters related to machinability in turning are shown in Figure 3.3.



t_0 : deforme olmamış talaş kalınlığı

t_c : deforme olmuş talaş kalınlığı

w : iş parçası genişliği

l_s : kayma düzlemi uzunluğu

ϕ : kayma düzlemi açısı

α : kesici takım talaş açısı

Figure 2. Factors Affecting the Processing Cost of a Part

Machinability and Test Methods

Factors such as the workpiece itself, tool wear, chip formation, and finishing surface determine the process ability characteristics. However, these factors vary considerably depending on the removal process. These factors are brief; wear, cutting forces, chip formation properties and final finishing surface, depending on the processing method used, cutting tool material, auxiliary materials and input variables such as cutting data. As discussed in Figure 3.6, it is possible to change or improve or deteriorate the results of the chip removal process, not only the workability. One of the above definitions has a specific logic. If the cutting speed is increased, better chip flow will occur, the increased cutting speed will lead to a higher amount of wear on the tool (Shintani, K., 1992). This will result in both good process ability and poor machinability, depending on the two definitions used. Obviously, such good and bad workability assessment is subjective and depends on a criterion that is considered more important. The workability of the materials is thus determined by the manufacturing process and the thermal behavior. For this reason, machinability can also be influenced by microstructural transformations in material by means of chip removal (Field, M., 1968).

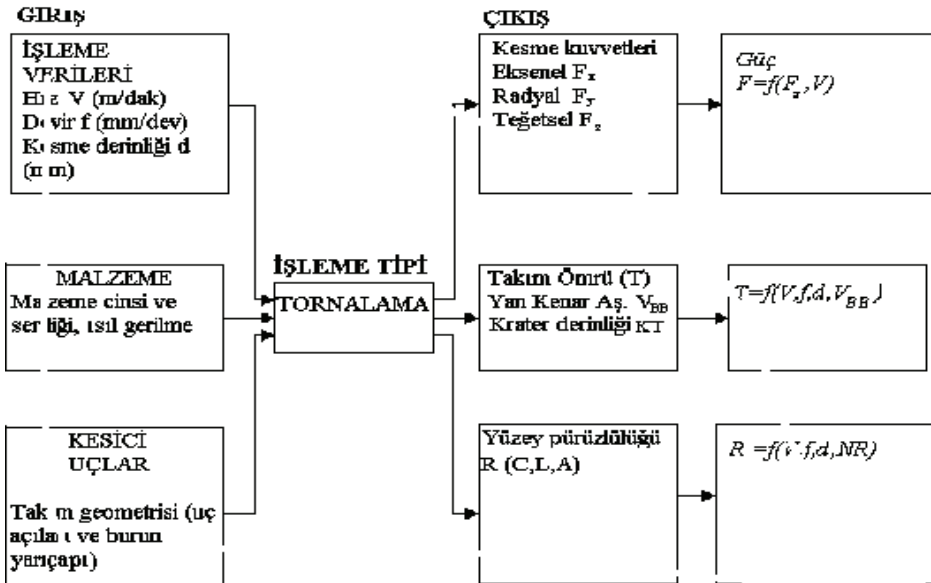


Figure 3. Machining and Input-Output Parameters in Turning

Factors Affecting Machinability

The following factors have positive or negative effects on the processability. These factors;

- 1- The effect of microstructure
- 2- Effect of heat treatment
- 3- Effect of alloying elements
- 4- It is the effect of mechanical properties.

Effect of Microstructure

The machinability of a metal is related to its microstructure and the presence of hard particles in the structure reduces the life of the cutting tool, and the tool life increases as the crystals in the structure become larger.

Heat-Processing

If the metal or alloy is annealed, the microstructure will change. Shear strength of metal; annealing, normalization, stress removal can vary considerably.

Effect of Alloy Elements

The alloying elements have an impact on the tool life. For example, the lower the amount of carbon, the lower the processability. Because when ductility increases, ductile material adheres to the cutting tool and accelerates blindness.

As the carbon content increases, the hardness of the material increases, and the increased hardness increases tool wear. Purpose of improving the workability of the material: a) Increasing the tool life,

- b) Better surface quality,
- c) Reduction of power consumption for chip removal.

The Effect of Mechanical Properties of Materials

Generally, there is a relationship between hardness and tensile strength in materials. As the hardness and the shear strength of a ma-

terial increases, the workability of that material decreases. For example; high alloy and stainless steels can be processed very low. This is due to the influence of alloying elements such as Ni, W and Mn present in the material.

Machinability of Nickel Based Super Alloys

There are many variables that affect machining operations in machinability. Among these, the small size and relatively inexpensive cutting tool are the most important criteria. In cutting tool materials used in the processing of nickel-based superalloys, the following properties are generally required.

1) good abrasion resistance, 2) high strength and hardness, 3) high thermal stiffness, 4) good thermal shock properties, 5) chemical stability in accordance with high temperatures.

Cemented carbide tools and high speed steels (HSS) are widely used in the processing of nickel-based superalloys. High-speed steels are generally suitable for intermittent metal removal operations (such as milling, drilling, etc.), whereas cemented carbide tools are used more often in continuous metal removal like turning or drilling (Ezugwu, E. O. and Pashby, I. R., 1992). Today, some ceramic tool materials ($Al_2O_3 - TiC$), Si_3N_4 silicon nitrite based ceramics and recently developed whisker reinforced aluminum oxide ceramics (25% SiCw whisker) are used in the processing of nickel based superalloys (Richards, N. and Aspinwall, D., 1989). Multi-layer coated carbide tools ($TiN + TiCN$ and TiN) showed a significant improvement in the processing of nickel-based superalloys (Drozda, T. J., 1985). These cutting tools are coated with PVD or CVD coating method. The cubic boron nitrite tools showed the best performance in the processing of nickel-based superalloys in all cutting tools (Jindal, P. C., 1999). Cubic boron nitrites have superior performance in the processing of nickel-based superalloys, although their main use is iron-based metals. However, having a very high cost limits their use.

Surface Integration in the Processing of Nickel Based Super Alloys

The strength of nickel-based superalloys is increased by heat treatment. The surface structure is highly sensitive to the change in the microstructure as a result of high resistance at high temperatures, high flow, high tendency to work hardening and high stresses. The treated surface layer can have the following important conditions.

- 1- Residual stresses may occur during machining.
- 2- The hardness of the surface layer may change as a result of work hardening.
- 3- Micro or macro cracks may occur in the grinding process.
- 4- During machining, defects such as severe sidewall wear, BUE, tears, folds or cracks may occur on the cutting tool.
- 5- Plastic deformation may occur as a result of cold or hot treatment.
- 6- Metallurgical structural changes may occur due to high temperature.
- 7- Chemical reactions such as diffusion movement and high temperature oxidation can occur between the workpiece and the tool.

During grinding of nickel-based superalloys, various residual stresses were observed on the ground surface (Sims, C.T., Hagel, W.C., 1972). As a result of the experiments, it was seen that different stress levels remained on the surface of the machined parts. With different metal removal amounts, residual stresses on the surface can be drawn or drawn. In single point turning, residual stresses can be minimized using positive chip angle and sharp tool. This reduces plastic deformation and work hardening. The shape of the cutting tool also affects the machined surface. Proper surface treatment and minimum surface damage can be achieved with round cutting tools. Continuous processing increases the hardness of the surface layer and disrupts the treated surface. This can be attributed to the partially machined surface of the workpiece and to the partial movement between the tool tip region and the side edge area, to severe sidewall wear and consequently to the increase in cutting forces. Another issue reported in the literature is that there are significant tears

and microstructural changes on the machined surface when processing nickel-based superalloys (Arunachalam, R., Mannan, M. A, 2000).

Inconel 718, one of the high yield strength superalloys, produces both tensile and compressive stresses during the material removal process at high temperatures. Excessive surface heat creates tensile stresses, as a result of more heat on the workpiece, the compression plastic deformation results in compression stress. Surface change in non-traditional chip removal processes is generally characterized by high surface roughness, interactions between the inner grains and the formation of a re-casting layer. Interaction of the inner beads is a form of corrosion that occurs on the surface grain boundaries and is usually seen as a sharp notch. The material is heat-treated after casting to obtain the required properties. Due to its ductile structure, continuous and long chips are obtained when Inconel 718 material is cut. Creep / adhesion with the mechanism of removal of particles from the tool and therefore leads to excess notch. It has been observed that the final finishing surface deteriorates when chip removal is performed with rhombic shaped ceramic tool, which is over-notched with high cheek wear (Shaw, M. C., 1989). Side edge abrasion and surface roughness values are shown in Table 3.1 when Inconel 718 is processed with ceramic tool tools. It has been observed that the last finishing surface has deteriorated when cutting with longer round ceramic tools. Surface roughness and side edge wear can be seen in Table 3.1.

Table 4. Side Edge Abrasion and Surface Roughness Values When Inconel 718 is Machined on Ceramic-Tipped Tools

Tool type	Cutting time (min.)	Average sidewall wear (mm)	Maximum sidewall wear (mm)	Surface roughness (μm)
Pure Oxide Ceramic (CNGN 120412T)	1*	0.336	0.769	7.94
	1	0.248	0.549	2.45
Pure Oxide Ceramic (RNGN 120712T)	2	0.283	0.561	2.60
	3	0.29	0.671	3.05
Ceramic with mixed oxides (CNGN 120412T)	1**	0.203	0.511	6.02
	1	0.157	0.404	1.13
Ceramic with mixed oxides (RNGN 120712T)	2	0.239	0.563	1.20
	3	0.229	0.472	2.11

Average flank wear and Maximum flank wear and 1 * if the cut is more than 1 minute after the cut is notch = 2.096 mm, and in 1 ** after 1 minute cutting, the overcutting amount: 4.125 mm.

As a result of the increase of the tool / workpiece contact area in the area of high cheek wear, a rougher surface is obtained, resulting in a reduced gap angle. This increases the friction of the side edge on the newly formed surface. The reason for their high cheek wear and surface roughness value is that they have very low fracture toughness and hardness of pure oxide ceramics.

Tool Life

The tool life is generally defined as the effective cutting time required to achieve a particular criterion or, as practically, the active working time between two sets of tools. Factors that affect wear due to tool life mainly due to wear, factors such as tool material and work material, tool and chip geometry, cutting speed, coolant, etc. also affect tool life. However, the most important factor is the cutting speed.

To optimize the cutting process, it is necessary to know the relationship between the cutting speed (V) and the tool life (T). The first study on this subject was done by Taylor and was expressed by the following empirical formula.

$$V \cdot T^n = C = \text{Fixed}$$

In this equation n: The tool base is shown and depends on factors such as tool material, work material, processing conditions, progress amount or depth of cut. Here again, V: Cutting speed (m / min.), T: Tool life (min.), And n are equal to $-1 / k$ [Shaw, M. C.,]. The formula is in this case;

$$T \cdot V^k = C = \text{Hard writeable.}$$

However, while the value of n is more affected by the tool material, the value of C depends on the material and cutting conditions. C refers to the cutting speed for 1 minute life. That is, the point where the line intersects the apse axis. Therefore, to find a more practical solution;

$$\log C = \log V + n \log T \text{ is used.}$$

The slope of (n) can be calculated as follows.

$$n = \frac{\log V_1 - \log V_2}{\log T_2 - \log T_1}$$

The cutting speed can be calculated as follows:

$$V_2 = V_1 (T_1 / T_2)^n$$

Cutting Tool Materials and Development

The cutting tool materials must have the following characteristics to enable the cutting tools to effectively cut for a long time due to high temperatures and stresses during machining:

- a) High hardness and hot hardness,
- b) high toughness,
- c) chemically directness to the workpiece,
- d) stability against oxidation and dissolution, resistance to thermal shocks,

The cutting tool materials which are widely used in industrial areas and their development are briefly summarized below.

Development of Uncoated Carbide Tools

These materials were first developed in the 1920s in Germany due to the expensive use of diamonds and to produce sufficient mold materials. It is made of abrasion-resistant, high temperature resistant material and it is produced by combining hard carbide particles with soft and ductile metals. It is hardly produced by tungsten carbide casting using cobalt binder. However, as a structure with many errors was observed, it was not found as satisfactory as cutting tool and die material. In 1923, fine tungsten carbide powders and fine iron, nickel or cobalt powders were pressed by powder metallurgy technique in France. It was then subjected to sintering at about 1300 °C and cobalt appeared as the best matrix. Since then, the foundation has been developed with carb-carbide materials based on WC-Co, different materials and different types of carbides for cutting operations. The properties of some carbides are shown in Table 3.2. 50% of the carbide production is used in metal removal processes. Carbide tools can be used effectively without losing their hardness and cutting up to a cutting speed of 40 m / min to 350 m / min [Shaw, M. C.,].

Table 5. Properties of Some Carbides (Shaw, M. C.)

Carbide types	Melting degree, °C	Hardness, (Hv 30)
TiC	3200	3200
V_4C_3	2800	2500
N_bC	3500	2400
TaC	3900	1800
WC	2850	2100

Hv 30: Vickers hardness, 30 kg weight used during measurement

Carbide cutters in ISO system; all processing degrees are divided into three-color coded series. These;

P series (blue): High-alloy tungsten carbide tool is used for machining long-chip materials.

M series (yellow): Alloy tungsten carbide tool, usually titanium ratio is less than the P series and is used in the processing of steels and cast irons.

K series (red): Tungsten cobalt alloy tool used for processing of non-ferrous metals, non-ferrous metals and non-ferrous metals.

Development of Coated Cemented Carbide Cutting Tools

Coating of a very thin hard layer on carbide tools with chemical evaporation method was started in 1980s. With this method, a thin layer of less than 10 μ m thickness is tightly attached to the coated tools and the coating material is used as TiN, Ti (C, N), Hf N and Al₂O₃. Here, TiN is used as the second layer, because it gives a lower coefficient of friction and decreases the BUE, because it is thinner, while Al₂O₃ provides chemical stability and abrasive wear resistance at high temperatures. Because the resistance and abrasion resistance is better on the main material, it forms the first layer [Shaw, M. C.,].

Research The main reason for the wear resistance of the TiN, TiN and Al₂O₃ coatings is due to their resistance to diffusion abrasion at the place of adhesion. However, in case of sudden high-speed steel cutting, the coatings cannot prevent adhesion on the surface, but they can destroy the low-speed chip build-up. Multi-layer coatings give the team a chance to use any kind of work. The physical evaporation method (PVD) is common in multi-layer coatings (Ezugwu, E. O. and Wang, Z. M., 1996). The surface to be coated with this method is first cleaned with an inert gas ion in a low pressure region and the pressure in this chamber is reduced. The metal atoms to be used in the coatings are evaporated in the space, ionized and emitted to the tool surface with high voltage. This process uses low pressure containing carbon atoms. The adhesion of the coatings to the tool surface is carried out on the tool at temperatures of 500 °C and lower. A lower coating temperature than the CVD (chemical evaporation method) creates less permanent stress and does not reduce the transverse breaking strength. In addition, PVD treatment is more attractive for sintered carbides, since it further thins the grain size of the coating layer [Shaw, M. C.,]. The researchers are aimed at coating sin-

tered carbide tools with different methods such as TR, TIN and Al₂O₃. With coated carbide tools, longer tool life, more production increase and easier chip flow are provided. Covering; It acts as a temporary lubricant by greatly reducing the cutting force, the heat generated and the wear. This allows higher speeds to be used during cutting, especially when a higher quality surface is desired. The ability of the coating to prevent lubricant and chip adhesion greatly reduces the amount of stress and heat generated during chip removal, thus greatly improving tool life. It is produced by covering a thin layer of approximately 0.25 mm thickness on the sawdust surfaces of the tools in order to provide the required superiority from the use-type tools. The main task of this layer consists of tough WC-Co alloys with thermal conductivity. It is possible to produce this type of composite by means of automatic press with powder metallurgy techniques.

REFERENCES

Arunachalam, R., Mannan, M. A., (2000). "Machinability of nickel-based high temperature alloys", *Machining Science and Technology*, Vol 4, Issue 1, 127-168.

Bartlay, E., (1988). "Super Alloys a Technical Guide", .

Brandt, G., Gerendas, A., Mikus, M.W., (1990). "Car mechanics of ceramic cutting tools when machining ferrous and non-ferrous alloys", *J. European Ceramic Soc.*, 6 (5), 273-290.

Chouldhury, I. A, El-Baradie, M. A., (1996). "Machinability assessment of nickel based alloys: tool life in turning Inconel 718", *In Proceedings of the Sixth Cairo University International MDP Conference*, 233-240, Cairo, Egypt.

Chouldhury, I. A., (1995). "Machinability studies of high strength materials and the development of a data base system", PhD thesis, *Dublin City University*.

Chouldhury, I. A., El-Baradie, M. A., (1997). "Machining nickel base superalloys: inconel 718", *Proc Instn Mech Engrs*, Vol 212, Part B, 195-205.

Drozda, T. J., (1985). "Ceramic tools find new applications", *Manuf. Eng.* 87, pp. 34-39.

Ezugwu, E. O., Bonney, J., Yamane, Y., (2003). "An overview of the machinability of aero engine alloys", *Journal of Materials Processing Technology*, 134, 233-253.

Ezugwu, E. O., Pashby, I. R., (1992). "High speed milling of nickel-based superalloys". *J.Mater Proc.technol.* 3 , 429-437.

Ezugwu, E. O., Tang, S. H., (1992). "Surface abuse when machining cast iron and nickel base superalloy (Inconel 718) with ceramic tools", *Proc. 9th Irish Manuf. Conf.*, Dublin, Sept., 436-450.

Ezugwu, E. O., Wang, Z. M., (1996). "Performance of PVD and CVD coated tools when nickel-based machining Inconel 718 alloy". IN: N.Narutaki et al. *Progress of Cutting and Grinding 111*, 102-107.

Ezugwu, E. O., Wanga, Z. M., Machadop A. R., (1998). "The machinability of nickel- based alloys: a review", *Journal of materials Processing Technology*, Volume 86, Issues 1-3, 1-16.

Field, M., (1968). "Machining aerospace alloys", *Iron and Steel Institute, Special Report 94*, 151-160.

Goossler, F.W., (1985). "High-speed machining of aircraft engine alloys, Proc." *Int. Conf. on High Productivity Machining Materials and Processing*, New Orleans, Louisiana, 7-9, 57-67

Groover, M. P., (1996). "Fundamentals of modern manufacturing-Materials, processes and systems", *Prentice Hall Inc.*, pp65,66

Hunn, J. D., Lee, E. H., Byun, T. S., Mansur, L. K., (2001). "Ion-irradiation-induced hardening in Inconel 718", *Journal of Nuclear Materials*, 296, 203-209.

Jindal, P. C., Santhanam, A. T., Schleinkofer, U., Shuster, A. F., (1999). "Performance of PVD TiN, TiCN, and TiAlN coated cemented carbide tools in turning", *International Journal of Refractory Metals & Hard Materials*, 17, 163-170.

Li, R. B., Yao, M., Liu, W. C., He X. C., (2002). "Isolation and determination for δ , γ' and γ'' phases in Inconel 718 alloy", *Scripta Materilia*, 46, 635-638.

Loria, E. A., (1992). "Recent development in the progress of super alloy 718", *J. Maler, Sci*, 44 (6), 33-36.

Richards, N., Aspinwall, D., (1989). "Use of ceramic tools for machining nickel-based alloys", *Int. J. Mach. tools Manuf.*, 294, 575-588.

Şahin, Y., (2000). "Talaş Kaldırma Prensipleri 1", *Nobel Yayın Dağıtım* pp45,46.

Şahin, Y., (2001). "Talaş kaldırma prensipleri 2", *Nobel Yayın Dağıtım* pp58,59.

Shaw, M. C., (1989). "Metal cutting principles", *Oxford University Press*, pp102,103.

Shintani, K., Kato, H., Maeda, T., Fujimera, Y., Yamamoto, A., (1992). "Cutting performance of CBN tools in machining of nickel-based superalloy", *J. Precis, Eng.* 58 10, 63-68.

Sims, C.T., Hagel, W.C., (1972). *The Superalloys Wiley*, New York p 25

Warbuton, P., (1967). "Problems of Machining Nickel-Based Alloys", *Iron and Steel Institute, Special Report 94*, 151-160.

White, C. H., (1986). "Nickel Base Alloys", *Wiggin Alloy*.p 12.

OPERATING PRINCIPLE OF AUTOMATIC ARTICULATOR

Mohammad RAFIGHI¹, Abdulkadir GÜLLÜ², Metin ORHAN³

Abstract: In order to determine the position of the upper (maxillary) and lower (mandibular) jaws in dentistry, an articulator that is a mechanical device is commonly used. In addition, the jaws shape and relationship disorders in orthognathic surgery are corrected using this device. In orthognathic surgery, the maxillary and mandibular position is changed relative to the skull -base. Hence, the dimension of the maxillary and mandibular is measured before the surgery and the jaw models are prepared using closing wax, thereafter the models are fixed to the articulator with a cast in patients who are going under orthognathic surgery. Afterward, the fixed models are released by cutting the cast, the desired adjustments are applied and the models are fixed back to the articulator. Small errors are inevitable in transferring the position of the models due to performing all processes manually. In the presented work, an automatic articulator was designed and produced which is controlled by a computer. Therefore, there is no need to cut and reattach the model from the articulator that decreases the pre-surgery duration and increases the operation precision significantly. The automatic articulator has three linear, two rotary axes, the upper and lower jaws can be brought to the desired reasonable position, and the movements can be recorded to use in the next possible operations.

-
- 1 Mechanical Engineering Department, University of Turkish Aeronautical Association, Ankara / Turkey, e-mail: mrafighi@thk.edu.tr, Orcid No: 0000-0002-9343-9607
 - 2 Manufacturing Engineering Department, Gazi University, Ankara / Turkey, e-mail: agullu@gazi.edu.tr, Orcid No: 0000-0003-1088-4105
 - 3 Faculty of Dentistry, Ankara Yıldırım Beyazıt University, Ankara / Turkey, e-mail: metinorhan@ybu.edu.tr, Orcid No: 0000-0002-6400-3695

Keywords: Automatic articulator, Orthognathic surgery, Design, Analysis, Manufacturing

INTRODUCTION

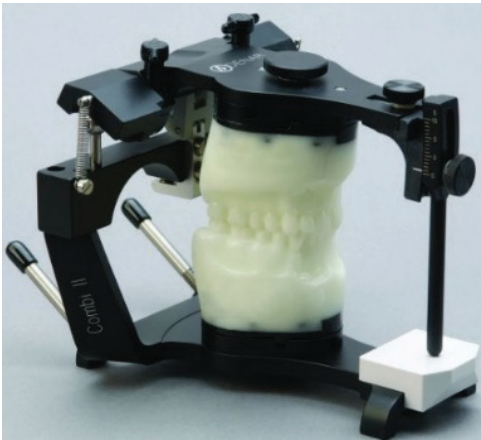
An articulator is a mechanical device, which is widely used in prosthetic dentistry and orthognathic surgery applications. It represents the temporomandibular joints and the jaw members to which maxillary and mandibular casts are attached to simulate jaw movements. The main purposes of the articulator are holding the maxillary and mandibular casts in a determined fixed position, simulating the jaw movements, producing border and intraborder movements of the teeth similar to those in the mouth, aiding to fabricate dental restoration, correcting and modifying the complete restoration. There are three types of articulators; Non-adjustable, Semi-adjustable, and Fully-adjustable (Starcke 1999; Kaur et al. 2017; Navneet et al. 2017).

Although there is not any data related to the automatic articulators according to the literature, many studies have been reported related to mechanical and virtual articulators, use of the device in orthognathic surgery applications, and problems, which dentists faced during prosthetic applications (Panula et al. 2001; Kordaß et al. 2002; Ghanai et al. 2010; Maestre-Ferrín et al. 2012).

This study aims to make an automatic articulator employing a new design. The most important task of the automatic articulator is simulating the positions of the model of the jaw related to each other precisely. The idea of this study was emerged by an orthodontist due to the limitations of mechanical articulators. One of the disadvantages of the mechanical articulators is rotating the jaw models only from one axis. However, jaw models in the automatic articulator can rotate from any axis in two directions which one of them simulate the opening and closing rotation and the other one simulate the right and left rotation. Measuring the position of the jaw models manually is another disadvantage of the mechanical hinge articulator. In the newly designed automatic articulator, the position of the jaw models will be measured fully automatically through the control screen.

LITERATURE SURVEY

Recently, many surgical robots have been designed and manufactured to use in surgical operations (Hockstein et al. 2005). Furthermore, mechanical (Figure 1a) and virtual articulators (Figure 1b) have been developed to use in orthognathic surgery (Gartner and Kordass 2003). Although many virtual articulators have been developed, the computer-assisted automatic orthognathic surgical articulator has not been fabricated yet.



(a)



(b)

Figure 1. (a) Mechanical Articulator, (b) Virtual Articulator

The use of mechanical articulators has been recommended due to statistically significant improvement in the accurate estimate of the maxillary position (Paul et al. 2012). In previous studies, it was reported that the positional accuracy of the cast on the articulator was affected by several factors. They are included; the age of the equipment, hygroscopic expansion of the installation cast, the time after assembly, the type of mounting cast, water and powder ratio, humidity, and temperature (Chung et al. 2001; Michalakis et al. 2012).

Proper positioning of the maxillary cast model in the articulator is very important in dentistry. Significant errors can occur in the final occlusion if the jaws relational transfer is not performed properly. There are also numerous problems in the articulator such as; cast expansion

and contraction, deformation of the biting material, and stability of the articulator.

Dentistry has made many important changes in recent years. The virtual articulator is designed to prevent mechanical articulator errors, reduce the duration of the operation, and perform detailed static and dynamic analysis of the occlusion (Shadakshari et al. 2012). The virtual articulator simulates the patient's specific chewing motion while the lower jaw calculates the area of the contact areas of the opposing teeth during the animation. The most important advantage of this technique is that it allows the dentist and/or dental technician to work in a digital environment without having to install a cast in the physical articulator.

Today, there are major changes due to the latest technological developments such as computer-aided design and computer-aided manufacturing (CAD/CAM) techniques in dentistry (Fuster Torres et al. 2009; Bai et al. 2010). Furthermore, new mounting materials, virtual articulator software, modern in-mouth scanners, and more efficient CAM machines and CAD / CAM systems are being used in the dental industry (Enciso et al. 2003; Yau et al. 2011; Logozzo et al. 2014).

Orthognathic surgery is performed to correct jaw and facial deformities, and it is usually planned by using a cast on the traditional articulator. Nowadays, use of the orthognathic surgery becomes widespread to repair deformities in the human jaw or the face. Such an operation is usually performed by changing the position of the maxilla relative to the patient's skull. The mounted cast is indispensable for surgeons because it guides surgeons in positioning the jawbones before surgery. The cast is usually installed on a semi-adjustable articulator. However, mechanical articulators have two major limitations; first, correct positioning of the upper teeth model, second, determination of maxilla's position according to the skull. Several types of articulators have been designed for orthognathic surgery applications, but none of them could be provided the correct position of the upper and lower jaws. Thus, repairing the position of the jaws in orthognathic surgery is mostly depends on the surgeon rather than using the mechanical articulator.

Traditional Articulator Operating Principle

For instance, in some cases, the lower jaw is not in the correct closing position relative to the upper jaw as shown in Figure 2. Thus, the surgeon cuts the cast of the lower jaw model attached to the articulator from the lower plate, brings the jaw model to the proper position, and fixes it back to the articulator.

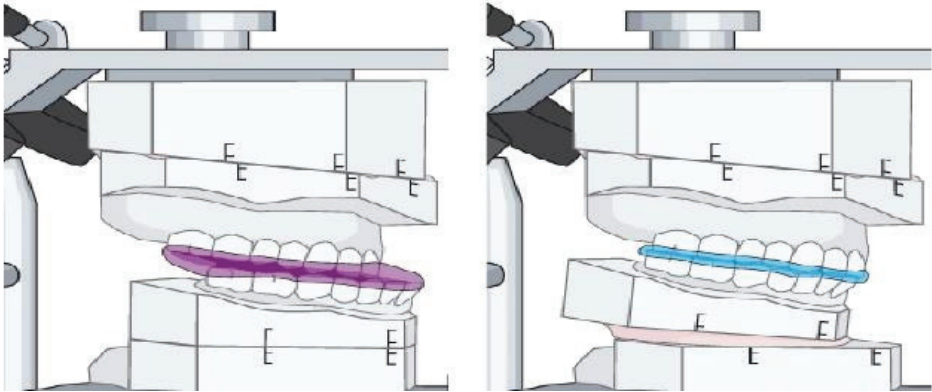


Figure 2. Asymmetric Mandibular

According to the measurements obtained from the face bow, the dentist transfers the lower and upper jaw model to the articulator employing cast. Then, as shown in Figure 3, horizontal and vertical lines are drawn on the cast for surgical planning. According to these lines, the jaw models, which are connected to the articulator by use of a cast, are cut off from the bottom and/or top plate and are released from the cast. Finally, the movements and rotations of the jaw model that are determined by cephalometric methods are made and it is fixed back again onto the articulator using the cast to obtain the final position.

Following the fixation of the jaw model on the mechanical articulator, the amount of displacement of the jaw models is obtained by measuring the difference between horizontal and vertical lines, which are drawn on the jaw models. Figure 3 shows two different cases for orthognathic surgery. In the left case, the upper jaw is shifted 2 mm to the right and in the right case, the upper jaw is shifted 3 mm forward. Since these operations are performed manually, mistakes can occur in transferring

the position of the jaws. However, if the surgeon will be able to measure the position of the jaw models automatically, it will be possible to estimate and apply the more precise, faster, and more accurate treatment without the necessity to cut the cast.

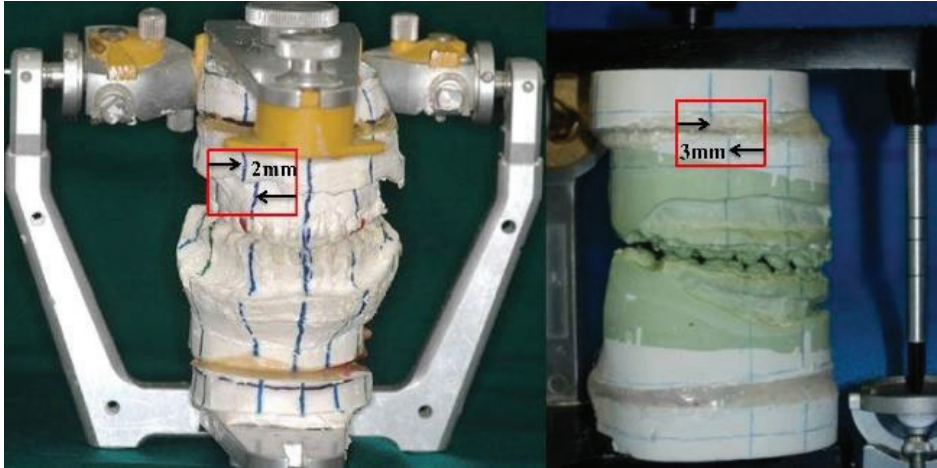


Figure 3. Orthognathic Surgery Planning

As a result, there are not any single automatic articulators according to the literature. The mechanical articulator, which is widely used until now, is controlled manually and generally is used in the treatment of prosthetic teeth. The purpose of this study is to design and fabricate of novel automatic articulator with new functions. In the automatic articulator, measuring the final position of the jaw models precisely and automatically is possible. There is no need to cut and release the jaw model cast and reattach it again. This step helps to reduce the pre-operation preparation time significantly. The other advantage of this device is rotating the upper and lower jaw models from any desired axis. Thus reducing the total duration of the treatment and increasing the precision of the surgical procedure in the jaw is aimed.

MATERIALS and METHOD

Various methods and programs can be used in the design and analysis of devices. Solid modeling programs such as SolidWorks and CATIA

are two of them. In this study, recent works have been examined and as a result of these investigations; the practical and functional device was targeted.

In this study, SolidWorks software has been used to design and analyze the automatic articulator. Aluminum 1060 alloy has been chosen as the material for automatic articulator due to its lightweight, ease of machining, and low cost. The finite element analysis was performed to check the strength of the components under applied loads. Regarding the analyses, some revisions have been done in the design of the automatic articulator, and finally, the best design was chosen. In the final step, the assembly of the automatic articulator has been done in SolidWorks. After all, components of the automatic articulator were manufactured and assembled in a mechanical workshop and the control of the device has been done using PLC's programming.

In this study, by considering the deficiencies of existing devices and advice of jaw surgeons, five axes automatic orthognathic articulator was designed and manufactured. This device has five degrees of freedom in the upper jaw and five degrees of freedom in the lower jaw. Three of five degrees of freedom meet linear movements (X, Y, Z axes), while the other two meet rotational movements (U, V rotation axes). The motion axes of the jaw model in the automatic articulator are shown in Figure 4.

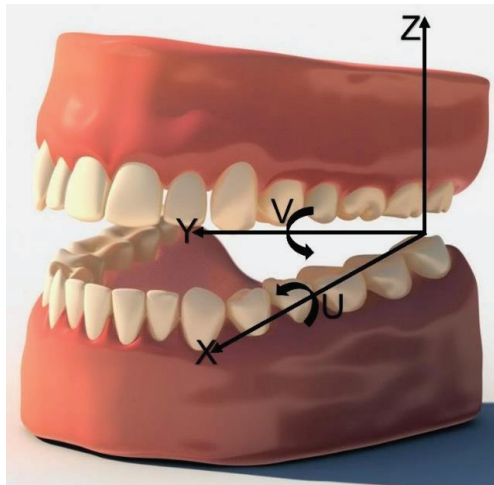


Figure 4. Motion Axes of the Jaw Model

Assembly of the Linear Mechanism

There are three linear movements in upper and lower jaws in the X, Y, and Z axes. These are; Back-forth, right-left, and up-down movements. Following the design of the solid parts, the assembly of the linear mechanism has been done as shown in Figure 5. The components of this mechanism are given in Table 1.

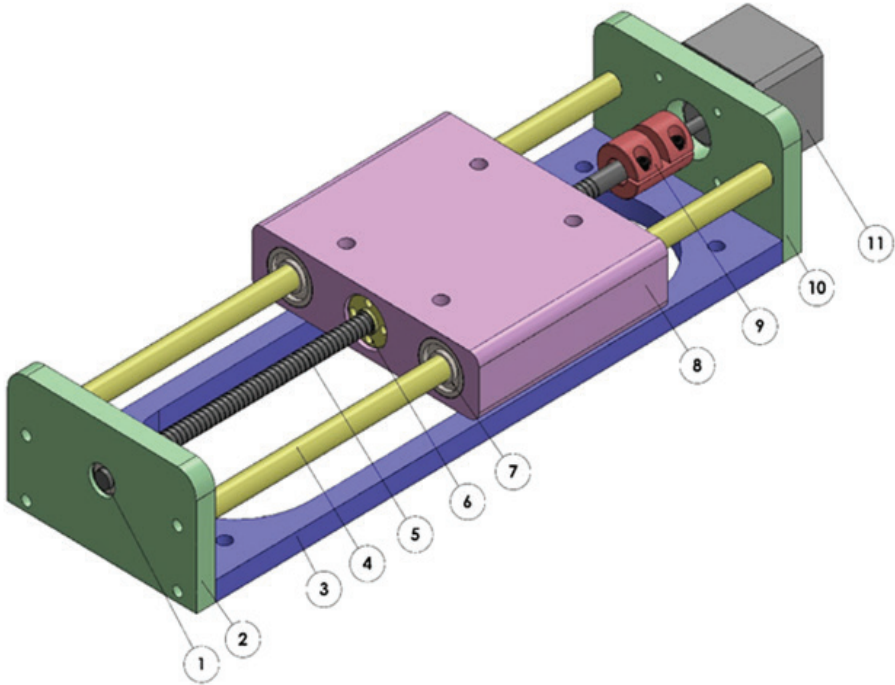


Figure 5. Assembly of the Linear Mechanism

Table 1. Mechanical Components of the Linear Mechanism

No	Name
1	Bearing
2	Bearing component
3	Base
4	Rail
5	Lead screw
6	Nut
7	Mechanical bush
8	carrier
9	Mechanical coupling
10	Stepper motor connecting component
11	NEMA-17 stepper motor

Assembly of the Rotary Mechanism

After designing the all necessary parts to perform the rotational movement, the virtual assembly of the rotary mechanism is given in Figure 6 and the solid parts of this mechanism are given in Table 2.

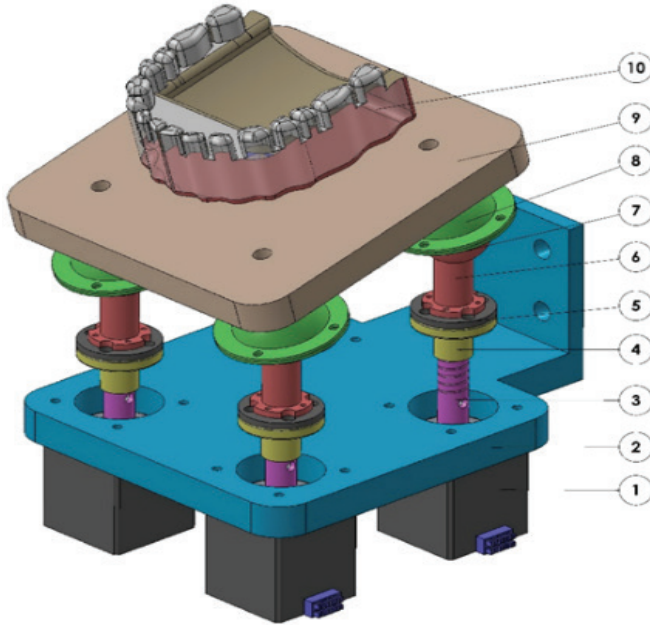


Figure 6. Assembly of the Rotary Mechanism

Table 2. Mechanical Components of the Rotary Mechanism

No	Name
1	NEMA-11 stepper motor
2	L-R connecting component
3	Lead screw
4	Nut
5	Connecting component
6	Spherical joint
7	Spherical bearing-down
8	Spherical bearing-up
9	Jaw holder component
10	Jaw model

Assembly of the Automatic Articulator

The aluminum 1060 alloy material is assigned to all designed parts in the SolidWorks environment and the mass and geometry of the parts are determined. Since the mounting of the lower jaw mechanism is the opposite of the upper jaw mechanism (mirroring), the following processes are performed only for the lower jaw mechanism.

The virtual assembly of the automatic articulator was carried out on a U shape designed table. First, the linear mechanism in the X-axis is placed on the right and left sides of the table. Second, the linear mechanism of the Y-axis is fixed to the X-axis linear mechanisms using bolt and nut. Third, the linear mechanism of the Z-axis is mounted vertically to the Y-axis linear mechanism through the L connecting component. Finally, the rotary mechanism is installed to the linear mechanism on the Z-axis through the L-R connecting component. The virtual assembly of the automatic articulator is given in Figure 7.

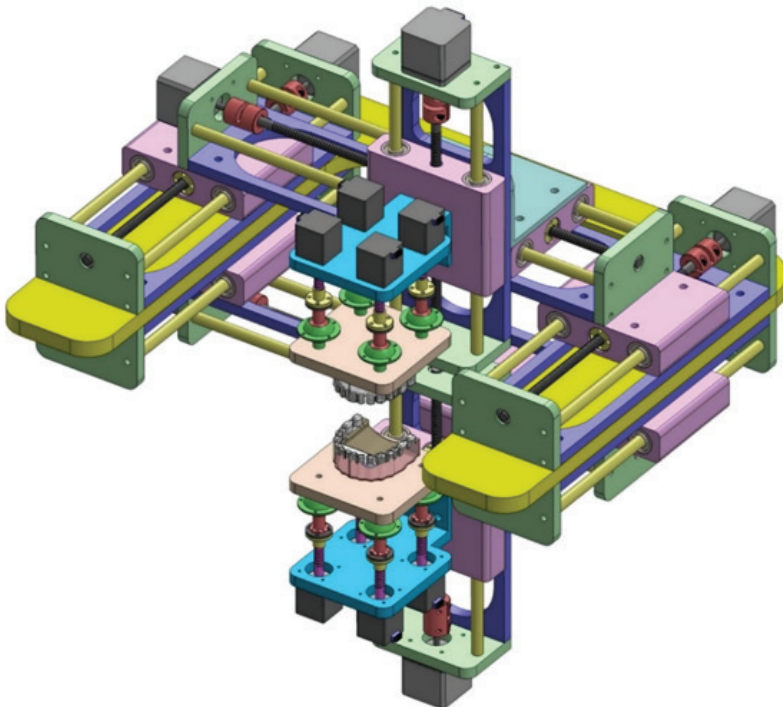


Figure 7. Assembly of the Automatic Articulator

RESULTS and DISCUSSION

The jaw models on the automatic articulator can rotate ± 25 degrees by a fully novel-designed rotary mechanism. According to Figure 8, there are four stepper motors and their associated spherical joints on the four corners of the L-R connecting component. This mechanism aims to ensure that the jaw holder, which carries the jaw model, can rotate from any desired axis. For instance, to rotate the jaw model in a clockwise direction on the U-axis; the spherical joints connected to the B and C stepper motors are remained in the same position, while the spherical joints connected to the D and A stepper motors move linearly up or down to provide the desired α angle to the jaw model. Similarly, the same processes are performed for the V-axis, and the β angle is given to the jaw model. Since the joints are spherical and could be easily rotated at the determined angles in the spherical bearings, it is possible to give any desired angles (± 25 degree) in the direction of U and V axes to the upper and lower jaw models.

To rotate the jaw models exactly from the middle on the U-axis, the B-C and D-A stepper motors must be work simultaneously. While the spherical joints, which are connected to the B and C stepper motors, go up, opposite side spherical joints must go down in the same distance to rotate the jaw models exactly from the middle.

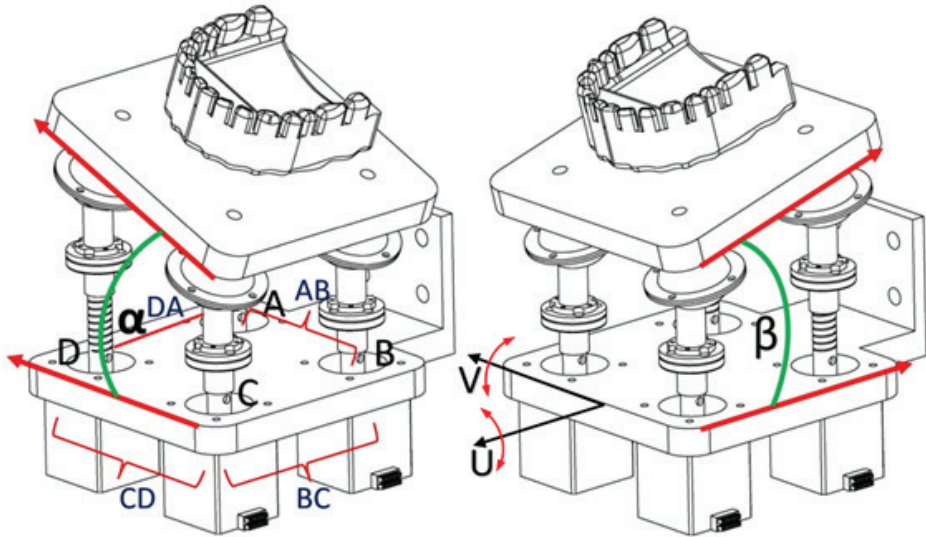


Figure 8. Working Principles of the Rotary Mechanism

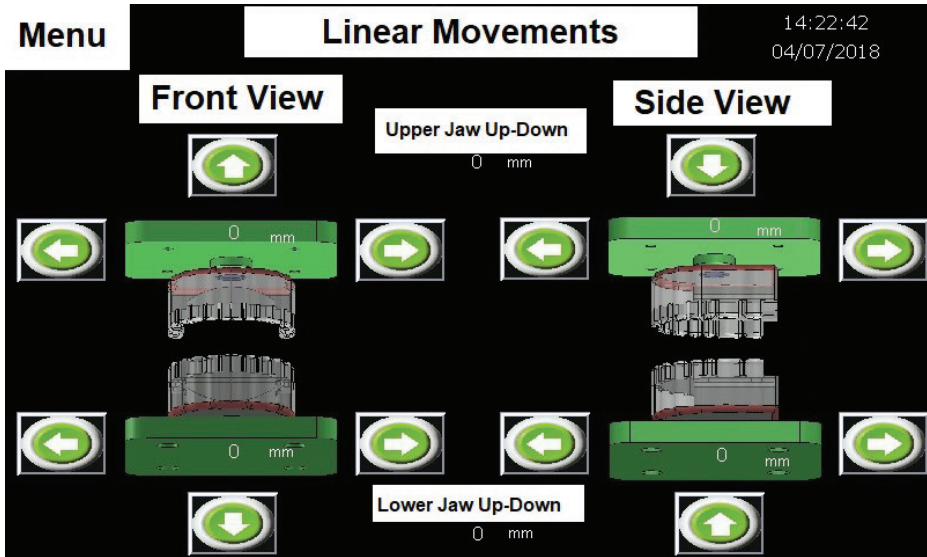
Automatic articulator control

In this step, the control and final assembly of the electrical-electronic components of the automatic articulator were carried out. Step motor, stepper motor drivers, PLCs, switches, power supply, communication cables, and operator control panel were used to provide control of the automatic articulator. Stepper motors, stepper motor drivers, and PLCs play an important role in this mechanism in the terms of precision and speed of operation. Servo motors are often used in places where large loads, high precision, and speed are required, such as CNC machines. However, the costs of the servo motor and the equipment connected to them are high. Therefore, stepper motors were chosen in this study due to their low cost, easy control, and precise positioning. In the automatic articulator, NEMA-17 stepper motors were used in the linear mechanism and NEMA-11 stepper motors were used in the rotary mechanism. Furthermore, 16 stepper motor drivers were used to control the 16 stepper motors. Switches were used to determine the starting and ending points in the linear and rotary mechanisms in the automatic articulator. Four Delta DVP-28SV PLCs were used to control the automatic articula-

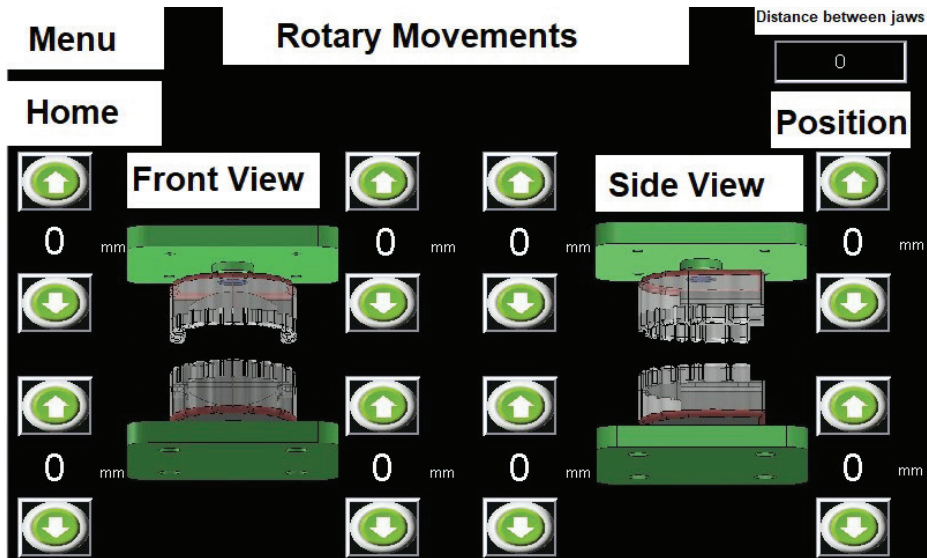
tor mechanism. Two of them are in the linear mechanism and the other two are in the rotary mechanisms.

Programming of the automatic articulator: The programming of the automatic articulator was performed using WPLSoft software. First, the program is written on the computer then it is transferred to PLC via an RS-232 communication cable. Also, the connection between the stepper motors and the PLCs is done with RS-458 communication cables. Thus, the program compiled in PLC enables stepper motors to operate at desired speed and direction through stepper motor drivers.

The DOPSoft software was used for the design of the operator control panel. In this section, the buttons designed for controlling the automatic articulator are explained. The linear and rotary mechanism control panel screens are shown in Fig. 9 (a) and (b) respectively.



(a)



(b)

Figure 9. a) Linear Mechanism and b) Rotary Mechanism Control Screen

Explanation of commands in the control panel:

Start/stop and emergency stop buttons: The automatic articulator mechanism is turned on or off via the start/stop button. The emergency button is used to stop the device immediately.

Zero-point (Home) button: The linear and rotary mechanisms are brought to the zero (Home) point.

The area for entering the distance between the jaw models: The upper and lower jaw models are quickly brought to an appropriate position by entering the distance in mm.

Linear movement's buttons: When the ◀ and ▶ buttons are clicked in the X and Y axes, the carrier moves back and forth or left and right precisely. As the same, when the ▼ and ▲ buttons are clicked in the Z-axis, the carrier moves up and down. Each motor has its starting and ending points. Switches were used to determine the start and endpoints. The parameters such as speed and direction of the stepper motors are determined by the program that is written into PLC.

Rotary movement's buttons: In rotary mechanism, ◀, ▶, ▼ and ▲ buttons on the U and V axes are used to give the desired angle between ± 25 degrees to the jaw models. The stepper motors work parallel (pairs) in the rotary mechanism. Eight NEMA-11 stepper motors were used for the upper and lower jaw models and these motors are named A, B, C, D, E, F, G, and H. As it is shown in Fig. 8, the lower jaw stepper motors are named A, B, C and D. Thus, there are four stepper motor pairs A-B (rear), B-C (right), C-D (front) and D-A (left). When the stepper motors are operated, the motor shaft and integrated lead screw rotate simultaneously. Thus, the spherical joint moves up and down along the lead screw thanks to the nut, hence it provides ± 25 degree to the jaw models.

Assembly of the Electrical and Electronic Equipment

In this step, eight NEMA-17 stepper motors are placed in the X, Y, and Z axes of the upper and lower jaws to perform the linear movements and eight NEMA-11 stepper motors are mounted on the mechanism to perform the rotary movements. Each stepper motor is connected to the TB6600 stepper motor driver through connection cables and each four

stepper motor driver is connected to the one DVP-SV28 PLC. Finally, stepper motor drivers, PLCs, connection cables, power supply and touch screen are placed into the electronic box. The complete assembly of the automatic articulator is shown in Figure 10.



Figure 10. Automatic Articulator

Case Study of the Automatic Articulator on a Jaw Model

As shown in Fig. 11 (a), the upper jaw is asymmetric to the lower jaw. The following operations have performed to obtain the correct closure of the jaw model:

- The upper jaw was moved 7 mm forward in the X-axis via the linear mechanism.
- The upper jaw was moved 5 mm to right in the Y-axis via the linear mechanism. Thus, the upper jaw is approximately in the same position as the lower jaw.
- The upper jaw was rotated 4 degrees in a clockwise direction from the U-axis using a rotary mechanism.
- The upper jaw was brought down 3 mm in the Z-axis via the linear mechanism. The upper jaw was rotated 2 degrees in a counterclockwise direction from the V-axis using a rotary mechanism. Then, it was moved 1 mm down in the Z-axis via a linear mechanism. Finally, as shown in Fig. 11 (b), the correct closure of the jaw models is obtained by applying the small changes.
- All positions obtained from the linear and rotary mechanism are saved to use in orthognathic surgery.

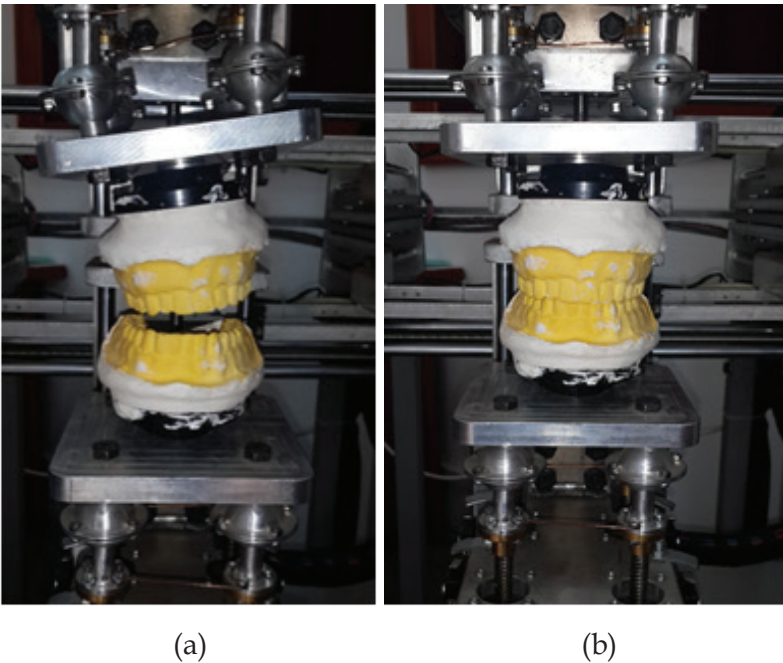


Figure 11. a) The Asymmetric Jaw Model and b) the Correct Closure of the Jaw Model

CONCLUSION

Nowadays dentists use mechanical articulators extensively in prosthetic dental processes or orthognathic surgery operations. However, since all the procedures are performed manually, the pre-operation preparation duration is long and the precision is low. The main idea of the automatic articulators is based on the demand of an orthodontist to facilitate the pre-operation procedure. The orthodontist described the deficiencies of the mechanical articulator and the desired functions in the automatic articulator. As a result, a novel automatic articulator has been designed and manufactured.

The innovative aspect of this work is the fabrication of the automatic articulator, which is capable to simulate the movement of the jaw model on any desired axis. According to the literature, there is not any similar device. Thus, firstly the automatic articulator's parts are designed, analyzed, and manufactured. Then, mechanical components are assembled on the U shape table and electrical-electronic equipment is located on the mechanism. Finally, PLC programmed stepper motors performed the movements in the linear and rotary mechanisms. Simulation of the jaw model was performed on the automatic articulator and the desired results were successfully achieved.

One of the most important functions of the automatic articulator is the ability to simulate the rotational movements of the jaw models. Thus, the rotary mechanism of this device could rotate the jaw model around any desired axes via spherical joints and bearings. This device has received great interest from orthodontists and dental laboratory experts due to innovation in the simulation of jaw models. Preparing the correct closure of the jaw model with mechanical articulators takes a long time due to the cutting and reattaching of the cast. However, since there is no need to cut and reattach the cast in the automatic articulator and also due to making all the processes automatically, providing the correct closure of the jaw model has been done much faster.

The reason for the long duration and low accuracy of the processes in the conventional articulators is based on determining the correct closure of the jaw model manually and by observation. In this method, the jaw

model is cut from the articulator, the correct closure is determined, and finally, reattach to the device, and the distance between the new and the previous position of the jaw model is measured with a ruler. However, in the automatic articulator, there is no need to cut and reattach the jaw models and all processes are done automatically and precisely. Thus, in orthognathic surgery applications, dentists have great advantages in terms of short pre-operation preparation time, high accuracy of the simulation due to the ability to rotate the jaw models in any desired axis.

REFERENCES

Bai, S., B. Bo, Y. Bi, B. Wang, J. Zhao, Y. Liu, Z. Feng, H. Shang and Y. Zhao (2010). "CAD/CAM surface templates as an alternative to the intermediate wafer in orthognathic surgery." *Oral Surgery, Oral Medicine, Oral Pathology, Oral Radiology, and Endodontology*, 110 (5), 1-7.

Chung, C.-C. J., J. Chai and L. M. Jameson (2001). "Interchangeability of a semiadjustable articulator." *International Journal of Prosthodontics*, 14 (5), 427-431.

Enciso, R., A. Memon and J. Mah (2003). "Three-dimensional visualization of the craniofacial patient: Volume segmentation, data integration and animation." *Orthodontics & craniofacial research*, 6, 66-71.

Fuster Torres, M., S. Albalat Estela, M. Alcañiz Raya and M. Peñarocha Diago (2009). "CAD/CAM dental systems in implant dentistry: update." *The International Journal of Prosthodontics*, 14 (5), 427-431.

Gartner, C. and B. Kordass (2003). "The virtual articulator: development and evaluation." *International journal of computerized dentistry*, 6 (1), 11-24.

Ghanai, S., R. Marmulla, J. Wiechnik, J. Muehling and B. Kotrikova (2010). "Computer-assisted three-dimensional surgical planning: 3D virtual articulator." *International journal of oral and maxillofacial surgery*, 39 (1), 75-82.

Hockstein, N. G., J. P. Nolan, B. W. O'Malley Jr and Y. J. Woo (2005). "Robotic microlaryngeal surgery: a technical feasibility study using the daVinci surgical robot and an airway mannequin." *The Laryngoscope*, 115 (5), 780-785.

Kaur, M. N., N. Pasriča, K. Sing and S. N. Man (2017). "The evolution of articulators: Part I." *Stomatološki glasnik Srbije*, 64 (3), 146-156.

Kordaß, B., C. Gärtner, A. Söhnel, A. Bisler, G. Voß, U. Bockholt and S. Seipel (2002). "The virtual articulator in dentistry: concept and development." *Dental Clinics*, 46 (3), 493-506.

Logozzo, S., E. M. Zanetti, G. Franceschini, A. Kilpelä and A. Mäkynen (2014). "Recent advances in dental optics-Part I: 3D intraoral scanners for restorative dentistry." *Optics and Lasers in Engineering*, 54, 203-221.

Maestre-Ferrín, L., J. Romero-Millán, D. Peñarrocha-Oltra and M. Peñarrocha-Diago (2012). "Virtual articulator for the analysis of dental occlusion: an update." *Medicina oral, patologia oral y cirugia bucal*, 17 (1), 160-163.

Michalakis, K. X., N. V. Asar, V. Kapsampeli, P. Magkavali-Trikka, A. L. Pissiotis and H. Hirayama (2012). "Delayed linear dimensional changes of five high strength gypsum products used for the fabrication of definitive casts." *The Journal of prosthetic dentistry*, 108 (3), 189-195.

Navneet, K. M., P. Neeta, S. Kavipal and S. M. Navjot (2017). "The evolution of articulators: Part II." *Stomatološki glasnik Srbije*, 64 (4), 184-193.

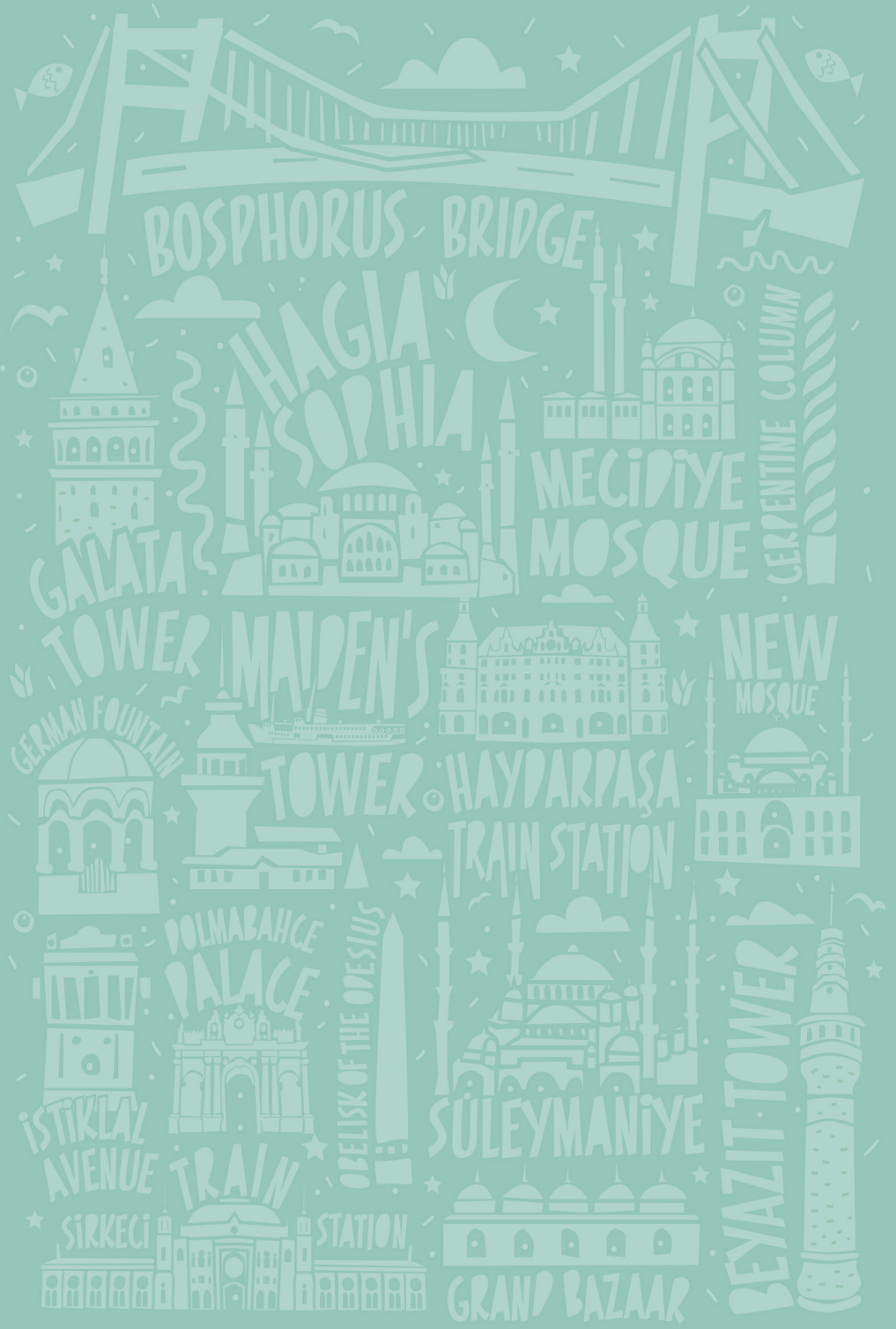
Panula, K., K. Finne and K. Oikarinen (2001). "Incidence of complications and problems related to orthognathic surgery: a review of 655 patients." *Journal of oral and maxillofacial surgery*, 59 (10), 1128-1136.

Paul, P., J. Barbenel, F. Walker, B. Khambay, K. Moos and A. Ayoub (2012). "Evaluation of an improved orthognathic articulator system. 2. Accuracy of occlusal wafers." *International journal of oral and maxillofacial surgery*, 41 (2), 155-159.

Shadakshari, S., D. Nandeeshwar and M. Saritha (2012). "Virtual articulators: a future oriented technology." *Asian Journal of Medical Sciences*, 1 (2), 98-101.

Starcke, E. N. (1999). "The history of articulators: A perspective on the early years, Part I." *Journal of Prosthodontics*, 8 (3), 209-211.

Yau, H.-T., H.-C. Chen and P.-J. Yu (2011). "A customized smart CAM system for digital dentistry." *Computer-Aided Design and Applications*, 8 (3), 395-405.



BOSPHORUS BRIDGE

HAGIA SOPHIA

MECIDIYE MOSQUE

CERPENTINE COLUMN

GALATA TOWER

MAIDEN'S TOWER

NEW MOSQUE

GERMAN FOUNTAIN

HAYDARPAŞA TRAIN STATION

DOLMABAHCÉ PALACE

OBELISK OF THE OPESIUS

SÜLEYMANIYE

BEYAZIT TOWER

ISTIKLAL AVENUE

TRAIN

STATION

SİRKECİ

GRAND BAZAAR

